Thèse de doctorat de l'Université Sorbonne Paris Cité

Préparée à l'Université de Paris

Ecole doctorale BioSPC ED 562

Institut Jacques Monod – Equipe Spécification des destins cellulaires

Role of Signaling Pathways in Cell-Fate Specification in the Early Mouse Embryo

Par Nicolas PORCHET

Thèse de doctorat de Biologie du Développement

Dirigée par Jérôme COLLIGNON

Présentée et soutenue publiquement à l'institut Jacques Monod le 20 décembre 2019

Rapporteuse : Dr Claire CHAZAUD, Université Clermont Auvergne

Rapporteuse : Dr Alice JOUNEAU, Université Paris Saclay

Examinateur : Dr Jérôme ARTUS, Université Paris Saclay

Examinateur : Dr Michel COHEN-TANNOUDJI, Institut Pasteur

Directeur de thèse : Dr Jérôme COLLIGNON, Université de Paris

ACKNOWLEDGMENTS

I especially wish to give a big thank you to Dr Jérôme COLLIGNON for recruiting me as a master's 1 intern and for transmitting its scientific interest that made me want to pursue his research during my PhD. I will keep in mind all the gossips and chit chats were shared during those 3 years in the lab! I have really appreciated the trust he ensured me with to conduct my research.

A special thank to the imaging facility at the IJM for their technical and, most and foremost their psychological back-up during those endless acquisitions at the confocal! A big thank you to Chloé, Nicolas, Orestis, Sophie, Vincent and Xavier for making work conditions so pleasant in your company.

A special thank to the mouse room facility of the IJM for taking such good care of my mice babies. I so glad that they were so well took care of until they unfortunately had to meet me… A big thank you to Andri, Camélia, Jennifer and Laetitia.

I am so grateful to Sabria for making all those genotyping PCR, I could not have done it without you.

I want to thank my two interns Marie and Thelma for their constant good mood and interest display during those months. You did a great job by making the βCATENIN project a reality.

I really want to thank newly appointed Dr Mathieu for welcoming me in the lab as my PhD student fellow. We had so much fun trying to make experiments work and still trying today, it will never get old.

A big thank you for all current lab members Annie, Mimmo and Nathalie for the good moments we shared. I want to especially thank any one of you for your support during these 3 years.

A huge thank you to all the IJM personal, and especially this wonderful 5th floor that makes all the other floors jealous. Jérémy, Laetitia, Line and Noémie you are very good friends to have, I wish you the best for the end of this "wonderful" PhD adventure!

A special thanks to my reporters and examiners for taking the time to get interest in my work, I hope you will be satisfied of your reading.

I want to personally thank my good friend Laina for your support and advices during this PhD, but let's be honest mostly for introducing me to ramens.

Finally, a huge thank you to my fiancée for both bearing me day to day and preventing me to kill myself during the conception of this damn Word document!

TABLE OF CONTENTS

FIGURES AND TABLES

PREFACE

The mouse early embryogenesis consists in two distinct periods divided by the time of the embryo implantation at the embryonic day 4.5 (E4.5). If the preimplantation stages see the first specifications of cell populations, the post-implantation period culminates with the gastrulation of the embryo leading to the differentiation of the germ layers and the massive cell rearrangements coming along. In the present manuscript I will be more focused on the pre-implantation stages of the mouse embryo and more precisely from the 8-cell stage (or morula) to the formation of the blastocyst consisting of a hollow sphere composed of three distinct tissues : the trophectoderm (TE), the primitive endoderm (PrE) and the Epiblast (Epi) (Figure 1).

The mouse early embryo has been well studied now for the past fifty years to understand how mammalian embryos develop. It is a robust and adaptive system capable of being cultured *in vitro* that presents key advantages for a biological model like a few numbers of tissues specified and their pseudo-transparency which is mandatory for light imaging.

One of the most challenging question in developmental biology is to understand how from the material contained in one fertilized egg the embryo can develop into a multicellular individual that is organized by specific axes. The paradigm of the mouse embryo is that it does not present any specific orientation – until it reaches the blastocyst stage – unlike in other metazoan models where the embryo clearly displays two poles (animal and vegetal) just after fertilization.

With no apparent embryo organization at the morula stage, we wonder how the specification of cell identities that will lead to the formation of distinct tissues observed at the blastocyst stage is triggered. Increasing evidence suggests that even though the blastomeres are phenotypically similar, key components including epigenetic modifications, transcription factors, signaling pathways etc. drive the blastomere to its fate while keeping a high degree of plasticity. After the first specification event separating the TE from the ICM, blastomeres within the ICM become competent for signaling cues that will drive their subsequent differentiation towards either PrE or Epi fate. ICM progenitors retain their ability to change fate until the late blastocyst stage where all cells are fully committed to their fate (Figure 1).

In recent years, with the combination of mass omics sequencing, advances in live-imaging and the increase use of computational models allowed researchers to propose mechanistic models from which the blastocyst is formed, and its tissues specified. These models revealed the increasing role of

signaling molecules that lead to a cascade of posttranslational protein modifications usually ending in transcriptional regulations of core genes and is establishing the signaling pathways network.

The aim of this manuscript is to highlight the roles of signaling pathways in regulating the events of cell-fate specification in the early mouse embryo. To that aim, I will present two distinct studies that used a combination of genetic and pharmacological approaches, as well as quantitative assessment of their impact on tissue specification. The first one will be focused on the role of the ACTIVIN/NODAL signaling which leads to the proper development of all the blastocyst lineages through a tissue-communication mechanism. The second will present the impacts of βCATENIN – member of the WNT/βCATENIN pathway – on cell-fate balance and cell differentiation via its interaction with other signaling pathways during blastocyst formation.

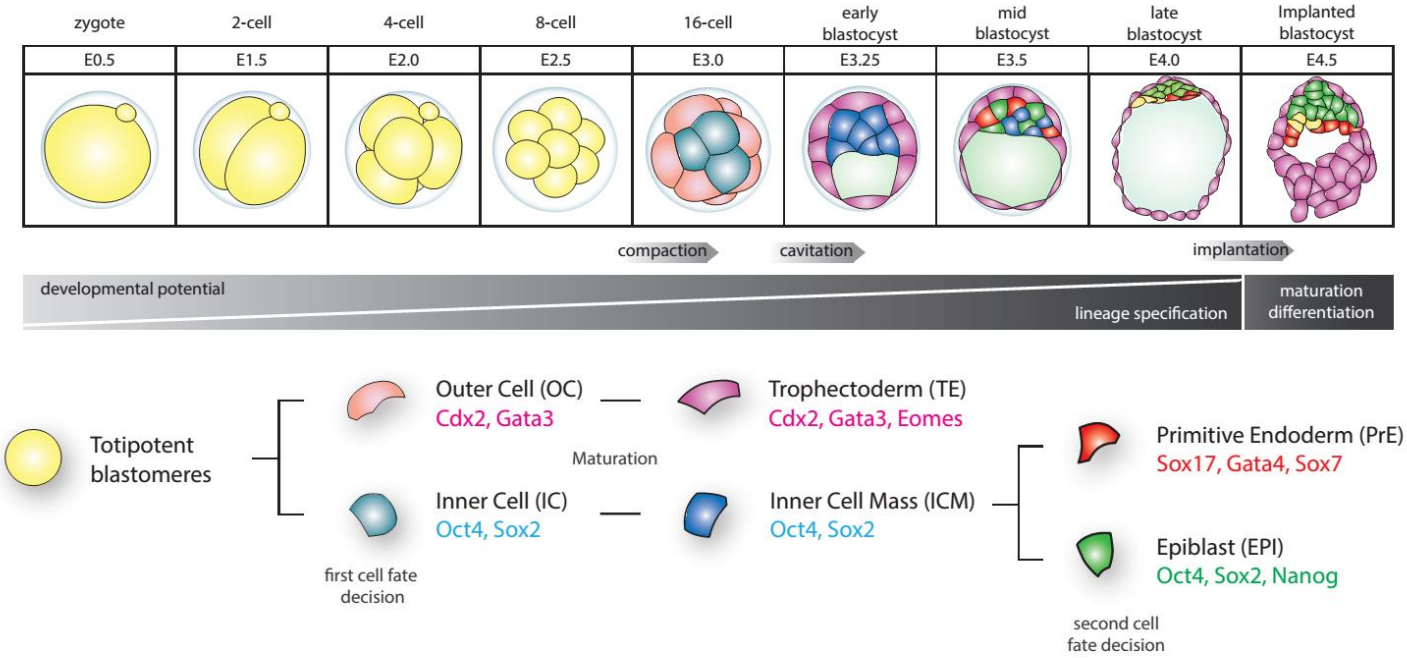

Figure 1 : Specification of cell fates throughout pre-implantation embryogenesis.

Adapted from V. Garg

Schematic representation of the different lineages formed from the zygote divisions and the morphological events occurring during this period. Following the cleavage stages, the blastomeres slowly lose their potential and become more specified. Once the late blastocyst stage is reached the cells are fully committed to their respective lineages. From that point the three lineages TE, PrE and Epi will undergo processes of maturation and differentiation allowing the late blastocyst to implant. During fate specification, cells will express gene repertoires that are specific to their lineage and this under the control of signaling pathways.

INTRODUCTION

I. THE MOUSE EARLY EMBRYOGENESIS

A. From fertilization to the morula stage

1. Cleavages of the zygote

The preimplantation period of the mouse embryogenesis starts with the formation of zygote consequently of the fertilization. The newly formed 1-cell stage will therefore undergo series of asynchronous cell divisions with the two first cleavages being approximately twice longer than the subsequent divisions. The mechanism controlling the time-line by which the embryo drives the different events controlling its development with the division rate of its blastomeres remains unclear[1]. One of the earlier events of the cleavage period is the activation of the zygotic genome (ZGA) occurring at the 1-cell stage with a burst of transcriptional activity at the 2-cell stage[2]. It is interesting to note that even though maternal RNAs are mostly degraded during this event, translated proteins from these messengers can withstand until the late blastocyst stage[3].

During the cleavages the embryo is encapsulated by a glycoprotein shell called the zona pellucida (ZP) limiting its expansion, but letting the embryo free of rotation movements, from which it will hatch at the late blastocyst stage around the 4th embryonic day (E4.0). Because of the space restriction, the embryo will divide keeping a constant global cytoplasmic volume leading to the formation of smaller blastomeres as development progresses. Even though the ZP is essential for the fertilization to occur it is completely dispensable for further development of the embryo until the late blastocyst stage – as shown in *ex vivo* culture experiments. However, some studies indicate that the deformation of the ZP prior to the embryo hatch guides the orientation of the blastocyst through the embryonic/abembryonic axis[4,5].

2. Self-organization and plasticity of the early embryo

The early stage of preimplantation development is a very robust and adaptative system mostly highlighted by blastomeres removal or aggregation experiments. In these experiments the embryo adapts in size and in cell specification through the regulation of the mitotic and apoptotic activities and fate reversal[6–8]. The plasticity of these early totipotent blastomeres is best illustrated by the fact that isolated blastomere from the 4-cell or 8-cell stage can develop into any tissues when combined with a host embryo[9,10]. However, even though the plasticity of this isolated blastomere and its viability in culture, no conceptus can be formed from these cells. Indeed, minima in terms of cell number exist and are required to form the individual because of the inability of the blastomere to divide further[6]. Until the 8-cell stage blastomeres forming the morula are totipotent and phenotypically identical; nevertheless, it is fair to wonder whether they are also similar at the molecular level.

For the last decade several studies have highlighted discrepancies between blastomeres from the 8-cell stage[11–14]. Taking in consideration that the mitotic division can be asymmetrical, it induces differences in term of the molecular material that is being spread between the cells. It is thus possible to imagine that some proteins will stochastically be accumulated in only one of the cell resulting in its further differentiation from its sister[8,14,15]. Moreover, with the emergence of single-cell sequencing technologies, heterogeneity in terms of gene expression levels has been observed in all blastomeres of the morula[11] (Figure 2).

A more sensitive and precise regulation has been identified following the assessment of transcription factors activity such as OCT4 and SOX2[12,13]. Indeed, the discrepancies observed in blastomeres from the 4-cell stage are not dependent of the expression levels of these factors but rather on the duration of their binding conducting their activity[12,13]. The duration length of these factors binding can predict a bias towards the first cell that will be allocated to the inner cell mass (ICM)[12,13]. Therefore, epigenetic regulations of early transcription factors can directly affect fate specification[8,12–14]. This early cell heterogeneity results in the emergence of two distinct cell populations by the 16-cell stage when the morula undergoes a process a compaction (Figure 2).

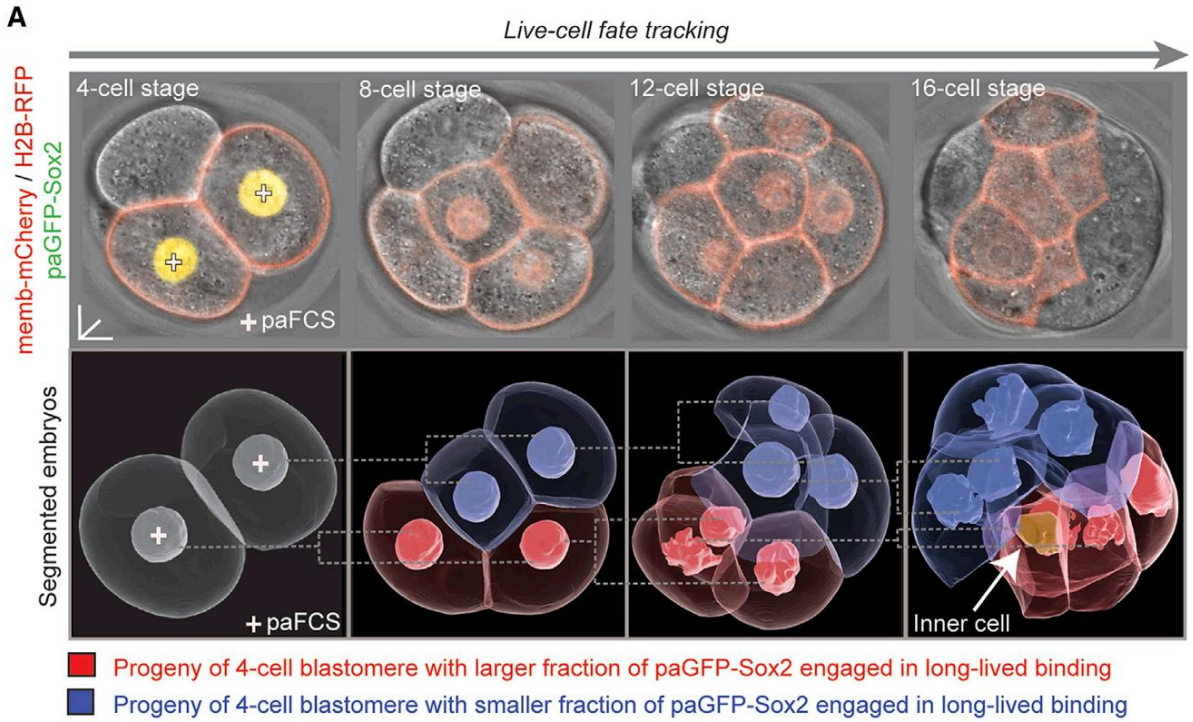

Figure 2: Difference in SOX2 binding durations in blastomeres from the 4-cell stage to the morula.

White et al. 2016

Once injected into one blastomere of the 2-cell stage, live imaging of SOX2 nuclear localization revealed different fractions according the duration of its DNA interactions. Progeny of the 4-cell blastomere can be divided in two groups: long-lived binding and short-lived binding. Blastomere presenting a longer DNA binding interaction of SOX2 are more likely to become ICM. Therefore, molecular heterogeneity at the 4-cell stage can drive the first fate specification.

B. Compaction and polarization of the morula

1. Compaction facilitates fate specification

Like other mammals the compaction of the mouse embryo is the first morphogenetic event occurring during the pre-implantation period. At the 8-cell stage, blastomeres of the newly formed morula will flatten increasing their intercellular contacts[16,17]. As a resultant, the boundaries between cells are not apparent and the embryo displays a more spherical shape[16,17]. This mechanism – taking few hours to be completed – utilizes forces from the cytoskeleton and more precisely the acto-myosin cortex to pull the blastomeres together[18]. Evidence suggested that the adherent junctions were responsible for the compaction as no compacted morula have been observed in a *Ecadherin* (encoding the protein of the same name involved in the adherent junction complex) maternal-zygotic (mz) double knock-out (KO) background[19]. However, more recent data showed that even though the adherent junctions were required to maintain the compaction in place, they were not responsible for its initiation as the forces they provided were insignificant compared to those coming from the acto-myosin cortex[18] (Figure 3).

But what is the mechanism behind this observation? The explanation nests in the position of the 8-cell stage blastomeres. Indeed, each blastomere has two types of contacts: i) the cell-cell contact with its neighbors through diverse junction complexes, ii) and the cell-liquid contact corresponding to the surface of the embryo – forming the apical domain – where the membrane is free of tension molecules. Pulses of contractions observed from the acto-myosin cortex will increase the surface tension at the apical domain of each blastomere. This cell-autonomous process leads to the formation of a driving force from the apical domain towards the basal side, resulting in the compaction of the cells through their cell-cell contact[17,18] (Figure 3).

During the transition from the 8-cell to the 16-cell stage, two distinct populations identified as the inner cells (IC) and the outer cells (OC) according to their position within or at the surface of the embryo respectively, are formed. If the compaction is not required for the establishment of these populations it does facilitate the internalization of the IC for pure geometrical reasons as the sphere can allocate more IC because of its low surface/volume ratio[20]. Still, we do not know yet what controls the contractility of the acto-myosin cortex. One explanation could be through the phosphorylation of the ECADHERIN. In fact, experiments using global inhibitors of kinases can trigger the compaction of the morula as early as at the 2-cell stage while inhibitors of phosphatases revert and block the compaction[21,22]. It is therefore tempting to associate the temporal regulation of the initiation of the

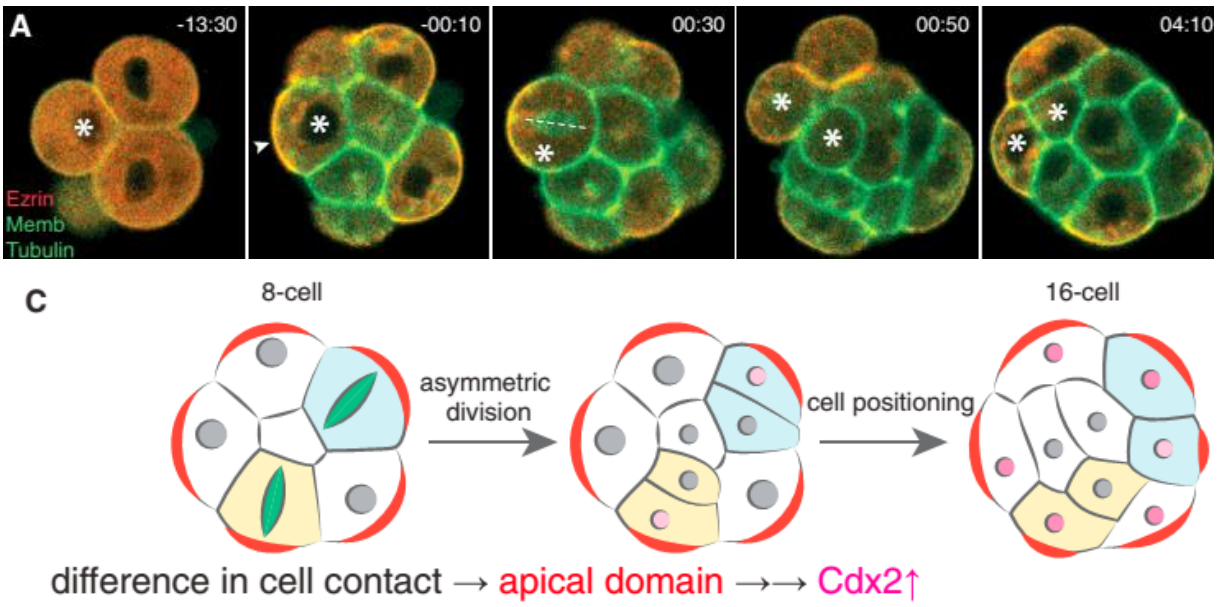

Figure 3: Formation of the apical domain on OC during the compaction of the morula.

Korotkevich et al. 2017

The upper panel shows the specification of both OC and IC depending on their position within the embryo. EZRIN labels the apical domain established in OC resulting in the establishment of the apical-basal polarity. Apolar cells that do not present the apical domain are fated to become IC.

The lower panel summarizes the events involved in the formation of the two spatially distinct populations. The polarization of the blastomere drives its position within the embryo and its linked with the expression of specific markers, here showed by the activation of *Cdx2*.

compaction with the inhibition and activation of these posttranslational modifiers occurring at the same time[23] (Figure 3).

2. Polarization specifies IC versus OC fate

Although, technically speaking, blastomeres become polarized at the 2-cell stage where they display two poles forming both cell-cell and cell-liquid contacts; the polarization of the blastomere is characterized at the 8-cell stage by the acquisition of the apical domain at the surface of the cells while the basal pole is formed at the cell-cell region. This apical domain is essential for further development of the embryo since it triggers the specification of both IC and OC. Indeed, the disruption of the apical domain by genetically removing some of its key components prevents the segregation of both IC and OC populations and their subsequent progression into ICM or trophectoderm (TE) cells respectively[24].

This cell-autonomous process taking approximately 5 hours is concomitant with the compaction of the embryo[17]. Still, these two events are completely independent to each other. Indeed, unpolarized blastomeres can flatten whilst blastomeres from a *mzEcadherin* KO background are polarized and present an apical-basal orientation[19,24–26]. Even if the mechanism behind the formation of the apical domain has no yet been elucidated, some studies have suggested that it is spatially restricted by molecules involved in cell-cell contacts since the apical domain is established in regions that are far away from cell junctions[16,17].

The apical domain constitutes a hub for different signaling pathways and components involved in the metabolic activity of the cell[16,17,27]. One of the earliest identified molecule to be part of the apical domain is the protein EZRIN which is involved in the orientation of microvilli[25]. Upon its phospho-activation EZRIN becomes excluded from the cell-cell contact regions and gets restricted to the apical domain of the cell where it will drive the formation of microvilli[28,29]. The protein kinase C (ζ isoform - PKCζ) has also been identified as a member of the apical domain and appear to be a good candidate for the phospho-activation of EZRIN[29]. More interestingly, the same study also identified RHO A (a small GTPase) as the main regulator of PKCζ during this process ; thus forming a tripartite complex that upon activation is localized at the apical domain and can trigger the OC differentiation[29] (Figure 3).

Even if the apical-basal polarization of the cell consists of a robust mechanism it still is plastic and can be reversible. Recent evidence have shown that – through mechanically applied surface tension – the apical domain could be suppressed whilst reversibly an unpolarized cell isolated from cell-cell contact recovers its apical-basal orientation[20,24]. Therefore, the maintenance of the polarization is a consistent and active process regulated by the embryo. Several molecules have been elucidated to provide such

perdurance of the apical domain. The partitioning defective complex (PARD3 – PARD6 – PRKCZ/i) components are first being expressed at the 2-cell stage where most of them are located in the nucleus[30,31]. However, from the 4-cell stage onwards these proteins are more often found in the cytoplasmic compartment until they are enriched at the apical domain specifically at the 8-cell stage. The localization of the complex at the apical surface does mainly depend on the activity of the RHO A GTPase – mentioned above[24,32]. The specific role of the PARD complex remains poorly understood but increasing evidence suggest that it is required for the establishment of tight junctions that are first initiated at the 8-cell stage and perdure further in development[30,33,34]. Indeed, disrupting the PARD complex prevents the correct patterning of the tight junction protein TJ-1 whilst does not affect the adherent junctions or the compaction[30,33,34].

C. First lineage specification

At the 16-cell stage, two spatially distinct cell populations are observed according to their position within the embryo: the IC and OC. More than being limited to a phenotypical separation these two populations present key differences in terms of transcriptomes, orientation and morphology that lead to the specification of two distinct lineages. The initiation of this process starts with the internalization of some blastomeres which become fully enclosed by their neighbors and form the IC. The mechanism underlying the positioning of each blastomeres is still investigated, but some recent studies have proposed models pointing towards the orientation of cell division from the 8-cell stage.

1. Two spatially distinct populations

a) Mitotic division and fate specification

b) The apical domain and spindle orientation

2. TE and ICM fate specification

a) From a polarized OC to a TE cell

b) From an apolar IC to an ICM cell

D. Formation of the blastocyst

At the 32-cell stage the emerging TE layer sees the establishment of an osmotic gradient caused by the asymmetric repartition of ionic canals within iTSC. Apical sodium exchangers allow the influx of cations while sodium-potassium pumps localized at the basal membrane are responsible for the efflux of water[59]. This osmotic regulation of the TE layer leads to the accumulation of water at the interface between TE and ICM cells and the subsequent formation of small lumens[60]. As the mitotic activity continues in these respective tissues the already established gradient leads to the formation of more pockets that at some point merge – through a mechanism that remains unknown – and extend asymmetrically to one side of the embryo to form a fluid-filled cavity named the blastocoel. The asymmetric localization of the blastocoel breaks the radial symmetry of the embryo creating an embryonic-abembryonic axe with the ICM pushed towards the embryonic pole and the cavity growing at the abembryonic pole. The newly formed early blastocyst then consists in a hollow sphere with the ICM lying on the top of the cavity that are both enclosed with the TE layer which acquires epithelial properties (Figure 7).

In order for the cavity to be formed, tight junctions should be formed and matured to tightly seal the TE in order to resist to the growing luminal pressure as more water is excluded from TE cells[61]. Tight junctions between TE cells are mostly composed of the CLAUDIN protein types 4 and 6 that are essential for the growth of the cavity[61]. Once established, the tight junctions will control both positioning and shape of the lumens via the connections between the cytoskeleton of TE cells creating an intercellular force within TE layer[16,61]. The growth of the cavity and the increased luminal pressure coming from it strengthens the tight junctions thus creating a stronger force within the TE layer, allowing the cavity to grow more, strengthening the epithelial TE etc….[62]. Even though, it has been shown that the compaction is not required for cavitation initiation, the essential role of the tight junctions makes the initial polarization of OC to be mandatory. Indeed, as we explained above, the establishment of the apical domain leads to the formation of the tight junction through a mechanism

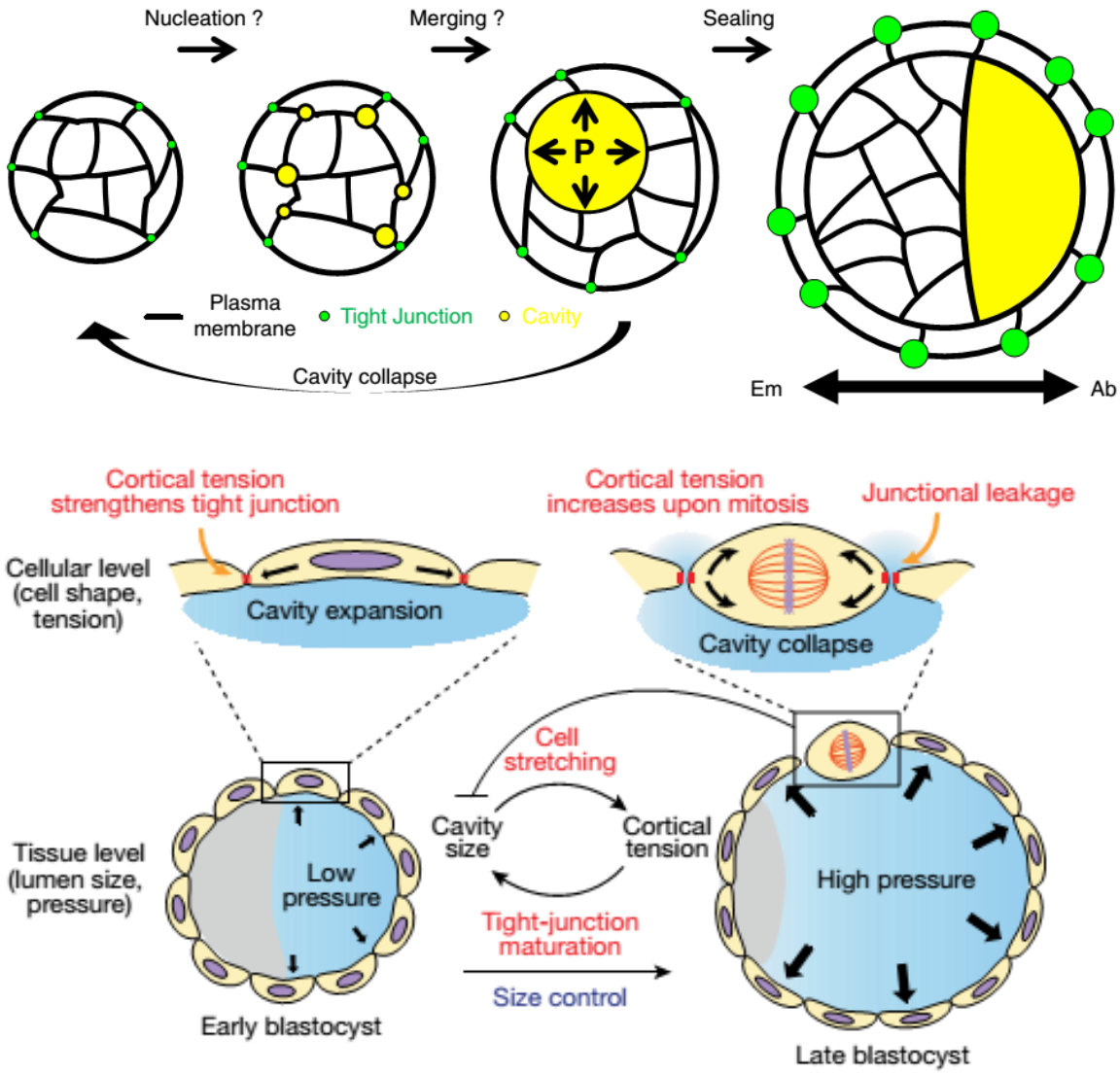

Figure 7: The formation of the blastocoel requires the consolidation of tight junctions.

Maitre 2017 ; Chan et al. 2019

Fluid is drawn at the contacts between TE and ICM as a consequence of an osmotic gradient within the TE layer. These small cavities merge to form the blastocoel at the early blastocyst stage. To allow the constant growth the blastocoel, tight junctions are strengthened between TE cells to support luminal forces. The cavity grows in expansion cycles depending on the mitosis activity of the mural TE. High pressure from the lumen stretches TE cells leading to increased cortical tensions and the rupture of the tight junctions. Thus, the cavity collapses, diminishing the luminal pressure allowing the tight junctions to be fully matured to resist a new growing phase.

involving the PARD-aPCK complex[33]. Therefore, embryos lacking elements for the PARD-aPCK complex are unable to cavitate and thus, their developmental progression arrests[33] (Figure 7).

The cavity grows according to expansion cycles that are a resultant of the mitotic activity within the TE layer[62,63]. Indeed, the asymmetric positioning of the cavity leads to discrepancies in cortical tensions between polar TE cells – close to the embryonic pole – and the mural TE – to the abembryonic pole[62]. The luminal pressure strengthens the mural TE cells and generates a mechanical stress through the tissue leading to the rupture of cell-cell junction, thus the collapse of the cavity and the reduction of the pressure[62]. Tight junctions will then regenerate after mitosis under luminal pressure, and the cavity will undergo a new expansion phase[63,62]. Therefore, the growth of the cavity is directly linked with the mitotic activity of mural TE cells through cycles of expansions and collapses. In contrast, the mitotic activity of the ICM that does not establish the same junctions as the TE is not affected by this process[62]. It is then noteworthy that low luminal pressure (i.e. at the early blastocyst stage) allows more cells to be internalized and limits the mitotic activity of mural TE cells leading to higher ICM/TE ratios whereas high luminal pressure (i.e. at the late blastocyst stage) results in the decrease of the ratio[62]. Thus, the cavitation of the blastocyst is required for the proper allocation of specified cells to their respective layer and the proper developmental progression of the embryo via its regulation of the proportion between fates (Figure 7).

E. Second lineage specification

1. Establishment of Epi and PrE fates

Once the first specification has terminated, ICM cells will progressively differentiate into two spatially and morphologically distinct tissues by the time of implantation. These populations are called the epiblast (Epi) and the primitive endoderm (PrE). The Epi is an embryonic tissue responsible for the specification of all tissues composing an individual while the PrE forms extra-embryonic populations that support the proper development of the embryo throughout gestation.

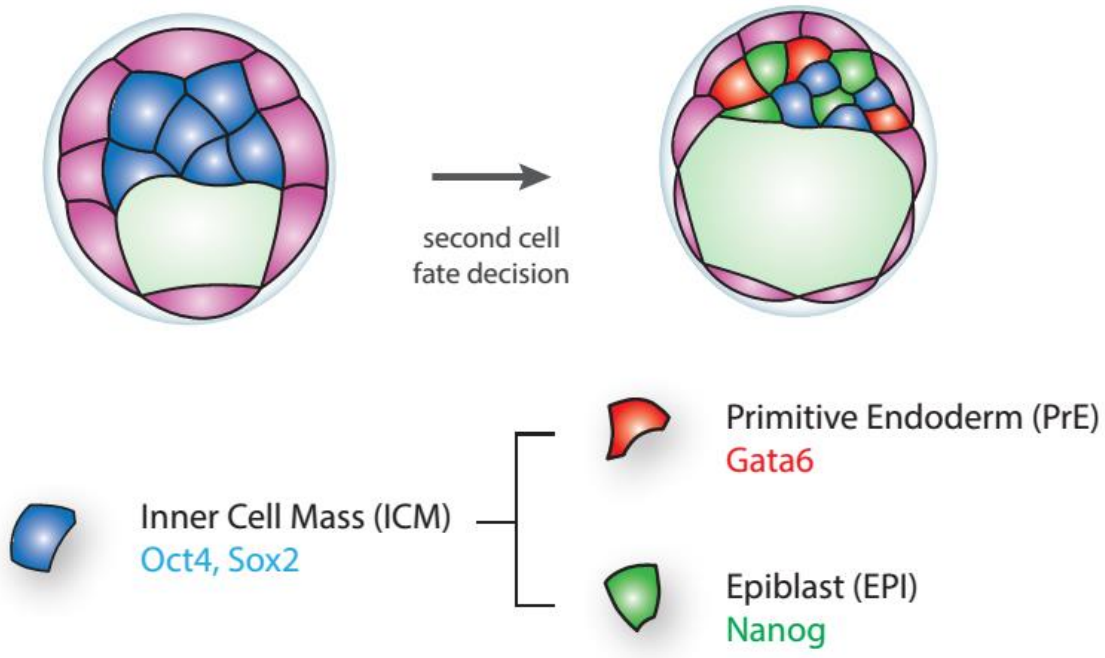

Figure 8: Acquisition of the salt-and-pepper distribution.

The second cell fate specification results in the differentiation of both the Epi and the PrE lineages. At the 32-cell stage ICM progenitors present stochastic difference in expression levels of NANOG and GATA6. This discrepancy is amplified by the action of molecules signals and transcription factors that promote the acquisition of each lineage program. The salt-and-pepper distribution observed by the mid blastocyst stage is the consequence of the asynchronous fate decision that occurs in each ICM progenitor. At this stage of development ICM cells remain plastic and upon reception of signals can switch fate.

a) The salt-and-pepper distribution

b) NANOG as the gatekeeper of the Epi fate

c) GATA6 and the adoption of the PrE fate

2. Balance between Epi and PrE fates

Since similar expression levels of both *Nanog* and *Gata6* are observed between the 8-cell stage and their respective fate-allocated cell at the mid blastocyst stage, it seems that fate specification depends on the downregulation of the opposite fate rather than the promotion of a specific factor[57]. As mentioned above, two main inhibition processes have been determined: the *Gata6* inhibition by NANOG and the *Nanog* inhibition by pERK. Thus, placing FGF/ERK signaling at the core of a tripartite regulatory system[68]. It is therefore imperative to understand the mechanism by which FGF signals are transmitted and what more does the activity of the pathway regulate.

a) Activity of FGF/ERK signaling

b) Regulation of FGF/ERK signaling

F. The ICM segregation

1. Cell sorting and survival

During the blastocyst development, as the cavity expands, another physical and mechanical event occurs: the segregation of the ICM. As they progress towards their respective fate ICM cells undergo rearranging movements resulting in the complete separation of both Epi and PrE at the late blastocyst stage. Not much is known regarding this cell reorganization. However, since it consists of PrE cells sorting out of the mixed ICM pool, some studies focused their interest on a link between PrE progression and cell sorting[97–100]. PDGF signaling is a RTK-dependent pathway involved in the progression of the PrE program via the presence of its receptor PDGFRA at the membrane of PrE cells from the 32-cell stage[100,101] (Figure 13).

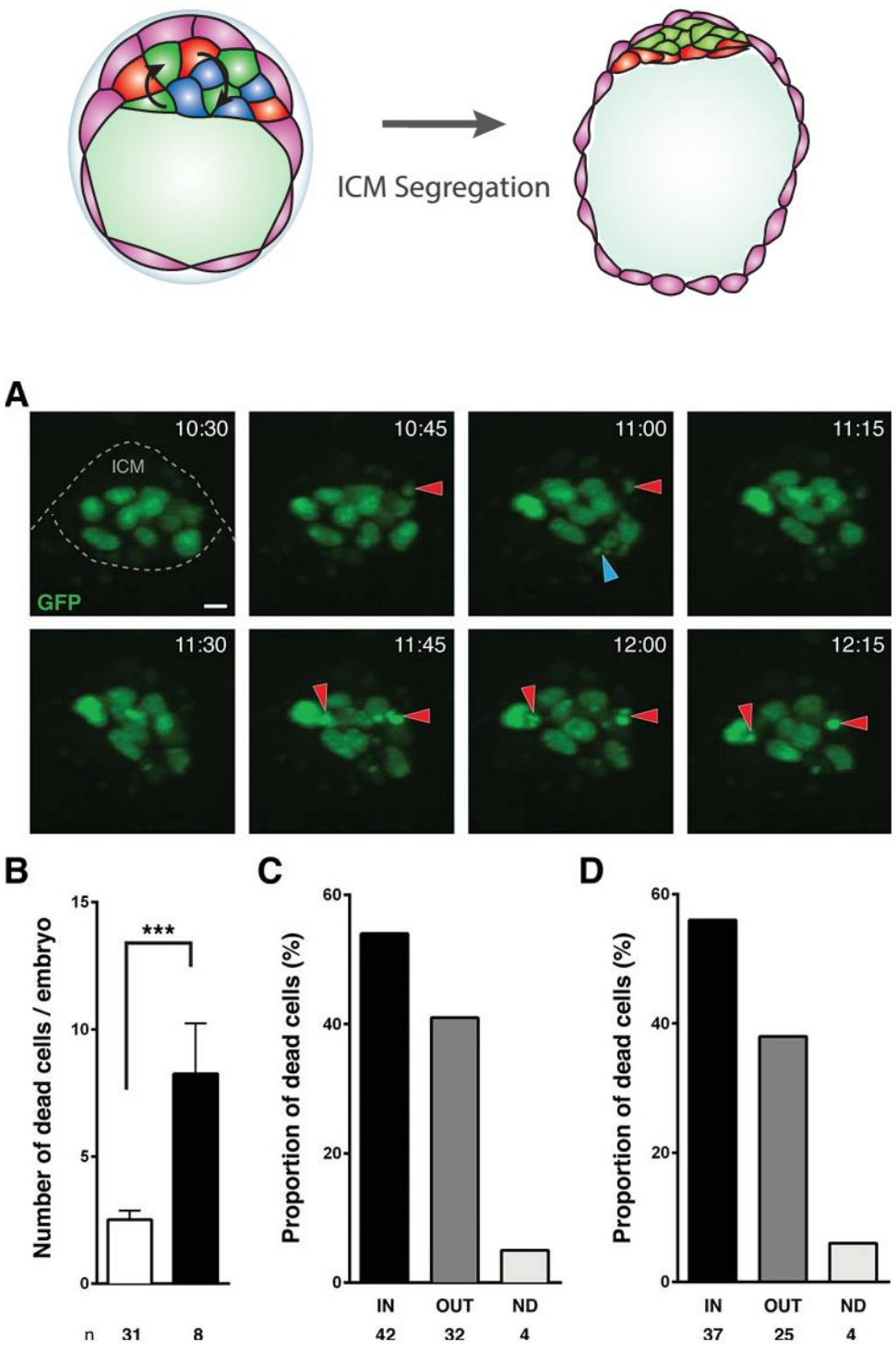

Figure 13: PDGF signaling sustains cell survival in the PrE independently of the cell position

Artus et al. 2013

During the specification of both Epi and PrE, cells from each lineage will undergo cell sorting rearrangements resulting in the complete separation of both populations in a process named ICM segregation. In the lower panel, time-lapse imaging of PdgfraH2B-GFP/H2B-GFP E3.5 embryos revealed an increase in apoptotic activity in the PrE layer. Since cell death occurs independently of the position of the PrE cell, it is unlikely that apoptosis is specifically triggered in misplaced PrE cells. Similar observations were made with inhibitors for PDGF signaling.

Although, the downregulation of the PDGF signaling does not affect the specification of the Epi or the PrE, it strongly reduces the number of PrE cells while not affecting the Epi number[98,102]. This would suggest that PDGF signaling is required for the maintenance of definitive PrE cells that die rather than convert to the Epi fate. Indeed, reducing the activity of the pathway leads to an increase of cell death within the PrE layer via apoptotic mechanisms depending on the action of the CASPASES[98]. However, even if the apoptotic activity was hypothesized for the proper sorting of the ICM cells, this study showed that cell death was increased in PrE cells independently of their position within the ICM upon PDGF downregulation[98,103]. Moreover, apoptotic events occur in both Epi and PrE via different mechanisms involving JAK/STAT signaling throughout the blastocyst progression suggesting that it is way for the embryo to control the number of cells from each tissue[102–105]. Therefore, even if cell death could be involved in order to select correctly positioned cells only, this regulation is undermined by the other roles of apoptosis during blastocyst development (Figure 13).

2. Cell sorting and epithelialization

As the blastocyst develops PrE cells acquire a robust organization leading to the formation of one layer of epithelialized cells separating the Epi from the blastocoel. Thus, at the late blastocyst stage, definitive PrE cells are linked together via both actions of adherent and tight junctions. This epithelium lays on a fully formed basal membrane – which is not a membrane – via the accumulation of extra-cellular LAMININ and COLLAGEN[106–108]. The acquisition of an apical-basal polarity is completed by the accumulation of LRP2 and DAB2 at the apical membrane and cytoplasm respectively[106–109]. The appearance of such epithelial makers before the cells are fully sorted could suggest that it has a role in the rearrangement of the populations[107,108]. Indeed, lack of DAB2 or aPKC – another apical marker located at the membrane of PrE cells – prevents the cells to maintain their position and are found mixed back in the ICM pool[99,106,109,110]. Interestingly, if DAB2 could be regulated by the TGFβ signaling pathway, aPKC appears to be directly controlled by FGF/ERK signaling and the PrE progression program[111,112,99,108]. Moreover, the activity of aPKC was required to sustain cell-survival within the PrE layer, and more specifically, suggested to sustain only properly segregated cells[99]. However, this appears to be unlikely since aPKC's role has been identified to maintain GATA4 levels, which are required for the activity of PDGF, and thus to maintain cell-survival in all PrE cells independently of their position as described above[99,101,113] (Figure 14).

Although not through apoptosis regulation, the epithelialization of the PrE could impact the cell-sorting through mechanical properties. Mathematical modelling and *in vitro* experiments have excluded

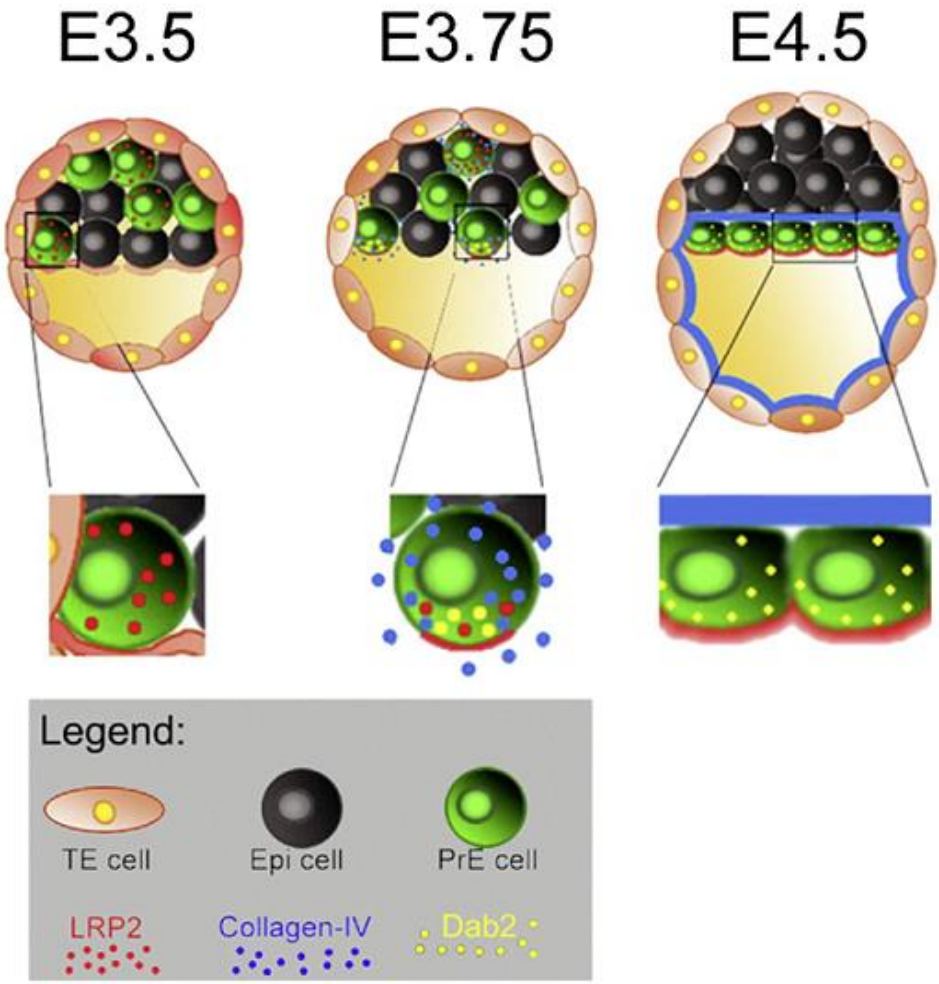

Figure 14: PrE cells are epithelialized and polarized at the late blastocyst stage

Gerbe et al. 2008

From the mid to late blastocyst stage, PrE cells progress expressing specific genes leading to their maturation. Among those expressed genes are found specific marker of epithelialization such as Dab2, Lrp2 or Collagen-IV. Once PrE cells have arisen at the surface of the ICM they assemble and form a proper epithelium with adherent junctions and the establishment of the apical-basal polarity represented by the apical accumulation of DAB2 and the formation of a basal membrane.

ECADHERIN driven adherent properties but not the impact of cortical forces[114,115]. Indeed, the presence of the cavity and the establishment of tight-junctions could govern the segregation in a similar way than the organization of the germ-layer in zebrafish[116]. Practically, the cortical tension exercised from the surface of the PrE by the molecules accumulated there reduce the contractility of the cell that result in force discrepancies between apical-basal polarized and apolar cells (i.e. Epi cells that are not epithelialized yet). Moreover, since about half of PrE cells were reported to lay against the cavity – as early as their specification could be detected – the lower surface tension from the blastocoel could be sufficient to maintain their position[20,100]. Thus, a similar contractility-based mechanism between IC internalization and PrE cell sorting could be possible[16]. To support this hypothesis, cytoskeleton inhibitors-based experiments have identified that the acto-myosin cortex and not the microtubules was responsible for the cell movements[103]. Alternatively, apoptosis regulation and directed cell migration could also play a role in the grand mechanism of Epi and PrE cell sorting that is yet to be completely understood (Figure 14).

G. Maturation and polarization of the late blastocyst

1. Progression into the PrE program

The maturation of the PrE is a multistep time gated process depending on the sequential activation of transcription factors controlled by mechanical cues and signaling pathways. To completely lock its fate and mature, a PrE cell needs to acquire specific properties and to activate a specific gene repertoire at each stage of the blastocyst development. Each step must be completed in order to progress to the next forming a linear process. The acquisition of these specificities during the blastocyst progression are regrouped in the so-called PrE program. As described above, the program starts with the initiation and maintenance of *Gata6* expression. However, GATA6 alone is not sufficient to progress into the program as illustrated in *Nanog* mutants where GATA6 positive cells fail to mature[67–69]. From the mid blastocyst stage onwards the activity of the FGF/ERK signaling and enough levels of GATA6 induce the expression of SOX17[67]. SOX17 is transcription factor expressed in PrE cells until the late blastocyst stage and is present in its derivatives after the implantation[97]. Although, its expression marks the commitment of the cell to further progress into the PrE program, its deletion did not reveal any requirements for the specification and maturation of the tissue[97]. Nevertheless, precise characterization of its binding during the gastrulation stages indicated that SOX17 was required to exclude SOX2 for its target genes, thus triggering the endoderm differentiation; such competitive

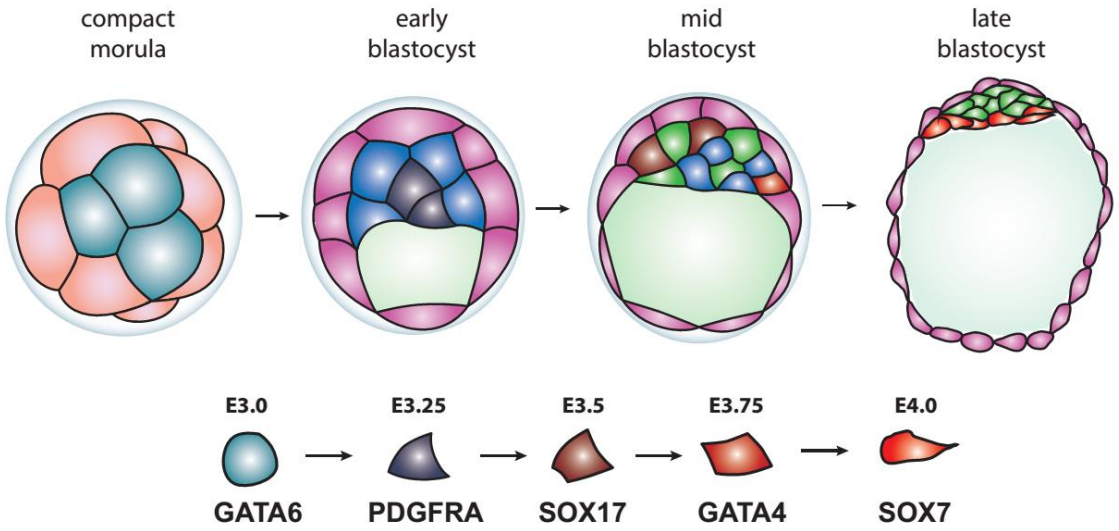

Figure 15: PrE acquisition program during the blastocyst maturation

Starting with Gata6 expression PrE cells will slowly commit to their fate and start to express a specific gene repertoire according to the developmental stage. Pdgfra is one of the earliest markers to be express in PrE cells after Gata6. Sox17 starts to be express at the mid blastocyst stage and is soon followed by the expression of Gata4 signifying that the cell has fully committed to the PrE lineage. The last marker of the PrE is Sox7 which expression is concomitant with the end of cell sorting and the epithelialization of the tissue. This linear acquisition of PrE markers makes a good tool to properly stage the embryos and identify at which step the development is affected.

mechanism at the preimplantation stages remains to be elucidated[97,117,118]. It is interesting to note that the restriction of *Sox2* expression to the Epi layer coincides nicely with the accumulation of SOX17 in emergent PrE cells and this restriction has been shown to be ERK signaling dependent like SOX17[58,119] (Figure 15).

Shortly after the initiation of *Sox17* expression, a combination of GATA6, ERK signaling OCT4 and some unidentified markers promotes the expression of *Gata4* at E3.75[55,58,67,120]. Unlike GATA6 and SOX17, that can label uncommitted cells, GATA4 is the first transcription factor to be expressed in definitive PrE cells, thus unable to switch back towards the Epi lineage[97,100,119,120]. Although the factors mentioned above are required for the expression of *Gata4*, its transcriptional regulation in the embryo is yet to be characterized. Similar to SOX17, the depletion of *Gata4* does not prevent the maturation of the tissue and its differentiation towards either the parietal endoderm (PaE) or the visceral endoderm (VE)[121]. Nonetheless, *in vitro* and similarly to GATA6, GATA4 is required and sufficient to differentiate ESC into PrE-like XEN cells[78,97]. Interestingly, since at this stage of development *Gata6* becomes sensitive to both ERK and OCT4 it is possible to imagine a combined complex including ERK/GATA6/OCT4 and GATA4 for further PrE maturation[55] (Figure 15).

SOX7 is the last known transcription factor being expressed by the PrE program at the late blastocyst stage where the initiation of its expression coincides, but does not requires, the completion of the ICM segregation[97]. Thus, SOX7 labels only definitive PrE cells and is known to regulate the epithelialization of the cell, even though its role in the PrE remains to be elucidated[122]. *Sox7* expression persists in the PrE derivatives tissues and is required for endothelial differentiation and hematopoietic stem cells differentiation[97,123]. However, unlike *Gata6* or *Gata4* its expression is dispensable for *in vitro* XEN cells differentiation[124]. Interestingly, most of the genes required for the maturation of the PrE are either expressed in both lineages and/or are Epi makers acting non cell-autonomously via signaling pathways suggesting that the Epi controls each step of the PrE maturation via the production of ligands[55,58,67] (Figure 15).

One such ligands is PDGFA involved in another RTK signaling pathway named PDGF. *Pdgfa* is expressed in Epi cells during the 16-cell to the 32-cell stage transition whereas its receptor PDGFRA is expressed and located in PrE cells at the 32-cell stage – although the activity of its locus starts earlier[96,98,119,125]. The activity of PDGF signaling in PrE cells starts shortly before the expression of *Sox17* and is responsible for the maintenance of PrE cell numbers[98,102]. Interestingly, the activity of the signaling is maintained by the mechanical properties of the cell and the conjoint activity of both GATA6 and GATA4[99]. Reciprocally, since PDGF signaling comes before the expression of *Gata4*, its activity is fully

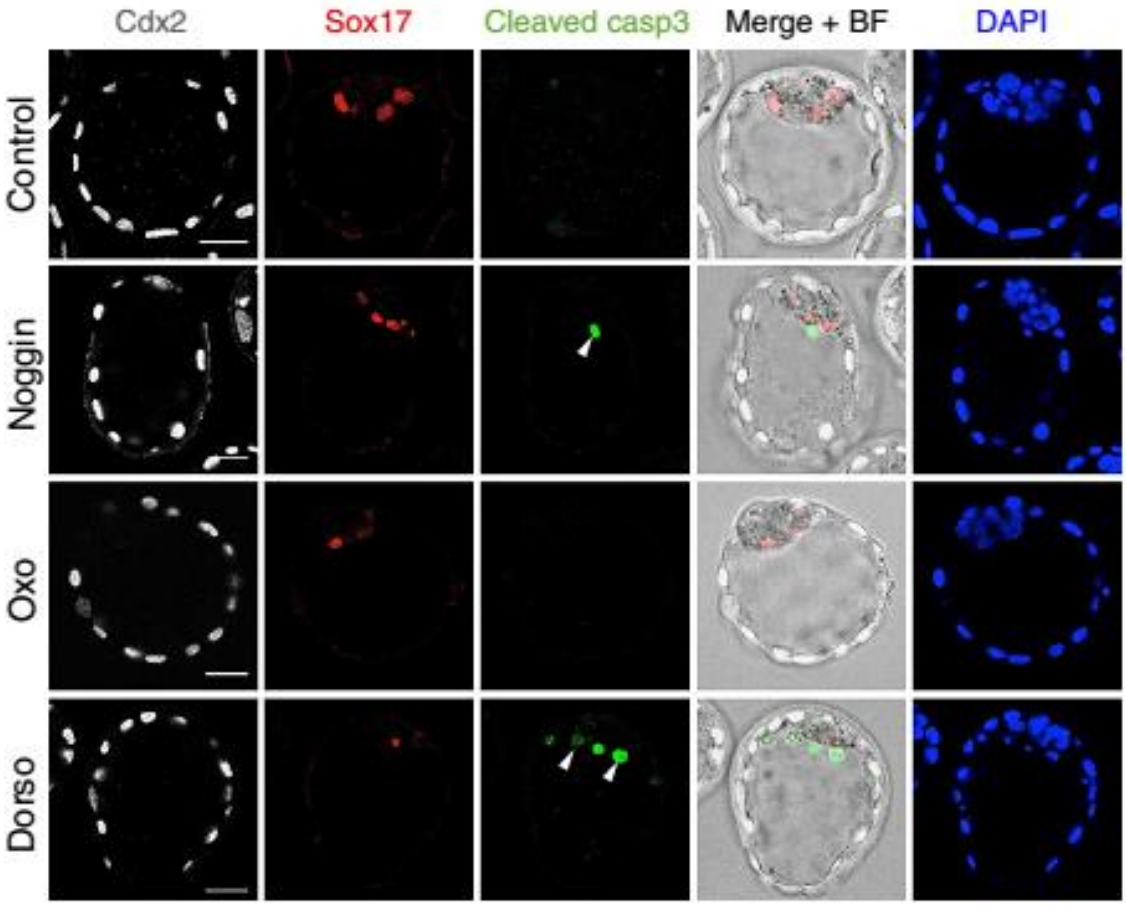

Figure 16: BMP signaling sustains cell survival within the PrE layer

Graham et al. 2014

BMP signals coming from the Epi are able to signal in PrE cells via receptors of the TGFβ family. Inhibition of these signals result in the activation of apoptosis in PrE cells preventing their subsequent maturation as seen by the downregulation of SOX17. BMP among with FGF and PDGF therefore demonstrate that the Epi sustains the maturation of the PrE via the expression of those signaling pathway ligands.

required for the progression of the PrE cell until it reaches a stage where *Gata4* is activated[99] (Figure 15).

Similar to PDGF, the BMP signaling pathway – member of the TGFβ superfamily – has been identified to be required for the maintenance of the PrE via the regulation of cell-survivability[105]. Indeed, reducing the activity of the SMAD1/5/9 – the effectors of BMP signaling – results in a striking increase of cell death but only in the PrE layer; thus, preventing the proper maturation of the tissue[105]. The activity of the pathway is mainly regulated by the ligand BMP4, expressed in a subpopulation of Epi cells at the early blastocyst stage[57,105,119] (Figure 16).

Therefore, a combination of cell-survival, transcription factors and Epi signals is controlling the progression of the cell though its PrE program. However, even though not much is known about the regulation of the mechanism driving a committed PrE cell and its late maturation, the expression profiles of the makers quoted above are an essential tool for researchers to properly stage the development of the blastocyst and to identify the state of maturation of the PrE layer. Lastly, it is remarkable than even though these transcription factors are spatially and temporally tightly regulated, none of their depletion – besides *Gata6* – presents a fully penetrant phenotype, highlighting the robustness of the mechanism and the possible redundancies between these factors.

2. The maturation of the Epi

a) The pluripotency factors in Epi maturation

b) Acquisition of the Epi gene repertoire

3. The polarization of the blastocyst

The polarization of the blastocyst – not to be mistaken with the apical-basal polarity of the cells – sets up a population of cells that can be oriented to one side of the embryo leading to a symmetry breaking. Not every event of polarization perdures and thus cannot be associated with embryonic axis establishment. The most noticeable polarization event occurs during the formation of the cavity and the pushback of the ICM towards one pole of the embryo. This mechanism described previously is essential for the cell sorting of the PrE during its maturation and the differentiation of the TE cells that are separated between a polar TE and a mural TE. Moreover, the adhesion between the polar TE and the Epi is for instance suggested to limit the movement of Epi cells, therefore driving PrE cells towards the cavity[137]. This radial symmetry breaking event will then control the orientation of the embryo

during its implantation into uterine horns[138]. Besides the cavitation process, the polarization of the embryo comes from the emergence of a subpopulation of cell within a tissue expressing a specific gene repertoire (Figure 19).

a) Lefty1 patterning and NODAL signaling

b) Hex positive population and BMP4 restriction

H. The implantation and building the egg cylinder

1. Preparation for the implantation

The implantation is initiating – once all the lineages are fully specified – by the hatch of the embryo out of the ZP. This acts as a checkpoint in order to verify that the embryo is ready for further development. Within the next few hours the hatched embryo invades the maternal tissues and implants into the uterine horns. While the embryo develops, increased levels of estrogen and progesterone are produced by the ovaries to synchronize the timing of uterine receptivity with the blastocyst progression[165]. More so, the levels of estrogen determine the time window by which the implantation can be started via the upregulation of "implantation genes"[165]. The regulation of estrogen can be controlled by each blastocyst via estrogen receptors at the membrane of their mural TE to postpone the implantation via the initiation of a dormant state called diapause[166,167]. This allows all

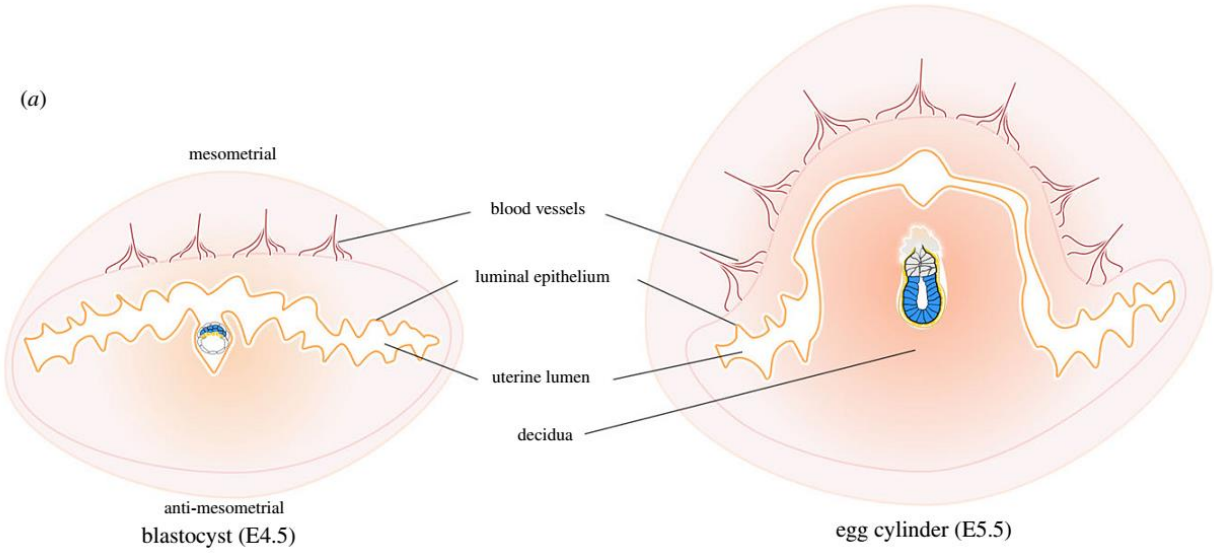

Figure 20: The implantation is concomitantly controlled by both the mother and the embryo

Bedzhov et al. 2014

After hatching, the embryo adheres to the LE and invades the stroma at the antimesometrial side of the uterus. The timing of the implantation is a resultant of the maturation of the blastocyst tissues and the estrogen signals sent by maternal tissues. During the penetration of the embryo, surrounding stromal cells differentiate into decidual cells regulating the directionality of the trophoblast invasion. Within the decidua the embryo induces massive proliferation of its cells resulting in the rapid growth of the embryo, allowed by the nutrients and gas exchanges made by decidual cells and the extra-embryonic tissues.

embryos to be implanted at the same developmental stage independently of the time spent in the uterus. This process is also taken advantaged off, in the case of embryo transfer experiments to synchronize as much as possible the developmental stages of each blastocyst[168]. Upon the initiation of the implantation, the embryos will progressively downregulate their estrogen receptor via a ubiquitin-proteasome mechanism; the completion of the degradation correlates with the termination of the uterine invasion[169] (Figure 20).

The process of implantation can be divided in three phases: apposition, attachment and penetration. During the apposition phase, the diameter of the uterus lumen becomes gradually reduced to position the floating embryo close the luminal epithelium (LE)[170]. Although, the first contact between the TE and LE is mediated by LE microvilli – responsible for grabbing and maintaining the embryo in place – it is not enough the permit its adhesion. Indeed, a glycoprotein layer of mucines covers the uterine tissue to act as a barrier for pathogens and prevents the embryo to adhere. At this step of the process maternal hormones and embryonic signal will suppress this layer allowing the embryo to be attached via a mechanism involving several adherent molecules[171,172]. Following to the penetration step, the contact between TE and LE triggers massive apoptosis at the site of attachment for the embryo to colonize the endometrial stroma[173]. This process is rapidly followed by the extensive proliferation of the surrounding stromal cells that differentiate into polyploid cells in order to form the decidua – responsible for nutrient and gas exchanges in top of immune protection[174,175]. The embryo implants at the antimesometrial side of the uterus – with the ICM pointing towards the mesometrial side – via the expansion of the TE that is directly controlled by the surrounding stromal cells[176]. The implantation process is a great example of the concomitant regulations coming from both maternal and embryonic cues (Figure 20).

2. TE differentiation and embryo implantation

Since the ICM points towards the mesometrial side, the mural TE is responsible for most of the regulation occurring during this event. Shortly after the adhesion phase, mural TE cells in contact with the LE will differentiate into trophoblast giant cells (TGC). TGC will invade in the endometrium through the directional control of decidual cells[177]. As the embryo invades deeper into maternal tissues, TGC will both secrete PROGESTERONE and type 1 INTERFERON in order to differentiate the surrounding cells, once again, and trigger the angiogenesis[178]. The local vasculature is remodeled by this process and the embryo can then grow while receiving nutrients and gas from the maternal circulatory system[172] (Figure 20).

On the other side, polar TE cells are actively differentiated by the time of the implantation to both form the ExE and the ecto-placental cone (EPC). This differentiation is initiated by the rapid increase in proliferation and the activation of the TE program, resulting in the expression or upregulation of a specific gene repertoire composed by *Cdx2*, *Eomes*, *Bmp4*, *Elf5* and *Ets2*[170]. The initiation of ExE and EPC differentiation mostly depends on EOMES activity downstream of CDX2[50]. Accordingly, genetic depletion of *Eomes* prevents any TE differentiation which in turn results in a developmental arrest at the implantation stage[50]. Interestingly, the proliferation and activation of the polar TE repertoire forms a multipotent lineage which keeps proliferating while maintaining a balance between self-renewal and EPC differentiation[170]. Indeed, the maintenance of these TE/ExE stem cells (TES) is essential for the constantly growing ExE and EPC – to attach the conceptus to a mass of differentiated TGC which mediates the early endometrial interactions[179]. During the formation of the egg cylinder at E5.0, this pool of TES is maintained in the ExE from which the EPC expansion is controlled[179].

The constant nature of this multi-potency is in part regulated by the concomitant action of the transcription factors ELF5 and ETS2[179–183]. Accordingly, the absence of either of these factors leads to the loss of the TES pool and a failure to maintain the ExE by the time of gastrulation[179–183]. Redundancies between these two factors were identified since the overexpression of ETS2 could rescue part of the *Elf5* mutant and double mutants embryos display a complete loss of the ExE by E5.5[179]. Interestingly these factors form a positive feedback loop with CDX2 and EOMES since the reduction of either protein levels lead to strong downregulation of *Eomes* and *Cdx2* and conversely[180,183].

Interestingly, the maintenance of the ExE is directly linked with the proper patterning of the adjacent Epi since ETS2 is able to maintain high level of NODAL and WNT3 – two Epi markers[179]. Reciprocally, the development and maintenance of the TES in the ExE is regulated by NODAL and FGF4 signaling that activate the core of genes described above, that culminates with the upregulation of BMP4 which in turn promotes a proper Epi patterning[160,162,184]. The EPC, on the other hand is mostly differentiated by the expression of *Mash2* expressed in TES cells by SP-1 following AKT/PI3K signaling[185–187]. Other transcription factors from the same family of MASH2 can also override FGF4 signals – essential for the TES maintenance – and promote the differentiation to the EPC[188].

1. PrE differentiation

Among the three lineages, the PrE undergoes the highest number of fate specification events, forming multiple cell populations by the time of the egg cylinder forms. Two main tissues are derived from the PrE by the time of the implantation: the VE and the PaE both contributing to the endoderm of the visceral yolk sac. The similarities between those three tissues (PrE, VE, PaE) make the reading of the differentiation quite challenging. Transcriptomic analyses of *in vitro* differentiations or more recently from the embryo itself identified specific markers that are lineage specific (i.e. *Ttr* and *Afp* for the VE; *Follistatin* and *Sparc* for the PrE)[189,190]. Tracking the expression of these genes will permit to precisely narrow the moment where a PrE cell will become a VE cell. It is however easier in the case of the PaE since it is considered that PaE cells are differentiating once they migrate distally over the mural TE[138] (Figure 21).

a) Differentiation of the VE

b) Forming the PaE layer

2. Epi morphogenesis

a) Reorganization of the Epi tissue

b) Patterning of the Epi

II. SIGNALING PATHWAYS PATTERN THE EARLY MOUSE EMBRYO

A. Active signaling pathways in a nutshell

Cell communication, via signal transduction, is essential for the proper patterning of the tissues composing the embryo. The action of signaling pathways appears to be fundamental for both spatial and temporal regulation of transcriptional and translational activities resulting in fate specification and morphogenesis. While introducing the different steps of lineage specification in the early mouse embryo we highlighted the vital nature of some of the mainstream signaling pathways; like HIPPO signaling for the first fate decision or the FGF/ERK signaling for the second specification event. Although, the main cascade pathway, following the capture of the ligand, can be drawn these days

with all the evidence available, numerous regulated factors are still being added regarding a specific process, cell-type or animal model. Indeed, even though the FGF/ERK signaling has been extensively studied in the context of Epi versus PrE fate decision the past decade, a very recent study has just elucidated a new role for a factor associated with FGF/ERK signaling[88]. Thus, the accumulation of knowledges that can fulfil blanks within the webs of signaling pathways is essential to properly understand the impact of such signals and the crosstalk they induce resulting in the establishment of more precise models concerning their action on fate specification.

1. NOTCH signaling backs HIPPO up during first cell-specification

If HIPPO signaling is at the core of TE versus ICM differentiation, another pathway has been found involved in this process; this pathway works concomitantly with HIPPO signaling to reinforce the TE identity via the transcriptional regulation of *Cdx2*. NOTCH signaling is activated by different ligands resulting in the activation and cleavage of an intracellular receptor which is translocated to the nucleus to bind transcription factors and initiate gene expression. One of these genes at preimplantation stages is *Cdx2* from which NOTCH activation allows the reinforcement of its levels during the 8-cell to 16-cell stage transition[48]. Accordingly, mutant embryos for the NOTCH associated binding sites or pharmacological inhibitions of the signaling lead to *Cdx2* downregulation albeit not sufficient to prevent TE specification[45]. Therefore, NOTCH signaling is suggested to act to maintain a fate identity that is initiated by HIPPO signaling. Recent evidence also suggested a role of NOTCH in the exit of naïve pluripotency of ESC leading to their differentiation; a process however depending mostly on FGF/ERK and ACTIVIN/NODAL signaling[48,218]. Indeed, striking phenotypic defects coming from the mutations of NOTCH signaling component are visible after the gastrulation where its overactivation leads to both impaired germ layer patterning and differentiation[225].

2. HEDGEHOG prepares the uterus for the implantation

Not much is known about HEDGEHOG (HH) signaling during the pre-implantation development of the mouse embryo. Upon receiving HH signals the constitutively inhibiting PATCH receptor releases the transmembrane protein SMOOTHEN resulting in the activation and nuclear translocation of the GLI proteins for transcriptional regulation. One of the first identified role of HH signaling in mice consisted in requirements for Indian HH for the differentiation of extra-embryonic endoderm[226]. A study also

provided evidence regarding the activity for the pathway for the proper implantation of the embryo[227]. Although, recent studies have demonstrated requirements of the signaling for oocyte maturation in different mammals it seems that it is not required in mouse oocytes and its action is restricted to either placental maturation or uterine receptivity[228–230].

3. IGF signaling redundancies play with many factors

The insulin-like growth factor family – comprises INSULIN, IGF1 and IGF2 – mediates cell responses such as apoptosis, mitosis and differentiation. IGF ligands can bind to specific binding protein (IGFBP) that regulate their availability to their respective receptors insulin receptor (IR), IGFR1 and IGFR2. Binding to those tyrosine kinase receptors activates both PI3K/AKT and MAPK cascades that, in the end, regulate transcriptional activity. The activated downstream pathway determines the cell response that depends on the activity of the cascade. While IGFR2's role is to internalize the complex IGF/IGFBP, IR and IGFR1 can either transduce their signal independently or form dimers with one another resulting in the formation of hybrids; each of them capable of transducing the signals from the three ligands but with different affinities. These redundancies between ligands and receptors make it challenging to investigate the different roles of the pathway.

Since the different KO of IGF ligands or receptor did not present any embryonic defects but size and weight reductions not much is known about IGF signaling in the early embryogenesis[231]. In the pre-implantation embryo *Igfr1* is expressed from the oocyte to the blastocyst stage[232]. While IGF1 addition to the culture media helps to proper develop the blastocyst, IGFR1 depletion resulted in cell number reduction via an increased apoptosis activity[233]. Accordingly, IGF1 signals increased the phosphorylation of AKT known to inhibit apoptotic activity[233]. PI3K/AKT is active very early in embryogenesis to promote the ZGA and the cleavages of the zygote[234,235]. Although minor, the inhibition of IGFR1 signaling was also shown to perturb mitotic spindle during the first division of the zygote[233]. mTOR is also a target in the PI3K/AKT cascade downstream of IGF signals which inhibition induce the diapause state of the blastocyst preventing tissues to mature and differentiate[167,236]. More recently, an *in vitro* study based on ESCs has demonstrated requirements for INSULIN to support naïve pluripotency via a selective increase of this population proliferation giving rise to high-contribution chimeras when transferred to pseudo-pregnant females[202]. Lastly, the antagonist effect of WNT/βCATENIN and IGF signaling was essential to allow extra-embryonic endoderm differentiation as it was suggested by IGF acting on the phosphorylation of GSK3 to prevent βCATENIN activation[206].

Therefore, IGF signaling could be involved in many specification events occurring during the formation of the blastocyst via its regulation of the several downstream pathways described.

4. BMP dynamic expression sustains cell-survival

BMP are members of the TGFβ superfamily of extracellular ligands signaling via the phosphorylation of SMAD1/5/9 through the activity of serine/threonine kinase type II (BMPRII) and I (ALK2/3/6) receptors. pSMAD1/5/9 can form a complex with the co-SMAD, SMAD4, resulting in the nuclear translocation of the complex and the transcriptional regulation of target genes. Although some SMAD can directly bind to the DNA, most of their roles consist in the activation of transcription or epigenetic factors to promote gene transcription. By its components and signal transduction mechanism BMP signaling is very closed to ACTIVIN/NODAL signaling, another TGFβ member. BMP signaling is required for the patterning, cell specification, cell proliferation and survival throughout the development of the embryo. Most of its early roles consist in the patterning of the VE and the ExE prior to gastrulation[237,238]. Since most of the genetic depletions of BMP components lead to post-implantation defects, not many studies have investigated the impact of the pathway at pre-implantation stages. Single-cell sequencing revealed however that all the components required for the pathway to be active are expressed at the morula stage with an activity of SMAD1 detected as early as at the 4-cell stage[57,119,239,240]. The early activity of BMP signaling is essential for the 16-cell to the blastocyst transition as most of the embryos inhibited for the pathway did not reach the blastocyst stage[240]. Moreover, similar to JAK/STAT3 and PDGF signaling, BMP signals are required to sustain cell-survival in the PrE layer[105].

Interestingly, as it is common for secreted growth factors, the ligands and receptors are expressed in different tissues: *Bmp1/4/7* are IC markers while *Bmpr1/2* are expressed in OC at the 16-cell stage[105]. Accordingly, *Id2* expression – a well identified target of BMP signaling – is specifically induced in the OC. From the blastocyst stage these genes present a highly dynamic expression pattern since from the mid blastocyst stage *Bmp4* and *Bmp7* are expressed in the early Epi and *Bmpr2* is in TE cells while at the implantation stage *Bmp4* is in the polar TE while *Bmpr2* is expressed in the PrE layer[57,105,144,241]. Consistent with these expression patterns, phenotypes linked with BMP signaling shut down affected the TE until E3.5 and the PrE at the late blastocyst stage[105]. Lastly, pSMAD1 activity at the late blastocyst stage is required for the specification of the DVE and probably VE differentiation from PrE cells[144,200,201]. Therefore, dynamic expression of BMP components can promote cell proliferation and survival in the proper tissue at a defined timeline.

B. ACTIVIN/NODAL signaling patterns the early mouse embryo

1. Structure of the ACTIVIN/NODAL pathway

ACTIVIN and NODAL are two TGFβ secreted factors binding to ACTIVIN receptors type I and type II. Upon fixation of the ligands the phospho-activation of the serine/threonine receptors will transduce the signal via the activation of the SMAD effectors through specific phosphorylation of their MH1 motif. Once activated, the SMAD form complexes with different factors leading to their nuclear translocation and transcriptional regulation of target genes (Figure 23).

a) Introducing the main components

b) Activity and regulation of the pathway

2. Patterning the early mouse embryo

a) Phenotypic descriptions of ACTIVIN/NODAL mutations

b) Nodal patterns the tissues of the egg cylinder

3. Dynamic expression sets the stage for embryo patterning

a) Activin expression and maternal cues

b) Mid blastocyst expresses all NODAL signaling components

c) NODAL requirements for early tissue patterning

C. WNT/βCATENIN signaling balances lineage specification

1. The canonical WNT/βCATENIN signaling pathway

a) Structure of WNT/βCATENIN signaling

b) Complexity of WNT signals

c) Transducing the signal

Most of WNT signaling components are however expressed prior to the implantation of the embryo. 10 out of the 19 WNT ligands expressed in mammals are present at the blastocyst stage, along with *Lrp5/6*, *Fzd* receptors and WNT antagonists *Sfrp* and display specific patterns and spatial distributions[466,467]. For example, *Wnt1* is specifically expressed in the ICM whilst *Wnt6* is present in the cells surrounding the blastocoel[466]. Despite the expression of these genes, the WNT/βCATENIN signaling pathway appears not to be active during the blastocyst formation. Indeed, GOF embryos at the oocyte stage did not present any nuclear localization of βCATENIN and these embryos developed correctly to the blastocyst stage[463]. Moreover, silencing the pathway did not affect preimplantation development either, albeit displaying some implantation defects[468].

In fact, several studies have highlighted the role of WNT/βCATENIN in the preparation of the uterus for the implantation and the subsequent decidualization[369,469–471]. As described previously, the success of the implantation depends on both the hormonal preparation of the receptive uterus and the proper maturation of the TE. Interestingly, *Wnt9a* is strongly expressed in the TE and the activation of βCATENIN specific genes such as *Cdx2* in both *in vivo* and *in vitro* models[471–473]. Therefore, WNT/ βCATENIN signaling could help the proper maturation of the TE to increase the efficiency of the implantation. Although, embryos mutants for *βcatenin* can still implant and form an egg cylinder this could be rescued by other factors and by maternal signals[474,475].

The earlier requirements for the transcriptional activity of βCATENIN before the implantation were identified at the implanted blastocyst stage for the activation of the PEE[70]. The dependence between PEE expression and βCATENIN activity was investigated at E6.5 during the PS formation[307]. A similar relation between these elements was found at E4.5 where embryos mutants for *βcatenin* failed to express the reporter PEE-GFP whereas *Apc* mutants presented an increase in PEE-GFP positive cells[70].

This demonstrates that βCATENIN is active in the Epi prior to the implantation. Analyses of the *Apc* mutants also revealed that a GOF of βCATENIN at this stage ectopically express mesoderm makers[461] (Figure 34).

Precisely assessing βCATENIN functions at these stages is quite challenging considering the mechanisms involved in the regulation of its activity and the signaling pathways in place. However, with the remodeling of the junctions during the blastocyst formation and the expression of epithelial markers, a specific regulation of βCATENIN could come from the membrane[16,17]. Indeed, as described previously many mechanisms of fate specification and tissue patterning are regulated by specific molecules involved at the membrane[16,17]. Therefore, βCATENIN could have an indirect role in these

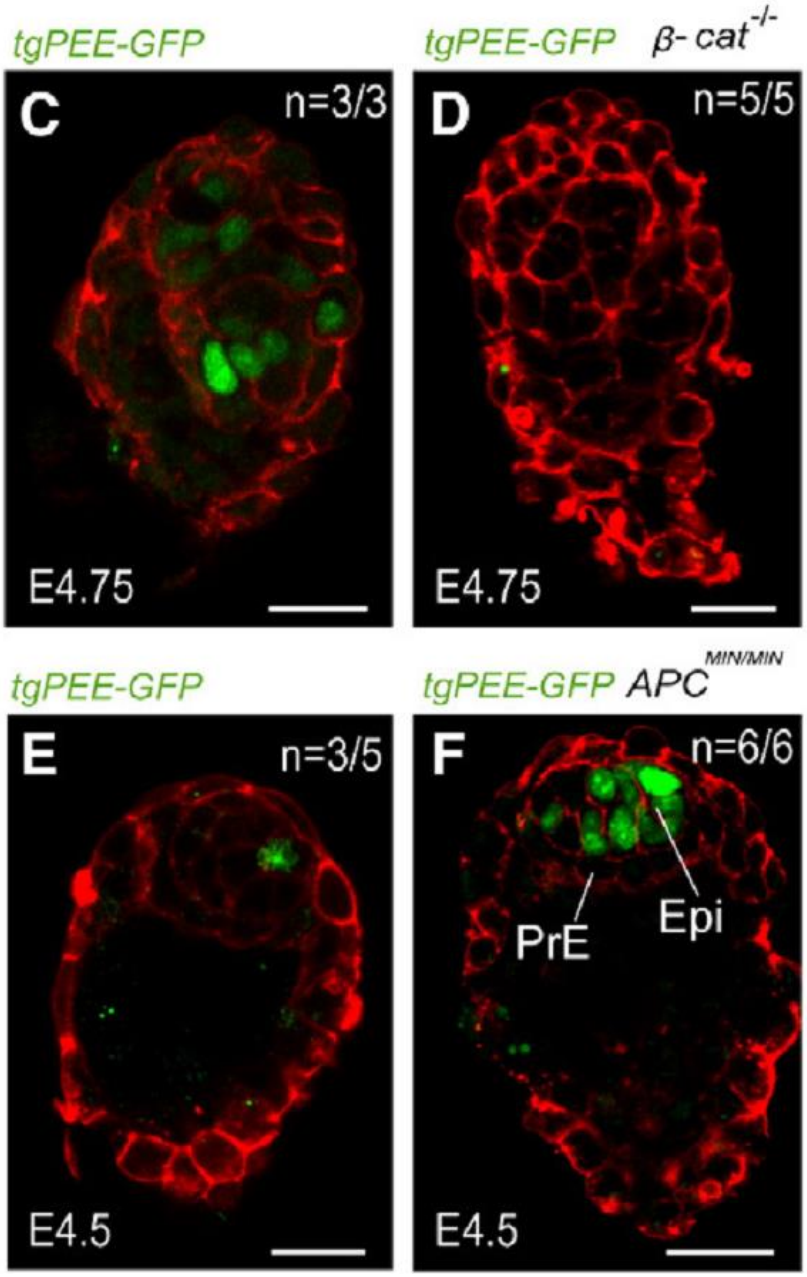

Figure 34: βCATENIN activity is found in the Epi of implanted blastocysts

Granier et al. 2011

Most of the phenotypical defects characterized in mutant embryo for *βcatenin* are observed at the egg cylinder and during gastrulation. One of the earliest roles of BCATENIN, is its regulation of the PEE of Nodal during the implantation of the blastocyst. Indeed, modulating the activity of BCATENIN directly impacts the levels of the PEE-GFP transgene. Therefore, BCATENIN is active prior to the formation of the egg cylinder and can regulate transcriptional activities within the Epi layer.

events via its interactions with these factors[471]. On the other hand, some of the main pathways (HIPPO, FGF, ACTIVIN/NODAL etc…) interacting with βCATENIN for their activity are required for

tissue patterning prior to the implantation[70,424,432]. It would thus be interesting to investigate the roles of βCATENIN in the events regulated by these pathways. Experiments conducted during the blastocyst formation however, disqualified βCATENIN in the ERK mediation of the PrE maturation[476].

III. DEVELOPING *IN VITRO* STRATEGIES TO STUDY EARLY EMBRYOGENESIS

A. Derivation of stem cells models

The study of the mouse embryo can be technically challenging considering different aspects: biological material availability, variety of tested conditions, developmental progression during culture experiments and genetic depletion. i) Indeed, although the isolation of cells from specific lineages is possible, the material provided by these few cells was not sufficient to conduct certain experiments. ii) Moreover, with the use of pharmacological inhibitors being more commonly used in laboratories, it is possible to compare different culture conditions, however limitation in terms of embryo number restricts the number of parallel conditions that can be conducted within a litter. iii) Lastly, studying a tissue at one specific developmental time point during development is in most of the case not possible considering the constant maturation of the lineage in correlation with the developmental progression of the blastocyst. Therefore, most of the conclusions from these experiments are subjected to causality-correlation conflicts. Short culture conditions and the use of time gated CRE lines can be used to counter this effect but they both present strong limitations. iv) Advances in the CRISPR technology allows the creation of several stem cell lines quite rapidly to analyze specific mutations whilst in mice although genetic depletion with the same technology is possible at the zygote stage, it is much more expensive and time consuming with restrictions in terms of line numbers. For these technical reasons among ethical considerations, stem cells models were derived to provide enough biological material, tissue specificity and control of the developmental stage.

1. Embryonic stem cells as a model for Epi maturation

By the time the ICM is fully segregated, the nascent Epi is sandwiched by two extra-embryonic lineages. The mechanisms by which this cell population emerges remains to be fully understood, even though several studies have elucidated many of the factors involved in this process. The nascent Epi will slowly acquire specific markers, indications of its maturation as the blastocyst progresses. During the implantation the Epi undergoes massive cell rearrangements and gene repertoire switch. The establishment of the germ layers is the main goal of the maturing Epi during the gastrulation. From it derives all the lineages forming the embryo proper; making the Epi the only pluripotent tissue of the mouse embryo.

For reasons described above, it is difficult to investigate the molecular mechanisms behind the acquisition of the pluripotency during the Epi maturation. To palliate in vivo difficulties and to study

the nature of pluripotency, Epi cells were derived from the late blastocyst stage and plated *in vitro* – historically on a layer of fibroblasts – in a culture media containing both BMP4 and LIF signaling molecules. These cells in culture represent the immortalized mESC, replicating the properties of the pre-implantation Epi[477,478]. Indeed, once injected in blastocysts these cells colonized preferentially the Epi without affecting the extra-embryonic lineages for the majority of stem cell lines[479]. Adaptations of the culture media were piloted to either maintain these self-renewing cells or, conversely, differentiate them into the three germ layers mimicking the gastrulation Epi[477,478]. Studies conducted in the embryo highlighted to main role of FGF/ERK signaling pathway to balance the differentiation between Epi and PrE. From these knowledges, mESC cultured in a medium composed of an ERK inhibitor and the inhibitor of GSK3 to maintain the identity of the nascent Epi[478,480]. These cells were stable and could sustain a state of pluripotency called naïve. Therefore, mESC with their close properties to Epi cells allow the investigations of molecular mechanisms involved in the maintenance of an early state pluripotency matching a specific developmental stage.

Although described as a pluripotent pool of cells the nascent Epi *in vivo* matures to its polarized version during the formation of the egg cylinder before being differentiated into any of the germ layers. Therefore, the nascent Epi forms a transient state between the ICM specification and the maturation of the competent Epi able to differentiate into both PS and neurectoderm lineages. The maturation of the Epi is an interesting process and the center of many studies conducted both *in vivo* and *in vitro*. Indeed, Epi cells at the egg cylinder stage can be derived and cultured *in vitro* into EpiSC[481,482]. EpiSC can be integrated back into the Epi of a gastrulating embryo but are not able to colonize the blastocyst, demonstrating that these cells acquire developmental and functional properties that diverge from the nascent Epi[127,482]. Moreover, the maintenance of EpiSC *in vitro* requires the activation of FGF and ACTIVIN/NODAL signaling in contrast to the BMP/LIF that are involved in mESC self-renewal[481,482]. These differences are highlighted by the clump morphology of these cells presenting more epithelial features and need to be cultured in colonies. Interestingly, once derived from human blastocysts, hESC are very similar to EpiSC[483]. This suggests that the mature Epi form the true pluripotent tissue of the mouse embryo and that the nascent Epi is specified before to trigger the formation of the egg cylinder required for the gastrulation to occur in rodents compare the disc morphology presented by other gastrulating mammal embryos.

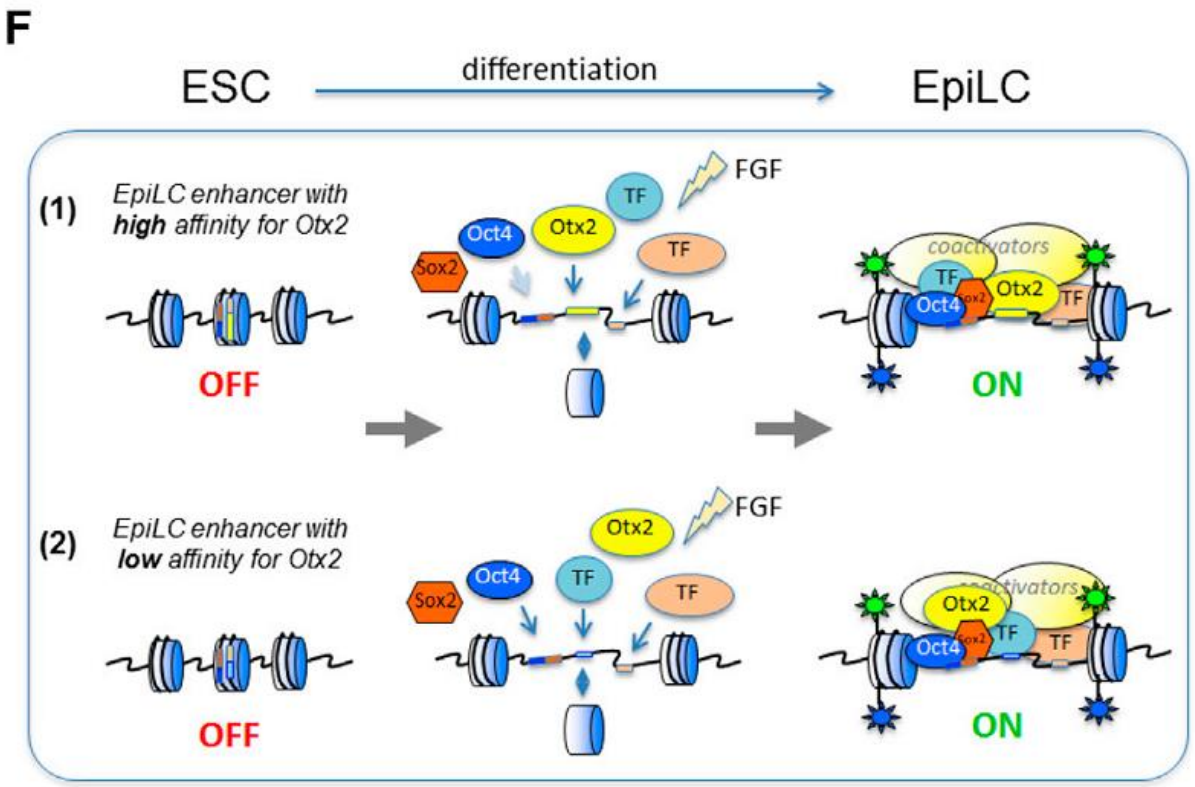

Figure 35: Enhancer switch drives the Epi maturation *in vitro*

Buecker et al. 2014

During the *in vitro* differentiation of mESC into EpiLC, mimicking the *in vivo* maturation of the Epi, cells activate of new network of pluripotency. Maintenance of the naïve pluripotency in mESC requires the expression of *Nanog*, *Pou5f1*, *Klf4*, *Tbx3* etc.… From the implantation onwards a new set of genes is expressed such as *Pou3f1*, *Esrrb*, *Otx2* etc.… This new gene repertoire encodes transcription factors able to promote the expression of specific genes associated with the maturation of the Epi. *In vitro*, the differentiation of mESC require the activity of FGF and ACTIVIN/NODAL signaling. pERK and pSMAD2/3 – the effectors of these pathways – form complexes with transcription factors to promote the activation of the new repertoire. In most of these genes their expression in EpiLC is controlled by regulative sequence with high affinity for the transcription factors involved in the primed core of pluripotency. These enhancers activation and for some genes, enhancers switch is a major tool to shut down transcription factors associated with naïve pluripotency and activate those associated with primed pluripotency.

Advances in culture conditions allowed researchers to develop in vitro conditions to induce the maturation of mESC to resemble EpiSC. These epiblast-like cells (EpiLC) are differentiating via the withdraw of the 2i medium and the addition of the FGF/ACTIVIN/knock-out serum medium[484]. Therefore, previously established mutant cell lines in mESC could now be differentiating into EpiLC to investigate the molecules involved in the maturation of the Epi. From these experiments, were identified two specific core of pluripotency factors each responsible for the respective maintenance of the naïve state and the now so-called primed pluripotency[79,80]. The downregulation of the first core and activation of the second core requires the precise regulation of transcriptional activities[79,80]. This has been identified as being depend of the specific activation and repression of genetic sequences and in some cases switches of activation between those sequences[79,80] (Figure 35).

The presence of these different states of pluripotency raises questions considering the ground state of pluripotency suggested to be shared by the Epi of mammalian embryos to control the germ layers differentiation. Derivation of ESC from different mammal models is mostly successful from the blastocyst stage. However, these ESCs do not share similar networks of gene with mESC as represented by the comparison with hESC[485]. This could be due to the necessity of the establishment of the egg cylinder in rodents prior to gastrulation that concomitantly requires the maturation of the Epi as previously mentioned. Another specificity of the mouse blastocyst is the diapause[167,236]. This development arrest occurs normally in rodents by the regulation of endometrial estrogen for the embryos to reach a similar stage of development before the implantation[167]. Self-renewal of Epi cells occurs during this period – albeit mitosis is strikingly reduced – in order to maintain the survivability of the embryo. The nascent Epi could thus be a state of ICM differentiation promoting pluripotent genes to maintain its identity while promoting its proliferation and maturation of the adjacent extra-embryonic tissues until the blastocyst implants. At this step the Epi will maturation to activate its specific network of pluripotency allowing it to differentiate into embryonic germ layers.

2. XEN cells as an advanced state of the PrE lineage

Stem cells can be derived from each tissue of the blastocyst, and the PrE does not rule this out via the establishment of the XEN stem cells[486]. XEN cells derived from the PrE can be maintained *in vitro* under serum conditions via the activation of ERK through PDGF signaling mostly[189,487]. Once injected back to the embryo, XEN cells colonize some cells in the PrE and contribute mostly to the PaE rather than the VE probably because of their interaction with the mural TE upon injections making them more susceptible to differentiate into PaE[202,486,488]. However, XEN cells can be differentiating *in vitro* into

both lineages via the addition of BMP4 and ACTIVIN[200,201,488]. Transcriptomic analyses conducted in XEN cells revealed a gene repertoire that share PrE, VE and PaE cells[189]. Notably XEN cells express *Hex* and *Dkk1* making them a powerful tool to study DVE specification[189]. Although derived from the PrE directly, XEN cells cannot be used – under the current culture conditions – to study the emergence and maturation of the PrE since they poorly contribute to this lineage defining a more advance state of differentiation[200–202,486,488].

XEN cells can be differentiated from mESC by the addition of external signaling cues that is sufficient for mESC to acquire an endoderm-like identity[489]. In fact, mESC cultured under serum conditions already express genes that are involved in the PrE repertoire such as *Gata6* and *Sox17*[108]. Accordingly, once transferred into embryonic hosts, these cells can contribute the PrE and found in the VE layer[108,461]. This suggests that, when not forced by the 2i medium, mESC resemble more to ICM cells in general than nascent Epi specifically. Consistent with what has been described *in vivo* to promote the PrE program, the activation of ERK is mandatory[489]. However, other signaling cues such as retinoic acid and ACTIVIN are required for the conversion to be initiated and the XEN identity to be maintained[489]. The transition between mESC to XEN cells can be investigated to better understand what is required to separate both Epi and PrE fates (Figure 36).

3. TE derived trophoblast stem cells

During the preimplantation embryogenesis, extra-embryonic lineages are specified prior to the Epi determination. In fact, the TE fate is the first to be acquired from OC at the compacted morula stage. The main goal of the TE is to allow the development of the embryo proper via its differentiation towards several cell types culminating with the formation of the embryonic placenta, connecting with cells derived from the PaE. Given the biological importance of the placenta and before that the implantation of the embryo and formation of extra-embryonic tissues. Studied have been conducted to establish an in vitro model ending with the formation of the immortalized trophoblast stem cell (TSC) line[490]. TSC can be maintained in culture via the addition of FGF and ACTIVIN similarly to EpiSC and can differentiate following the withdraw of these signaling molecules[490]. It is noteworthy that the derivation of TSC was not successful in human blastocysts unlike their ESC counterpart, although TS-like human cells can be converted from hESC[491,492]. Mouse TSC provide thus the only *in vitro* tool to investigate the molecular mechanisms responsible for both maintenance of identity and differentiation of the TE.

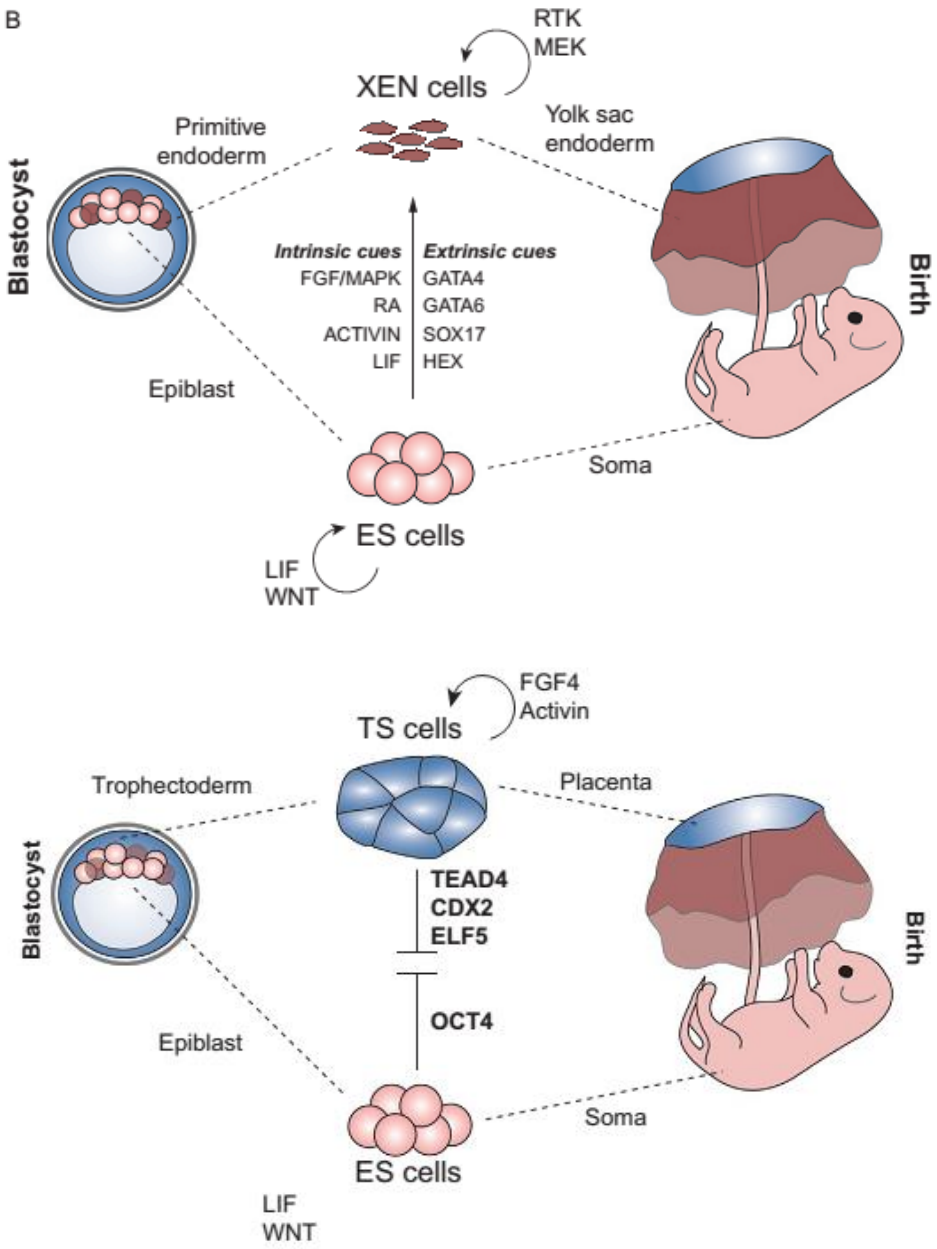

Figure 36: Stem cells can be derived from the blastocyst and interconvert fates

Watts et al. 2018

Three different stem cell types are derived from the blastocyst stage: mESC, TSC and XEN cells, respectively representing the Epi, TE and PrE derivatives. Each stem cell type can be immortalized and maintained in culture under specific conditions. LIF and βCATENIN activation with pERK inhibition maintains the pluripotency and self-renewing capabilities of mESC whereas TSC are cultured in FGF and ACTIVIN and, lastly, XEN cells are cultures in serum like conditions. Although, derived from delimitated lineages, those cell types can be interconverted in vitro if cultured with the specific cues associated with the stem cell type. Indeed, ESC to XEN cells differentiation requires the activation of FGF signaling and is supported by the activities of both retinoic acid and ACTIVIN. For TSC differentiation, conditions developed to this day require the genetic depletion of Pou5f1. Indeed, lack of OCT4 is required to activate the TSC gene repertoire composed of Cdx2, Gata3 and Tead4 mainly. A reverse differentiation is possible by the genetic ablation of Cdx2 that results in the upregulation of OCT4 and the activation of the ESC gene repertoire.

Being derived from the same developmental stage TSC and ESC are suggested to be completely distinct in terms of tissue identity. However, since totipotent stem cell lines have not been derived from pre 16-cell stage embryos, some studies attempted to differentiate ESC to TSC in order to mimic the first cell specification[49,50]. The core of the mechanisms requires the double inhibition of both CDX2 and OCT4. Indeed, both factors are required to maintain the identity of their respective stem cell line and thus imbalance in terms of expression levels of OCT4 and CDX2 is sufficient for the stem cells to acquire either ESC or TSC-like properties. The identity barrier between these two cell types can therefore be overcame to investigate the molecular events required for the acquisition and promotion of each lineage; providing more knowledges regarding the first cell fate specification (Figure 36).

B. Patterning embryonic tissues

Cells have a remarkable intrinsic ability to self-assemble and self-organize into complex and functional tissues. By taking advantage of this ability, embryoids, organoids and gastruloids have recently been generated *in vitro*, providing a unique opportunity to deeper explore complex embryological events. These self-assembly models were mostly formed through the conjoint action of physical restrictions and signaling cues applied to aggregated stem cell types. Forming these structures allows the reproduction of patterned tissues composing the embryo to properly study tissue organization and symmetry breaking events[493]. Several features occurring during the early embryogenesis were mimicked and studied *in vitro* like: lumen formation, cell sorting, cell polarization, cell epithelialization via mechanical influences and geometric confinement[493–496]. Finally, since the derivation of hESC and the application of technics developed in mESC, these self-organized structures provide a powerful tool to study the human embryology[483,495].

1. Models for symmetry breaking events

Attempts to build an *in vitro* structure that can recapitulate tissue patterning and orientation were made to properly assess the correlation between specific development processes and molecular cascades[497,498]. For that purpose, aggregates of mESC were plated *in vitro* and their arrangement assessed[220,499]. A specific structure emerged from these aggregates, cultured in a given media, forming a hollow cylinder[220,499]. The number of mESC was determinant for the viability and patterning of these structures requiring between 100 and 300 cells, corresponding the number of Epi cells by the time of

gastrulation is initiated[220]. The main interest coming from these structures is the fact that they are able to establish specific orientations and fate specifications although being composed of only mESC[500,501]. Indeed, the AP orientation was sort of mimicked by the restriction of *T/Bra* expression to one side of the structure therefore named gastruloids for their ability to form an oriented mesoderm-like pool of cells[220,500]. Similar to what has been described *in vivo* the specification and orientation of this cell population is directly regulated by the combined action of both ACTIVIN/NODAL and WNT canonical signaling[220,500].

Symmetry breaking has been of a main interest for developmental biologists. Since these gastruloids – composed solely of mESC – are forming specific axis orientations, they enter in a direct opposition of the currently established model from which extra-embryonic lineages are required to orientate the Epi. Indeed, in the embryo both VE and ExE are essential for the proper patterning of the maturing Epi[162,193]. However, although composed of mESC, gastruloids structures do not fully recapitulate the pattern of a mature Epi, becoming evident by the activation of *Cdx2* – an ExE specific gene – localized next to the *T/Bra* expression pattern[500]. As described above, mESC have a remarkable ability to differentiate and specify distinct populations upon signaling activation, which appears to be the case for the formation of the gastruloids. Indeed, the addition of external mature ligands for NODAL and WNT3 that have shown to be either processed of their expression initiated in extra-embryonic tissues is a way to bypass these tissues to activate specific genes in an oriented fashion[162,193,500]. More interestingly, is the fact that these gastruloids can be culture beyond the gastrulation-like stages where they present gene expression that resembles E9.5 gene repertoire[501]. At the end of the culture gastruloids present structures oriented multi-axially that can be useful to study the AP orientation of the forming brain tissues[501]. Thus, instead of being fully true with the developing embryo, the gastruloid model offers an interesting *in vitro* model to study symmetry breaking events occurring at different stages during mouse early embryogenesis and organogenesis.

2. Physical constraints and fate specification

During the different events of fate specification throughout early embryogenesis, mechanical cues and physical properties acted in concert to promote the activation of signaling pathways. Combined, these elements can promote tissue differentiation and their proper organization in the mouse embryo from the blastocyst to the gastrulation stages. One of the major considerations of using embryonic bodies is to correlate the activation of signaling pathways in response to diverse physical elements such as size, adhesion, cell proportions of certain fate, shape etc.… Given space to grow, embryonic bodies

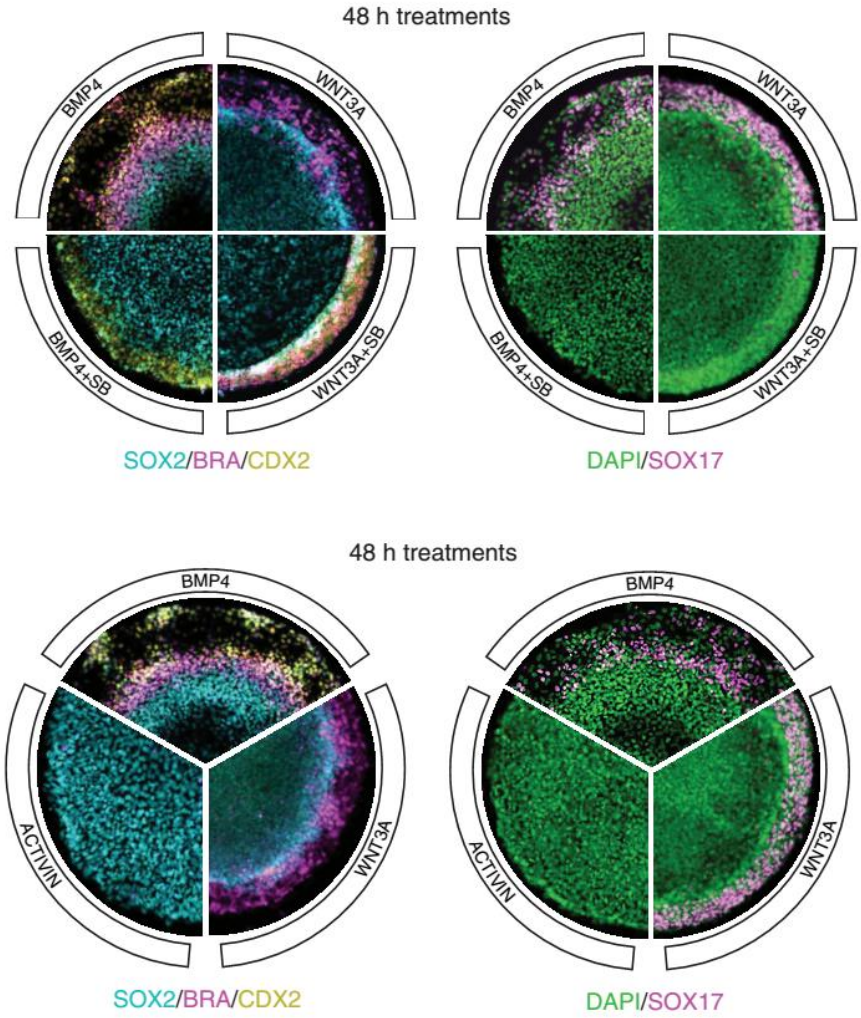

Figure 37: Cooperation between BMP, WNT and ACTIVIN/NODAL signaling can specify the gastrulation lineages of hESC

Yoney et al. 2018

In a geometrically confined environment and upon BMP treatment, hECS differentiate a radially symmetric pattern displaying markers for all gastrulation lineages. According to the proximity of BMP signals the ExE is specified in the outer layer while the ectoderm receiving the least amount of signals is specified in the inner circle. Although the pattern is established by a unidirectional gradient of BMP signals, the differentiation of the cells requires both WNT/βCATENIN and ACTIVIN/NODAL signaling to be active. Different treatments conditions revealed that WNT3A signals mostly promoted the endoderm and mesoderm layers whereas ACTIVIN differentiate all cells toward the ectoderm fate. However, the mesoderm differentiation although dependent on WNT signals requires the activity of pSMAD2/3 to be induced.

made of mESC will usually adopt a hollow sphere-like shape in order to reduce physical constrains and allow the formation of junctions between cells without affecting their shape or structure too much. However, although the mouse blastocyst presents similar shape properties, upon implantation the embryo is constrained by mechanical forces from the maternal tissues and the Epi endure these tensions from the extra-embryonic lineages. Such tensions are fully required for the gastrulation to occur properly[502].

Advances in biophysical methods allow researchers to apply mechanical constraints in their stem cell cultures. Spatially confining hESC in 2D onto submillimeter circles was made possible by the elaboration of the micropattern technology[503,504]. These circles of different sizes made by Matrigel confined cells in a physical constraint setting from the edge[503,504]. Upon application of BMP4 and adhesive molecules – forming a layer on top of which hESC are plated – hESC differentiate into a radially symmetric pattern[503,504]. The resultant pattern mimics the onset of gastrulation displaying layers of cells expressing specific makers that can differentiate them in ExE, endoderm, mesoderm and ectoderm[503,504]. These layers are differentiated according to the amount of TGFβ signals they receive starting with ExE receiving the most of BMP4 and the inner layer of ectoderm receiving the least. This is due to the formation of a single morphogen gradient with TGFβ receptors being expressed on the edge of the colony and BMP4 antagonists being express from the center in response to the signals[503,504]. The specification of cell fate depends on the response from other signaling pathways including ACTIVIN/NODAL and WNT canonical signaling[221,505]. Interestingly, adapting the diameter of the micropattern and the cell density directly affects the formation of the layers as shown with the absence of the inner layers in smaller settings[221,503–505] (Figure 37).

This technology allows the study of the human gastrulation in combination with already developed tools such as genetic engineering of hESC and pharmacological treatments. It is also a great tool to analyze the mechanisms behind secretion-diffusion properties and the impact of size, cell number and mechanical tensions to fate specification events. Further differentiation of the derived tissues has been induced to study the formation of cardiomyocytes[506]. The micropattern technology has been adapted to the mouse model more recently but displays some differences in term of the tissues derived and the conditions applied for the differentiation of the mESC[219]. This is not surprising considering the major differences between the mESC and the hESC properties as described before. The availability of this technology in mice allows the study of different features and signaling cues of the gastrulating mouse embryo, although not competent to analyze the embryo in all its complexity at these stages.

C. Forming embryo-like structures

The variety of developed *in vitro* models forms a solid base to investigate different features of the developing mouse embryo. However, none of these technics recapitulate the entire complexity of the mouse embryo. The constant communication, segregation and differentiation of cells occurring concomitantly with one other add a degree of interactions that cannot be mimicked via the isolation of specific cell populations; preventing a full understanding of the mechanisms responsible for the developmental progression of the embryo. To counter this, research teams have looked for the elaboration of technics based on embryo-derived stem cells to faithfully reproduce embryonic structures. This allows to take advantage of the stem cells engineering combined with the *in vivo* complexity and fidelity of the embryo resulting in a major breakthrough in the developmental biology field.

1. Pre-implantation blastoids

With recent advances in culture conditions, blastocyst-derived stem cell can be maintained in specific states matching developmental stages and subsequently combined to form embryonic structures. The blastocyst model with its apparent simplicity was favored *in vivo* to study fate specification from a unique progenitor cell. Since ESC and TSC were derived from this model, a team has recently been able to combined those two cell types in blastocyst-like structures they named blastoids[507]. With specific culture conditions and a precise proportion between these two cell types, ESC and TSC can aggregate resulting in the formation of a hollow sphere resembling a blastocyst[507]. These blastoids express specific makers of the three lineages composing the blastocyst and have the ability to implant upon uterus transfers[507]. However, the viability of these blastoids has not been confirmed after the implantation[507]. It is noteworthy that their developmental viability depends on the joint actions of two TGFβ signaling molecules, BMP4 and NODAL that are responsible for the expansion of the cavity and to support the TE layer[507]. This system could be used in the future to combine ESC and TSC carrying different genetic modifications in order to investigate the requirements of factors involved in the formation and maturation of the blastocyst.

2. Post-implantation ETX embryos

The ability of the mouse embryo to be cultured and developed *in vitro* is the consequence of its remarkable robustness and self-organizing properties. Pre-implantation and post-implantation embryos have been cultured *ex vivo* for many years now allowing to test the impact of external cues to the development of their tissues. However, the barrier of the implantation represents a challenge for developmental biologists and most studies investigate separately both early embryogenesis periods. This leads to the formation of uncharted territories at the edge of peri-implantations stages and the disjunctions between mechanisms involved in pre-implantation and post-implantation development. Therefore, negatively affecting our understanding of the maturation and differentiation of the blastocyst tissues. To counter these effects several culture conditions were elaborated to allow the progression of the blastocyst to the egg cylinder stages. And so, with no apparent success since no consensus was found in the utilization and on the performance of these technics.

Like the blastoid model, researchers have tried to combined stem cells derived from the blastocyst to aggregate them and allow their maturation to form a conceptus. The association between ESC and TSC cultured in a specific medium resulted in the formation of ETS embryos composed of an ExE and a matured Epi resembling embryos at the egg cylinder stage[222]. Those embryos were found to establish specific boundaries between the ExE and the Epi and the formation of a basal membrane surrounding the conceptus[222]. Moreover, upon specific signals these ETS embryos arbore a specific axial asymmetry similar to the AP orientation of the Epi during gastrulation; displayed by the posterior orientation of *T/Bra* expression[222]. A more resembling version of the mouse embryo was made shortly after via the addition of XEN cells in addition with ESC and TSC[223,224]. Different combinations of these cell populations revealed that the ETX embryos were predominant meaning that the three cell types and thus the three tissues are required to properly form the mouse egg cylinder[223,224]. Indeed, these ETX embryos fully formed a VE surrounding both Epi and ExE[223,224]. Strikingly, these embryos displayed axes orientation and expressed specific genes regulated both spatially and temporally[223,224]. This was sufficient for these structures to gastrulate and express definitive endoderm markers along with displaying typical features of an oriented mesoderm similar to a properly gastrulated embryo[223,224]. Finally, uterus transfers of ETX embryos resulted in the initiation, although with a low penetrance, of their implantation[224]. Such complex structures recapitulate the interactions between the tissues composing the embryo and their concomitant progression, characteristic of the early embryogenesis (Figure 38).

The utilization of such models can vastly contribute to our understanding of the mouse developmental biology and can be applied to the human model once the derivation and the culture of TSC and XEN cells will be possible; which, obviously raises ethical questions considering the formation of *in vitro* early human embryos…

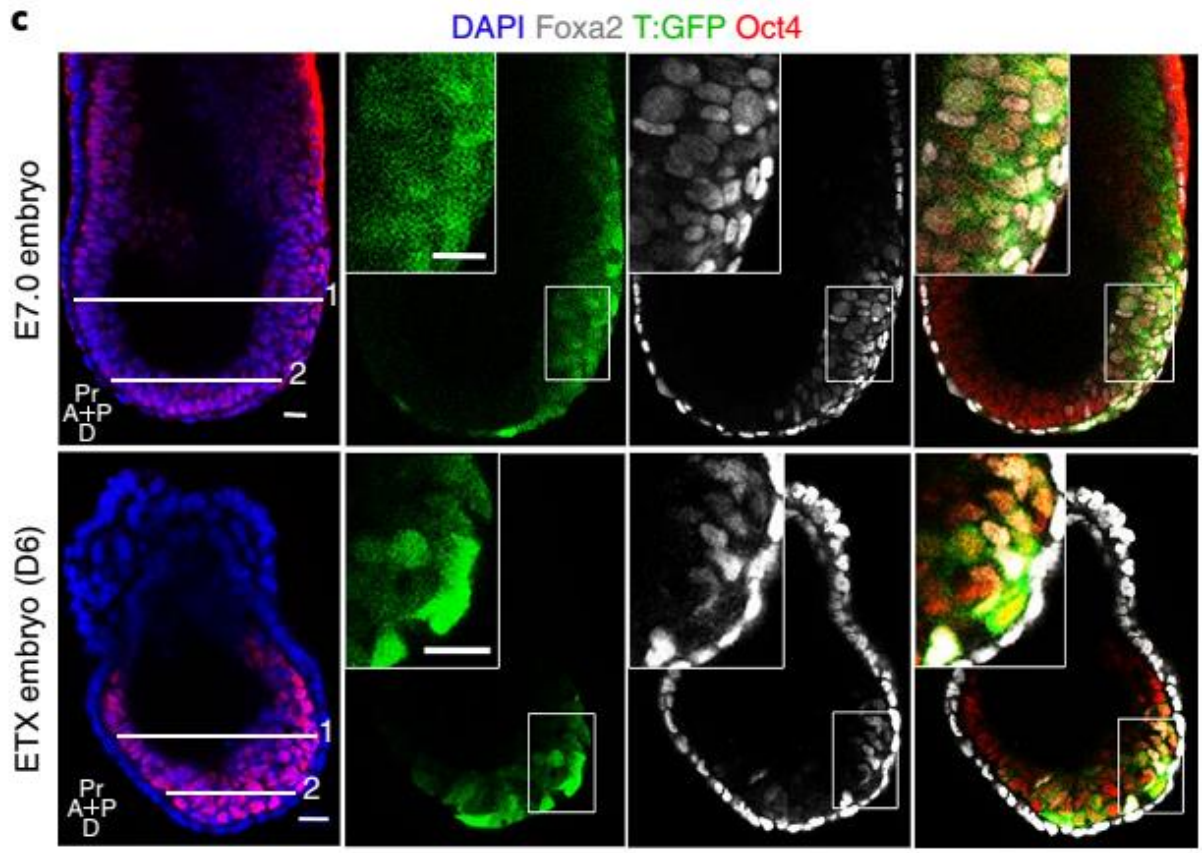

Figure 38: ETX embryos in culture can properly gastrulate

Sozen et al. 2019

The aggregation of mESC, TSC and XEN cells cultured in vitro can form embryonic structures called ETX embryos. These structures are very similar to mouse embryos at the egg cylinder stage. Presenting all three lineages at this stage, these ETX embryo also display axis orientation similar to the AP orientation of gastrulating embryos. Moreover, once cultures to day 6 posterior Epi cells from ETX embryos can undergo the EMT and migrate distally to form the PS. During this migration both endoderm and mesoderm fates are specified characteristics of the proper gastrulation of these embryonic structures.

CONTEXT

During the pre-implantation development of the mouse embryo, numerous fate specification events are associated with metabolic and structural changes to ultimately form the implanted blastocyst. The specification of cell populations is directed by a linear progression with fates being acquired from a previous progenitor and initiated according to the developmental stage of the embryo. Once specified each cell will deeply commit to its lineage via the activation of specific gene repertoires that is usually strengthened by its ability to directly inhibit the factors associated with a concurrent fate. In addition to transcriptional regulations, fate specification is accompanied by morphological and structural events. Cell polarization and cortical tensions can either restrict or promote the ability of a cell to acquire its identity. All those processes involved in the specification of the blastocyst populations are governed by the establishment and subsequent activation of signaling pathways.

Signaling pathways have the ability to transduce a signal, regulating key processes of the cell metabolism, from either external sources or from a different cell compartment. Most of these signaling molecules diffuse their message via the assemble of a molecular cascade, often found to self-regulate, ensuring the robustness of the process. During the formation of the blastocyst, several signaling pathways have been identified to drive a given fate to a competent cell. ACTIVIN/NODAL and WNT/βCATENIN are two signaling pathways required for the proper tissue patterning and axes orientation of the mouse embryo.

Most of the impacts of these signaling pathways have been characterized shortly after the implantation at the egg cylinder stages. They were found to be required for the maintenance of the Epi identity and for the proper patterning of extra-embryonic tissues. Lack of either one of these signals results in in a developmental arrest of the embryo a consequence to AP axis establishment failures and ectopic differentiation of the Epi.

Considering that both fate specification and tissue patterning depend on the completion of previous events, it is interesting to wonder whether the impacted tissues observed in mutant embryos lacking either *Nodal* or *βcatenin* are of the resultant of earlier requirements for the molecules that both genes encode. Supporting this hypothesis comes from the fact that the phenotypic defects of embryos carrying those mutations occur very shortly after the implantation, thus suggesting that prior to this, the proper patterning of the blastocyst tissues is affected.

Not much is known about pre-implantation requirements for these signaling pathways since mutant embryos for the main signal/effector can implant and present an organization resembling early egg cylinders. However, with increasing evidence showing phenotypic rescues via molecular redundancies and maternal cues, it is fair to investigate the roles of both signaling pathways during the pre-implantation development.

The main components of the signaling cascades are found expressed in the early stages of the development and in the case of *Nodal* show indications of activity. In contrast, the WNT/βCATENIN pathway does not seem to be activated at these early stages. However, βCATENIN does not depend only on WNT signals and can its activity can be induced by several mechanisms, mostly interconnected with already established signaling cascades.

Therefore, I aimed here to investigate the roles and requirements for both ACTIVIN/NODAL and βCATENIN activities in the different fate specifications that contribute to the formation and maturation of the blastocyst. For that purpose, I will use different combinations of genetic mutations and pharmacological treatments to assess the impacts of modulating the activity of both signaling pathways in the acquisition and balance of cell fates. Lineage associations and quantifications were made to precisely identify the molecular mechanism behind the phenotypic characterization.

In two distinct studies, for each signaling pathway respectively, I was able to identify specific requirements for the molecules involved in those cascades to the proper formation and maturation of the blastocyst lineages. Indeed, disrupting the activity of these two signaling pathways resulted in cell populations specification failures and profound imbalance between the lineages composing the embryo. If the study focused around ACTIVIN/NODAL reflected tissues communication processes and maternal cues requirements for the concomitant maturation of the cell populations; the second study displayed βCATENIN as an intermediate of signaling cascades to regulate tissue differentiation of the blastocyst and beyond implantation.

MATERIALS AND METHODS

Mouse husbandry and embryo collection

Mouse strains used in this study were *Nodal*$^{LacZ/+}$ [250], *Pgk*$^{Cre/+}$, *βcatenin*$^{\Delta ex2\text{-}6/+}$ [442], *βcatenin*$^{flex3/+}$ [462], *Hex*$^{GFP/+}$ [508], *Pdgfra*$^{H2B\text{-}GFP/+}$ [509], H2B-GFP$^{+/-}$ [510]. Mice were maintained on a mixed bred Swiss, 129sv/C57BL6 or CBA background under a 12h light/dark cycle according the guidelines of the Animaliance – Paris Diderot-Institut Jacques Monod guidelines. For fluorescent cassettes mice were crossed with Swiss females to either recover heterozygous or wild-type embryos. Wild-type embryos were obtained from Swiss by Swiss crosses. Embryos were collected according to the date of the vaginal plug which was considered as embryonic day 0.5 (E0.5). Pre-implantation embryos were dissected in M2 media (Sigma) their ZP removed by a short treatment of pre-warmed Tyrode's acid solution (Sigma) and then washed 2 times in M2 before being transferred in the culture media .Post-implantation embryos were dissected in DMEM/F-12 (Gibco) enriched with 5% new born calf serum (Invitrogen) their Reichert's membrane was removed using tungsten needles and fine forceps. *Nodal*$^{LacZ/LacZ}$ embryos were genotyped by nested PCR using the primers listed in Table 1. *βcatenin* mutants from both lines were genotyped as described in[442,462].

Name	Sequence	Company	Purpose
N2E-F	CACCGTCATTCCTTCTCAGGT	Eurofins	Nodal genotyping external PCR
N2E-R	CTCCCCCACAGGGTTAGGA	Eurofins	Nodal genotyping external PCR
N2I-F	TCTCAGGTCACGTTTGCCTC	Eurofins	Nodal genotyping internal PCR
N2I-R	CACCTGGAACTTGACCCTCC	Eurofins	Nodal genotyping internal PCR

Table 1 : primers used in the nested PCR to genotype Nodal$^{LacZ/LacZ}$ *embryos*

Immunostaining

For immunofluorescent staining, embryos were fixed in 4% paraformaldehyde (PFA) in PBS at room temperature (RT) for 5' (E3.25 – E4.0), 10' (E4.25, E5.0) or 15' (E5.5, E6.5) and washed three times 5' in 0.1% PBS Triton-X100 (PBX) and stored at 4°C protected from light. From this step immunostaining was performed according to different protocols depending on the antibodies used (Table 2). For multiple staining, all primary antibodies were combined in one step of primary incubation. Secondary

incubation was made using Dylight (488, 550, 650 - Thermofisher) species-specific secondary antibodies diluted 1:500. Nuclear coloration was obtained by a short incubation in Hoechst 33342 10µg/ml (Life Technologies) at the end of the protocol. Embryos were then washed in 0.1% PBX and stored at 4°C protected from light until confocal imaging.

Name	Species	Reference	Dilution	Blocking buffer
aCaspase3	rabbit	CST	1 :500	5% HS
aPKC	mouse	Santa cruz	1 :200	3% BSA
DAB2	rabbit	Abcam	1 :200	3% BSA
Ecadherin	rat	Sigma	1 :500	5% HS
Gata4	goat	Santa cruz	1 :200	5% HS
Gata6	goat	RD system	1 :200	5% HS
GFP	chicken	Abcam	1 :500	5% HS
Laminin	rabbit	Sigma	1 :200	5% HS
LRP2	rabbit	Abcam	1 :200	3% BSA
Nanog	rat	BD bioscience	1 :500	5% HS
Nanog	rabbit	Abcam	1 :500	5% HS
Oct4	mouse	Santa cruz	1 :100	5% HS
Otx2	rabbit	Abcam	1 :200	5% HS
Pecam	rabbit	Abcam	1 :500	5% HS
pHistone3	rabbit	CST	1 :500	5% HS
Sox17	goat	RD system	1 :200	5% HS
Sox2	rabbit	Milipore	1 :500	5% HS
Sox7	goat	RD system	1 :200	5% HS
Sparc	rabbit	Abcam	1 :200	5% HS
βcatenin	rabbit	Milipore	1 :500	5% HS

Table 2 : reference of all the antibodies used with their respective dilution and blocking buffer

Image acquisition and processing

Images were acquired using a Zeiss LSM780 confocal microscope and raw data were processed using ZEN Black software and ImageJ. Fixed embryos were imaged in drops of PBX on glass bottom MatTek II dishes using an EC Plan-Neofluar 40x/1.30 oil immersion objective with 1.6µm z-stacks. Multi-positionning set ups were established to keep constant parameters during the imaging of the embryos from one experiment. Fluorescence was excited with a 405-nm diode laser, 488-nm argon laser, 561-nm DPSS laser and a 633-bn HeNe laser. Brightfield and *in situ* photos of cultured embryos were taken using a Zeiss Axio observer Z.1 equipped with a CCD Zeiss HRc color camera and processed with ZEN Blue software. Time-lapse imaging was performed using a CSU-XI spinning disk head mounted on a Zeiss Axio observer Z.1 equipped with sCMOS Prime 95 (Photometrics) camera. GFP was detected with

a 514-nm Argon laser using an EC Plan-Neofluar 40x/1.30 oil immersion objective with 2µm z-stacks. Cultured embryos were scanned every 15' for indefinite cycles until they reached the correct developmental stage. Images obtained from time-lapse imaging were acquired using the Metamorph software and processed using ImageJ or Imaris. All imaged embryos, fixed or alive, were imaged in separate drops with one embryo each.

Embryo culture and treatments

Pre-implantation embryos were cultured in G2-plus (Vitrolife) medium in an incubator at 37°C with 5% CO_2. Embryos were regrouped in drops according to the culture conditions in a 35mm culture dish (TPP) covered in mineral oil (Sigma). Embryos were carefully transferred using glass capillary and a mouth pipette and positioned into the culture drop in order to avoid embryos aggregations. Culture times were defined to reach specific developmental stages. Embryos were treated in the presence of different molecules as shown in Table 3. Control conditions were made using the molecular carrier of the given molecule. The different molecules were resuspended in the indicated solvent. All recombinant proteins were purchased from Cell Guidance System and all inhibiting molecules were purchased from Sigma.

Traitement	[stock]	[final]	[intermediate]	Dilution	V G2 µl	V add µl	Solvent
SB431542	10mM	40µM	4mM	2,5	20	0,2	DMSO
CHIR9910	3mM	3µM	300µM	10	20	0,2	DMSO
CHIR9910	3mM	10µM	1mM	3	20	0,2	DMSO
Activin	20µg/ml	20ng/ml	2µg/ml	10	20	0,2	PBS/1% BSA
Fgf4	0,1mg/ml	1µg/ml		0	20	0,2	PBS/1% BSA
XAV939	5mM	5µM	500µM	10	20	0,2	DMSO
PD0325901	1mM	1µM	100µM	10	20	0,2	DMSO
Follistatin	0,1mg/ml	1µg/ml		0	20	0,2	PBS/1% BSA
Nodal	0,2mg/ml	1µg/ml	0,1mg/ml	2	20	0,2	PBS/1% BSA
Lefty	0,5mg/ml	1µg/ml	0,1mg/ml	5	20	0,2	PBS/1% BSA
BMS	10mM	10µM	1µM	10	20	0,2	DMSO
Verteporfin	2,5mM	2,5µM	250 µM	10	20	0,2	DMSO
INK128	2mM	40nM		50	20	0,4	DMSO

Table 3 : Recombinant proteins and molecular inhibitors used in embryo culture

RNA whole-mount *in situ* hybridization

RNA probes for *Nodal*, *Fgf4*, *Otx2*, *Bmp4*, *T/Bra* and *Cripto* were synthesized using *in vitro* transcription protocols with DIG labeling mix (Roche). RNA probes were purified on RNA columns and resuspended in TE10:1 (Macherey-Nagel). Whole-mount *in situ* hybridization was performed as previously described[163]. Briefly, embryos were fixed overnight in 4% PFA in PBS at 4°C, washed three times 5' in PBS, and dehydrated in Ethanol/Saline series to be stored at -20°C. Embryos were rehydrated and permeabilized 20' in RIPA solution. They were then post-fixed 20' in 0.2% glutaraldehyde/4% PFA in 0.05% PBS-Tween20 at RT, pre-hybridized in hybridization buffer for 2h at 70°C and hybridized overnight at 70°C with the denatured RNA probe (1µg/ml). After post-hybridization washes the embryos were blocked in 20% fetal bovine serum and 2% BBR (Roche) for 1h30 at RT and incubated in blocking buffer with DIG antibody 1:2000 (Roche). Staining was revealed at RT using BM purple (Roche) in PBT 0.05%.

Embryo lysis and RT-qPCR

For mRNA quantifications embryos were lysed in pools according to their culture conditions (Macherey-Nagel). The lysate was then frozen at -70°C until the RNA extraction using purification columns (Macherey-Nagel). Total RNA were purified and suspended in 10µl of water. RT enzyme and buffer were added to the suspension and incubated 10' at RT 2h at 42°C and inactivated at 85°C for 5'. qPCR was performed according to the Roche protocol of the LightCycler480 using the SyBR Green solution (Roche). cDNA concentrations were obtained according to a standard of serial dilutions made of the cDNA of all conditions. Calculations were performed by the LightCycler480 using the CPs for each primer combination. Relative expression of the genes was obtained by dividing the mean of the concentration over the mean of the *Gapdh* levels. Standard deviations were calculated using the CoVar for each primer combination (Table 4).

Name	Sequence	Name	Sequence
Apela F 4	CTCCTTGGAGCTTTGCAGAGA	Pou5f1 F	AGTTGGCGTGGAGACTTTGC
Apela R 168	GCAAGTGAACAATAGCTCTTC	Pou5f1 R	CAGGGCTTTCATGTCCTGG
Aplnr F 10	CTGTGCTGGATGCCTTACCA	Gapdh F	TTCAACAGCAACTCCCACTCTTC
Aplnr R 137	TGAGAATGGCTGATGCAGGT	Gapdh R	CCCTGTTGCTGTAGCCGTATTC
SMAD4 F	AGGTGGCCTGATCTACACAAG	Lefty2 F	CAGCCAGAATTTTCGAGAGGT
SMAD4 R	ACCCGCTCATAGTGATATGGATT	Lefty2 R	AGTGCGATTGGAGCCATCC
SMAD7 F	GACAGCTCAATTCGGACAACA	Fgf5 F	TGTACTGCAGAGTGGGCATC
SMAD7 R	CAGTGTGGCGGACTTGATGA	Fgf5 R	ACAATCCCCTGAGACACAGC
GATA6 F	CTCATCAAGCCACAGAAGCG	Nodal F	CTGTGAGGGCGAGTGTCCTA
GATA6 R	CCCTCAGCATTTCTACGCCA	Nodal R	CAGTGGCTTGGTCTTCACGG
FGF4 F	GAGGCGTGGTGAGCATCTTC	Klf4 F	GGAAGGGAGAAGACACTGCG
FGF4 R	CGGGGTACGCGTAGGATTC	Klf4 R	ATGTGAGAGAGTTCCTCACGCC
SMAD6 F	GCAACCCCTACCACTTCAGC	Cripto F	GTC TTT CCA GTT TGT GCC TTC
SMAD6 R	GTGGCTTGTACTGGTCAGGAG	Cripto R	GTT CAC AGT TGC GTC CAT AGA
T/Bra F	CCAGCTCTAAGGAACCACCG	Otx2 F	CTGTTTGCCAAGACCCGGTA
T/Bra R	ACTCCGAGGCTAGACCAGTT	Otx2 R	TGGCGGCACTTAGCTCTTC
Sox2 F	GCTCGCAGACCTACATGAAC	Pou3f1 F	TCG AGG TGG GTG TCA AAG G
Sox2 R	GCCTCGGACTTGACCACAG	Pou3f1 R	GGC GCA TAA ACG TCG TCC A

Table 4 : primers used for RT-qPCR experiments

Cell culture and aggregation chimera

mESC were cultured at 37°C in 5% CO_2 in either 2i+LIF medium[127] or in 15% FBS depending to establish chimera experimental conditions. *Nodal*$^{-/-}$ mESC were made by the depletion of the exon2 by CRISPR technology on the HM1 background. *Nodal-YFP* mESC were made as described previously described but derived on a R1 background expressing a H2B-mCherry cassette[163]. Wild-type HM1 mESC were used as control for the chimera. For the aggregation wild-type, *Nodal*$^{LacZ/LacZ}$ and *Hex*$^{GFP/+}$ E2.5 embryos were collected and their ZP removed. Embryos were positioned in small holes created in 35mm plastic culture dish by aggregation needles. Each hole contained a specific number of mESC and one embryo. Different drops containing several holes were formed to separate cell types and culture conditions. Aggregation chimera were cultured for 48h in G2-plus media as previously mentioned.

Embryo transfer

To assess the impact of the inhibitor to post-implantation tissues, E2.5 wild-type or *Hex*$^{GFP/+}$ embryos were cultured for 48h in presence or absence of SB in the culture conditions described above. Pseudo-

pregnant females were obtained by crossing Swiss females with vasectomized males. At the end of the culture, embryos were washed in M2 medium and transferred in one uterine horn. Embryos were transferred in the pseudo-pregnant females at E3.5 and dissected at E6.5 or E7.5 as described above according to the day of the plug of the pseudo-pregnant female and not according to the embryonic stage. Peudo-pregnant females were anesthetized using a solution of Ketamin/Xylazin at 15ml/100g of weight.

Quantification and post-acquisition computational analysis

Nuclei were segmented from confocal z-stack images using the algorithm MINS (Modular Interactive Nuclear Segmentation)[511] for fluorescence intensity and nuclear volume quantification. The number of VE cells was manually determined using the Cell Counter plugin on ImageJ. GFP-positive cells were tracked using the tracking spot function on Imaris software. Movies were made from TIFF file sequences produced by ImageJ and regrouped using VLC media player. All raw data coming from the different software have been analyzed through Excel and presented in clustered histograms using PrismGraphpad. Statistical analysis has been performed using different statistical tests as indicated and calculated by the matrix of PrismGraphpad: * $p<0.05$, ** $p<0.01$, *** $p<0.001$. All representing schemes were made using Adobe Illustrator, all figures were assembled using the same software.

RESULTS

NODAL Signals in the Epiblast to Ensure the Proper Development of the Blastocyst and its Derivatives

ACTIVIN/NODAL signalling is required to ensure the proper development of the blastocyst

To analyse the contribution of ACTIVIN/NODAL signalling to blastocyst development E2.5 morulas were cultured with or without the ALK4,5,7 inhibitor SB431542 (SB) for 48h. At the end of the culture SB-treated embryos were smaller than control embryos, their blastocoel cavity underdeveloped (Fig. 1a, b, c). Immunostaining that allowed the identification of Epi and PrE cells showed that SB-treated embryos failed to segregate them into separate layers. Cell counting revealed a significant deficit in total cell number, associated with a reduction in TE and PrE cell numbers (Fig. 1a, b ,c). E3.25 embryos cultured for 30h in the presence of SB presented slightly less severe versions of the same defects (Fig. S1a, d). Moreover, the percentage of embryos that reached the late blastocyst stage was strongly lowered in SB-treated embryos as shown the lower ratio of segregated ICM and the higher ration of NANOG positive embryos (Fig. S1b, c). These results showed that ACTIVIN/NODAL signalling promotes blastocyst development as soon as it is formed.

To precisely narrowed the time window of which ACTIVIN/NODAL signalling inhibition impacted developmental progression we scored the ratio of segregated ICMs in E2.5 embryos cultured for 48h and exposed to SB for different lengths of time (Fig. 1d, e, f). Only 9% of embryos that were with SB for 48h had completed their segregation against 77% for control embryos (Fig. 1d, e, f). Embryos treated with SB for 24h, regardless of whether it was in the first or the second half of the culture, reached a ratio of about 50%. In contrast, embryos that were relieved from SB exposure for the last 12 hours of the culture were almost as affected as those treated for the full 48h, while embryos exposed to SB just for these last 12h appeared unaffected (Fig. 1d/e, f). All together these observations thus revealed that ACTIVIN/NODAL signalling was continuously required for up to 36 h, from the morula stage, to ensure the proper segregation of the ICM-derived Epi and PrE layers in these conditions.

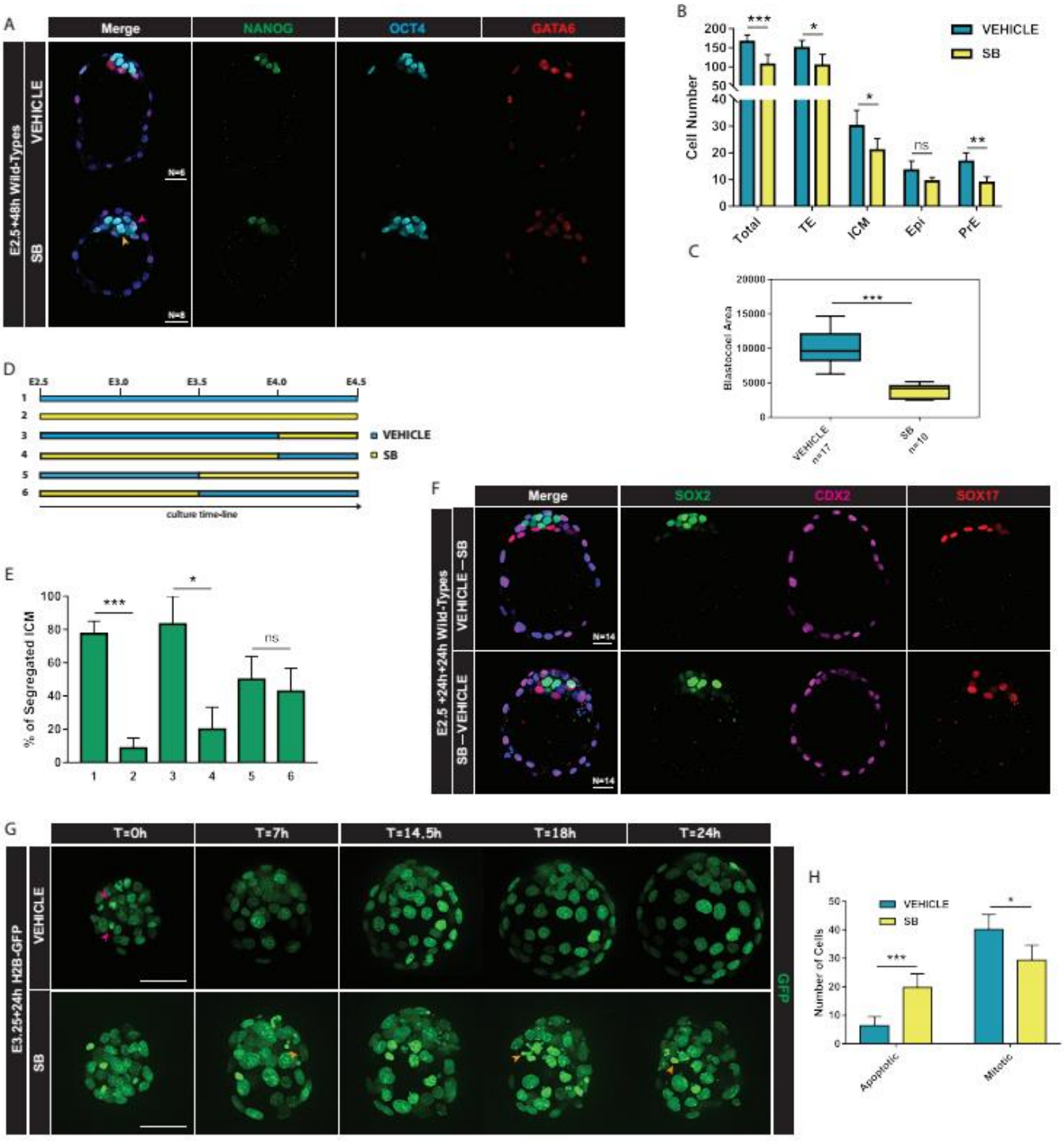

Figure 1: ACTIVIN/NODAL signaling is required to ensure the proper development of the blastocyst

A. Maximum intensity projection (MIP) of confocal images rendering the inner views (2D) of whole-mount immunostained wild-type embryos cultured from E2.5 for 48h in either control (VEHICLE) or inhibitor (SB) conditions showing inner cell mass (ICM) segregation with the labelling of its derivatives: NANOG (Epi), OCT4 (ICM), GATA6 (PrE). Magenta arrow shows non segregated PrE cell. Orange arrow shows a NANOG+;GATA6+ double positive cell. Scale bar = 20µm. **B.** Histogramm displaying the cell numbers of each tissue present at the blastocyst stage and their total cell number from the embryos cultured as described in (**A.**). Vehicle (N=11) ; SB (N=7). **C.** Box plot showing discrepancies in the blastocoel area measured in a.u. of embryos cultured in the same conditions as in (**A.**). **D.** Schematic

representation of the different culture conditions applied for the following experiments shown in (**E.**) and (**F.**). All cultured embryos shared the same starting and ending point with only the treatment duration as difference. Couple conditions (1-2 ; 3-4 ; 5-6) were processed from the same batch for a total of three distinct experiments. **E.** Histogram displaying the percentages of embryos with proper segregated ICMs at the end of each culture conditions. Row numbers represent the culture conditions explained in (**D.**)**.** 1 (N=31); 2 (N=23); 3 (N=6); 4 (N=10); 5 (N=14); 6 (N=14). **F.** MIP rendered inner views (2D) of whole-mount immunostained wild-type embryos cultured from E2.5 for 48h in the presence of the inhibitor either for the first or the last 24h labeling all tissues of the blastocyst: SO2 (Epi), CDX2 (TE), SOX17 (PrE). Scale bar = 20µm. **G.** 3D reconstruction rendered by confocal MIP of different time points from E3.25 showing the blastocyst development of embryos cultured in VEHICLE (N=5) or SB (N=5) conditions carrying the H2B-GFP transgene which labels all nuclei. Orange arrow shows apoptotic cells. Magenta arrow shows mitotic cells. Scale bar = 50µm. **H.** Histogramm displaying the total number of apoptotic and mitotic cells of the embryos during the entirety of the movies time-line for both conditions presented in (**G.**). Statistical significance is calculated using T.tests with Pvalues represented as following: *<0.05 ; **<0.01 ; ***<0.001.

ACTIVIN/NODAL signalling sustains cell-survival of the blastocyst lineages

To investigate what was affected in SB-treated embryos that lead to lower cell numbers, we performed live imaging of E2.5 transgenic embryos expressing ubiquitously the H2B-GFP nuclear fluorescent label[510] and cultured with or without SB for 48h (Fig. 1g). Analysis of these recordings detected a 3-fold increase of apoptotic cells and showed a ~30% decrease in the number of mitotic cells (Fig. 1h). Failures of ICM segregation and fewer cell numbers indicated that the PrE layer was the most affected tissue. To confirm this hypothesis the experiment was repeated using embryos harbouring a nuclear fluorescent reporter knock-in, PDGFRα::H2B-GFP[509]. This reporter is expressed in uncommitted cells but subsequently becomes restricted to PrE cells as they specify[100] (Fig. S1e). Analysis of these recordings revealed again a strong increase of apoptosis in the GFP-positive cells of SB-treated embryos (Fig. S1f). Lineage association of activated CASPASE3 positive cells revealed increased apoptosis in both the ICM and the TE of SB-treated ones (Fig. S1g, h). These increases correlated with the downregulation of the TE markers CDX2 and GATA3 and of the PDGFRα reporter – showed to reflect the activity of PDGF signalling, known to promote PrE cell survival[98] (Fig. S1i, j, k).

These results indicate that ACTIVIN/NODAL signalling promotes cell-survival in all cell layers of the blastocyst throughout its development, and suggest that SB-treated embryos have a lower cell count because they fail to compensate for increased apoptosis.

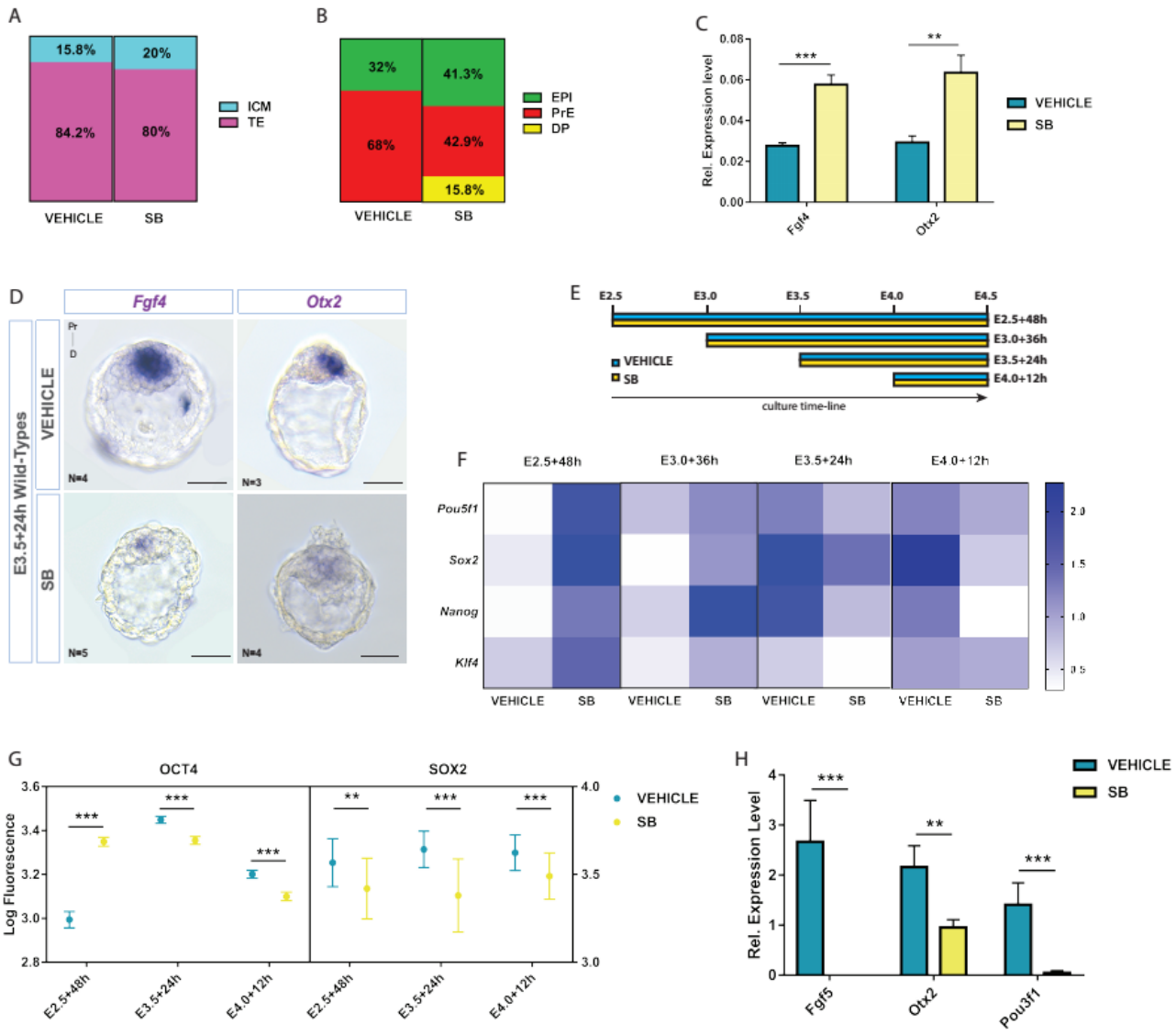

Figure 2: Lack of ACTIVIN/NODAL signalling impairs the maintenance of the Epi identity

A. Representation of the blastocyst tissue composition in percentages from the total cell numbers in the embryos shown in (**Fig. 1A.**). OCT4+ cells were counted as ICM cells while OCT4- were labeled as TE cells. B. Representation of the ICM composition in percentages from the total ICM cell numbers in the embryos shown in (**Fig. 1A.**). DP represents NANOG+/GATA6+ double positive cells. NANOG+ cells were labeled as Epi while GATA6+ cells were labeled as PrE. **C.** Histogramm displaying RT-qPCR data from whole-mount lysed E2.5 embryos cultured for 48h in control or SB conditions. Fgf4 and Otx2 relative expression were obtained after being normalized by Gapdh. **D.** WMISH for Fgf4 and Otx2 on wild-type embryos cultured from E3.5 for 24h in control or SB conditions. Scale bars = 50µm. **E.** Schematic representation of the different culture conditions applied for the following experiments shown in (**F.**) and (**G.**) All cultured embryos shared the same ending point with only the start of the culture being changed. **F.** Heatmap displaying the normalized relative expression of Pou5f1, Sox2, Nanog and Klf4 obtained from a unique RT-qPCR experiment on the embryos (N≥6) cultured in the conditions presented in (**E.**). The color scale on the right represents the normalized expression values with darker blue indicating higher enrichment of cDNAs. Each couple experiment (control/inhibitor) was conducted using embryos from the same litter for a total of 4 separated experiments for all conditions. **G.** Interleaved scatter plots showing the corrected mean ± SEM fluorescence intensity of

OCT4 and SOX2 in the Epi of embryos cultured as in E. without the E3.0 starting point. For both OCT4 and SOX2 quantifications: E2.5+48h Vehicle (n=25), SB (n=21); E3.5+24h Vehicle (n=38), SB (n=35); E2.5+48h: Vehicle (n=29), SB (n=27) embryos were used. **H.** Histogramm displaying relative gene expression from RT-qPCR data obtained after the lysis of whole-mount E4.0 embryos cultured for 12h in control or SB conditions. Statistical significance is calculated using T.tests with Pvalues represented as following: *<0.05 ; **<0.01 ; ***<0.001.

Lack of ACTIVIN/NODAL signalling impairs the maintenance of the Epi identity resulting in PrE maturation defects

Most of the studies indicate that the progression of the Epi lineage is essential for the maturation of the PrE[27] via the sequential activation of transcription factors forming the PrE program (Fig. S2a). Taking this into account we examined how ACTIVIN/NODAL signalling inhibition affected the development of both layers at different stages of development (Fig. S2b). The impact of the inhibitor on cell numbers affected the composition of the blastocyst lineages. Indeed, E2.5 embryos cultured in the presence of SB for 48h had a higher percentage of ICM cells than controls (Fig. 2a). Their ICM had a higher percentage of Epi cells than that of controls, a lower percentage of PrE cells, and still harboured nearly 16% of undetermined GATA6-NANOG double positive cells (Fig. 2b), an indication of specification failures. The upregulation of the early Epi-specific markers *Fgf4* and *Otx2* in such SB-treated embryos (Fig. 2c), was likely reflecting the over-representation of this tissue in their ICM, correlated with a higher expression of SOX17 in their PrE (Fig. S2c/d). In contrast, E3.5 embryos cultured with SB for 24h had a lower expression of GATA4 than controls in their PrE (Fig. S2e/f), associated this time with a concomitant loss of *Fgf4* and *Otx2* expression in the Epi (Fig. 2d). Lastly, embryos cultured from E4.0 with SB for 12h resulted in the complete absence of SOX7 (Fig. S2g). Taken together these results indicated that ACTIVIN/NODAL was required for the maturation of the PrE lineage to its definitive state.

Since SB treatment impacted Epi markers differently depending on the time-length of the incubation, we then characterized how added the inhibitor at different developmental stages affected its impact on Epi progression (Fig. 2e). The expression of *Pou5f1 (*OCT4*)*, *Sox2*, *Nanog*, and *Klf4*, which encode master regulators of the pluripotency network, served as a readout. We found that when the treatment started before E3.5, their expression at the end of the culture was maintained at a higher level than in control embryos (Fig. 2f) correlated with the pan-ICM expression of SOX2 (Fig. S2c), an indication that the maturation of the Epi was delayed. In contrast, when started after E3.5 the treatment resulted in the four genes being expressed at lower level, indicating that identity of the nascent Epi was prematurely extinguished. Quantification of fluorescence in individual Epi cells after

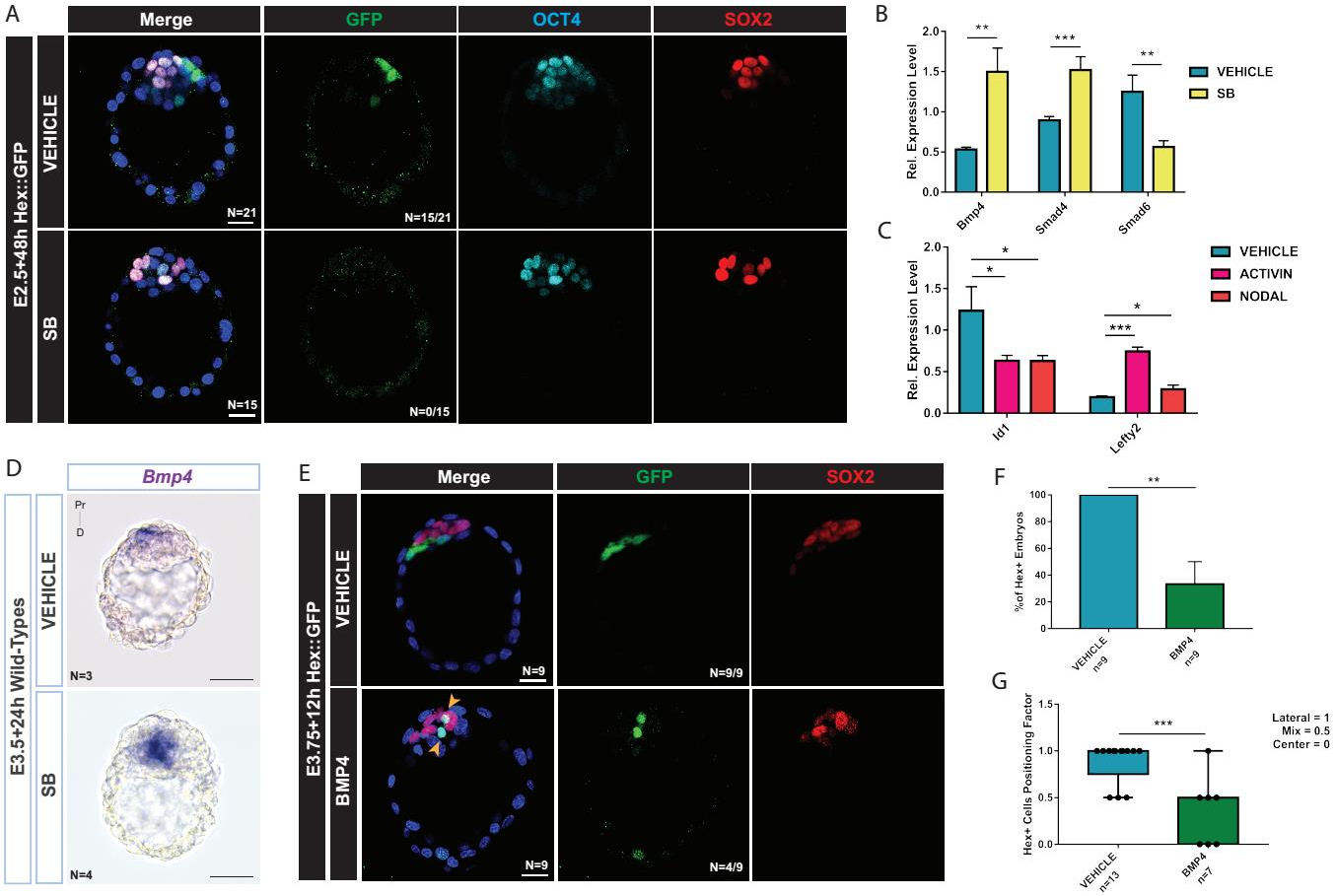

Figure 3: ACTIVIN/NODAL signalling counters BMP signals to pattern the PrE

A. Maximum intensity projection (MIP) of confocal images rendering the inner views (2D) of whole-mount immunostained embryos cultured from E2.5 for 48h in either control (VEHICLE) or inhibitor (SB) conditions and carrying the Hex::GFP transgene showing the expression pattern of Hex. N in the GFP column indicates the number of Hex-GFP+ embryos/total embryos. Scale bar = 20µm. **B.** Histogramm displaying RT-qPCR data of the BMP signaling members from whole-mount lysed E2.5 embryos cultured for 48h in control or SB conditions. Bmp4, Smad4 and Smad6 relative expression were obtained after being normalized by Gapdh. **C.** Histogramm displaying normalized RT-qPCR data for both BMP and ACTIVIN/NODAL signaling targets from embryos cultured 48h in presence of either ACTIVIN or NODAL recombinant proteins. **D.** WMISH on wild-type embryos cultured from E3.5 for 24h in control or SB conditions showing the expression pattern of Bmp4. Scale bars = 50µm. **E.** MIP rendered inner views (2D) of whole-mount immunostained Hex::GFP embryos cultured from E3.75 for 16h in either control or in presence of recombinant BMP4. N in the GFP column indicates the number of Hex-GFP+ embryos/total embryos. Orange arrows indicate GFP+ cells mixed in the ICM. Scale bar = 20µm. **F.** Histogramm displaying the percentage of embryos showing a GFP staining at the end of the culture as shown in (**E.**). **G.** Box plot showing discrepancies in Hex+ cell positioning in the ICM of the embryos cultured in (**E.**) and in (**Fig. S3E.**) conditions. Hex+ embryos were categorized according to the positions of their GFP+ cells. Embryos with GFP+ cells correctly positioned on one side of the PrE layer got a score = 1 while embryos displaying cells mixed within the ICM received a score = 0; embryos with both cell behavior were categorized as score = 0.5. Statistical significance is calculated using T.tests with Pvalues represented as following: *<0.05 ; **<0.01 ; ***<0.001.

immunodetection of OCT4 and SOX2 found differences between treated and control embryos that were consistent with the changes in gene expression seen in whole embryos (Fig. 2g). RT-qPCR measurements of *Fgf5*, *Otx2* and *Pou3f1*, which normally see their expression increase in maturing Epi cells, found missing or drastically reduced expression in E4.0 embryos cultured for just 12h in the presence of SB (Fig. 2h), confirming that their maturation was curtailed and suggesting that they were on a path to premature differentiation.

These results reveal a for ACTIVIN/NODAL signalling in the developing Epi, acting first to promote its maturation, and then maintaining its identity after E3.5. They also show that ACTIVIN/NODAL signalling is continuously required to ensure proper PrE development but suggest that much of the defects seen in the PrE are a consequence of what happens in the Epi.

ACTIVIN/NODAL signalling counters BMP signals to pattern the PrE

To study how ACTIVIN/NODAL signalling controls later aspects of PrE development we focused on its patterning and how the AP orientation is initiated. It begins before implantation, as subsets of PrE cells start to express markers distinguishing them from other cells in the layer such as *Hex*[140,343]. We found that E2.5 embryos carrying the Hex::GFP reporter transgene failed to express it when cultured for 48h in the presence of SB (Fig. 3a), a finding consistent with PrE development being stalled in these embryos. To assess if the lack of staining was a consequence of earlier defects, we cultured embryos with SB from E3.5 shortly prior to the initiation of *Hex* expression. This was enough to prevent the expression of the transgene (Fig. S3a, b). In contrast, E4.0 Hex::GFP embryos cultured in the presence of SB for just 12h all activated the transgene, implying that ACTIVIN/NODAL signalling was required for the initiation of this expression but not for its maintenance (Fig. S3c, d).

Previous work had shown that BMP ligands restricted *Hex* expression at E5.5[154]. As ACTIVIN/NODAL signalling inhibition is known to enhance BMP signalling in early mouse embryos[144,343], we wondered whether something similar underlay the lack of Hex::GFP expression in SB-treated embryos. *Bmp4* is expressed in the ICM and in the nascent epiblast but this expression is normally downregulated as the epiblast matures, while it starts to be expressed in the polar TE[352]. RT-qPCR measurements showed *Bmp4* and *Smad4* expression levels in our SB-treated embryos were 2-3 times of those in controls (Fig. 4b), while the expression of *Smad6*, which encodes a potent inhibitor of BMP signalling, was strongly reduced, changes all conducive to higher BMP signalling levels. In contrast, wildtype embryos cultured in the presence of ACTIVIN or NODAL saw a two-fold decrease in the expression of *Id1* (Fig. 4c), a target

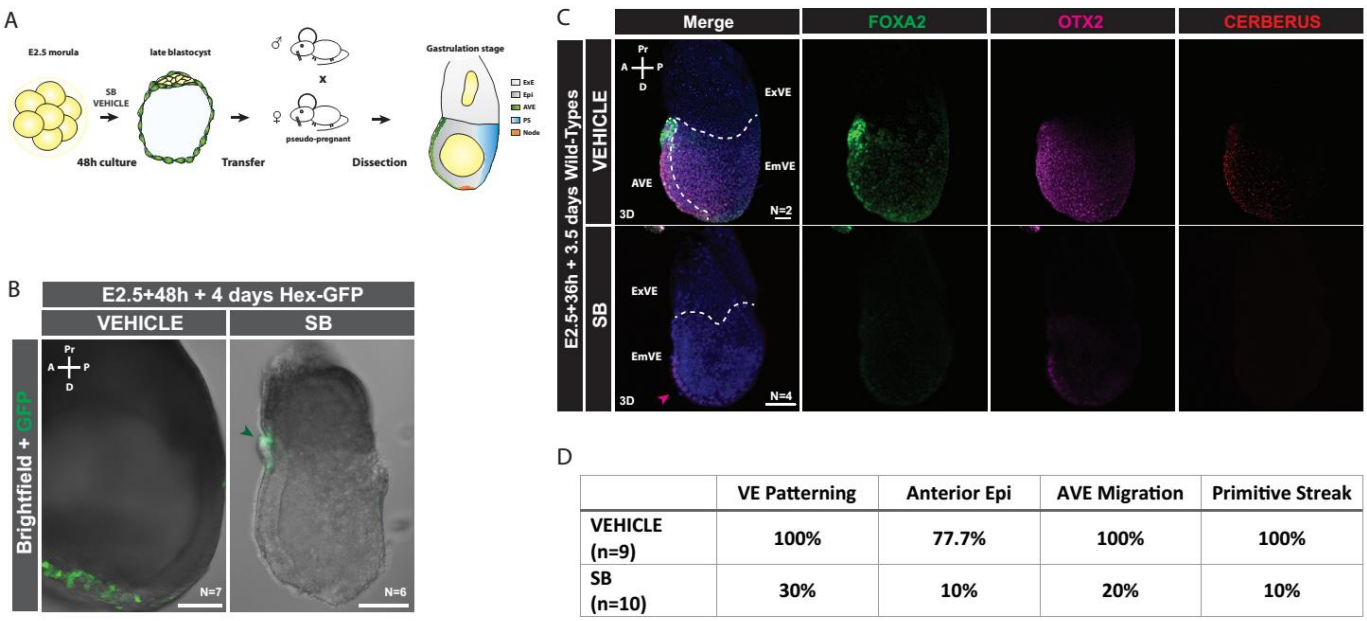

	VE Patterning	Anterior Epi	AVE Migration	Primitive Streak
VEHICLE (n=9)	100%	77.7%	100%	100%
SB (n=10)	30%	10%	20%	10%

Figure 4: Inhibition of ACTIVIN/NODAL signalling impairs the development of the blastocyst derivatives

A. Schematic representation of the experimental design where wild-type or *Hex*::GFP embryos were cultured for 48h from E2.5 and transferred into pseudo-pregnant mice and analyzed at either E6.5 or E7.5 during gastrulation. **B.** MIP rendered inner views (2D) of whole-mount immunostained *Hex*::GFP embryos cultured as explained in (**A.**) and dissected at E7.5 labelling the global morphology of the embryo in brightfield and the *Hex* expression pattern – marker of the anterior visceral endoderm – with an antibody against the GFP. Green arrow shows the disturbed expression of *Hex* in SB treated embryos. Scale bar = 50µm. **C.** MIP of confocal images rendering the surface (3D) of whole-mount immunostained wild-type embryos cultured as explained in (**A.**) and dissected at E6.5 labelling the embryonic visceral endoderm, endoderm, anterior Epi (FOXA2; OTX2) and anterior visceral endoderm (CERBERUS). Magenta arrow shows a deem staining of OTX2 in the embryonic visceral endoderm. Scale bar = 50µm. **D.** Table showing the percentage of embryos with the indicated affected feature from the analyzed embryos from both (**B.**) and (**C.**). These percentages were obtained through the ration of embryos displaying either lack of staining or a misplaced pattern over the total number of embryos analyzed for each condition.

of BMP signalling, while the expression of *Lefty2*, a target of ACTIVIN/NODAL signalling, showed expected increases. These results confirmed that at this stage ACTIVIN/NODAL signalling acts to keep BMP signalling in check.

Since the proximity with BMP ligands was responsible for turning Hex expression off we investigated the expression pattern of *Bmp4* in embryos lacking ACTIVIN/NODAL activity. Embryos cultured from E3.5 in presence of SB for 24h hours resulted in the aberrant persistence of *Bmp4* expression in the epiblast of these embryos (Fig. 3d). We then tested whether excessive or prolonged BMP signalling was the cause of the defective Hex::GFP expression seen in SB-treated embryos. Culture of E3.75 Hex::GFP embryos in the presence of recombinant BMP4 resulted in a drastic reduction in the ratio of fluorescent embryos and in the number of fluorescent cells they harboured (Fig. 3e, f, g – Fig. S3e), confirming that the number of Hex::GFP-expressing PrE cells is at least in part determined by the antagonistic action of BMP signals on ACTIVIN/NODAL signalling. Moreover, BMP4 treatments affected the pattern of Hex::GFP preventing expressing cells to become polarized to the lateral side of the embryo (Fig. 3e, g). These defects were attenuated when the embryos were cultured for 48h suggesting a rescuing mechanics (Fig. S3f, g).

However, the impact of BMP treatment on the formation of Hex::GFP-positive cells in the PrE was never as drastic as that of SB treatment. These results indicate that ACTIVIN/NODAL signalling is required for the specification of *Hex*-positive cells concomitantly to the inhibition of BMP signalling ensuring the proper pattern of the PrE.

Inhibition of ACTIVIN/NODAL signalling impairs the development of the blastocyst derivatives

With all the defects to the blastocyst development induced by the lack of ACTIVIN/NODAL signalling we wanted to investigate if those embryos could develop beyond the implantation as suggested by the phenotypes of embryos carrying the double mutations for Smad2/3[306]. To assess whether this was the case E2.5 embryos cultured for 36 or 48h in the presence or absence of SB were transferred in pseudo-pregnant females, and collected 3.5 or 4 days later for analysis (Fig. 4a). Although, SB-treated embryos were able to implant and to develop into egg-cylinders, their anterior orientation was not properly established as shown by the pattern of Hex::GFP that usually layers the anterior visceral endoderm (AVE) (Fig. 4b). Moreover, SB-treated embryos presented tissue morphological defects resulting in their smaller size compared to those of the controls (Fig. 4b). Immunostaining for an array of markers showed that the development of both PrE and Epi derivatives was defective. A majority of SB-treated

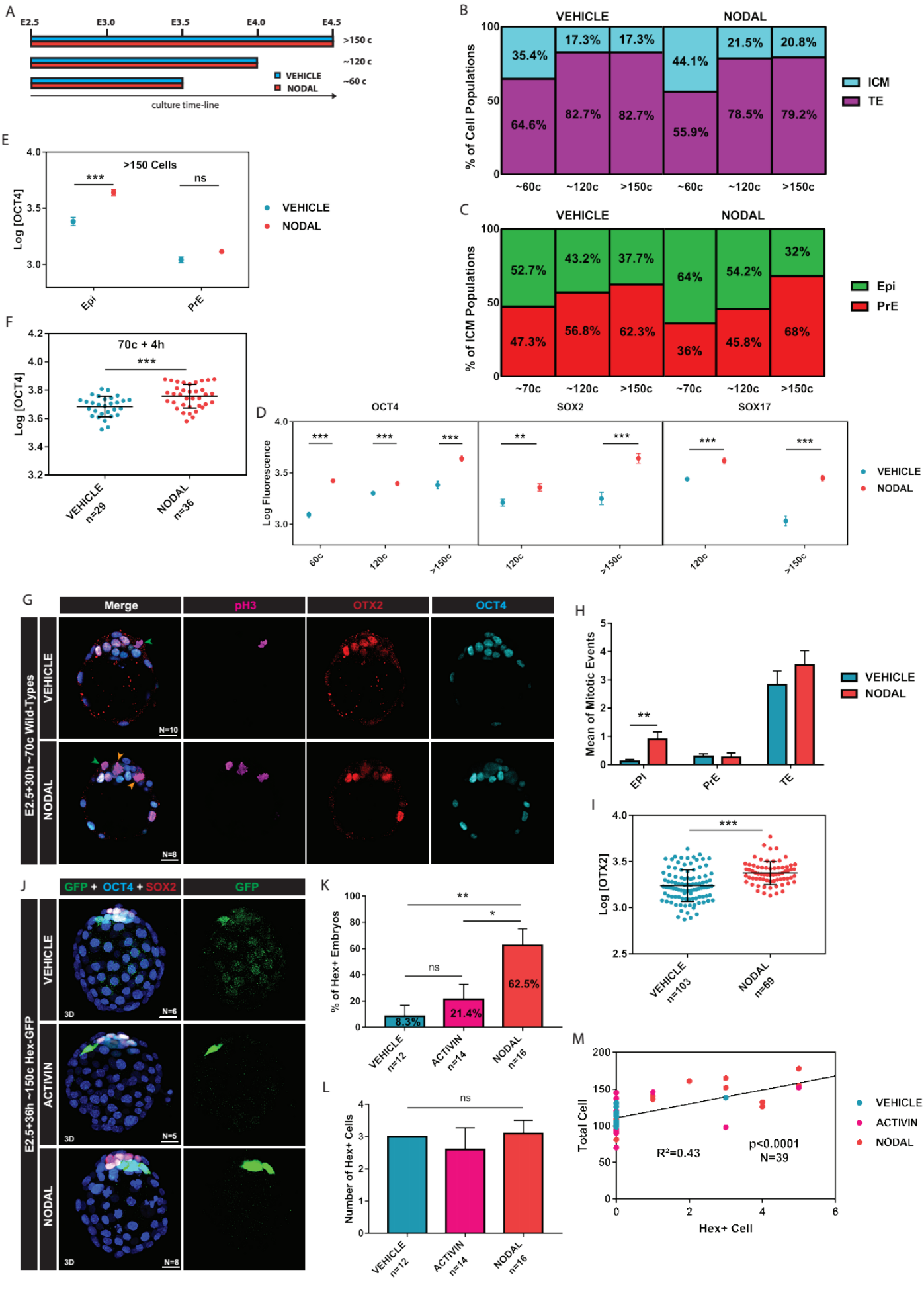
A
E2.5
E3.0
E3.5
E4.0
E4.5
>150 c
~120 c
~60 c
VEHICLE
NODAL
culture time-line
B
VEHICLE
NODAL
% of Cell Populations
35.4%
64.6%
17.3%
82.7%
17.3%
82.7%
44.1%
55.9%
21.5%
78.5%
20.8%
79.2%
~60c
~120c
>150c
~60c
~120c
>150c
ICM
TE
C
VEHICLE
NODAL
% of ICM Populations
52.7%
47.3%
43.2%
56.8%
37.7%
62.3%
64%
36%
54.2%
45.8%
32%
68%
~70c
~120c
>150c
~70c
~120c
>150c
Epi
PrE
D
OCT4
SOX2
SOX17
Log Fluorescence
60c
120c
>150c
120c
>150c
120c
>150c
VEHICLE
NODAL
E
>150 Cells
Log [OCT4]
***
ns
Epi
PrE
VEHICLE
NODAL
F
70c + 4h
Log [OCT4]
***
VEHICLE n=29
NODAL n=36
G
Merge
pH3
OTX2
OCT4
E2.5+30h ~70c Wild-Types
VEHICLE
NODAL
N=10
N=8
H
Mean of Mitotic Events
**
EPI
PrE
TE
VEHICLE
NODAL
I
Log [OTX2]
***
VEHICLE n=103
NODAL n=69
J
GFP + OCT4 + SOX2
GFP
E2.5+36h ~150c Hex-GFP
VEHICLE
ACTIVIN
NODAL
3D
N=6
N=5
N=8
K
% of Hex+ Embryos
**
*
ns
8.3%
21.4%
62.5%
VEHICLE n=12
ACTIVIN n=14
NODAL n=16
L
Number of Hex+ Cells
ns
VEHICLE n=12
ACTIVIN n=14
NODAL n=16
M
Total Cell
R²=0.43
p<0.0001
N=39
Hex+ Cell
VEHICLE
ACTIVIN
NODAL

Figure 5: NODAL signals in Epi cells to promote the whole ICM maturation

A. Schematic representation of the different culture conditions with or without recombinant NODAL applied for the following experiments shown in (**Fig. 5, S4**). All cultured embryos shared the same starting point with only the end of the culture being changed. Each ending time point corresponds to an approximative total cell number obtained after nuclear segmentation of each embryo which was then categorized in the three categories. **B.** Representation of the blastocyst tissue composition in percentages from the total cell numbers in the embryos shown in (**Fig S4**) for each condition presented in (**A.**). OCT4+ cells were counted as ICM cells while OCT4- were labeled as TE cells. **C.** Representation of the ICM composition in percentages from the total ICM cell numbers in the embryos shown in (**Fig. S4**) for each condition presented in (**A.**). SOX2+;SOX17- cells were labeled as Epi while SOX17+ cells were labeled as PrE. **D.** Interleaved scatter plots showing the corrected mean ± SEM fluorescence intensity of OCT4, SOX2 in the Epi and SOX17 in the PrE of embryos cultured as in (**A.**) without the ~60 cells point for the last two since the Epi and PrE are not fully specified yet. OCT4 is quantified in all ICM cell at ~60 cells then only in the Epi for both ~120 and ~150 cells. **E.** Interleaved scatter plots showing the corrected mean ± SEM fluorescence intensity of OCT4 in the Epi or PrE of embryos cultured to the >150 cells stage in presence (N=8) or absence (N=6) of recombinant NODAL. **F.** Scatter plots showing the corrected OCT4 fluorescence intensity of each nuclei in the embryos cultured from the ~70 cells stage for 4 hours without (N=3) or with (N=3) recombinant NODAL. n represents the number of nuclei used in this quantification. **G.** MIP rendered inner views (2D) of whole-mount wild-type E2.5 embryos immunostained against phosphoHistone3 at the end stage of 30h culture without or with recombinant NODAL. Orange arrows show mitotic Epi cells colocalizing pH3 and OTX2. Green arrows show mitotic TE cells as they are OCT4 negative. Scale bar = 20µm. **H.** Histogramm displaying the number of mitotic events per cell population in each embryo cultured in the conditions described in **I.** Scatter plots showing the corrected OTX2 fluorescence intensity of each nuclei in the embryos cultured from the ~70 cells stage for 4 hours without (N=10) or with (N=8) recombinant NODAL. n represents the number of nuclei used in this quantification. **J.** MIP of confocal images rendering the surface (3D) of whole-mount immunostained *Hex*::GFP embryos cultured from E2.5 for 36h until they reach a cell number of ~150 cells in either control condition or in presence of recombinant ACTIVIN or NODAL. **K.** Histogramm displaying the percentage of embryos showing a GFP staining at the end of the culture as shown in (**J.**). **L.** Histogramm displaying the number of Hex+ cells in each embryo cultured as shown in (**J.**). **M.** Correlation plot between the total cell number of each embryo and its GFP+ cells at the end of the culture described in (**J.**). The linear regression was calculated from a X,Y table showing the best fit ±SE. The pearson correlation factor of r=0.6517 for a R^2= 0.4247 shows a significant correlation for the 39 pairs analyzed with a Pvalue<0.0001. The three different treatments are colored coded in the plot with one dot equals one embryo. Three different experiments using the same conditions were conducted and the embryos pooled for statistical significance. Besides the correlation plot as mentioned above, statistical significance is calculated using T.tests with Pvalues represented as following: *<0.05 ; **<0.01 ; ***<0.001.

embryos had failed to pattern their VE properly and to form a primitive streak reflecting a failure to establish the anterior-posterior axis (Fig. 4c, d).

The failure of SB-treated embryos to develop normally after implantation, even though signals during the implantation overcame their failure to segregate Epi and PrE cells, showed that most of the tissue patterning defects finds its origin at pre-implantation stages.

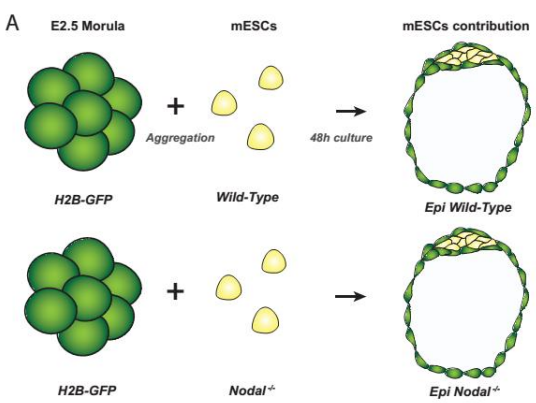

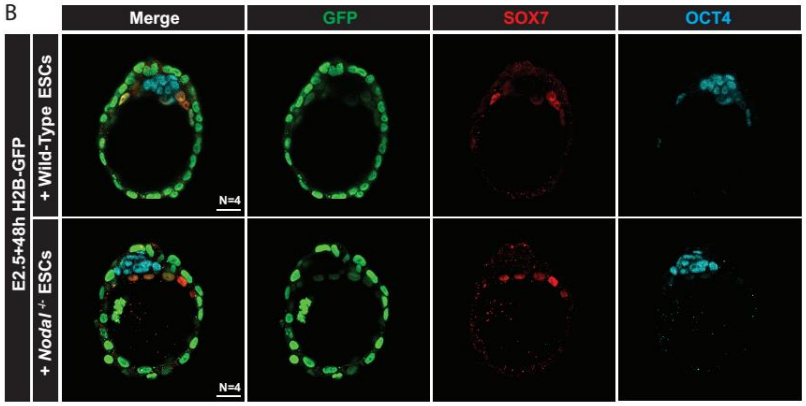

C

E2.5+48h in VEHICLE	Epi Contribution	PrE Contribution	Segregated ICM
+Wild-Type ESCs (n=6)	100%	0%	100%
+Nodal$^{-/-}$ ESCs (n=11)	99.25%	0%	100%

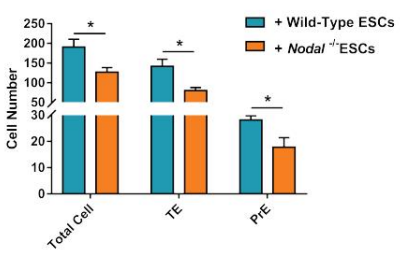

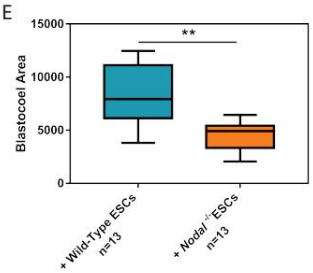

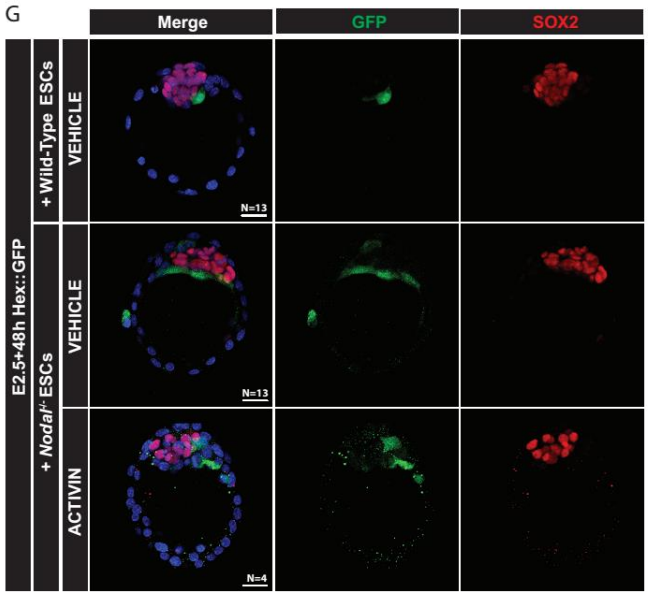

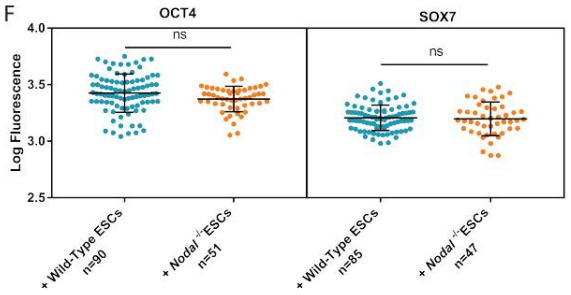

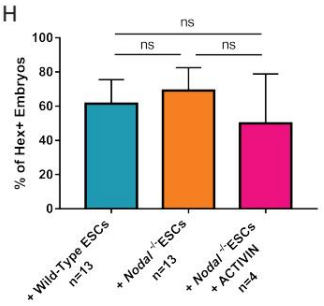

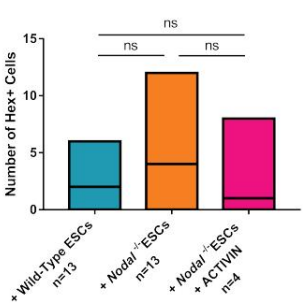

J

E2.5+48h in VEHICLE	4-6 Cells n=3	6-8 Cells n=10	12-16 Cells n=8	>22 Cells n=2
% of Embryos with a PrE Layer	100%	100%	100%	0%

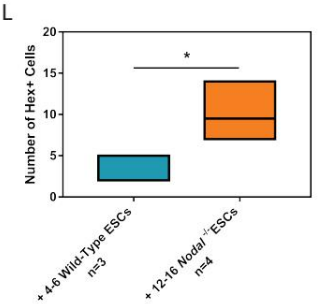

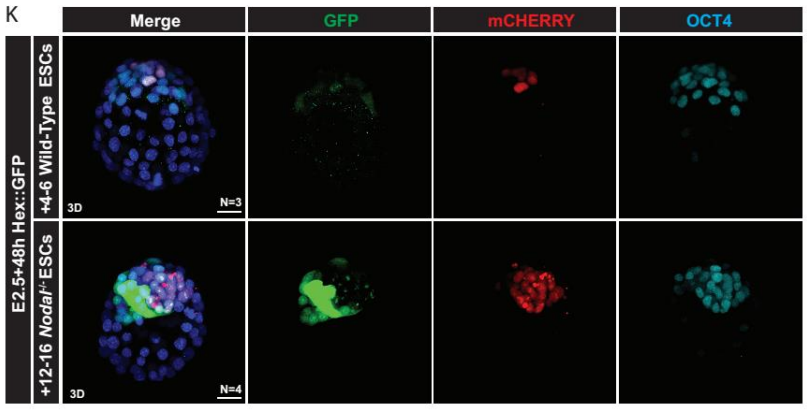

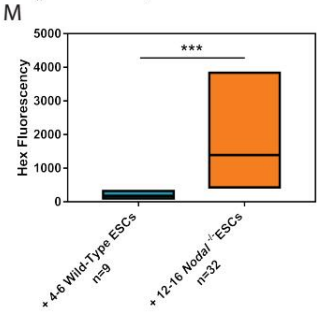

Figure 6: The initial Nodal expression in the PrE is sufficient to drive ICM maturation

A. Schematic representation of the experimental design where wild-type, H2B-GFP or *Hex*::GFP E2.5 embryos were dissected and aggregated with either wild-type, *Nodal*$^{-/-}$ or Nodal::YFP embryonic stem cells (ESCs). Then the newly formed chimeras were cultured for 48h in either control or with ACTIVIN or NODAL. **B.** MIP rendered inner views (2D) of whole-mount immunostained H2B-GFP chimeras aggregated with either wild-types or *Nodal*$^{-/-}$ ESCs and cultured 48h, showing Epi only colonization of the ESCs and the patterning of both ICM (OCT4) and PrE (SOX7). **C.** Table summarizing the tissue contribution for both wild-type and *Nodal*$^{-/-}$ ESCs after the aggregation and the percentage of correctly segregated ICMs; This table was obtained by pooling the results of two different experiments led in a similar manner. **D.** Histogramm displaying the cell numbers of TE, PrE and their total cell number from the embryos aggregated with wild-type (N=6) or *Nodal*$^{-/-}$ (N=6) ESCs as described in (**B.**). **E.** Box plot showing discrepancies in the blastocoel area measured in a.u. of embryos cultured in the same conditions as in (**B.**). **F.** Interleaved scatter plots showing the corrected mean ± SEM fluorescence intensity of OCT4 in the Epi and SOX7 of embryos cultured as in (**B.**). For OCT4: wild-type ESCs (N=6), *Nodal*$^{-/-}$ ESCs (N=3) and SOX7: wild-type ESCs (N=6), Nodal$^{-/-}$ ESCs (N=6). **G.** MIP rendered inner views (2D) of whole-mount immunostained *Hex*::GFP chimeras aggregated with either wild-types or *Nodal*$^{-/-}$ ESCs and cultured 48h in control or ACTIVIN in the case *Nodal*$^{-/-}$ aggregated embryos. The *Hex*::GFP expression pattern is shown using an anti-GFP antibody. **H.** Histogramm displaying the percentage of embryos showing a GFP staining at the end of the culture as shown in (**G.**). **I.** Histogramm displaying the number of GFP+ cells in each embryo cultured as shown in (**G.**) **J.** Table summarizing the percentage of embryos with a PrE layer depending on the number of wild-types ESCs aggregated. **K.** MIP rendered surface views (3D) of whole-mount immunostained *Hex*::GFP chimeras aggregated with either 4-6 wild-types or 12-16 *Nodal*$^{-/-}$ ESCs and cultured 48h. The *Hex*::GFP expression pattern is shown using an anti-GFP antibody. **L.** Histogramm displaying the number of GFP+ cells in each embryo cultured as shown in K. Box plot showing the fluorescence of the GFP in *Hex*+ cells in embryos cultured as described in **K.** Scale bars = 20µm. Statistical significance is calculated using T.tests with Pvalues represented as following: *<0.05 ; **<0.01 ; ***<0.001.

NODAL signals in Epi cells to promote the whole ICM maturation

The suggestion that ACTIVIN/NODAL signalling inhibition affected PrE development in correlation with its impact on Epi, raised the question of how the embryo responded to either of these two ligands. Since, both are present in the embryo at these stages, we wanted to address the respective impacts of these molecules on the phenotypes we characterized[352].

To find out whether this was the case we cultured wild-type morulas in the presence of recombinant NODAL for 24, 36 and 48h, until they reached a specific stage (Fig. 5a), and analysed how it affected cell lineage allocation in the resulting blastocysts (Fig. S4.1a, b, c, d, e, f). All NODAL-treated embryos showed gains in the percentage of ICM cells (Fig. 5b, c). In ~60 and ~120 cell-stage embryos the higher percentage of ICM cells resulted from an increase in the number of Epi cells while the number of PrE cells was no different than in controls (Fig. 5b, c). However, the percentage of PrE cells was strongly increased in >150 cell-stage NODAL-treated embryos, displaying a belated acceleration of the pace of proliferation in this lineage. The dynamics of the ratios of Epi and PrE cells in NODAL-treated embryos

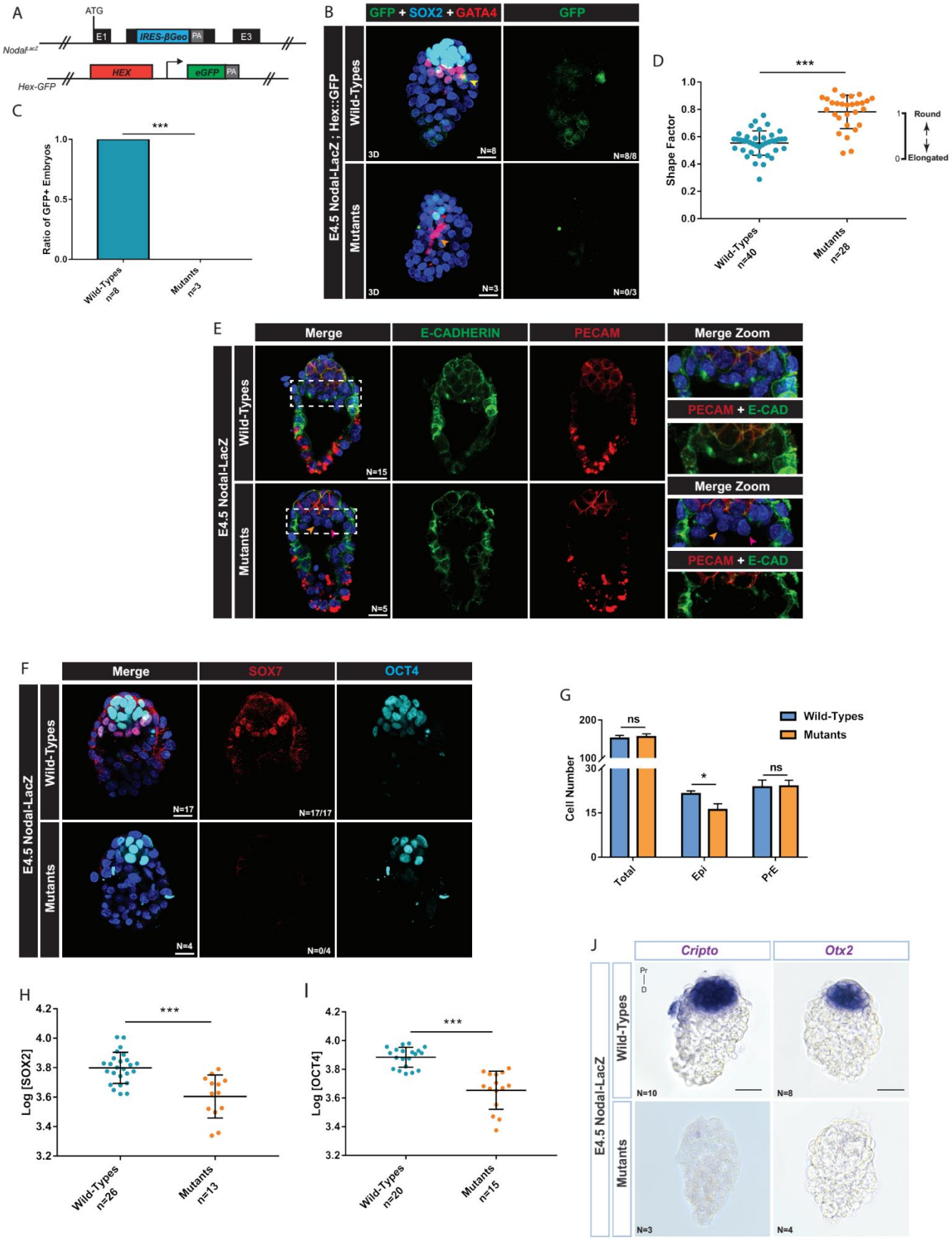
A
ATG
E1
IRES-βGeo
PA
E3
Nodal lacz
HEX
eGFP
PA
Hex-GFP
B
GFP + SOX2 + GATA4
GFP
E4.5 Nodal-LacZ ; Hex::GFP
Wild-Types
Mutants
3D
N=8
N=8/8
3D
N=3
N=0/3
C
***
Ratio of GFP+ Embryos
1.0
0.5
0.0
Wild-Types n=8
Mutants n=3
D
***
Shape Factor
1.0
0.8
0.6
0.4
0.2
0.0
Wild-Types n=40
Mutants n=28
1
Round
0
Elongated
E
Merge
E-CADHERIN
PECAM
Merge Zoom
E4.5 Nodal-LacZ
Wild-Types
Mutants
N=15
N=5
PECAM + E-CAD
Merge Zoom
PECAM + E-CAD
F
Merge
SOX7
OCT4
E4.5 Nodal-LacZ
Wild-Types
Mutants
N=17
N=17/17
N=4
N=0/4
G
Wild-Types
Mutants
Cell Number
200
100
30
15
0
ns
*
ns
Total
Epi
PrE
H
***
Log [SOX2]
4.2
4.0
3.8
3.6
3.4
3.2
Wild-Types n=26
Mutants n=13
I
***
Log [OCT4]
4.2
4.0
3.8
3.6
3.4
3.2
Wild-Types n=20
Mutants n=15
J
Cripto
Otx2
E4.5 Nodal-LacZ
Wild-Types
Mutants
Pr
D
N=10
N=8
N=3
N=4

Figure 7: Zygotic NODAL is essential for late PrE and Epi patterning

A. Schematic representation of the formation of the Nodal-LacZ ; Hex::GFP mouse line. Nodal-LacZ KiHet males were crossed with Hex:GFP Hom females. F1 males Nodal-LacZ KiHet;Hex::GFP Het were crossed with Nodal-LacZ KiHet females to obtain the Nodal-LacZ KiHom;Hex::GFP Het embryos. **B.** Ratio of GFP+ wild-types and mutant embryos from one litter. **C.** MIP rendered surface views (3D) of whole-mount immunostained Nodal-LacZ;*Hex*::GFP embryos. Hex::GFP expression is detected using an antibody against GFP. Merge displays Epi (SOX2) and PrE (GATA4) markers. Numbers in the GFP column corresponds to the number of GFP+ embryos over the total number of embryos stained. Orange arrow indicate GFP+ cell. **D.** Scatter plots showing the shape factor of nuclei from both wild-types (N=5) and mutant (N=3) embryos. Nuclei adopting a spherical shape will present a number closed to 1 while more rectangular nuclei will be associated with numbers closed to 0. The embryos used for this analysis are shown in (**Fig. S7A**.). n represents the number of nuclei used in this quantification. **E.** MIP rendered inner views (2D) of whole-mount immunostained Nodal-LacZ embryos showing the adherent junctions (ECADHERIN) and Epi membranes (PECAM). White rectangle dashes indicate the numerical zoom made of this zone and displayed to the right side of the panel. **F.** MIP rendered inner views (2D) of whole-mount immunostained Nodal-LacZ embryos showing the late PrE (SOX7) and Epi (OCT4). Numbers in the SOX7 column corresponds to the number of SOX7+ embryos over the total number of embryos stained**. G.** Histogramm displaying the number of Epi and PrE cells as well as the total cell number of the wild-types (N=3) and mutants (N=2) embryos seen in (**Fig. S7A**.). **H.** Scatter plots showing the corrected SOX2 fluorescence intensity of each nuclei in the wild-type (N=3) or mutant (N=2) embryos shown in (**Fig. S7A**.). n represents the number of nuclei used in this quantification. **I.** Scatter plots showing the corrected OCT4 fluorescence intensity of each nuclei in the wild-type (N=3) or mutant (N=2) embryos shown in (**Fig. 7F**) n represents the number of nuclei used in this quantification. **J.** WMISH for *Cripto* and *Otx2* on wild-type and mutant embryos. Scale bars = 50µm. Statistical significance is calculated using T.tests with Pvalues represented as following: *<0.05 ; **<0.01 ; ***<0.001. Scale bars = 20µm.

thus indicated that the Epi was the first to respond to the ligand while that of the PrE, which came later.

Accordingly, quantification of the early ICM/late Epi factors OCT4 and SOX2 and of the PrE marker SOX17 in individual cells showed important changes in the expression levels of OCT4 and SOX2 already at the ~60 and ~120 cell stage whereas the most important variation in SOX17 expression took place from the ~150 cell stage (Fig. 5d). While OCT4 is expressed in both the Epi and the PrE, it was primarily in the Epi that its expression was increased in >150 cell NODAL-treated embryos (Fig. 5e). Also, exposure to NODAL elicited an increase in OCT4 expression in just 4h in ~70 cell embryos, a speed consistent with a direct response to the ligand (Fig. 5f). Moreover, exposure to NODAL until the ~60 cell stage for 24h hours lead to the overexpression of both NANOG and GATA6, in correlation with the positive impact on OCT4 (Fig S5g). Finally, staining of E2.5 embryos cultured with or without recombinant NODAL until they reached a total cell number of ~70 confirmed that the only significant increase in the number of mitotic cells detected at this stage was in the Epi (Fig. 5g, h). This increased mitotic activity was associated with an overexpression of OTX2, which is known to promote the Epi lineage at the mid blastocyst stage[132] (Fig. 5i). Taken together these data shown that NODAL specifically

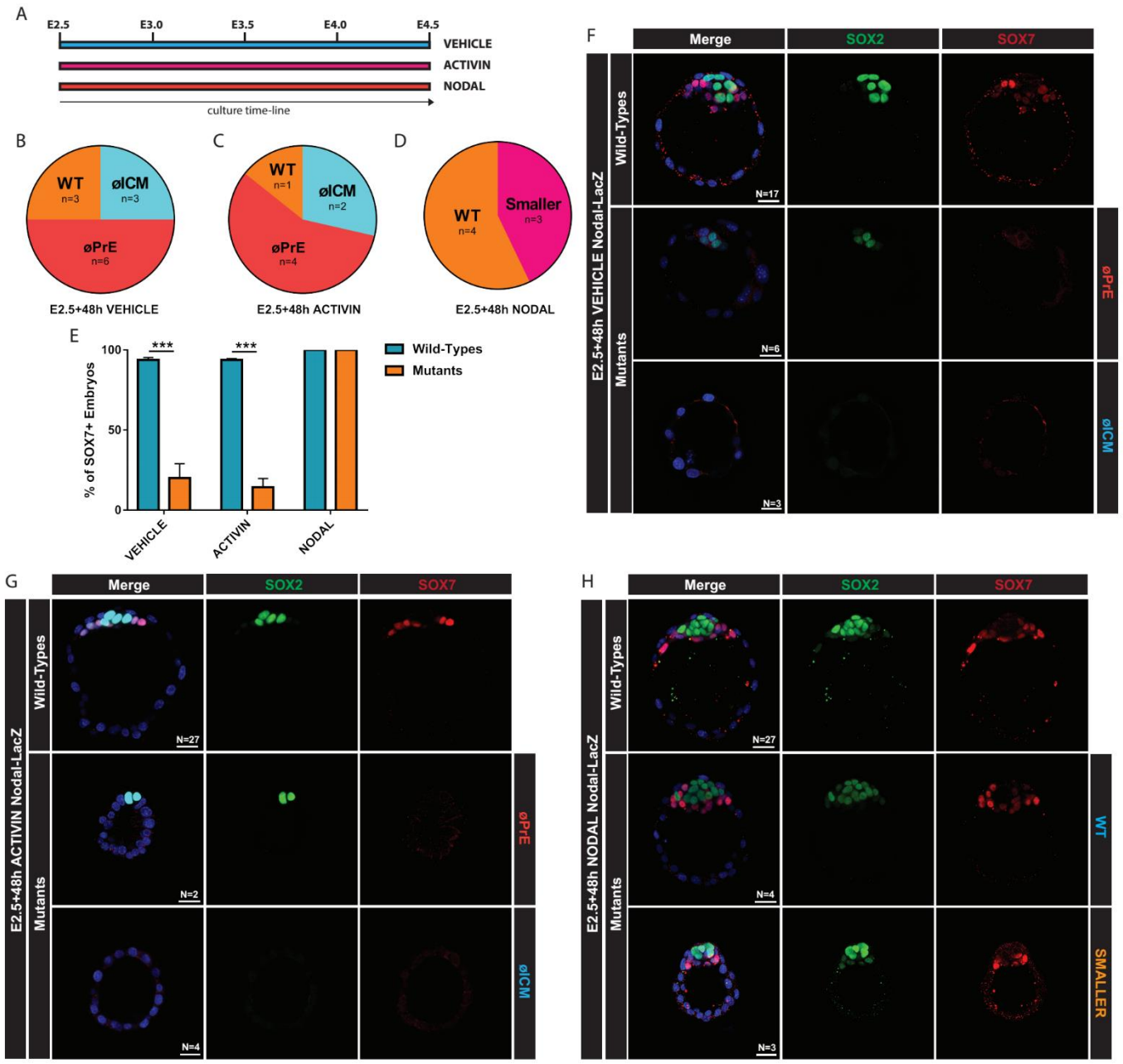

Figure 8: NODAL presence conditions early steps of ICM development

A. Schematic representation of the different culture conditions applied for the following experiments. Embryos from *Nodal-LacZ* KiHet x *Nodal-LacZ* KiHet were cultured for the same time with either control, with recombinant ACTIVIN or NODAL. At the end of the culture the embryos were fixed, analyzed and then genotyped. **B.** Pie representation of the different phenotypes observed in the *Nodal* mutants' embryos at the end of a 48h culture in vehicle (**F.**). øPrE: embryos without SOX7; øICM: embryos without SOX2 and SOX7; WT: embryos resembling wild-type embryos. **C.** Pie representation of the different phenotypes observed in the *Nodal* mutants' embryos at the end of a 48h culture in ACTIVIN (**G.**). **D.** Pie representation of the different phenotypes observed in the *Nodal* mutants' embryos at the end of a 48h culture in NODAL **(H.**). Smaller: embryos presenting both SOX2 and SOX7 expression but being smaller to their counterparts; WT: embryos resembling wild-type embryos. **E.** Histogram displaying the percentages of embryos expressing SOX7 at the end of all cultured conditions shown in (**F. G. H.**) **F.** MIP rendered inner views (2D) of whole-mount immunostained *Nodal-LacZ* KiHet

x *Nodal-LacZ* KiHet embryos cultured from E2.5 for 48h in vehicle showing both Epi (SOX2) and PrE (SOX7) expression patterns. Mutants embryos are categorized according to their phenotype as described in (**B.**). **G.** MIP rendered inner views (2D) of whole-mount immunostained *Nodal-LacZ* KiHet x *Nodal-LacZ* KiHet embryos cultured from E2.5 for 48h in ACTIVIN showing both Epi (SOX2) and PrE (SOX7) expression patterns. Mutants embryos are categorized according to their phenotype as described in (**C.**). H. MIP rendered inner views (2D) of whole-mount immunostained *Nodal-LacZ* KiHet x *Nodal-LacZ* KiHet embryos cultured from E2.5 for 48h in NODAL showing both Epi (SOX2) and PrE (SOX7) expression patterns. Mutants embryos are categorized according to their phenotype as described in (**D.**). Scale bar = 20µm. Statistical significance is calculated using T.tests with Pvalues represented as following: *<0.05 ; **<0.01 ; ***<0.001.

signal in Epi cells to promote the expansion of the Epi lineages resulting in the maturation of the whole ICM tissues.

ACTIVIN promotes to the development of the PrE layer

In contrast to what we saw with NODAL, the culture of E2.5 embryos for 48h in the presence of ACTIVIN did not alter cell counts in any of their lineages (Fig. S5a). However, the ratio of embryos having completed the segregation of their ICM was significantly increased in the ACTIVIN-treated lot (Fig. S5b), suggesting that ACTIVIN promoted PrE development. To obtain more evidence about this the same experiment was performed on E2.5 Hex::GFP embryos. ACTIVIN treatment was found to increase the percentage of GFP-positive embryos, and the number of GFP-positive cells they contained at the end of the culture (Fig. S5c, d). The same effect was detected in E3.5 Hex::GFP embryos cultured in ACTIVIN for just 24h, narrowing down the time during which this exposure is effective (Fig. S5e). A slight increase in the expression of the PrE-determining factor GATA6 was also measured in E2.5 embryos cultured with ACTIVIN for 48h (Fig. S5f), another indication that the ligand was affecting this layer. However, we could not detect any effect of a 36h exposure on the mitotic activity measured in the various cell layers (Fig. S5g), a result consistent with our observation that cell counts were not affected. Therefore, while NODAL is signalling to Epi cells specifically, the impact of ACTIVIN is restricted to the PrE layer.

NODAL conditions the specification of the blastocyst polarization

Given the differences in the effect NODAL and ACTIVIN had on blastocyst development we compared their impact on the expression of the Hex::GFP reporter. E2.5 embryos harbouring the transgene were cultured for 36h with or without NODAL or ACTIVIN, pass the point at which the ~120-cell embryos start to express it (Fig. 5j). In these conditions, we found that although the percentage of GFP-positive embryos was higher in the ACTIVIN-treated lot, the difference with controls was not significant (Fig.

5k). In contrast, the percentage of GFP-positive embryo was significantly higher in the NODAL-treated lot. Although the number of fluorescent cells in GFP-positive embryos was about the same, regardless of the treatment they underwent (Fig. 5l), we found that the number of GFP-positive cells was correlated to the total cell number of the embryo (Fig. 5m). No such correlation was found with the number of Epi or PrE cells. This nevertheless suggested that the gain in Epi cell number seen in these embryos affected the pace of development of their PrE and its patterning.

These results indicate that NODAL and ACTIVIN play quite distinct roles in the development of the ICM. They suggest that NODAL directly promotes the formation and maturation of the Epi, which in turn promotes PrE development, while ACTIVIN appears to promote PrE development directly.

The initial *Nodal* expression in the PrE is sufficient to drive ICM maturation

Nodal-expressing ICM cells appear to downregulate this expression when they adopt an Epi identity while it gains in strength in emerging PrE cells[70]. As both lineages mature *Nodal* expression increases in the Epi but declines in the PrE (Fig. S6a). To assess the respective contributions of these distinct phases of *Nodal* expression to blastocyst development we investigated what happened in chimeric embryos where the Epi is mutant for *Nodal*. Chimeric embryos can be obtained when aggregating E2.5 morulas with a clump of ESCs, and culturing them up to blastocyst stage (Fig. 6a). To address the impact of Epi maturation, ESCs were cultured in either 2i or serum affected their contribution to the Epi of such aggregation chimeras, and found that 100% contribution was routinely obtained with ESCs cultured in 2i (Fig. S6a, b, c). These conditions were thus used to generate late blastocysts where the TE and PrE derived from host H2B::GFP embryos while the entire Epi derived from *Nodal*$^{-/-}$ ESCs (Fig. 6b). Although all cell layers seemed to develop normally, with properly segregated ICMs and unchanged expression of SOX7 and OCT4 in ICM derivatives (Fig. 6b, c, f), these embryos were smaller than controls and had a lower total cell number, associated with lower cell counts in all cell layers (Fig. 6d, e; Fig. S6d). This suggested that the lack of *Nodal* expression in the Epi only affected the growth of these layers. We generated chimeras using E2.5 Hex::GFP morulas, to find out whether the absence of *Nodal* in the Epi affected the patterning of the PrE, but the percentage of GFP-positive embryos and the number of GFP-positive cells in these embryos was no different than in controls (Fig. 6g, h, i). Moreover, the addition of ACTIVIN was not able to promote a different patterning in those *Nodal*^{Epi} depleted embryos (Fig. 6g, h, i). These results suggested that *Nodal* expression in the ICM and the PrE was enough to ensure the emergence and maturation of all ICM derivatives, including *Hex*-positive PrE cells.

Given our previous finding that the number of *Hex*-positive cells correlated with the total cell number of the embryo we investigated whether this remained true with a *Nodal*-defective Epi. Aggregation chimeras were generated using E2.5 Hex::GFP morulas and increasing numbers of ESCs to identify conditions that were still allowing the establishment of a PrE layer (Fig. 6j). Chimeric embryos generated using 12-16 *Nodal*$^{-/-}$ ESCs were then found to harbour more GFP-positive cells at the end of the culture than chimeric embryos generated with 4-6 wildtype cells, and these cells were also more fluorescent. This confirmed that the total cell number of the embryo is a determinant of the number of *Hex*-positive cells, and that *Nodal* from the Epi is not essential for their specification.

Zygotic NODAL is essential for late PrE and Epi patterning

To further our understanding of the contribution and origin of the various ligands signalling via ACTIVIN receptors during blastocyst development we characterized the phenotype of *Nodal*$^{LacZ/LacZ}$ embryos. The failure to express Hex::GFP being one of the latest defects we characterized in SB-treated blastocysts we first assessed how the absence of zygotic NODAL affected the transgene's expression (Fig. 7a). No GFP was detected in E4.5 *Nodal*$^{LacZ/LacZ}$ embryos carrying the transgene (Fig. 7b, c), but the scattering of PrE cells observed in these embryos revealed that the entire cell layer was disorganized. Measurements of the aspect ratio of PrE mutant nuclei, itself a reflection of cell shape, showed they were more rounded, less stretched, than their wildtype counterparts (Fig. 7d, S7a), presumably affecting the structures or mechanisms that ensure its cohesion. Immunodetection of E-CADHERIN revealed the absence of staining foci in the PrE of mutant embryos, confirming that mutants PrE cells fail to form or to maintain a cohesive epithelium (Fig. 7e). Finally, *Nodal*$^{LacZ/LacZ}$ embryos did not present any expression of DAB2 and LRP2, which are hallmarks of the apical-basal polarity of PrE cells (Fig. S7b, c). These results showed that NODAL is required to ensure the epithelialization of the PrE layer. Immunodetection of earlier markers of fully specified PrE cells revealed in E4.5 *Nodal*$^{LacZ/LacZ}$ embryos a complete absence of SOX7, while GATA4 levels were strongly downregulated (Fig. 7f, S7d, e). This confirmed that although the absence of zygotic NODAL does not prevent the specification of PrE fate, nor its segregation from Epi cells, it clearly affects the subsequent developmental progression of the layer. Our previous analyses of SB and NODAL-treated embryos strongly suggested that this defect stemmed directly from a defect in the Epi.

Although the comparison between E4.5 *Nodal*$^{LacZ/LacZ}$ and wildtype embryos after staining found no difference in their total cell number and PrE cell number, mutant embryos showed a specific deficit in their Epi cell number (Fig. 7g), an indication that the development of this tissue was indeed affected. Immunodetection of the Epi factors NANOG, SOX2 and OCT4 showed that the expression of both was

significantly reduced in the Epi of *Nodal*$^{LacZ/LacZ}$ embryos (Fig. 7h, i, S7f). In addition, *in situ* hybridization experiments failed to detect the expression of *Cripto* and *Otx2*, which both promote the maturation of the Epi at this stage (Fig. 7j). The defects we found in the Epi of E4.5 *Nodal*$^{LacZ/LacZ}$ embryos were thus quite similar to what we saw in E3.5 embryos cultured in the presence of SB.

These results thus identify key requirements for zygotic NODAL in the developmental progression of both the Epi and the PrE after E3.5. However, the fact that in no affected phenotype could be detected prior to E4.25 and in some of implantation stages mutants for *Nodal* suggested that other signals could rescue the defects.

NODAL presence conditions early steps of ICM development

The discrepancy between the capacity of ICM cells to respond to NODAL from an early stage and the relatively late defects we characterized in *Nodal*$^{LacZ/LacZ}$ blastocysts raised the possibility that the absence of zygotic NODAL was partially compensated by ligands of maternal origin in these embryos. *Nodal* and ACTIVIN-coding genes are known to be expressed by the endometrium as the morula enters and progresses through the uterus (Park and Dufort, 2011; Jones et al., 2006). To assess whether such ligands of uterine origin compensated for the absence of zygotic NODAL we cultured E2.5 morulas obtained from crosses between *Nodal*$^{LacZ/+}$ mice in the presence or absence of recombinant ACTIVIN or NODAL for 48h (Fig. 8a). We were surprised to find at the end of the culture embryos that presented phenotypes we had never seen before, more severe than that of SB-treated embryos and characterized by a complete absence of ICM, or a complete absence of PrE associated with a residual ICM or Epi (Fig. 8f/b). Genotyping confirmed that these embryos were homozygous for the mutation, but showed also that some homozygotes (3/12) appeared to develop normally (Fig. 6b, f). These results were not altered when using a different culture medium (Fig. S8a, b, c, d). While treatment with ACTIVIN did not seem to affect the range of phenotypes or their frequency in mutant embryos, treatment with NODAL totally (4/7) or partially (3/7) rescued these phenotypes (Fig. 6c, d, e, g, h). All rescued embryos expressed SOX7, which we found previously dependent on NODAL signalling. However, some of them were much smaller than normal, even smaller than the blastocyst chimeras harbouring *Nodal*-defective Epi we characterized previously, implying that recombinant NODAL was not always sufficient to compensate for the absence of zygotic NODAL.

These results demonstrate that the development of the ICM is dependent on NODAL from an early stage, and that uterine products compensate for its absence up to blastocyst stage. The range of phenotypes seen in mutant and rescued embryos suggests some heterogeneity among the E2.5 embryos used in these experiments, possibly reflecting the extent to which they were exposed to

NODAL from neighbouring wildtype embryos while they were cultured. The fact that cultured *Nodal*$^{LacZ/LacZ}$ morulas develop a phenotype far more severe than SB-treated morulas could suggest that part of NODAL action at this early stage is independent of its canonical signalling pathway.

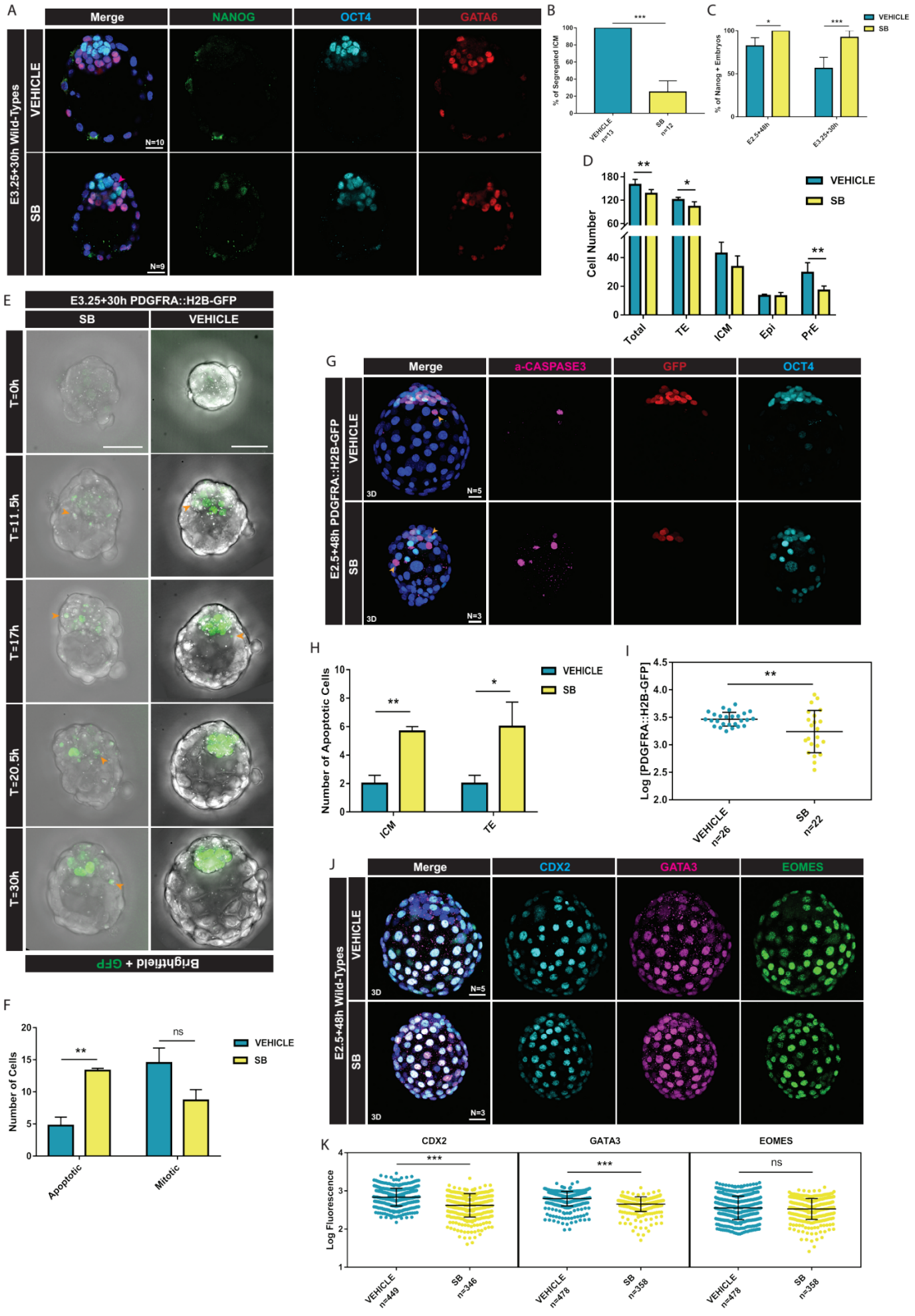
A
Merge
NANOG
OCT4
GATA6
E3.25+30h Wild-Types
VEHICLE
SB
N=10
N=9
B
% of Segregated ICM
VEHICLE n=13
SB n=12
C
% of Nanog + Embryos
VEHICLE
SB
E2.5+48h
E3.25+30h
D
Cell Number
VEHICLE
SB
Total
TE
ICM
Epi
PrE
E
E3.25+30h PDGFRA::H2B-GFP
SB
VEHICLE
T=0h
T=11.5h
T=17h
T=20.5h
T=30h
Brightfield + GFP
F
Number of Cells
VEHICLE
SB
Apoptotic
Mitotic
G
Merge
a-CASPASE3
GFP
OCT4
E2.5+48h PDGFRA::H2B-GFP
VEHICLE
SB
3D
N=5
N=3
H
Number of Apoptotic Cells
VEHICLE
SB
ICM
TE
I
Log [PDGFRA::H2B-GFP]
VEHICLE n=26
SB n=22
J
Merge
CDX2
GATA3
EOMES
E2.5+48h Wild-Types
VEHICLE
SB
3D
N=5
N=3
K
CDX2
GATA3
EOMES
Log Fluorescence
VEHICLE n=449
SB n=346
VEHICLE n=478
SB n=358
VEHICLE n=478
SB n=358
ns

Supplementary figure 1: ACTIVIN/NODAL signaling is required to ensure the proper development of the blastocyst

A. Maximum intensity projection (MIP) of confocal images rendering the inner views (2D) of whole-mount immunostained wild-type embryos cultured from E3.25 for 30h in either control (VEHICLE) or inhibitor (SB) conditions showing inner cell mass (ICM) segregation with the labelling of its derivatives: NANOG (Epi), OCT4 (ICM), GATA6 (PrE). Magenta arrow shows non segregated PrE cell. Orange arrow shows a NANOG+;GATA6+ double positive cell. Scale bar = 20µm. **B.** Histogram displaying the percentages of embryos with proper segregated ICMs at the end of both cultured conditions shown in (**A.**). **C.** Histogram displaying the percentages of NANOG+ embryos cultured for both conditions from either E2.5 (Vehicle: N=17 ; SB: N=22) or E3.25 (Vehicle: N=16 ; SB: N=13) indicating the stage of developmental progression. **D.** Histogramm displaying the cell numbers of each tissue present at the blastocyst stage and their total of embryos cultured in the same conditions as in (**A.**). Vehicle (N=7) ; SB (N=8). **E.** 3D reconstruction rendered by confocal MIP of different time points from E3.25 showing the specification and arrangement of the PrE layer of *Pdgfra*$^{H2B\text{-}GFP}$ knock-in embryos cultured in VEHICLE (N=4) or SB (N=3) conditions. Orange arrow shows apoptotic cells. Scale bar = 50µm. **F.** Histogramm displaying the total number of apoptotic and mitotic cells of the embryos during the entirety of the movies time-line for both conditions presented in (**E.**). **G**. Maximum intensity projection (MIP) of confocal images rendering the surface (3D) of whole-mount *Pdgfra*$^{H2B\text{-}GFP}$ knock-in embryos immunostained against activated-CASPASE3 at the end stage of the 48h culture in control or SB conditions. PrE cells are labeled using an anti-GFP antibody. Orange arrow shows apoptotic cells in both TE and ICM populations. Scale bar = 20µm. **H.** Histogramm displaying the number of apoptotic cells in either ICM (OCT4+) or TE (OCT4-) populations of embryos cultured as in (**G.**). **I.** Scatter plots showing the corrected GFP fluorescence intensity of each nuclei in the embryos cultured as in (**G.**). conditions. n represents the number of nuclei used in this quantification**. J.** Maximum intensity projection (MIP) of confocal images rendering the surface (3D) of whole-mount immunostained wild-type embryos cultured from E2.5 for 48h in control or SB conditions labelling several TE markers. Scale bar = 20µm. **K.** Scatter plots showing the corrected fluorescence intensity of each nuclei for CDX2, GATA3 and EOMES in the embryos cultured as in (**E.**). conditions. n represents the number of nuclei used in this quantification. Statistical significance is calculated using T.tests with Pvalues represented as following: *<0.05 ; **<0.01 ; ***<0.001.

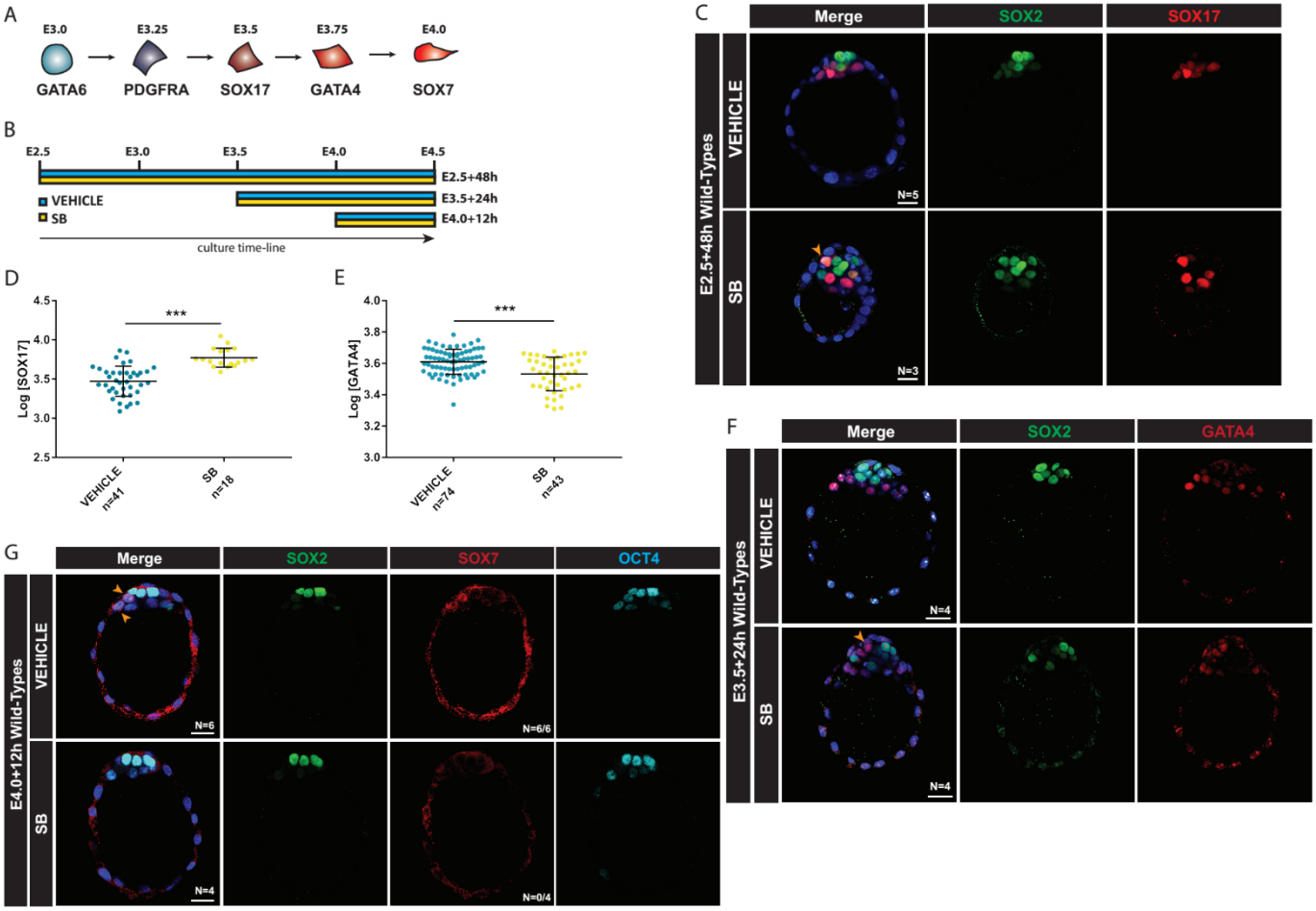
A
E3.0
E3.25
E3.5
E3.75
E4.0
GATA6
PDGFRA
SOX17
GATA4
SOX7
B
E2.5
E3.0
E3.5
E4.0
E4.5
E2.5+48h
E3.5+24h
E4.0+12h
VEHICLE
SB
culture time-line
C
Merge
SOX2
SOX17
E2.5+48h Wild-Types
VEHICLE
SB
N=5
N=3
D
Log [SOX17]
***
VEHICLE n=41
SB n=18
E
Log [GATA4]
***
VEHICLE n=74
SB n=43
F
Merge
SOX2
GATA4
E3.5+24h Wild-Types
VEHICLE
SB
N=4
N=4
G
Merge
SOX2
SOX7
OCT4
E4.0+12h Wild-Types
VEHICLE
SB
N=6
N=6/6
N=4
N=0/4

Supplementary figure 2: ACTIVIN/NODAL signaling is required for the maturation of the PrE

A. Schematic representation of the time-gated maturation of the PrE through the sequential expression of several marker from E2.5 to E4.0. The cells are color coded according to its identity from an ICM fate (cyan) to a definitive PrE cell (red) **B.** Schematic representation of the different culture conditions applied for the following experiments. All cultured embryos shared the same ending point with only the start of the culture being changed in order to precisely investigate the impact on the factor expression pattern. **C.** MIP rendered inner views (2D) of whole-mount immunostained wild-type embryos cultured from E2.5 for 48h in either control (VEHICLE) or inhibitor (SB) conditions showing the expression pattern of both SOX2 (Epi) and SOX17 (PrE). **D.** Scatter plots showing the corrected SOX17 fluorescence intensity of each nuclei in the embryos cultured as in control (N=5) or SB (N=3) condition as described in (**C.**). n represents the number of nuclei used in this quantification. **E.** Scatter plots showing the corrected GATA4 fluorescence intensity of each nuclei in the embryos cultured as in control (N=6) or SB (N=7) condition as described in (**F.**). n represents the number of nuclei used in this quantification. **F.** MIP rendered inner views (2D) of whole-mount immunostained wild-type embryos cultured from E3.5 for 24h in either control or SB conditions showing the expression pattern of both Epi (SOX2) and PrE (GATA4). Orange arrow indicates a missorted PrE cell. **G.** MIP rendered inner views (2D) of whole-mount immunostained wild-type embryos cultured from E4.0 for 16h in either control or SB conditions showing the expression pattern of ICM derivatives: Epi (SOX2), ICM (OCT4), PrE (SOX7). Orange arrows indicate SOX7 labeled nuclei. N in the SOX7 column indicates the number of SOX7+ embryos/total embryos. Scale bars = 20µm. Statistical significance is calculated using T.tests with Pvalues represented as following: *<0.05 ; **<0.01 ; ***<0.001.

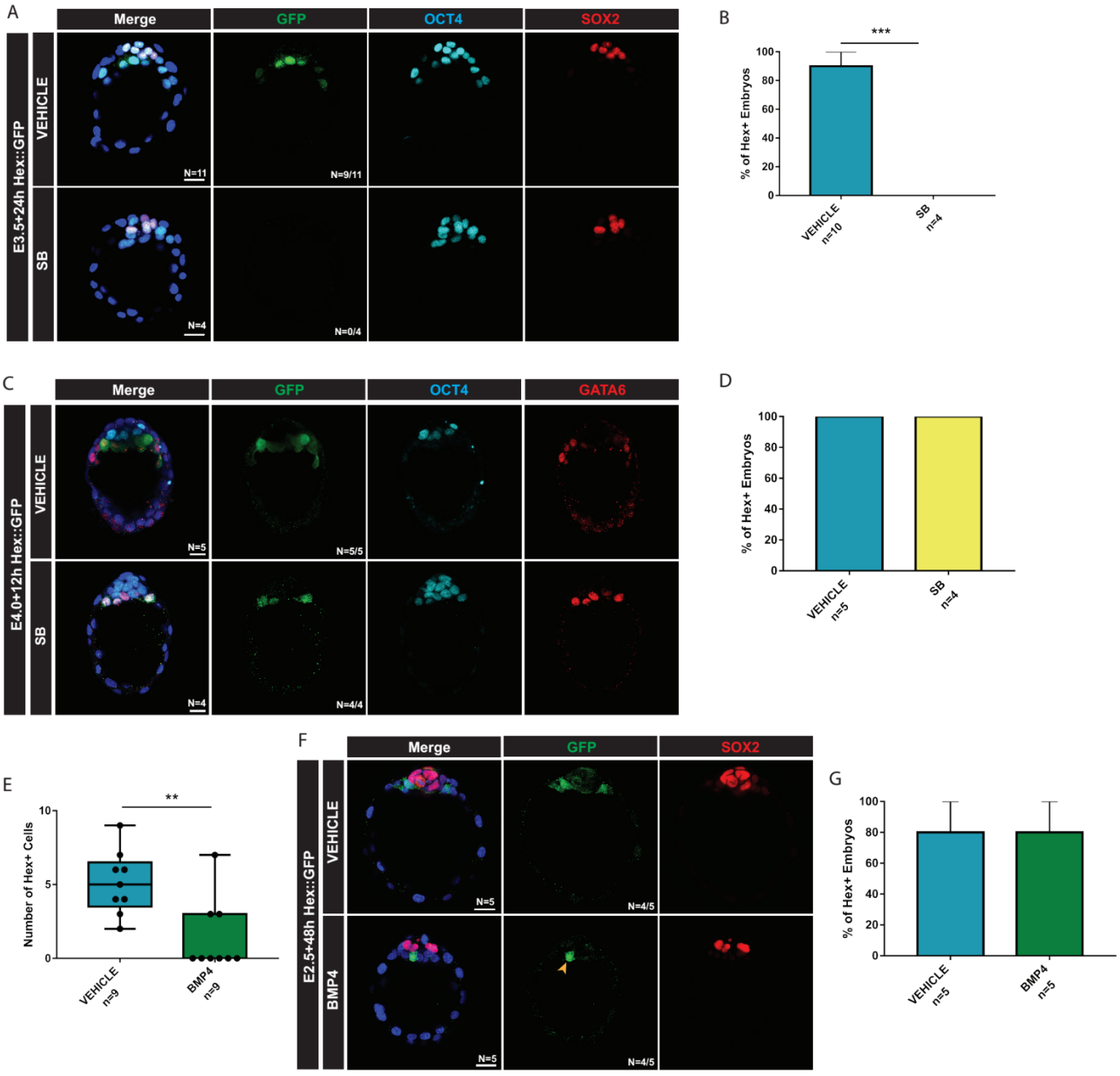
A
Merge
GFP
OCT4
SOX2
E3.5+24h Hex::GFP
VEHICLE
SB
N=11
N=9/11
N=4
N=0/4
B
***
% of Hex+ Embryos
VEHICLE n=10
SB n=4
C
Merge
GFP
OCT4
GATA6
E4.0+12h Hex::GFP
VEHICLE
SB
N=5
N=5/5
N=4
N=4/4
D
% of Hex+ Embryos
VEHICLE n=5
SB n=4
E
**
Number of Hex+ Cells
VEHICLE n=9
BMP4 n=9
F
Merge
GFP
SOX2
E2.5+48h Hex::GFP
VEHICLE
BMP4
N=5
N=4/5
N=5
N=4/5
G
% of Hex+ Embryos
VEHICLE n=5
BMP4 n=5

Supplementary figure 3: ACTIVIN/NODAL signalling counters BMP signals to pattern the PrE.

A. Maximum intensity projection (MIP) of confocal images rendering the inner views (2D) of whole-mount immunostained embryos cultured from E3.5 for 24h in either control (VEHICLE) or inhibitor (SB) conditions and carrying the *Hex*::GFP transgene showing the expression pattern of *Hex*. N in the GFP column indicates the number of Hex-GFP+ embryos/total embryos. Scale bar = 20µm. **B.** Histogramm displaying the percentage of embryos showing a GFP staining at the end of the culture as shown in (**A.**). **C.** MIP rendered inner views (2D) of whole-mount immunostained *Hex*::GFP embryos cultured from E4.0 for 12h in either control or SB conditions. N in the GFP column indicates the number of Hex-GFP+ embryos/total embryos. Scale bar = 20µm. **D.** Histogramm displaying the percentage of embryos showing a GFP staining at the end of the culture as shown in (**C.**). **E.** Histogramm displaying the number of GFP+ cells in each embryo cultured as shown in (**Fig. 3E.**). **F.** MIP rendered inner views (2D) of whole-mount immunostained Hex::GFP embryos cultured from E2.5 for 48h in either control or in presence of recombinant BMP4. N in the GFP column indicates the number of Hex-GFP+ embryos/total embryos. **G.** Histogramm displaying the percentage of embryos showing a GFP staining at the end of the culture as shown in (**F.**). Statistical significance is calculated using T.tests with Pvalues represented as following: *<0.05 ; **<0.01 ; ***<0.001.

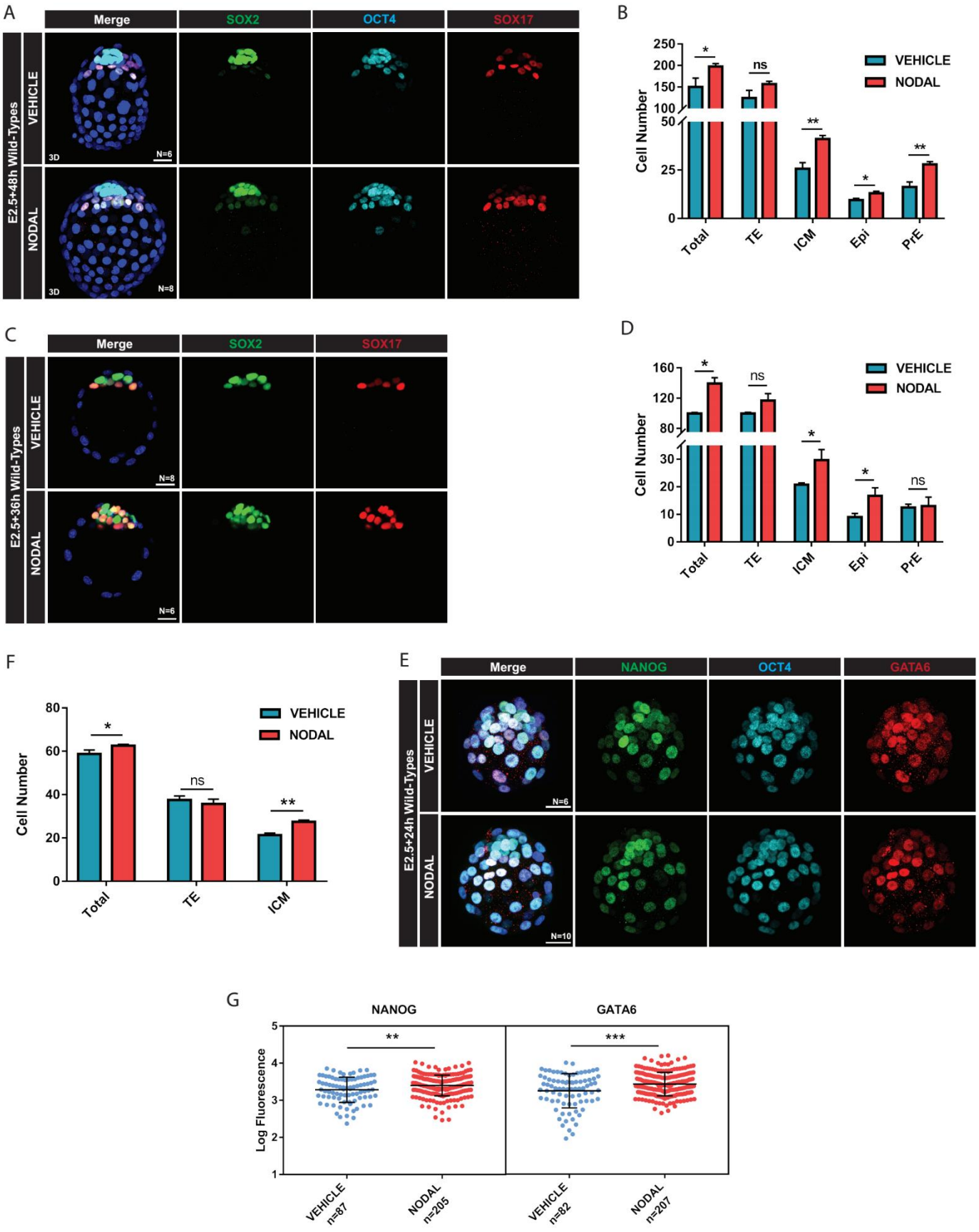
A
Merge
SOX2
OCT4
SOX17
E2.5+48h Wild-Types
VEHICLE
NODAL
3D
N=6
N=8
B
Cell Number
VEHICLE
NODAL
Total
TE
ICM
Epi
PrE
ns
C
E2.5+36h Wild-Types
N=8
N=6
D
E
NANOG
GATA6
E2.5+24h Wild-Types
N=10
F
G
Log Fluorescence
VEHICLE n=87
NODAL n=205
VEHICLE n=82
NODAL n=207

Supplementary figure 4: NODAL signals in Epi cells to promote the whole ICM maturation

A. MIP of confocal images rendering the surface (3D) of whole-mount immunostained wild-type embryos cultured from E2.5 for 48h reaching a total cell number >150 cells in either control condition or in presence of recombinant NODAL. **B.** Histogramm displaying the cell numbers of each tissue present at the blastocyst stage and their total cell number from the embryos cultured as described in (**A.**). **C.** MIP rendered inner views (2D) of whole-mount immunostained wild-type embryos cultured from E2.5 for 36h reaching a total cell number ~120 cells in either control condition or in presence of recombinant NODAL. **D.** Histogramm displaying the cell numbers of each tissue present at the blastocyst stage and their total cell number from the embryos cultured as described in (**C.**). **E.** MIP of confocal images rendering the surface (3D) of whole-mount immunostained wild-type embryos cultured from E2.5 for 24h reaching a total cell number ~60 cells in either control condition or in presence of recombinant NODAL. **F.** Histogramm displaying the cell numbers of each tissue present at the early blastocyst stage where the Epi and PrE are not fully specified and thus not analyzed and their total cell number from the embryos cultured as described in (**E.**). **G.** Scatter plots showing the corrected NANOG and GATA6 fluorescence intensity of each nuclei in the embryos cultured as described in (**E.**). n represents the number of nuclei used in this quantification. Scale bars = 20µm. Statistical significance is calculated using T.tests with Pvalues represented as following: *<0.05 ; **<0.01 ; ***<0.001.

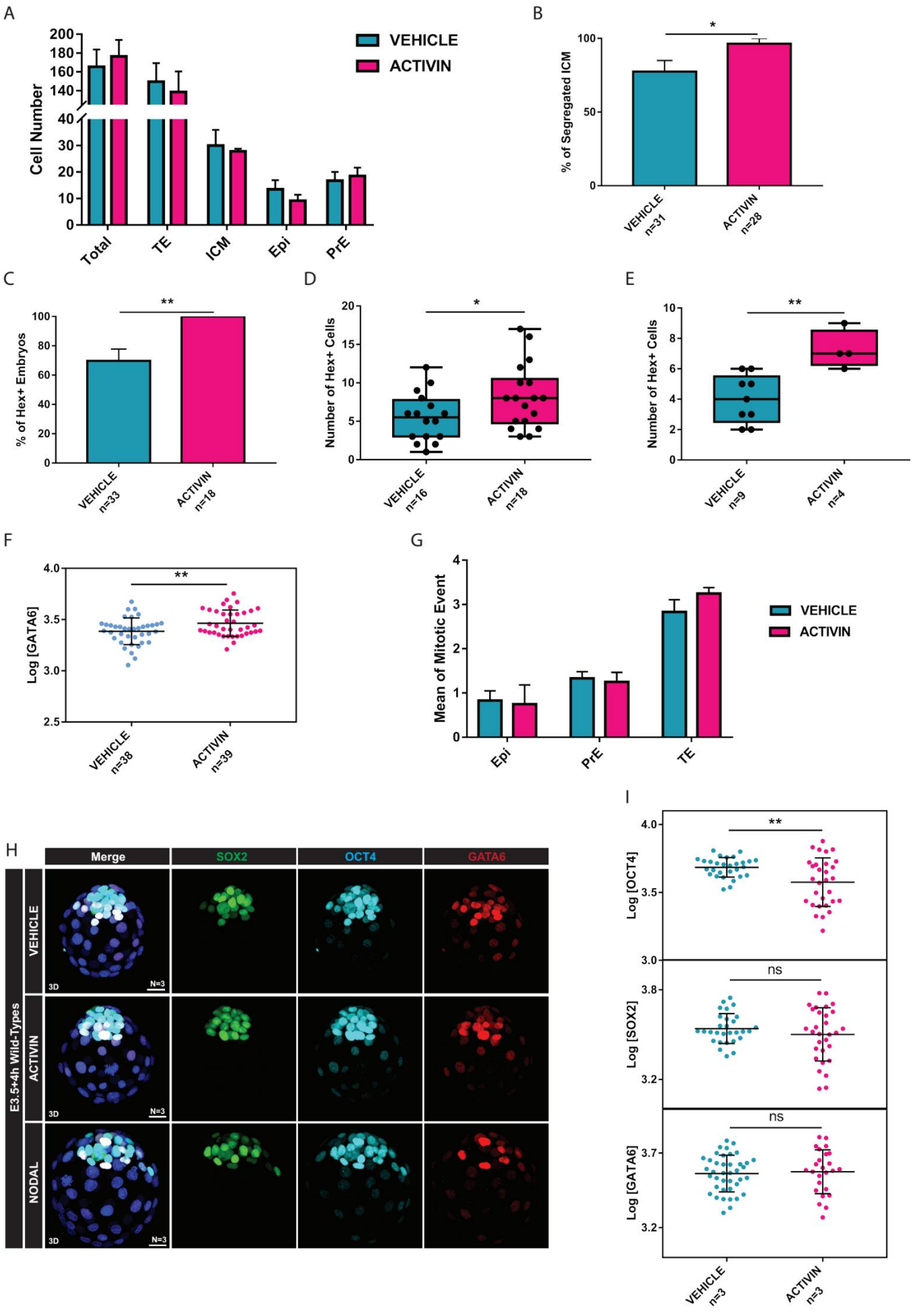
A
VEHICLE
ACTIVIN
Cell Number
Total
TE
ICM
Epi
PrE
B
% of Segregated ICM
VEHICLE n=31
ACTIVIN n=28
C
% of Hex+ Embryos
VEHICLE n=33
ACTIVIN n=18
D
Number of Hex+ Cells
VEHICLE n=16
ACTIVIN n=18
E
Number of Hex+ Cells
VEHICLE n=9
ACTIVIN n=4
F
Log [GATA6]
VEHICLE n=38
ACTIVIN n=39
G
Mean of Mitotic Event
Epi
PrE
TE
VEHICLE
ACTIVIN
H
Merge
SOX2
OCT4
GATA6
E3.5+4h Wild-Types
VEHICLE
ACTIVIN
NODAL
3D
N=3
I
Log [OCT4]
Log [SOX2]
Log [GATA6]
ns
VEHICLE n=3
ACTIVIN n=3

Supplementary figure 5: ACTIVIN promotes to the development of the PrE layer

A. Histogramm displaying the cell numbers of each tissue present at the blastocyst stage and their total cell number from E2.5 embryos cultured in recombinant ACTIVIN for 48h without showing any significant difference. **B.** Histogram displaying the percentages of embryos with proper segregated ICMs at the end of the culture described in (**A.**). **C.** Histogramm displaying the percentage of *Hex*::GFP embryos showing a GFP staining at the end of a 48h culture in either control or ACTIVIN. **D.** Box plot displaying the number of GFP+ cells in each *Hex*::GFP embryo cultured as shown in (**C.**). Each dot represents one embryo. **E.** Box plot displaying the number of GFP+ cells in each E3.5 *Hex*::GFP embryo cultured for 24h. Each dot represents one embryo. **F.** Scatter plots showing the corrected GATA6 fluorescence intensity of each nuclei in the embryos cultured from E2.5 for 48h as described in (**A.**). n represents the number of nuclei used in this quantification. **G.** Histogramm displaying the number of mitotic events per cell population in each E2.5 embryo cultured for 36h until they reach a total number of ~120 cells. No significance difference in mitotic events was observed in these conditions. **H.** MIP of confocal images rendering the surface (3D) of whole-mount immunostained wild-type embryos cultured from E3.5 for 4h in either control condition or in presence of recombinant ACTIVIN or NODAL. Scale bars = 20µm. **I.** Scatter plots showing the corrected OCT4, SOX2 and GATA6 fluorescence intensity of each nuclei in the embryos cultured as described in (**H**.). Statistical significance is calculated using T. tests with Pvalues represented as following: *<0.05; **<0.01 ; ***<0.001.

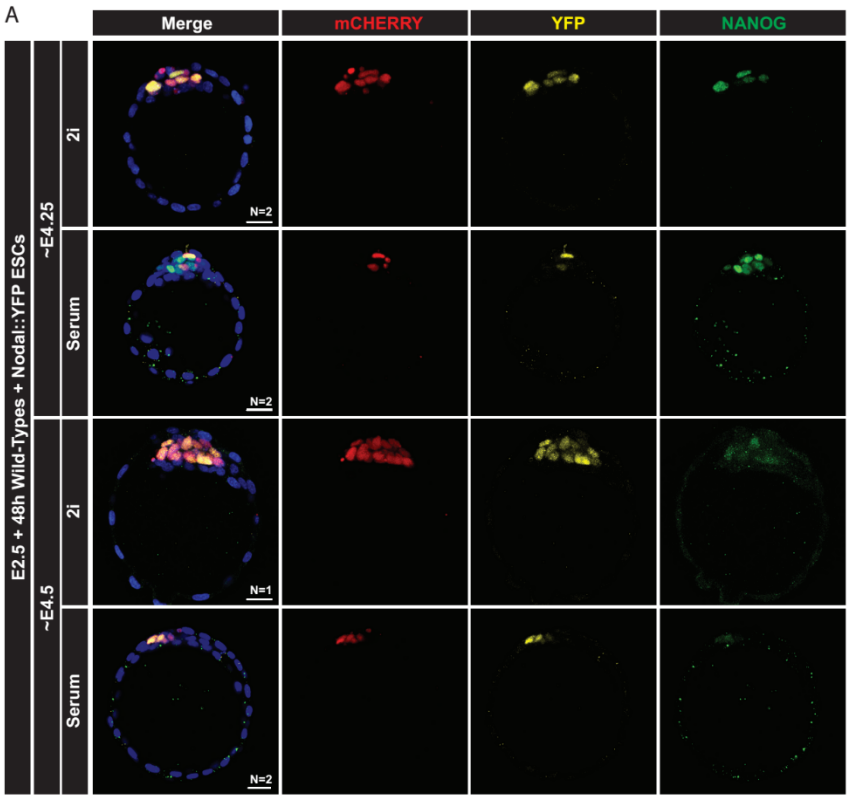
A
Merge
mCHERRY
YFP
NANOG
E2.5 + 48h Wild-Types + Nodal::YFP ESCs
~E4.25
~E4.5
2i
Serum
2i
Serum
N=2
N=2
N=1
N=2

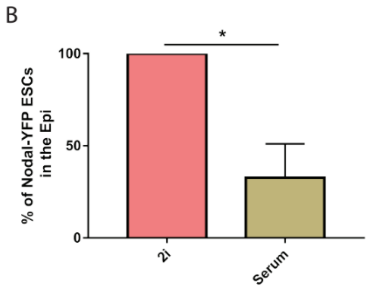
B
% of Nodal-YFP ESCs in the Epi
100
50
0
*
2i
Serum

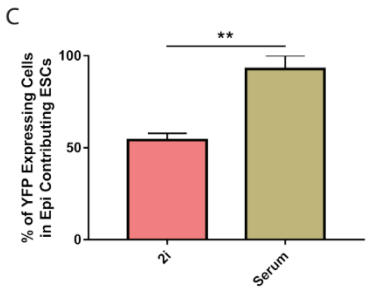
C
% of YFP Expressing Cells in Epi Contributing ESCs
100
50
0
**
2i
Serum

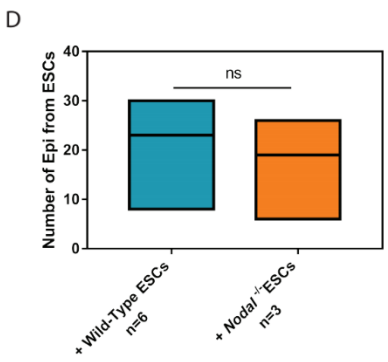
D
Number of Epi from ESCs
40
30
20
10
0
ns
+ Wild-Type ESCs n=6
+ Nodal -/- ESCs n=3

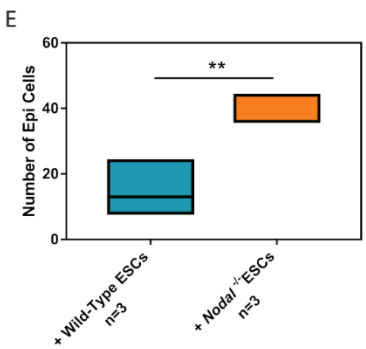
E
Number of Epi Cells
60
40
20
0
**
+ Wild-Type ESCs n=3
+ Nodal -/- ESCs n=3

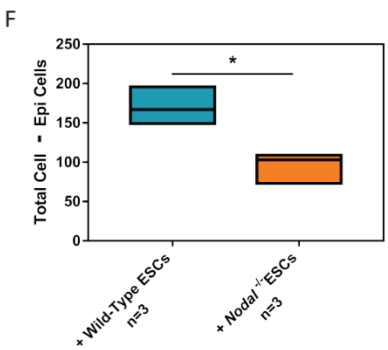
F
Total Cell - Epi Cells
250
200
150
100
50
0
*
+ Wild-Type ESCs n=3
+ Nodal -/- ESCs n=3

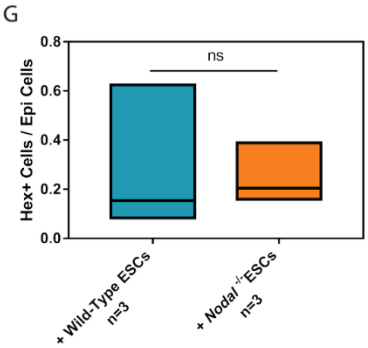
G
Hex+ Cells / Epi Cells
0.8
0.6
0.4
0.2
0.0
ns
+ Wild-Type ESCs n=3
+ Nodal -/- ESCs n=3

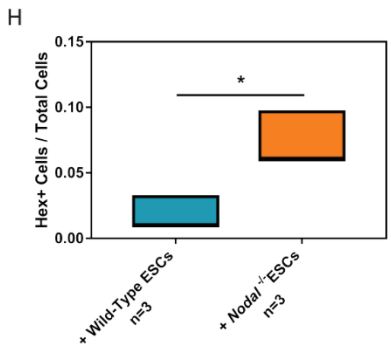
H
Hex+ Cells / Total Cells
0.15
0.10
0.05
0.00
*
+ Wild-Type ESCs n=3
+ Nodal -/- ESCs n=3

Supplementary figure 6: The initial *Nodal* expression in the PrE is sufficient to drive ICM maturation

A. MIP rendered inner views (2D) of whole-mount immunostained wild-type chimeras aggregated with *Nodal*::YFP ESCs that used to be cultured in either 2i media or in serum. Embryos were staged ~E4.25 or ~E4.5 depending on the expression pattern of NANOG. The *Nodal*::YFP expression pattern is shown using an anti-GFP antibody. ESCs are tracked following mCherry expression. Scale bars = 20µm. **B.** Histogram displaying the contribution of *Nodal*::YFP in the Epi in the embryos cultured as described in (**A.**). **C.** Histogram displaying the percentage YFP/mCherry double positive cells in the embryos cultured as described in (**A.**). **D.** Box plot showing the number of Epi cells derived from the ESCs in the embryos at the end of the culture as described in (**Fig. 6B**.). **E.** Box plot displaying the number of Epi cells from the embryos cultured in (**Fig. 6K**.). **F.** Box plot displaying the total cell number without the number of Epi cells from the embryos cultured in (**Fig. 6K**.). **G.** Box plot displaying the ratio of Hex+ cells over the number of Epi cells from the embryos cultured in (**Fig. 6K**.). **H.** Box plot displaying the ratio of Hex+ cells over the total number of cells from the embryos cultured in (**Fig. 6K**.). Statistical significance is calculated using T. tests with Pvalues represented as following: *<0.05; **<0.01 ; ***<0.001.

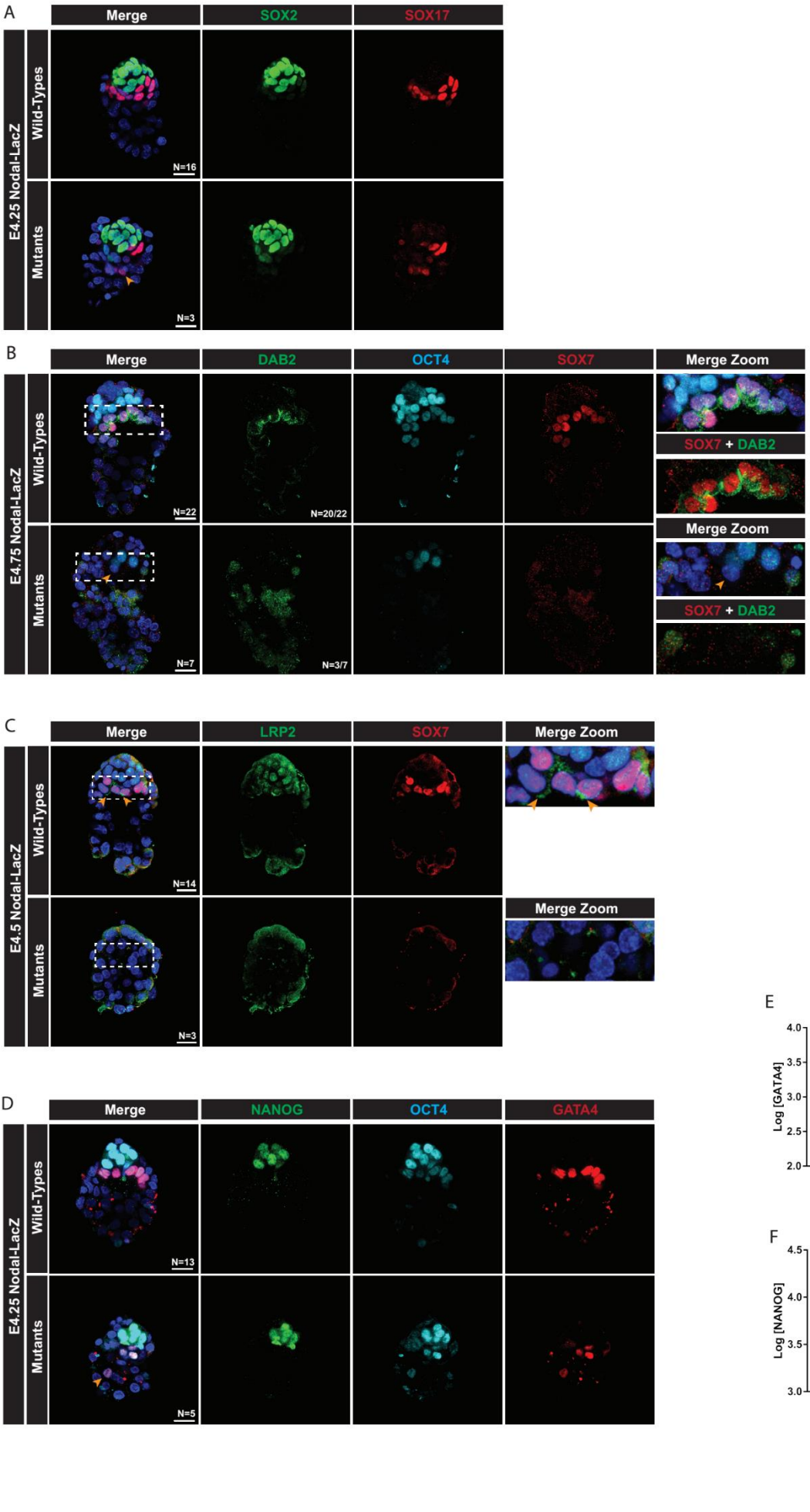
A
Merge
SOX2
SOX17
E4.25 Nodal-LacZ
Wild-Types
Mutants
N=16
N=3
B
Merge
DAB2
OCT4
SOX7
Merge Zoom
E4.75 Nodal-LacZ
Wild-Types
Mutants
N=22
N=20/22
N=7
N=3/7
SOX7 + DAB2
Merge Zoom
SOX7 + DAB2
C
Merge
LRP2
SOX7
Merge Zoom
E4.5 Nodal-LacZ
Wild-Types
Mutants
N=14
N=3
Merge Zoom
D
Merge
NANOG
OCT4
GATA4
E4.25 Nodal-LacZ
Wild-Types
Mutants
N=13
N=5
E
***
Log [GATA4]
4.0
3.5
3.0
2.5
2.0
WT
n=14
Mutants
n=13
F
***
Log [NANOG]
4.5
4.0
3.5
3.0
Wild-Types
n=21
Mutants
n=15

Supplementary figure 7: Zygotic NODAL is essential for late PrE and Epi patterning

A. MIP rendered inner views (2D) of whole-mount immunostained E4.25 Nodal-LacZ embryos showing the Epi (SOX2) and PrE (SOX17) lineages. Orange arrow indicates a misplaced PrE cell. **B.** MIP rendered inner views (2D) of whole-mount immunostained E4.5 Nodal-LacZ embryos showing apical-basal polarity of the PrE (DAB2). White rectangle dashes indicate the numerical zoom made of this zone and displayed to the right side of the panel. Numbers in the DAB2 column corresponds to the number of DAB2+ embryos over the total number of embryos stained **C.** MIP rendered inner views (2D) of whole-mount immunostained E4.5 Nodal-LacZ embryos showing apical-basal polarity of the PrE (LRP2). White rectangle dashes indicate the numerical zoom made of this zone and displayed to the right side of the panel **D.** MIP rendered inner views (2D) of whole-mount immunostained E4.25 Nodal-LacZ embryos showing the Epi (NANOG), PrE (GATA4) and ICM (OCT4) populations. Orange arrow indicates a misplaced PrE cell. **E.** Scatter plots showing the corrected GATA4 fluorescence intensity of each nuclei in the wild-type (N=2) or mutant (N=2) embryos shown in (**D.**). n represents the number of nuclei used in this quantification. **F.** Scatter plots showing the corrected NANOG fluorescence intensity of each nuclei in the wild-type (N=2) or mutant (N=2) embryos shown in (**D.**). n represents the number of nuclei used in this quantification. Scale bars = 20µm. Statistical significance is calculated using T.tests with Pvalues represented as following: *<0.05 ; **<0.01 ; ***<0.001. Scale bars = 20µm.

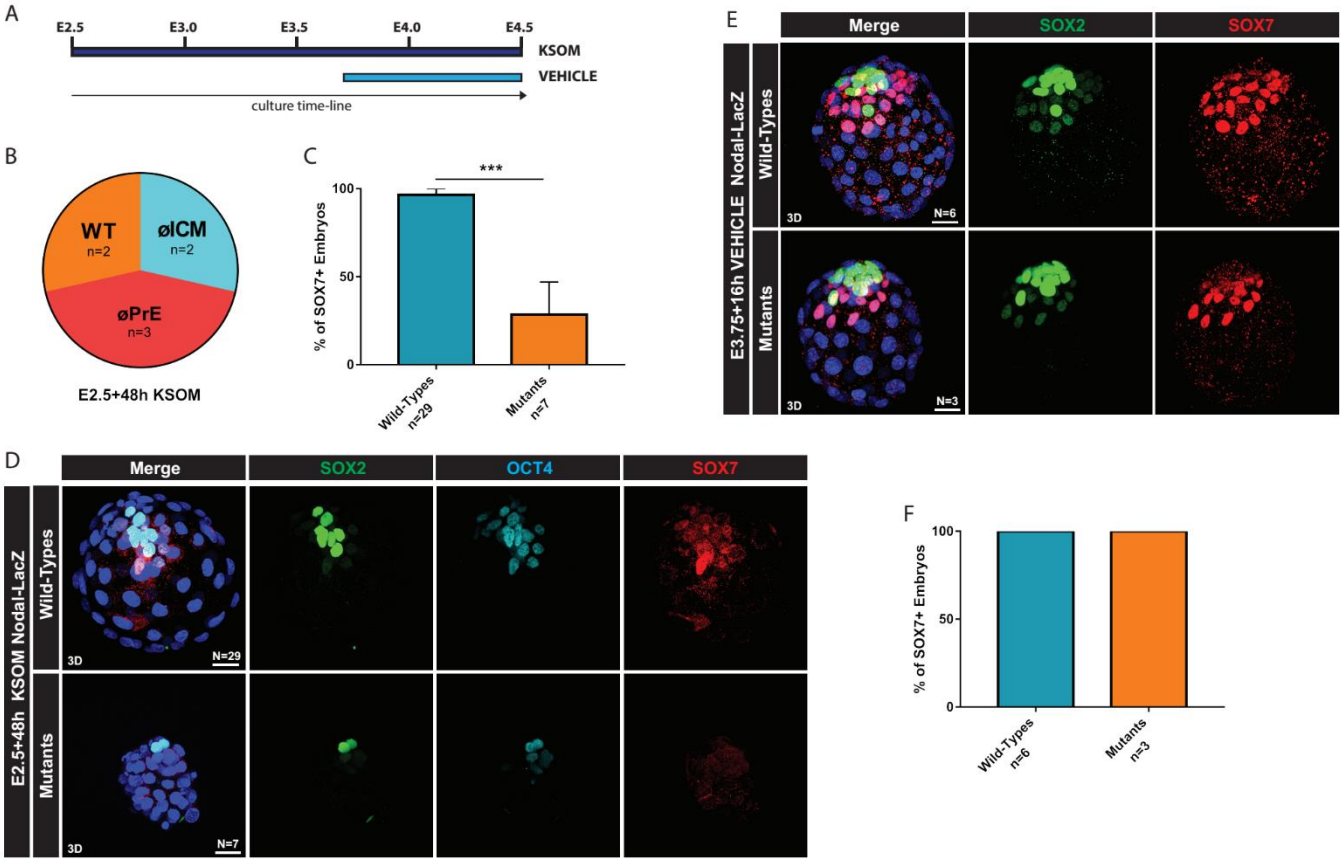
A
E2.5
E3.0
E3.5
E4.0
E4.5
KSOM
VEHICLE
culture time-line
B
WT
n=2
øICM
n=2
øPrE
n=3
E2.5+48h KSOM
C
***
% of SOX7+ Embryos
100
50
0
Wild-Types
n=29
Mutants
n=7
D
Merge
SOX2
OCT4
SOX7
E2.5+48h KSOM Nodal-LacZ
Wild-Types
Mutants
3D
N=29
N=7
E
Merge
SOX2
SOX7
E3.75+16h VEHICLE Nodal-LacZ
Wild-Types
Mutants
3D
N=6
N=3
F
% of SOX7+ Embryos
100
50
0
Wild-Types
n=6
Mutants
n=3

Supplementary figure 8: NODAL presence conditions early steps of ICM development

A. Schematic representation of the different culture conditions applied for the following experiments. Embryos from *Nodal-LacZ* KiHet x *Nodal-LacZ* KiHet were cultured in either another media (KSOM) for 48h or from E3.75+16h. At the end of the culture the embryos were fixed, analyzed and then genotyped. **B.** Pie representation of the different phenotypes observed in the *Nodal* mutants' embryos at the end of a 48h culture in KSOM (**D.**). øPrE: embryos without SOX7; øICM: embryos without SOX2 and SOX7; WT: embryos resembling wild-type embryos. **C.** Histogram displaying the percentages of embryos expressing SOX7 at the end of all cultured conditions shown in (**D.**). **D.** MIP rendered surface views (3D) of whole-mount immunostained *Nodal-LacZ* KiHet x *Nodal-LacZ* KiHet embryos cultured from E2.5 for 48h in KSOM (**A.**) showing ICM derivatives expression patterns: Epi (SOX2), ICM (OCT4) and PrE (SOX7). Mutants embryos are categorized according to their phenotype as described in (**B.**). **E.** MIP rendered surface views (3D) of whole-mount immunostained *Nodal-LacZ* KiHet x *Nodal-LacZ* KiHet embryos cultured from E3.75 for 16h in vehicle (**A.**) showing both Epi (SOX2) and PrE (SOX7) expression patterns. **F.** Histogram displaying the percentages of embryos expressing SOX7 at the end of all cultured conditions shown in (**E.**). Scale bar = 20µm. Statistical significance is calculated using T.tests with Pvalues represented as following: *<0.05 ; **<0.01 ; ***<0.001.

βCATENIN Regulates Cell Differentiation of the Blastocyst Lineages

βCATENIN activity restrains HIPPO signalling and the specification of TE fate

Two conditional alleles of Ctnnb1 were used to study the role of the transcriptional activity of βCATENIN (also known as CTNNB1) in the developing blastocyst (Fig. 1A). The loss-of-function (LOF) allele Ctnnb1 tm2Kem[442], where exons 2 to 6 are floxed, so that their deletion generates a truncated protein that can still perform its function in cellular adhesion, but not in signalling[471]. The gain-of-function (GOF) allele Ctnnb1 tm1Mmt[462], where exon 3 is floxed, so that its deletion generates a protein that can no longer be targeted for degradation, and is therefore stabilised.

Homozygote LOF embryos were generated by crossing heterozygotes carrying one copy of the deleted version of the allele. GOF embryos were obtained by crossing heterozygotes carrying the floxed version allele with PGK-Cre transgenic mice.

Immunostaining for markers that allowed ICM and TE cells to be counted showed that E3.5 embryos homozygote for the LOF allele had a higher percentage of TE cells than wildtype embryos (Fig. 1B, C). This was associated with a higher level of expression of CDX2 and GATA3 in these cells (Fig. 1D). In contrast, E3.5 embryos homozygote for the GOF allele had a lower percentage of TE cells than wildtype embryos (Fig. 1E, F), associated with lower and more heterogeneous expression of GATA3 (Fig. 1G). To understand the role of βCATENIN in how the balance between ICM and TE is established, we looked at YAP, which is known to promote the specification of a TE identity in cells where it is translocated to the nucleus. We found that E3.25 embryos homozygote for the LOF allele maintained higher levels of nuclear YAP in their cells than wildtype embryos (Fig. 1H, I).

These results therefore identify a role for βCATENIN in the allocation of TE and ICM fates and suggest it normally acts to restrain the expression and nuclear localization of YAP. The fact that the two alleles had opposite effects on the development of the blastocyst confirms that the function affected in the LOF allele is the one of interest to us.

βCATENIN activity delays the emergence of the PrE during the second cell-fate specification

Cell counting revealed that most of the difference in TE allocation in homozygote LOF embryo resulted from a decrease in ICM cell number (Fig. 2A). The ICM at this stage contains NANOG-positive

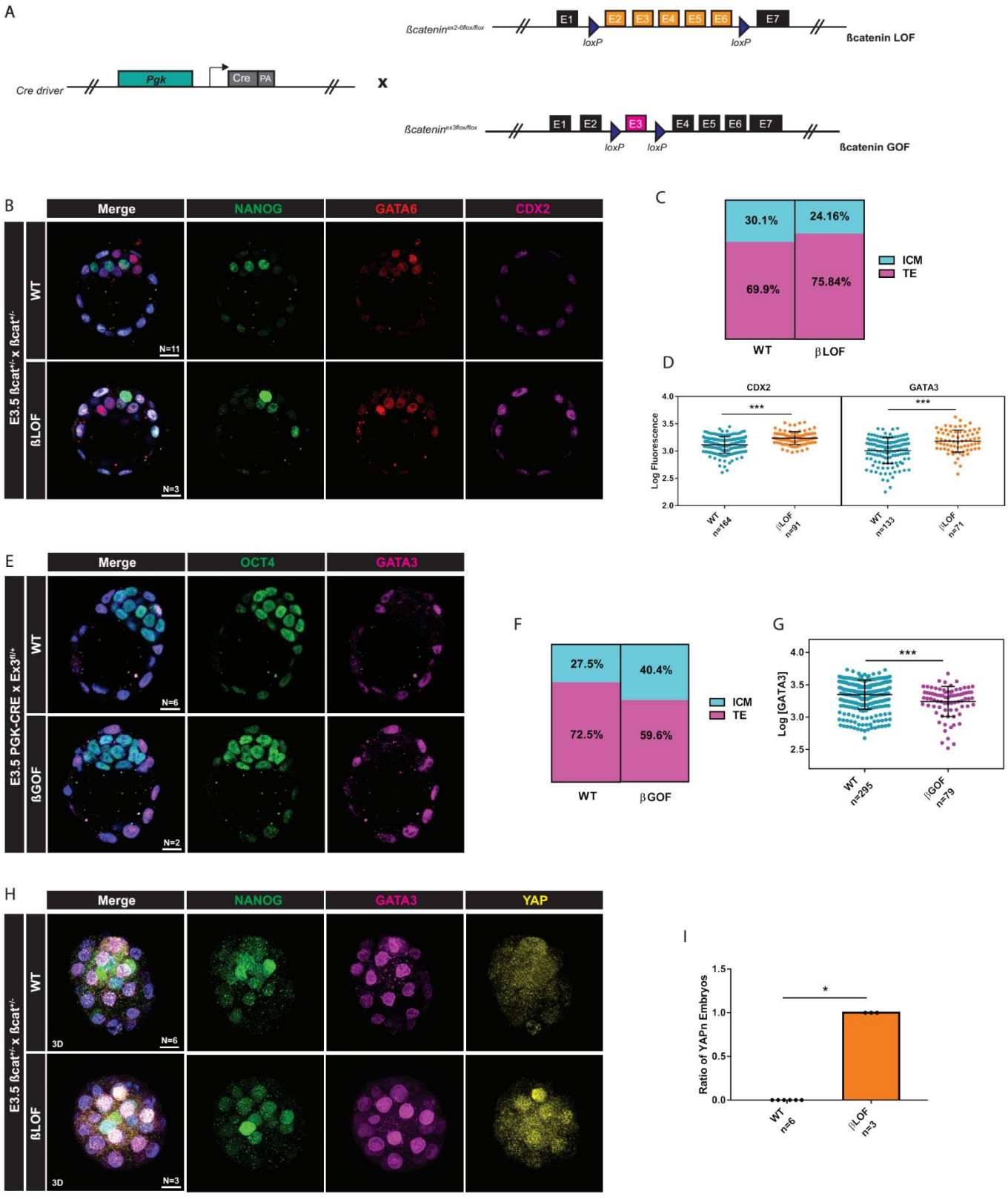
A
ßcatenin ex2-6flox/flox
E1
E2
E3
E4
E5
E6
E7
loxP
loxP
ßcatenin LOF
Cre driver
Pgk
Cre
PA
x
ßcatenin ex3flox/flox
E1
E2
E3
E4
E5
E6
E7
loxP
loxP
ßcatenin GOF
B
Merge
NANOG
GATA6
CDX2
E3.5 ßcat+/- x ßcat+/-
WT
ßLOF
N=11
N=3
C
30.1%
24.16%
69.9%
75.84%
ICM
TE
WT
βLOF
D
CDX2
GATA3
***
***
Log Fluorescence
4.0
3.5
3.0
2.5
2.0
WT n=164
βLOF n=91
WT n=133
βLOF n=71
E
Merge
OCT4
GATA3
E3.5 PGK-CRE x Ex3fl/+
WT
ßGOF
N=6
N=2
F
27.5%
40.4%
72.5%
59.6%
ICM
TE
WT
βGOF
G
***
Log [GATA3]
4.0
3.5
3.0
2.5
WT n=295
βGOF n=79
H
Merge
NANOG
GATA3
YAP
E3.5 ßcat+/- x ßcat+/-
WT
ßLOF
3D
N=6
3D
N=3
I
*
Ratio of YAPn Embryos
1.5
1.0
0.5
0.0
WT n=6
βLOF n=3

Figure 1: βCATENIN activity restrains HIPPO signalling and the specification of TE fate

A. Schematic representation of the crosses made to recover βLOF and βGOF mutant embryos. The ubiquitously expressed *Pgk* gene drives the expression of the Cre that removes the loxP sites and excludes the exon 2 to 6 for βLOF and the exon 3 for βGOF. **B.** Maximum intensity projection (MIP) of confocal images rendering the inner views (2D) of whole-mount immunostained E3.5 βLOF embryos showing the Epi (NANOG), PrE (GATA6) and TE (CDX2) lineages. **C.** Histogram displaying the percentages of tissue composition of the embryos shown in (**B.**): ICM (cyan) counted from both NANOG+ and GATA6+ cells; TE (pink) counted from CDX2+ cells. The numbers are reported to the total cell number of the embryos to obtain the percentage. WT: N=6; βLOF: N=3. **D.** Scatter plots showing the corrected fluorescence intensity of each nuclei for CDX2 and GATA3 in WT (N=6) or βLOF (N=3) embryos shown in (**B.**) and in (**H.**). n represents the number of nuclei used in this quantification. **E.** MIP rendering the inner views (2D) of whole-mount immunostained E3.5 βGOF embryos showing the ICM (OCT4) and TE (GATA3) lineages. **F.** Histogram displaying the percentages of tissue composition of the embryos shown in (**E.**): ICM (cyan) counted from OCT4+ cells; TE (pink) counted from CDX2+ cells. The numbers are reported to the total cell number of the embryos to obtain the percentage. WT: N=13; βLOF: N=6 **G.** Scatter plots showing the corrected fluorescence intensity of each nuclei for GATA3 in WT (N=6) or βGOF (N=3) embryos shown in (**B.**) and in (**H.**). n represents the number of nuclei used in this quantification. **H.** MIP rendering the surface views (3D) of whole-mount immunostained E3.25 βLOF embryos showing the ICM (NANOG) and TE (GATA3) lineages and the nuclear localization for YAP. **I.** Histogram displaying the ratio of embryos with TE cells positive for nuclear YAP as shown in (**H.**). Scale bar = 20µm. Statistical significance is calculated using T.tests with Pvalues represented as following: *<0.05 ; **<0.01 ; ***<0.001.

presumptive Epi cells, GATA6-positive presumptive PrE cells and GATA6-NANOG double positive cells, which are still awaiting specification[27]. Within the ICM of homozygote embryos, the main change was a 40% reduction in the percentage of these GATA6-NANOG double positive cells (Fig. 2B), an indication that their specification towards an Epi or PrE fate took place at a faster pace than in wildtype embryos. We measured an increase in the expression of GATA6 in these embryos (Fig. 2C), while the expression of NANOG was unchanged, suggesting βCATENIN was involved in the regulation of *Gata6*.

In contrast, E3.5 embryos carrying the activated form of the GOF allele had a lower total cell number than wildtype embryos. It resulted from a drastic 35% reduction in the number of TE cells. These embryos also saw a concomitant 35% rise in their number of Epi cells (Fig. 2E), while their number of PrE cells was unchanged, which translated into a gain of 8% in the percentage of Epi cells in their ICM (Fig. 2F). The expression levels of the Epi-specific SOX2 and PrE-specific SOX17 were however unchanged (Fig. 2G).

These results therefore suggest that βCATENIN signalling also interferes with the second cell-fate specification, where it appears to delay the emergence of the PrE and to promote that of the Epi.

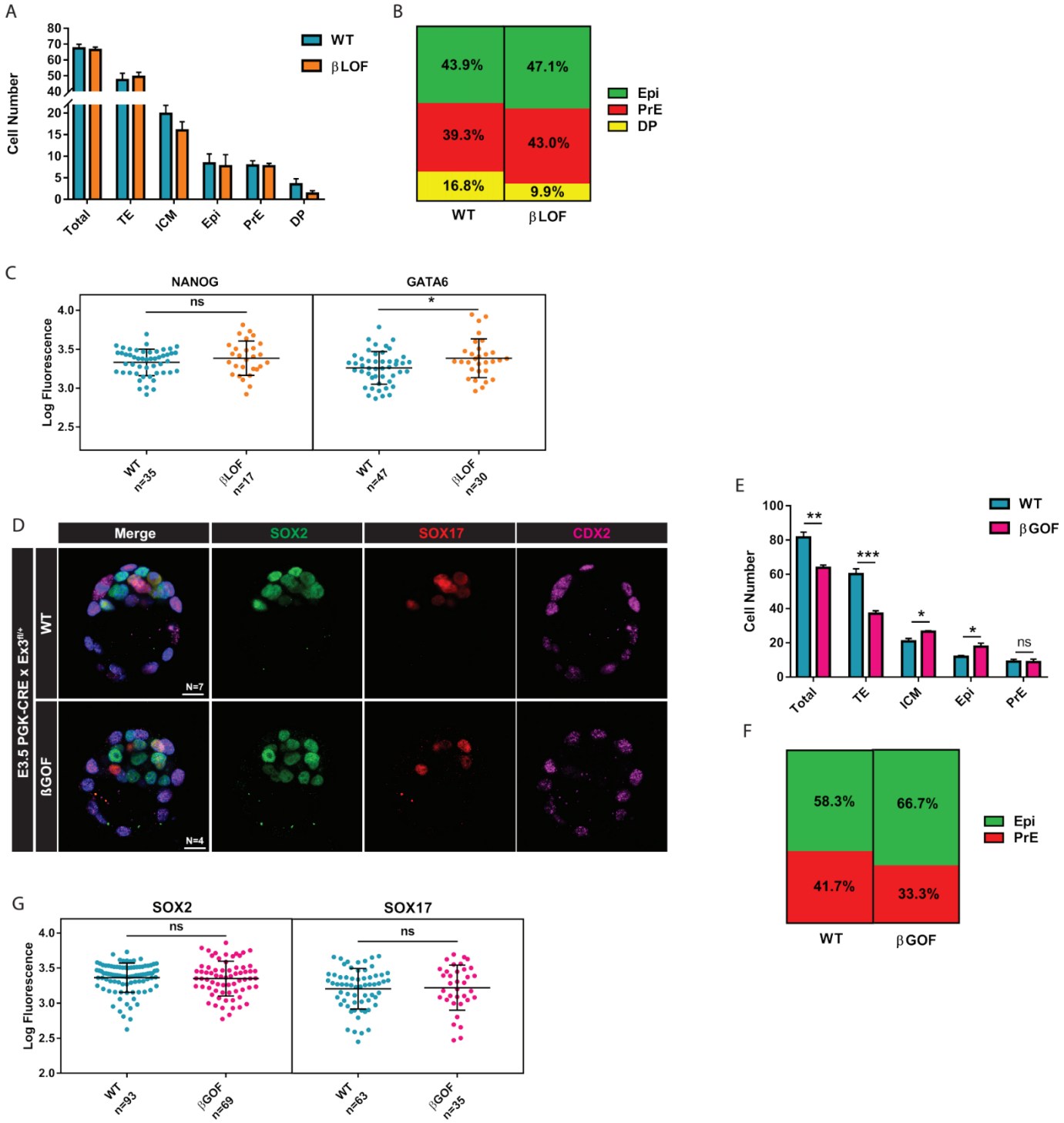
A
Cell Number
WT
βLOF
Total
TE
ICM
Epi
PrE
DP
B
43.9%
47.1%
39.3%
43.0%
16.8%
9.9%
WT
βLOF
Epi
PrE
DP
C
NANOG
GATA6
ns
*
Log Fluorescence
WT n=35
βLOF n=17
WT n=47
βLOF n=30
D
Merge
SOX2
SOX17
CDX2
E3.5 PGK-CRE x Ex3fl/+
WT
βGOF
N=7
N=4
E
Cell Number
WT
βGOF
**
***
*
*
ns
Total
TE
ICM
Epi
PrE
F
58.3%
66.7%
41.7%
33.3%
Epi
PrE
WT
βGOF
G
SOX2
SOX17
ns
ns
Log Fluorescence
WT n=93
βGOF n=69
WT n=63
βGOF n=35

Figure 2: βcatenin activity delays the emergence of the PrE during the second cell-fate specification

A. Histogram displaying the number of cells associated with each lineage and the total cell number of E3.5 WT (N=6) and βLOF (N=3) embryos shown in (**Fig. 1B.**). DP cells correspond to NANOG+; GATA6+ cells that are not allocated to either Epi or PrE yet. **B.** Representation of the ICM composition in the embryos shown in (**Fig. 1B.**). Epi (green) counted from NANOG+ and PrE (red) counted from GATA6+ cells. The numbers are reported to the total cell number of the embryos to obtain the percentage. WT: N=6; βLOF: N=3. **C.** Scatter plots showing the corrected fluorescence intensity of each nuclei for NANOG and GATA6 in WT (N=6) or βLOF (N=3) embryos shown in (**Fig. 1B.**). n represents the number of nuclei used in this quantification. **D.** MIP rendering the inner views (2D) of whole-mount immunostained E3.5 βGOF embryos showing the ICM (SOX2) and PrE (SOX17) lineages. **E.** Histogram displaying the number of cells associated with each lineage and the total cell number of E3.5 WT (N=7) and βGOF (N=4) embryos shown in (**D.**) **F.** Representation of the ICM composition in the embryos shown in (**D.**). Epi (red) counted from SOX2+; SOX17- and PrE (green) counted from SOX17+ cells. The numbers are reported to the total cell number of the embryos to obtain the percentage. WT: N=7; βGOF: N=4. **G.** Scatter plots showing the corrected fluorescence intensity of each nuclei for SOX2 and SOX17 in WT (N=7) or βGOF (N=4) embryos shown in (**D.**). n represents the number of nuclei used in this quantification. Scale bar = 20μm. Statistical significance is calculated using T.tests with Pvalues represented as following: *<0.05 ; **<0.01 ; ***<0.001.

CHIR-treated embryos fail to develop properly and prevent the maturation of the PrE

To characterize in greater detail the role of βCATENIN during blastocyst development we cultured E2.5 embryos in the presence or absence of the glycogen synthase kinase 3 (GSK3) inhibitor CHIR99021, which prevents βCATENIN degradation and therefore acts as a βCATENIN activator. We found that only 20% of embryos cultured for 48h in the presence of 3μM CHIR completed the segregation of their ICM into separate Epi and PrE layers, against 80% for controls (Fig. 3A, B). However, the treatment had no impact on the expression levels of *Fgf4*, which encodes the Epi-produced ligand promoting PrE development, and *Gata4*, the expression of which is specific of committed PrE cells (Fig. 3C). A comparison of the impact of 3μM and 10μM CHIR treatments on the expression of the WNT/ βCATENIN signalling pathway target *Axin2* in 48h cultured E2.5 embryos found that the higher concentration of the inhibitor was far more effective at activating the pathway. Embryos treated with 10μM CHIR were as likely to complete the segregation of their ICM than embryos treated with 3μM CHIR (Fig. 3E, F), but they expressed *Gata4* at a significantly lower level than controls while Gata6 levels appeared unaffected (Fig. 3H). This fit with our previous results suggesting that βCATENIN delays PrE specification and promotes Epi development. The findings that these CHIR-treated embryos saw a drastic increase in the expression of *Nanog* (Fig. 3G), but were less likely to express the mature PrE marker *Sox7* (Fig. 3I, J) were also consistent with this interpretation. We thus decided to use CHIR at a

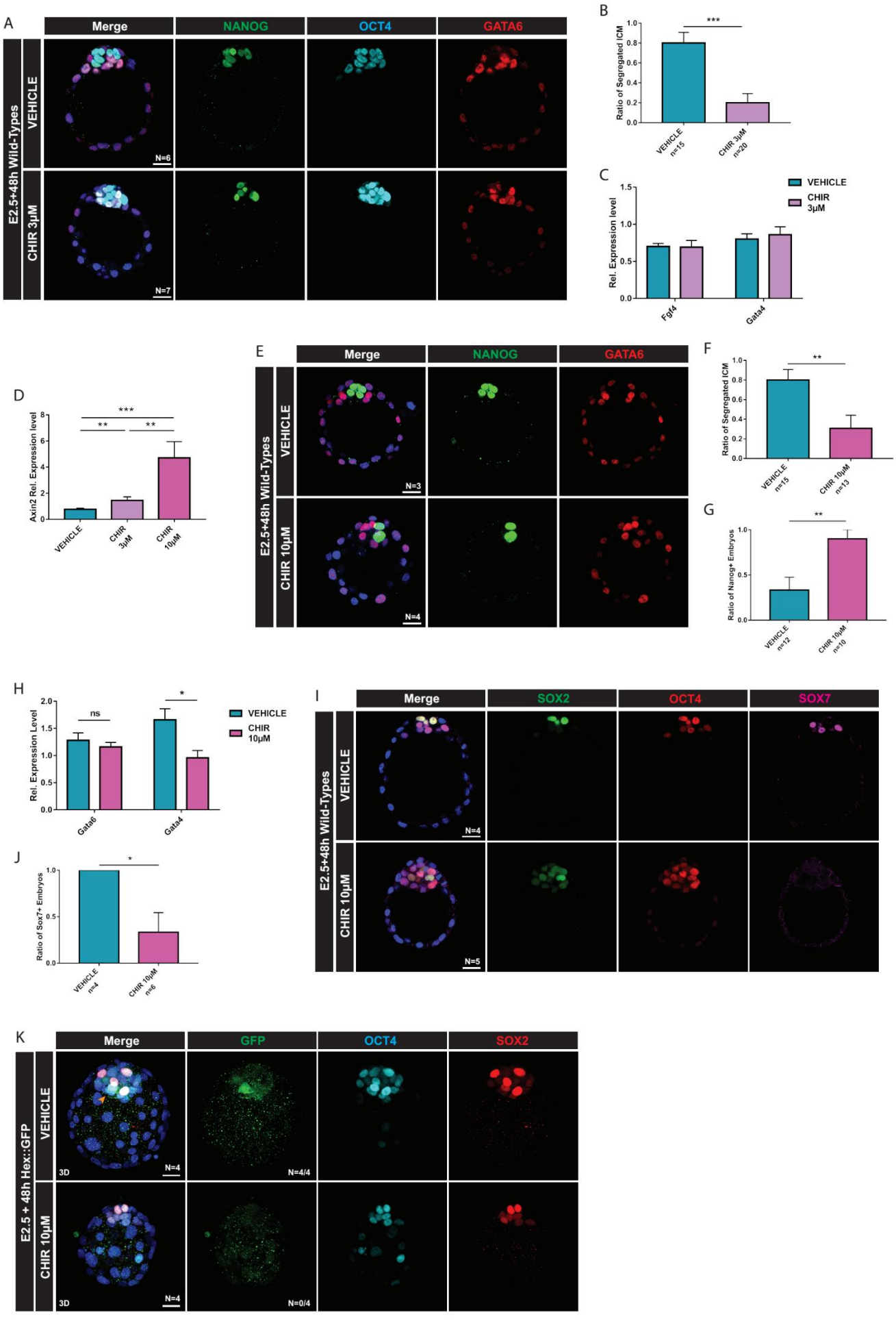
A
Merge
NANOG
OCT4
GATA6
E2.5+48h Wild-Types
VEHICLE
CHIR 3µM
N=6
N=7
B
Ratio of Segregated ICM
***
VEHICLE n=15
CHIR 3µM n=20
C
Rel. Expression level
VEHICLE
CHIR 3µM
Fgf4
Gata4
D
Axin2 Rel. Expression level
***
**
**
VEHICLE
CHIR 3µM
CHIR 10µM
E
Merge
NANOG
GATA6
E2.5+48h Wild-Types
VEHICLE
CHIR 10µM
N=3
N=4
F
Ratio of Segregated ICM
**
VEHICLE n=15
CHIR 10µM n=13
G
Ratio of Nanog+ Embryos
**
VEHICLE n=12
CHIR 10µM n=10
H
Rel. Expression Level
ns
*
VEHICLE
CHIR 10µM
Gata6
Gata4
I
Merge
SOX2
OCT4
SOX7
E2.5+48h Wild-Types
VEHICLE
CHIR 10µM
N=4
N=5
J
Ratio of Sox7+ Embryos
*
VEHICLE n=4
CHIR 10µM n=6
K
Merge
GFP
OCT4
SOX2
E2.5 + 48h Hex::GFP
VEHICLE
CHIR 10µM
3D
N=4
N=4/4
N=0/4

Figure 3: CHIR-treated embryos fail to develop properly and prevent the maturation of the PrE

A. MIP rendering the inner views (2D) of whole-mount immunostained E2.5 WT embryos cultured for 48h in control (VEHICLE) or in 3µM CHIRION (CHIR 3µM) showing the ICM (OCT4), Epi (NANOG) and PrE (GATA6) lineages. **B.** Histogram displaying the ratio of correctly segregated ICM in control (N=15) or treated embryos (N=20) shown in (**A.**) **C.** Histogramm displaying RT-qPCR data from whole-mount lysed E2.5 embryos cultured for 48h in control or CHIR 3µM conditions. *Fgf4* (Epi) and *Gata4* (PrE) relative expression were obtained after being normalized by *Gapdh*. **D.** Histogram displaying the expression level of *Axin2* by RT-qPCR obtained from lysed E2.5+48h cultured embryos in increasing dose of CHIR (CHIR 3µM; CHIR 10µM). **E.** MIP rendering the inner views (2D) of whole-mount immunostained E2.5 WT embryos cultured for 48h in control or in CHIR 10µM showing the Epi (NANOG) and PrE (GATA6) lineages. **F.** Histogram displaying the ratio of correctly segregated ICM in control (N=15) or treated embryos (N=13) shown in (**E.**). **G.** Histogram displaying the ratio of NANOG+ E3.5+24h cultured embryos in control or CHIR 10µM conditions. **H.** Histogramm displaying RT-qPCR data for the early (*Gata6*) and definitive (*Gata4*) PrE markers from whole-mount lysed E2.5 embryos cultured for 48h in control or CHIR 10µM conditions. **I.** MIP rendering the inner views (2D) of whole-mount immunostained E2.5 WT embryos cultured for 48h in control or in CHIR 10µM showing the ICM (OCT4), late Epi (SOX2) and late PrE (SOX7) lineages. **J.** Histogram displaying the ratio of SOX7+ embryos cultured as described in (**I.**). **K.** MIP rendering the surface views (3D) of whole-mount immunostained E2.5 *Hex*::GFP embryos cultured for 48h in control or in CHIR 10µM showing the expression pattern of the blastocyst polarization marker *Hex*. *Hex* expression is renderer using an anti-GFP antibody. N in the GFP columns represents the number of embryos GFP+ over the total number of *Hex*::GFP cultured in their condition. Orange arrowhead indicates a GFP+ cell in the PrE lineage. Scale bar = 20µm. Statistical significance is calculated using T.tests with Pvalues represented as following: *<0.05 ; **<0.01 ; ***<0.001.

10µM concentration for the rest of our study. To investigate further the impact of this treatment on PrE development we looked at the expression of Hex, which normally appears at E3.75 in a subset of asymmetrically positioned PrE cells[343], using embryos carrying the Hex::GFP reporter transgene[154]. We found that exposure of these embryos to CHIR prevented the expression of the transgene, further evidence that early βCATENIN activity hampers the maturation of the PrE.

Stage-dependent BCATENIN activity leads to early retention of ICM markers and subsequent ectopic mesoderm differentiation

The development and the maturation of the PrE are known to depend on events taking place in the Epi. We thus investigated the impact of CHIR treatment on the Epi. Although the expression of the genes encoding the pluripotency factors OCT4, NANOG and KLF4 was not affected in CHIR-treated embryos (Fig. 4A) all ICM cells were found to retain both SOX2 and OCT4 a delay in Epi maturation

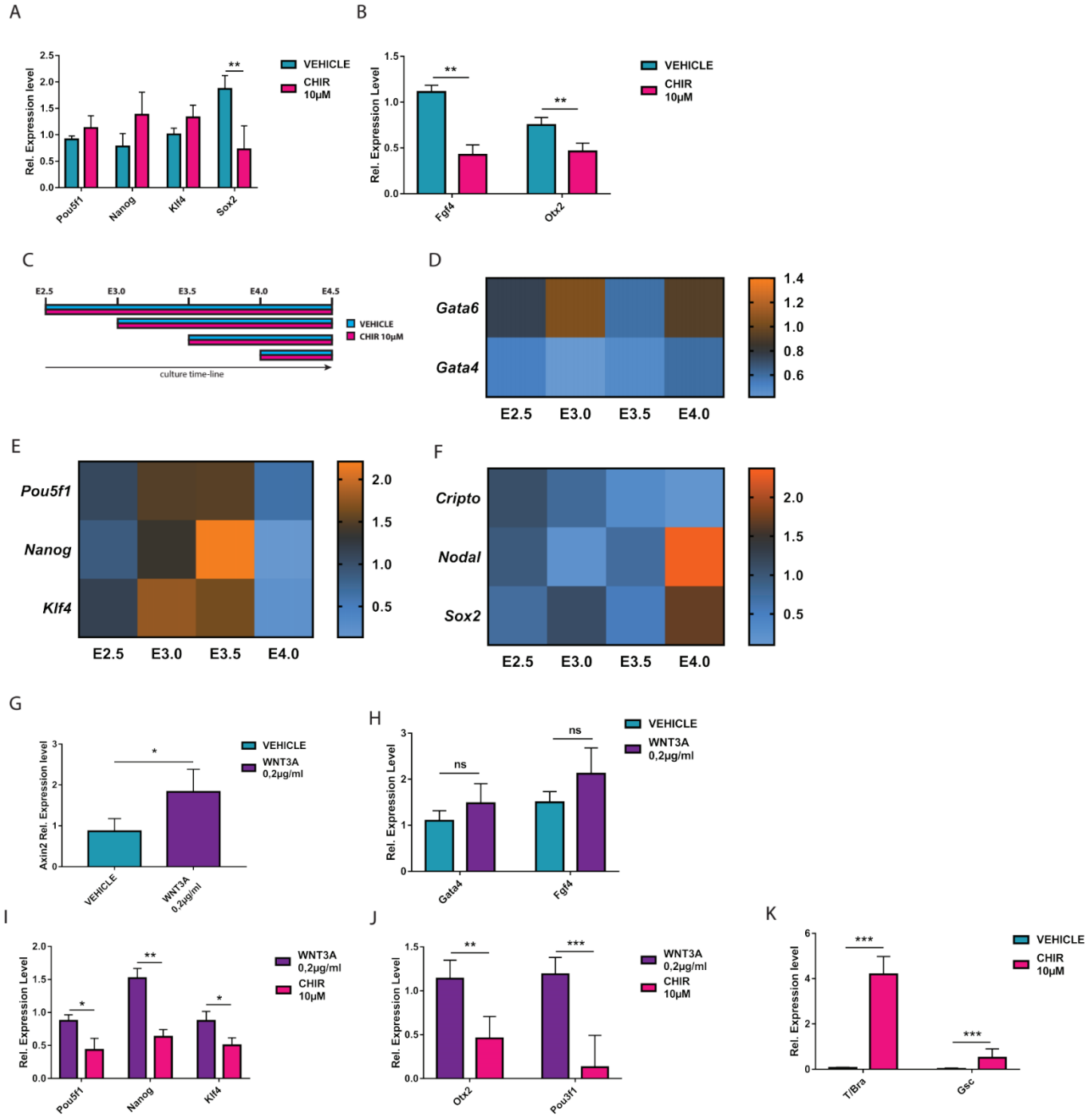

Figure 4: Stage-dependent βCATENIN activity leads to early retention of ICM markers and subsequent ectopic mesoderm differentiation

A. Histogramm displaying the expression levels of the so-called pluripotency factors by RT-qPCR on whole-mount lysed E2.5 embryos cultured for 48h in control or CHIR 10µM conditions. **B.** Histogramm displaying the expression levels of Epi specific genes by RT-qPCR on whole-mount lysed E2.5 embryos cultured for 48h in control or CHIR 10µM conditions. **C.** Schematic representation of the different culture conditions applied for the following experiments shown in (**F.**, **G.** and **H.**) All cultured embryos shared the same ending point with only the start of the culture being changed. **F.** Heatmap displaying

the normalized relative expression of PrE genes obtained from a unique RT-qPCR experiment on the embryos (N≥6) cultured in the conditions presented in (**C.**). The double color scale on the right represents the normalized base-1 expression values with the orange indicating higher and light blue lower enrichment of cDNAs. Each couple experiment (control/inhibitor) was conducted using embryos from the same litter for a total of 2 separated experiments for all conditions. All gene expression in control condition are normalized to a base-1. **D.** Heatmap displaying the normalized relative expression of pluripotency factors obtained from a unique RT-qPCR experiment on the embryos (N≥6) cultured in the conditions presented in (**C.**). **E.** Heatmap displaying the normalized relative expression of Epi genes obtained from a unique RT-qPCR experiment on the embryos (N≥6) cultured in the conditions presented in (**C.**). **F.** Histogramm displaying the expression levels *Axin2* by RT-qPCR on whole-mount lysed E3.5 embryos cultured for 24h in control or WNT3A 0.2µg/ml conditions. **G.** Histogramm displaying the expression levels of *Fgf4* (Epi) and *Gata4* (PrE) by RT-qPCR on whole-mount lysed E3.5 embryos cultured for 24h in control or WNT3A 0.2µg/ml conditions**. H.** Histogramm displaying the expression levels of the so-called pluripotency factors by RT-qPCR on whole-mount lysed E4.0 embryos cultured for 12h in WNT3A 0.2µg/ml or CHIR 10µM conditions. **I.** Histogramm displaying the expression levels of the late Epi markers by RT-qPCR on whole-mount lysed E4.0 embryos cultured for 12h in WNT3A 0.2µg/ml or CHIR 10µM conditions. **J.** Histogramm displaying the expression levels of the mesoderm-associated genes by RT-qPCR on whole-mount lysed E3.5 embryos cultured for 24h in control or CHIR 10µM conditions. Statistical significance is calculated using T.tests with Pvalues represented as following: *<0.05 ; **<0.01 ; ***<0.001.

(Fig. 3I), a result consistent with such embryos maintaining *Nanog* expression longer than controls (Fig. 3G). In contrast, the expression of *Sox2* was halved compared to control embryos. This CHIR treatment also resulted in lower expression levels for *Fgf4,* something we had not detected at lower CHIR concentration, and *Otx2*, which at this stage can be considered as promoting the maturation of the Epi (Fig. 4C). These results thus confirmed that factors that are critical to epiblast developmental progression are responsive to βCATENIN, and this in turn has the potential to affect PrE development.

To assess how the response to CHIR changed with time we started the started the treatment at different time points and compared how it impacted the expression of Epi and PrE markers at the equivalent of E4.5 (Fig. 4C). While none of the treatments appeared to affect the expression of *Gata6* much, *Gata4* was found to be expressed at lower levels in all treated embryos (Fig. 4D). Although the expression of *Pou5f1*, *Nanog* and *Klf4* was barely affected when the treatment started at E2.5 (Fig. 4E), as we had seen before (Fig. 4A), starting the treatment at E3.0 or E3.5 led to these embryos retaining higher expression levels for these genes, suggesting βCATENIN at these stages is promoting pluripotency and preventing the maturation of the Epi. Consistent with this interpretation is the lower expression in these embryos of the genes encoding the TGFβ family member NODAL and its co-receptor CRIPTO (Fig. 4F). In contrast, starting the CHIR treatment at E4.0 resulted in a drastic downregulation of *Pou5f1*, *Nanog* and *Klf4*, and a concomitant upregulation of *Nodal* and *Sox2*

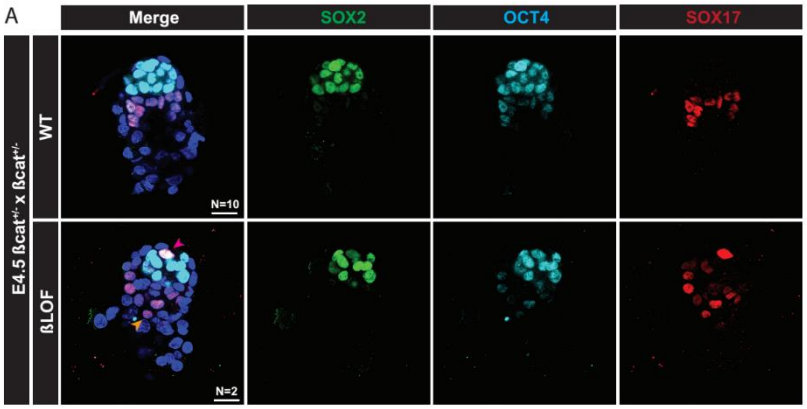
A
Merge
SOX2
OCT4
SOX17
E4.5 ßcat+/- x ßcat+/-
WT
ßLOF
N=10
N=2

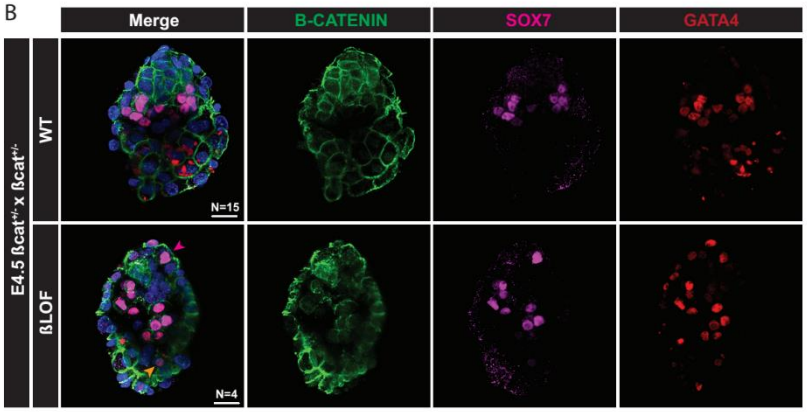
B
Merge
B-CATENIN
SOX7
GATA4
E4.5 ßcat+/- x ßcat+/-
WT
ßLOF
N=15
N=4

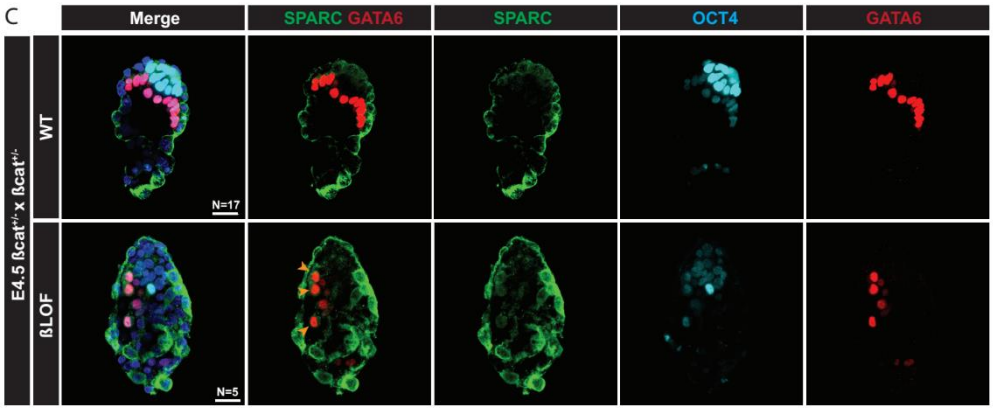
C
Merge
SPARC GATA6
SPARC
OCT4
GATA6
E4.5 ßcat+/- x ßcat+/-
WT
ßLOF
N=17
N=5

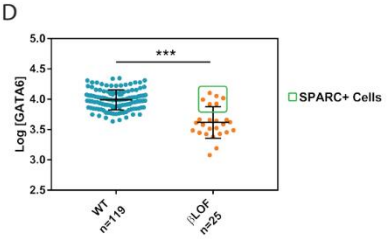
D
***
Log [GATA6]
5.0
4.5
4.0
3.5
3.0
2.5
WT n=119
ßLOF n=25
SPARC+ Cells

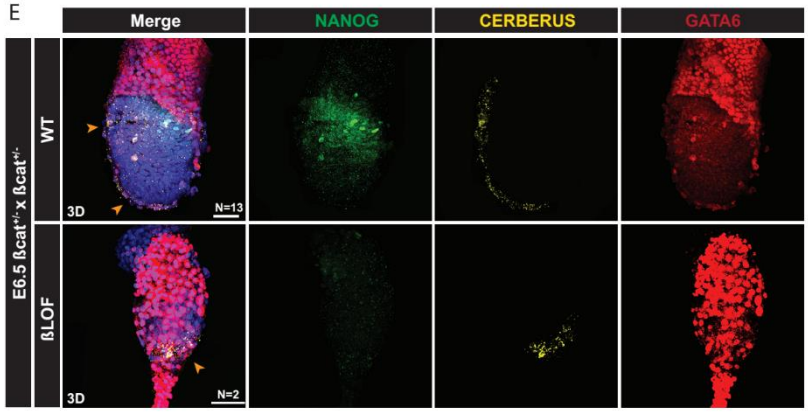
E
Merge
NANOG
CERBERUS
GATA6
E6.5 ßcat+/- x ßcat+/-
WT
ßLOF
3D
N=13
3D
N=2

Figure 5: Lack of βCATENIN activity results in PrE disorganization and premature PaE differentiation

A. MIP of confocal images rendering the inner views (2D) of whole-mount immunostained E4.5 βLOF embryos showing the Epi (SOX2), PrE (SOX17) and ICM (OCT4) populations. Orange arrow shows unorganized PrE cells. Magenta arrow shows unsegregated PrE cells. **B.** MIP of confocal images rendering the inner views (2D) of whole-mount immunostained E4.5 βLOF embryos showing PrE maturation markers (GATA4, SOX7) and the βCATENIN accumulation at the cell membranes. Orange arrow shows unorganized PrE cells. Magenta arrow shows unsegregated PrE cells. **C.** MIP of confocal images rendering the inner views (2D) of whole-mount immunostained E4.5 βLOF embryos showing the PrE (GATA6) and ICM (OCT4) populations. SPARC staining is accumulated in the cytoplasm of PaE differentiating cells. Orange arrows show overexpressing GATA6 cells co-expressing SPARC. **D.** Scatter plots showing the corrected fluorescence intensity of each nuclei for GATA6 in WT (N=8) or βLOF (N=4) embryos shown in (**C.**). Green rectangle indicates the SPARC+ cells among the GATA6+ nuclei. n represents the number of nuclei used in this quantification. **E.** MIP of confocal images rendering the surface views (3D) of whole-mount immunostained E6.5 βLOF embryos showing the Epi (NANOG), PrE-derivatives (GATA6) and the DVE/AVE subpopulations (CERBERUS). Orange arrows indicate the anterior positioning in WT embryos while pointing towards the distal tip of βLOF embryos. Scale bars = 20µm. Statistical significance is calculated using T.tests with Pvalues represented as following: *<0.05 ; **<0.01 ; ***<0.001.

(Fig. 4E, F), suggesting that βCATENIN is now repressing the pluripotency network and promoting differentiation.

Although the treatment E3.5 embryos with recombinant WNT3A ligands could elicit an increase in the expression of the WNT/ βCATENIN signalling target *Axin2* (Fig. 4G), this treatment had no detectable impact on the expression of *Gata4* and *Fgf4* (Fig. 4H), unlike CHIR. E4.0 embryos were also found to be far more responsive to CHIR than to WNT3A (Fig. 4I, J). The fact that the downregulation of *Pou5f1*, *Nanog* and *Klf4* was not associated with an increase in the expression of *Otx2* and *Pou3f1*, which promote the maturation of the Epi, suggested the possibility that the Epi might prematurely differentiate. This was further supported by our finding that E3.5 embryos treated with CHIR for 24h prematurely expressed the mesodermal markers *T/Bra* and *Gsc* (Fig. 4K).

Lack of βCATENIN activity results in PrE disorganization and premature PaE differentiation

While we found evidence that E3.5 LOF mutant embryos saw their PrE specified earlier than wildtype embryos, we repeatedly obtained evidence that the gain of βCATENIN activity delayed the maturation of this layer. We thus went back to LOF embryos to find out how the development of their PrE was affected at later stages.

E4.5 embryos homozygote for the LOF allele were found to have a disorganized PrE, SOX17-expressing cells being found scattered in the blastocoel cavity or still trapped in the Epi (Fig. 5A). These PrE cells nevertheless expressed GATA4 and SOX7, indicating that they had matured (Fig. 5B). Immunostaining against βCATENIN indicated that although matured PrE cells, among Epi cells, failed to maintain a proper cell structure as shown by disorganized membranes within the ICM (Fig. 5B). Their distribution suggested they might have prematurely formed parietal endoderm (PaE) cells, which normally migrate along the mural TE lining the blastocoel cavity. To find out we stained embryos with GATA6, which is normally upregulated in migrating PaE cells, and SPARC, which is also expressed in these cells[205,211] (Fig. 5C). We found that GATA6 cells indeed co-localized with SPARC in some of the endodermal cells that colonized the blastocoel of E4.5 mutant embryos and those cells have higher levels of GATA6 (Fig. 5C, D) By E6.5 the smaller egg-cylinder of mutant embryos appeared completely enmeshed in parietal endoderm-like cells as shown by the strong GATA6 staining the tissue morphology forming a PaE tail at the distal tip of the conceptus (Fig. 5E). The other PrE derivative, the VE is also affected by the lack of transcriptional βCATENIN as shown by the failure of the DVE to migrate anteriorly (Fig. 5E), consistent with previous reports[465].

DISCUSSION

How, with the biological material contained in one fertilized egg, a fully formed individual composed of several cell identities can be formed? Providing answers to this question has been one of the main goals of developmental biologists. Studying the specification of different cell fates can be challenging and require a system that presents the least possible complexity and the ability of researchers control of the developing environment. For those reasons, the blastocyst model has recently been at the center of many studies investigating the events of fate specification resulting in the formation of the three lineages that is composed of. These studies have highlighted the progression of lineages specification regulated by both the developmental stage and the activity of signaling pathways. Although, much has been found regarding the signaling molecules required for the specification of the lineages, the signals responsible for their maturation remain to be known.

Here I have uncovered new roles for two signaling pathways in the maturation and the balance of regulation of the lineages specified during blastocyst development. Although, ACTIVIN/NODAL and βCATENIN signaling pathways were already well identified for their impacts on early post-implantation embryos for tissue patterning and axis orientation establishment, not much was investigated regarding their earlier requirements. Both signaling pathways, are active at pre-implantation stages and involved in the different events regulating the formation of the developing blastocyst. Most of the defects I characterized during those early stages, consequently to the inactivity of both pathways, reflect the phenotypes described at the egg cylinder stage, suggesting that these phenotypes were of the resultant of earlier requirements.

NODAL Signals in the Epiblast to Ensure the Proper Development of the Blastocyst and its Derivatives

Although, previous reports have demonstrated the activity of ACTIVIN/NODAL signaling at pre-implantation stages, not much is known regarding its impact on the formation of the blastocyst[70,142,163]. A recent study has suggested that NODAL signals were involved in the developing PrE as supported by the requirements of the signaling pathway in the mESC differentiation towards an endoderm-like fate[202]. Moreover, although well characterized, part of the defects induced by the lack of Nodal at post-

implantations stages find its origin during the pre-implantation development[140]. Therefore, to better understand the roles of ACTIVIN/NODAL signaling during the early embryogenesis, I characterized the impacts of modulating the activity of the pathway to the lineages forming the blastocyst.

First, I investigated the impact of inhibiting the signaling pathway from the morula to the late blastocyst stage using a small inhibiting molecule preventing the phosphorylation of the ALK4/5 receptors. From these experiments I was able to determine that all the blastocyst lineages were affected by the lack of ACTIVIN/NODAL signaling. This resulted in a failure of the ICM to segregate properly in addition with a decrease in the blastocoel size and in cell numbers. Cells without ACTIVIN/NODAL signals failed to mature and undergo processes of apoptosis. Time gated experiments revealed that from the morula stage the ACTIVIN/NODAL signaling pathway was continuously required to support the blastocyst development (Fig. 1, S1).

BMP crosstalk and the blastocyst polarization

ACTIVIN/NODAL signals are received and translocated via the ACTRI/II located at the cell membrane. The expression patterns of these receptors during the development of the blastocyst remains to be fully elucidated. However, *in vivo* and *in vitro* experiments suggest that ACTRI/II are found in both TE and ICM lineages during the first event of fate specification. Supporting this, my data showed that both ICM and TE lineages were affected by apoptosis and the expression of markers specific to these populations was downregulated (Fig. 1, S1). It is interesting to note that similar requirements in both of these lineages were found in the context of inactive BMP signaling[105]. Indeed, consistent with our data on ACTIVIN/NODAL, BMP signaling was required to sustain cell-survival of PrE cells and to support the TE layers involving both SMAD-dependent and independent pathways[105]. Most of biochemicals studies show that ACTRI/II and BMPRI/II are very similar and that the ligands from both pathways can signal to these receptors mixing the activity of both signaling cascades together[265,266,268]. It would thus be worthy to investigate by which receptors both BMP and ACTIVIN/NODAL signal and what directly results from the activity of those receptors. It is possible than rescue mechanisms are also induced by the cells to compensate for the lack of either of the ligands.

Although, able to signal via each other receptors complexes, BMP and NODAL are shown to compete for different factors of their respective signaling cascades and thus characterized as antagonists[161,512]. The competition between these signaling pathways is responsible for the proper patterning of both the Epi and ExE after the implantation of the embryo[162,343]. The analysis of target genes expression for BMP signaling in different conditions modulating ACTIVIN/NODAL signaling indicates that the competition also occurs at pre-implantation stages (Fig. 3). Lack of pSMAD2/3 activity resulted in the

upregulation of BMP signaling, that was not countered anylonger, leading to failures of the blastocyst to be properly polarized by restricting the emergence of the *Hex* positive subpopulation of the PrE (Fig. 3, S3). Although BMP treatments negatively affected the patterning of this subpopulation, the defects were never as drastic as embryos inhibited for ACTIVIN/NODAL displayed (Fig.3, S3). Indeed, the addition of the inhibitor shortly prior to the *Hex* initiation prevented the expression of the gene, demonstrating that ACTIVIN/NODAL is essential for the early polarization of the blastocyst (Fig 3.). ChIP-seq data indicated that pSMAD2 was found at the promoter of Hex suggesting a direct control of the *Hex* expression by the ACTIVIN/NODAL signaling[164]. However, treated embryos past the time of *Hex* initiation failed to downregulate its expression indicating that different mechanisms were responsible for its initiation and maintenance (Fig. S3). Moreover, upregulation of both NODAL and ACTIVIN did not significantly increased the number of specified *Hex* positive cells suggesting that either not all PrE cells are competent for ACTIVIN/NODAL signaling to express *Hex* or that negative feedbacks are established to counter the ectopic specification of this subpopulation (Fig. 5). ACTIVIN treatment resulted in the induction of more *Hex* positive cells after the implantation, showing that VE cells are competent for the signal[144]. Interestingly, a recent study has shown that the feedback loop between NODAL and LEFTY1 was responsible for the maintenance of *Lefty1* positive subpopulation, suggested to co-express *Hex*[142]. It is therefore tempting to speculate that NODAL signals promote the specification of this lateral PrE population via the expression of both *Hex* and *Lefty1* and that the subsequent negative feedback loop from LEFTY1 is preventing the ectopic activation of this gene repertoire to the rest of the PrE layer, thus leading the polarization to one side of the embryo, later involved in the AP axis establishment.

Thus, BMP and ACTIVIN/NODAL signaling show similar roles in cell metabolism and tissue patterning. It would be interesting to investigate deeper the molecular mechanisms by which those ligands can transduce their message in order to better understand the impacts induced by the association of both signaling cascades.

NODAL promotes and maintain the identity of the Epi lineage

At post-implantation stages, *Nodal* is required for the patterning of the posterior proximal Epi and the maintenance of its pluripotency[145,343]. Although my first results regarding the inhibitor effects revealed stronger defects in the PrE layer, preventing its maturation and patterning, kinetics experiments revealed that those defects coincided with changes in the expression of Epi genes (Fig. 2, S2). Many studies have highlighted the Epi progression and the genes it expresses as essential for the maturation of the differentiating PrE[27]. My own data revealed that in SB-treated embryos, the expression of the

factors involved in the differentiation of the PrE was strongly affected, and this, depending on the developmental stage of which the embryos were incubated (Fig. 2). Starting from the morula stage the presence of the inhibitor resulted in the strong increase of *Fgf4*, *Pou5f1* and *Sox2*, known to promote the progression of cells into the PrE program as shown by the overexpression of SOX17 (Fig. 2, S2). Moreover, the retention of the so-called pluripotency network was suggested to prevent subsequent maturation of the whole ICM (Fig. 2). However, starting from the mid-blastocyst stage these genes were found downregulated in correlation with the reduction of GATA4 levels and the absence of SOX7 (Fig.2, S2). This indicated that ACTIVIN/NODAL signaling was required for the proper progression of the Epi lineage resulting in the exit of its cells from the naïve state that reflects the nascent Epi, preventing the subsequent progression of PrE cells. Consistent with *in vitro* experiments, the requirements for ACTIVIN/NODAL to maintain the Epi identity at the late blastocyst stage did not lead to its premature differentiation as shown by the lack of *Pou3f1* and *Fgf5* (Fig. 3)[80,484]. Post-implantation analyses demonstrate that Epi cells lacking NODAL were differentiating towards a neural fate[351]. It would thus be interesting to assess the identity of these cells by looking at specific markers indicating an ectopic neural induction and the signaling cascades involved in the activation of such genes. The association between FGF2 and βCATENIN has been shown to promote the differentiation of neural crest cells in hESC in absence of *Nodal*[409]. Considering the roles of FGF signaling in PrE specification and TE maturation, it would be interesting to assess the impact of pERK in a pSMAD2/3 depleted context.

Although, NODAL addition to the blastocyst promoted the Epi fate and its expansion, it still remains to understand by which mechanism the Epi depends on NODAL signals (Fig. 5). Short treatment and tissue specific effects of recombinant NODAL indicated that the ligand was specifically targeting Epi cells and activating the expression of OCT4 (Fig. 5, S4). This was consistent with *in vitro* experiments showing that during the differentiation of EpiLC, pSMAD2 was specifically promoted genes responsible for the primed pluripotency core[80,512]. Among those genes are found *Otx2*, essential for enhancers activation during the EpiLC differentiation[80,135]. *In vivo*, *Otx2* is also responsible to enhance mitosis activity and was found at the blastocyst stage to directly bind *Nanog* to promote the Epi expansion[132,513]. This was consistent with the impact of NODAL treatment to early stages of the blastocyst. Interestingly, at the mid blastocyst stage, where OTX2 promotes *Nanog* expression, the levels of OTX2 were significantly upregulated upon recombinant NODAL addition (Fig. 5, S4). Moreover, in other models OTX2 was found to depend on pSMAD2/3 to be expressed[327]. Therefore, considering the connections between NODAL and OTX2, it would thus be interesting to investigate whether the upregulation in *Otx2* expression was responsible for the early effects of NODAL in the Epi layer (Fig. 5, S4). Although, since pSMAD2/3 is involved in so many complexes with most of the Epi lineage factors, NODAL effects would

probably result in the activation of a network via protein-protein interactions and combined transcriptional regulations making the reading its direct targets more challenging.

Distinct roles for NODAL and ACTIVIN in the early embryo

The characterization of the impacts of recombinant protein for ACTIVIN and NODAL to the formation of the blastocyst revealed distinct roles for both ligands (Fig. 5, S5). Indeed, ACTIVIN treatment although shown useful for the progression of the PrE layer did not recapitulate any of NODAL impacts on the Epi layer, suggesting that both ligands have respective signaling capabilities. Although sharing the same receptors, NODAL requires the presence of the EGF-CFC co-receptor family to signal[143]. Both *Cripto* and *Cryptic* encode co-receptors of this family, but differentiate from their expression patterns[333]. If *Cripto* is restricted to the Epi lineage and express early from the mid blastocyst stage, *Cryptic* expression starts in the PrE of the implantation blastocyst[333]. Those patterns of expression support the conclusion that NODAL signals in early Epi cells (Fig. 5). However, the analysis of implantation blastocyst carrying the mutation for *Nodal* presents global defects within the PrE layer (Fig. 7, S7). Although, most of the maturation failures could be due to the lack of proper signals from the Epi, the PrE of E4.5 embryos is mostly regulating itself (Fig. 2, S2). Interestingly, my characterization revealed that most of *Nodal* mutant embryos lacked the expression of *Dab2*, which is required for the proper epithelialization of the tissue as shown by the rest of the immunostainings (Fig. 7, S7)[107,109]. Interestingly, *Dab2* expression and translation has been found to be regulated by TGFβ[110,112]. It would thus be interesting to assess whether the epithelialization defects observed in *Nodal* mutant embryos could be rescued by the promotion of DAB2 using retinoic acid. Therefore, NODAL could supposedly promote late PrE proper patterning via its potential signaling capacities through CRYPTIC.

How ACTIVIN signals remain however to be elucidated. Some studies have suggested that ACTIVIN signaling is inhibited by CRIPTO[265]. Albeit a possible explanation of why ACTIVIN does not recapitulate NODAL Epi promotion, EpiSC are cultured in ACTIVIN while expressing strong levels of *Cripto*. Moreover, my own analysis revealed that *Lefty2*, an Epi marker (data not shown), was overexpressed upon ACTIVIN treatment (Fig. 3). ACTIVIN restriction to the PrE could also be due to the inhibition induced by the presence of NODAL protein at the ACTRI/II of Epi cells. It is interesting to note that ACTIVIN signaling in PrE correlates with the activity of pSMAD2 as shown by antibody staining and reporter activity[70,144]. Indeed, most of the tools showing the dynamic of pSDMAD2 revealed an active signaling in PrE cells, suggesting that at these stages NODAL does not depend on pSMAD2/3 to transduce its signals. However, this needs to be taken carefully as a dynamic investigation of the

pSMAD2/3 activity as yet to be done, since the available tools do not recapitulate the kinetic of the effector capacities.

Tissue communication pattern the whole ICM

Nodal presents an interesting expression pattern as it is highly regulated depending on the developmental stage and the lineage[70,142,163]. *Nodal* is supposed to shortly be expressed in early Epi cells before getting restricted to the PrE layer between E3.75 and E4.0[70,142,163]. To assess whether Epi *Nodal* or PrE *Nodal* was responsible for the developmental progression of the blastocyst, I performed chimera experiments with mESC mutants for *Nodal* (Fig. 6, S6). The analysis revealed that the effects of Epi *Nodal* was irrelevant compared to the PrE contribution (Fig. 6, S6). This was quite interesting since it displays a loop of activation shared by both lineages of the ICM (Figure 38). Indeed, NODAL expressed from PrE cells will signal to the early Epi leading the proliferation and maturation of the lineage (Figure 38). This results in the amplification of Epi markers responsible for the differentiation of the PrE, thus subsequently leading to the maturation and patterning of the PrE lineage (Figure 38). Interestingly, this therefore shows that contrary to the believe that the Epi triggers PrE specification and not vice-versa[7], signals coming from PrE cells can promote the maturation and proper patterning of the Epi lineage.

Since *Nodal* expression is regulated by so many combinations of factors it is quite challenging to elucidate what triggers the initiation of tissue communication process described above. In addition to many Epi and ICM factors acting on the HBE, the ASE directly responds to pSMAD2/3[70,163,514]. However, in SB-treated embryos lacking any pSMAD2/3 activity, *Nodal* expression was not affected (data not shown). This raised questions regarding the role of the ASE, indeed, this expression pattern of this regulative sequence recapitulates most of *Nodal* dynamics, but its inactivation does not seem to affect its expression[70,515]. In my culture experiments, I found that *Nodal* expression at the blastocyst stages responded to both p38 and βCATENIN activities (data not shown, βCATENIN Fig. 4). This was quite surprising since, from what we know, p38 acts to amplify pSMAD2/3 signals but its inhibition did not recapitulate its effect on *Nodal* expression, although the inhibition of both proteins separately lead to similar effects among the pool of genes I tested (data not shown). It would therefore be interesting to precisely investigate what does control the early *Nodal* expression to better understand its contribution to the blastocyst development.

Maternal signals compensate for the lack of zygotic NODAL

The characterization of embryos mutant for Nodal revealed strong defects at the implantation stages (Fig. 7, S7). However, those defects, albeit similar in some ways, did not recapitulate the phenotype of SB-treated embryos (Fig. 1, 2). This could suggest that other molecules than NODAL could activate pSMAD2/3 and therefore compensate for the lack of the ligands. Although possible at pre-implantation stages, this appears to be unlikely since *Nodal* mutants and *Smad2/3* double KO shared similar phenotypes[145,306]. Moreover, these mutants were surprisingly not affected compared to embryos cultured for 48h in presence of SB, suggesting that during the implantation, the early phenotypes I characterized could be rescued (Fig.1, 2). Therefore, in order to test whether compensation mechanics are of a possibility, I transferred SB-treated embryos into wild-types pseudo-pregnant females (Fig. 4). The phenotypes I observed confirmed that post-implantation defects are of a consequence to previous requirements for the pathway during blastocyst formation (Fig. 4).

However, similar to *Nodal* mutants those embryos implanted and could adopt an egg cylinder-like shape. This suggests that during the implantation signals are emitted to rescue the miss-patterned tissues of the blastocyst. Interestingly, *Nodal* is expressed in the uterus until the embryo implants but is rapidly removed from the implantation zones[358]. This was surprisingly concomitant with the time of the first defects from *Nodal* mutants were observed, suggesting that maternal NODAL could probably compensate for the absence of zygotic NODAL. To address this hypothesis, I cultured embryos carrying the mutation for *Nodal* to remove signals from the mother (Fig. 8, S8). To my surprise, these embryos displayed stronger defects than SB-treated embryos suggesting that NODAL's actions are not limited to promote the activation of pSMAD2/3 (Fig. 8, S8). Moreover, since these embryos were rescued by the addition of NODA,L and not ACTIVIN, it was indicating that the latter was not able to compensate for the complete lack of *Nodal*, and that among the maternal signals rescuing the zygotic depletion was probably found NODAL itself (Fig. 8, S8). It would therefore be very interesting to investigate the mechanisms behind the maternal recue, and how the signals are emitted and received by the embryos. Although a simple protein transfer is possible, recent studies have pointed towards the transport of exosomes, carrying proteins and mRNA, from the uterus. A better understanding of the mechanism by which the mother communicate with pre-implantation embryos could be of a huge impact on our understanding in the different specification events controlling the formation of the blastocyst.

To conclude, NODAL signals are required for the proper development of the blastocyst via its signals to the Epi and according to an elaborate tissue communication process. Most of the data suggest that NODAL does not solely signal via pSMAD2/3 and that ACTIVIN is therefore not able to compensate for its absence. As a TGFβ secreted protein NODAL can form dimers with several other factors that complexify our ability to understand it signaling mechanics. The fact that maternal NODAL could

theoretically compensate for the lack of zygotic NODAL opens news ways to elucidate the roles of secreted proteins in cell fate specification. Finally, with the considerable roles of NODAL in early human embryogenesis, it would be interesting to complete our knowledges of the mechanisms behind NODAL signaling to better understand how the human Epi is specified[516].

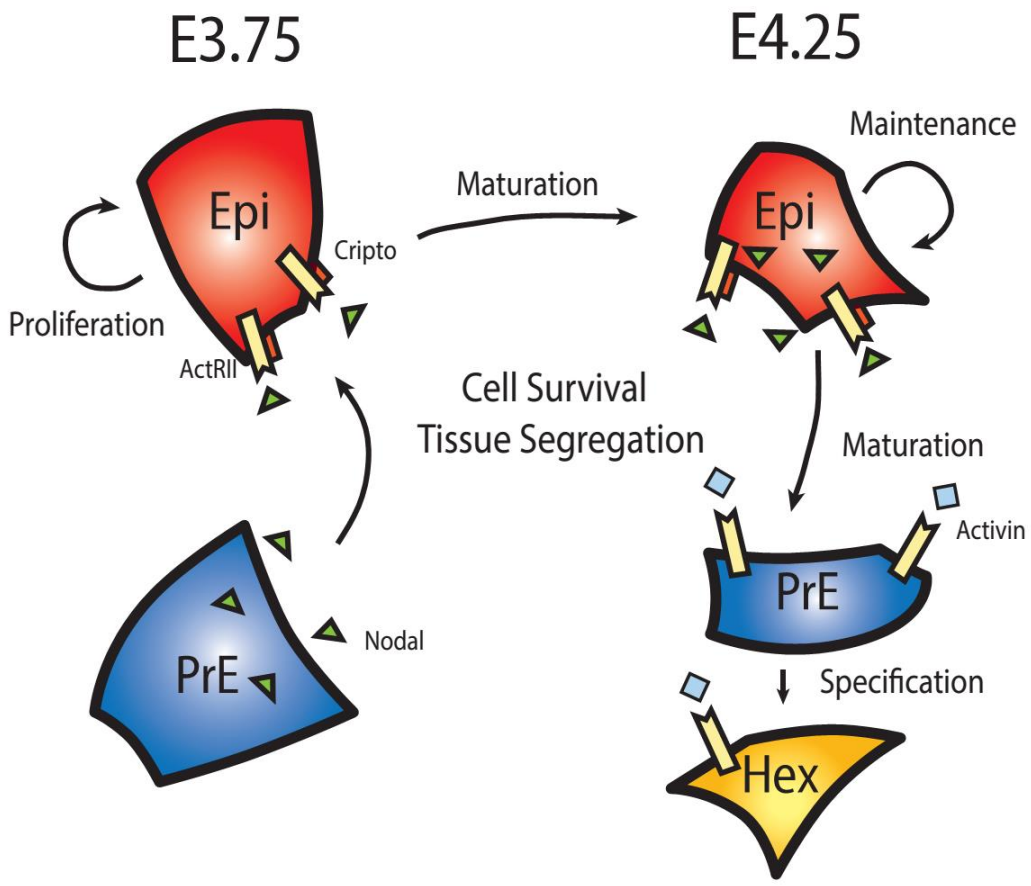

Figure 39 : Working model explaining how NODAL can promote the patterning of the ICM via lineage communications

At the mid blastocyst stage NODAL proteins expressed from PrE cells can signal in Epi cells via the presence of the co-receptor CRIPTO. This leads to the expansion and maturation of the lineage. During this process Epi signals amplified by NODAL can promote the progression of the PrE lineages resulting in its maturation and the specification of its lateral subpopulation expressing *Hex*. ACTIVIN on the other hand signals directly in PrE cells to support the maturation of the lineage. Combined action of NODAL and ACTIVIN sustain cell-survival and promote the proper development of the whole blastocyst.

βCATENIN Regulates Cell Differentiation of the Blastocyst Lineages

βCATENIN is mostly described as the effector of the canonical WNT/βCATENIN signaling pathways, although its activity does not entirely depend on the WNT signals. Indeed, many factors have been found to induce the release of the protein from its destruction complex. Among those factors are found molecules essential for the events of fate specification occurring at the pre-implantation stages such as YAP and ERK – respectively effectors of the HIPPO and FGF signaling pathways[408]. During these stages most of the components of the WNT/βCATENIN signaling pathways are expressed and regulated[466,467]. However, previous reports indicate that the WNT/βCATENIN signaling pathway is inactive as shown by the different genetic depletions of the pathway members[454]. However, taken separately, βCATENIN mutants present stronger defects that any of the WNT mutations demonstrating that βCATENIN is activated by other cues in early embryogenesis.

To investigate the impacts of modulating the transcriptional activity of βCATENIN at pre-implantation stages, I used two different mouse lines allowing to induce either a LOF or a GOF of the protein (Fig. 1)[442,462]. Characterization of those mutant embryos revealed considerable impacts of βCATENIN in fate specification and cell differentiation at pre-implantation stages.

βCATENIN and the modulation of HIPPO signaling in the first fate specification

The first event of specification leads to the formation of both ICM and TE lineages. To assess whether βCATENIN was involved in this event I analyzed the ICM composition of mutant embryos for both mutations (Fig. 1). This analysis indicated that the transcriptional activity of βCATENIN is involved in the balance between those fate as shown by the higher percentage of ICM in GOF embryos and the higher percentage of TE in LOF embryos (Fig. 1). Cell counting for each lineage and the expression levels of tissue specific markers revealed that βCATENIN was actively inhibiting the TE fate (Fig. 1). Indeed, I found that *Cdx2* and *Gata3* expression levels were affecting by both mutations of βCATENIN and that was correlated with the nuclear retention of YAP (Fig. 1). Several combined regulations between YAP and βCATENIN have been identified in different models[419,422]. YAP can in fact restrict βCATENIN to the destruction complex and vice-versa leading to the degradation of both effectors[419,422]. It is therefore interesting to constate that in LOF mutants, where the exon 2 to 6 are deleted and among those are found the exon 3 responsible for βCATENIN attachment to the destruction complex, YAP is specifically retained in the nuclei (Fig. 1). This would suggest that βCATENIN is able to promote the degradation of YAP via confining it to the destruction complex. It will therefore be interesting to correlate the localization of both effectors during the event of the first specification to see if βCATENIN is able to act

in the decision-making process. Moreover, TCF3 binding sites are found close to TEAD binding sites at *Cdx2* enhancers (data analyzed from [47]). It is thus tempting to interpret the downregulation of *Cdx2* in GOF mutants by the accumulation of βCATENIN at those binding sites preventing YAP fixation to the TEAD factors responsible for *Cdx2* expression[38]. Therefore, βCATENIN function would be to act indirectly on the first fate specification via the modulation of HIPPO/YAP activity. Further experiments and mutant embryos collection will be necessary to properly test this hypothesis.

βCATENIN regulates the ICM progression through the pluripotency factors

Cell counting also revealed an increase of ICM cells in GOF embryos suggesting that βCATENIN was involved in the proliferation of the ICM (Fig. 1, 2). Lineage association experiments indicated that this increase in ICM cells came from a higher number of Epi cells (Fig. 2). However, in my first experiment I was not able to identify a specific marker susceptible to explain this increase in cell number (Fig. 2). Interestingly however, GATA6 levels were upregulated in the context of βCATENIN LOF suggesting that the PrE fate was promoted over the Epi in this genetic background (Fig. 2). The fact that no significant difference in cell number for each lineage was found suggested that this impact was quite limited (Fig. 2). Additional litters for this mutation will be required to properly assess the impact of βCATENIN in the second fate specification. Considering that the two mutations presented opposite effects suggested however an implication of βCATENIN in this event (Fig. 2). Embryos in culture with CHIR resulting in a GOF of βCATENIN showed similar effects by promoting the ICM fate and conversely preventing the proper maturation of the PrE (Fig. 3). Indeed, CHIR-treated embryos stained for late PrE markers showed either a downregulation of their levels or a complete absence (Fig. 3).

The effect I found using CHIR, albeit being consistent with the phenotypes observed in the mutant background, was challenged by a previous report suggesting that CHIR did not affect the pre-implantation development[476]. The main difference between our two studies find its origin in the concentration of the inhibitor we used (Fig. 3). Indeed, if CHIR at 3µM used in mESC cultures did not affect the blastocyst formation too much, its concentration used at 10µM however, resulted in a stronger increase of the *Axin2* levels – a target of βCATENIN – and prevented the proper patterning of the ICM (Fig. 3). The fact that the embryo required higher concentration than mESC can be however debated. Using these conditions, I was able to further characterize the impact of βCATENIN on the ICM.

A striking evidence while analyzing the expression patterns of ICM markers such as SOX2 and OCT4 was that their expression failed to be either restricted or amplified in the Epi lineage as it is normally the case (Fig. 3). The retention of SOX2 in PrE cells particularly is known to prevent the proper

maturation of the PrE as shown by the competition between SOX2 and SOX17 and the inhibition of SOX2 mediated by pERK in PrE cells[117,118]. In addition with its pan-ICM expression, the levels of *Sox2* were downregulated suggesting that the Epi also failed to mature as shown by the constant upregulation of *Sox2* levels as the Epi progresses (Fig. 4)[57]. Therefore, the ICM of CHIR-treated embryos appeared to share similarities with its earlier state during the blastocyst formation. Indeed, time gated experiments revealed that starting from the morula stage, CHIR treatment prevented the maturation of both Epi and PrE and this was correlated with a strong upregulation of the pluripotency factors (Fig. 4). Strong indications support that βCATENIN is able to bind OCT4 in order to promote naïve pluripotency in mESC[434,435]. It is therefore possible that βCATENIN upregulates the pluripotency network and that is sufficient to maintain the ICM as a naïve state with both Epi and PrE failing to mature. More interestingly, is the recent advance regarding the diapause state of the blastocyst. If historically diapause was induced experimentally by the addition of progesterone and tamoxifen, a study indicated that inhibition of mTOR could reflect similar properties[236]. βCATENIN has shown interaction with the mTOR/PI3K in the embryo, it would thus be interesting to investigate whether the upregulation of βCATENIN resulted in a diapause state subsequently assessing its correlation with mTOR.

βCATENIN promotes cell differentiation in association with signaling pathways

Starting the CHIR treatment from the late blastocyst stage, when the ICM could mature properly, showed that the Epi lineage failed to maintain its identity and, as suggested by the upregulation of *Sox2* and *Nodal,* underwent a premature differentiation (Fig. 4). NODAL and SOX2 are known to promote the Epi maturation during the implantation before being restricted to each Epi populations according to the AP orientation[217,343]. However, none of the markers characteristics of the Epi maturation were expressed in late blastocyst embryos treated with CHIR suggesting that another fate was acquired (Fig. 4). As it has been well identified, βCATENIN and NODAL are known to promote the mesendoderm differentiation of the posterior proximal Epi during gastrulation[145,193]. Analysis of the two mesoderm markers T/Bra and Goosecoïd indicated that the CHIR treatment induced an ectopic differentiation of the Epi to a mesoderm fate more than 2 days before the initiation of the gastrulation (Fig. 4). This was consistent with a previous report showing that in embryos carrying a mutation for *Apc* – therefore resulting in a βCATENIN GOF – *T/Bra* was found expressed at the implantation stage[461]. To address whether pSMAD2/3 was required to allow the mesoderm induction in CHIR-treated embryos, I combined genetic ablations and pharmacological treatments for the two signaling pathways and assessed the combined impact on the Epi lineage (data not shown). These results indicated that both pathways communicated with each other to promote the proper maturation and differentiation

of the Epi. Considering the impact of βCATENIN LOF at early post-implantation stages, it will be interesting to assess the contribution of pSMAD2/3 modulation in the phenotypes displayed by βCATENIN mutants[465].

Further characterization of βCATENIN LOF embryos revealed that the PrE was strongly disorganized, as shown by the βCATENIN immunostaining and the distribution of PrE cells (Fig. 4). Since I hypothesized that the PrE progression was accelerated in LOF mutants, I investigated the differentiation of the PrE derivatives (Fig. 4). This analysis revealed that some of the PrE cells at the implantation stage prematurely acquired a PaE fate (Fig. 4). *In vitro* experiments showed that the inhibition of WNT/βCATENIN by IGF2 is sufficient to allow PaE differentiation[206]. It is thus interesting that the βCATENIN LOF recapitulates the changes identified in this study as shown by the upregulation of GATA6 and the SPARC staining (Fig. 4). Not much is known about IGF signaling at these stages, since most of the genetic mutations developed allowed the birth of the embryos[232,233]. However, modulation of the IGF signaling directly affects the activation levels of PI3K/AKT[517,518]. It would thus be interesting to investigate the impact of IGF signaling on the transcriptional activity of βCATENIN during the formation of the blastocyst.

The activation of βCATENIN does not recapitulate WNT signaling

In order to understand what does control the activity of βCATENIN, I tested the impact of recombinant WNT3A on cultured embryos (Fig. 4). Although, this treatment resulted in a small increase in *Axin2* levels, suggesting that all the components of the cascade were functional, WNT3A addition did not recapitulate any of the phenotypes described with the genetic mutations and the CHIR treatment (Fig. 4). Even though WNT3A does not represent all WNT molecules, its protein structure allows this ligand to activate βCATENIN with the highest efficiency[379]. Therefore, other factors than WNT are responsible for the modulation of βCATENIN activity.

βCATENIN finds itself as the crossroad of many signaling pathways. Indeed, IGF/PI3K/AKT, HIPPO/YAP, FGF/ERK and NODAL/SMAD2/3 were found to be able to either control the interaction between βCATENIN and its destruction complex or to make protein-protein interactions for transcriptional regulation purposes. Although quite challenging to address, the identification of the factors responsible for βCATENIN modulation could lead to new insights regarding the mechanism by which this factor controls an event of the blastocyst formation.

To conclude, although the WNT/βCATENIN does not seem to be involved in the pre-implantation development, I was able to uncover new roles for βCATENIN in the specification and differentiation of

the blastocyst lineages. However, much remains to be addressed and confirmed, I identified βCATENIN as an effector playing in different signaling cascades in order to control different events of the forming blastocyst.

REFERENCES

1. Artus, J. & Cohen-Tannoudji, M. Cell cycle regulation during early mouse embryogenesis. *Mol. Cell. Endocrinol.* **282**, 78–86 (2008).

2. Aoki, F., Hara, K. T. & Schultz, R. M. Acquisition of transcriptional competence in the 1-cell mouse embryo: Requirement for recruitment of maternal mRNAs. *Mol. Reprod. Dev.* **64**, 270–274 (2003).

3. Johnson, M. H. & McConnell, J. M. L. Lineage allocation and cell polarity during mouse embryogenesis. *Semin. Cell Dev. Biol.* **15**, 583–597 (2004).

4. Honda, H., Motosugi, N., Nagai, T., Tanemura, M. & Hiiragi, T. Computer simulation of emerging asymmetry in the mouse blastocyst. *Development* **135**, 1407–1414 (2008).

5. Kurotaki, Y., Hatta, K., Nakao, K., Nabeshima, Y. I. & Fujimori, T. Blastocyst axis is specified independently of early cell lineage but aligns with the ZP shape. *Science (80-.).* **316**, 719–723 (2007).

6. Morris, S. A., Guo, Y. & Zernicka-Goetz, M. Developmental Plasticity Is Bound by Pluripotency and the Fgf and Wnt Signaling Pathways. *Cell Rep.* **2**, 756–765 (2012).

7. Saiz, N., Williams, K. M., Seshan, V. E. & Hadjantonakis, A. K. Asynchronous fate decisions by single cells collectively ensure consistent lineage composition in the mouse blastocyst. *Nat. Commun.* **7**, (2016).

8. Piotrowska-Nitsche, K., Perea-Gomez, A., Haraguchi, S. & Zernicka-Goetz, M. Four-cell stage mouse blastomeres have different developmental properties. *Development* **132**, 479–490 (2005).

9. Tabansky, I. *et al.* Developmental bias in cleavage-stage mouse blastomeres. *Curr. Biol.* **23**, 21–31 (2013).

10. Rossant, J. Postimplantation development of blastomeres isolated from 4 and 8 cell mouse eggs. *J. Embryol. Exp. Morphol.* **36**, 283–290 (1976).

11. Shi, J. *et al.* Dynamic transcriptional symmetry-breaking in pre-implantation mammalian embryo development revealed by single-cell rna-seq. *Dev.* **142**, 3468–3477 (2015).

12. White, M. D. *et al.* Long-Lived Binding of Sox2 to DNA Predicts Cell Fate in the Four-Cell Mouse Embryo. *Cell* **165**, 75–87 (2016).

13. Plachta, N., Bollenbach, T., Pease, S., Fraser, S. E. & Pantazis, P. Oct4 kinetics predict cell lineage patterning in the early mammalian embryo. *Nat. Cell Biol.* **13**, 117–123 (2011).

14. Torres-Padilla, M. E., Parfitt, D. E., Kouzarides, T. & Zernicka-Goetz, M. Histone arginine methylation regulates pluripotency in the early mouse embryo. *Nature* **445**, 214–218 (2007).

15. Hupalowska, A. *et al.* CARM1 and Paraspeckles Regulate Pre-implantation Mouse Embryo Development. *Cell* **175**, 1902-1916.e13 (2018).

16. Maître, J. L. Mechanics of blastocyst morphogenesis. *Biol. Cell* **109**, 323–338 (2017).

17. Mihajlović, A. I. & Bruce, A. W. The first cell-fate decision of mouse preimplantation embryo development: Integrating cell position and polarity. *Open Biol.* **7**, (2017).

18. Maître, J. L., Niwayama, R., Turlier, H., Nedelec, F. & Hiiragi, T. Pulsatile cell-autonomous contractility drives compaction in the mouse embryo. *Nat. Cell Biol.* **17**, 849–855 (2015).

19. Stephenson, R. O., Yamanaka, Y. & Rossant, J. Disorganized epithelial polarity and excess trophectoderm cell fate in preimplantation embryos lacking E-cadherin. *Development* **137**, 3383–3391 (2010).

20. Maître, J. L. *et al.* Asymmetric division of contractile domains couples cell positioning and fate specification. *Nature* **536**, 344–348 (2016).

21. Aghion, J., Gueth-Hallonet, C., Antony, C., Gros, D. & Maro, B. Cell adhesion and gap junction formation in the early mouse embryo are induced prematurely by 6-DMAP in the absence of E-cadherin phosphorylation. *J. Cell Sci.* **107**, 1369–1379 (1994).

22. Kawai, Y., Yamaguchi, T., Yoden, T., Hanada, M. & Miyake, M. Effect of protein phosphatase inhibitors on the development of mouse embryos: Protein phosphorylation is involved in the E-cadherin distribution in mouse two-cell embryos. *Biol. Pharm. Bull.* **25**, 179–183 (2002).

23. Levy, J. B., Johnson, M. H., Goodall, H. & Maro, B. The timing of compaction: Control of a major developmental transition in mouse early embryogenesis. *J. Embryol. Exp. Morphol.* **VOL. 95**, 213–237 (1986).

24. Korotkevich, E. *et al.* The Apical Domain Is Required and Sufficient for the First Lineage Segregation in the Mouse Embryo. *Dev. Cell* **40**, 235-247.e7 (2017).

25. Dard, N. *et al.* In vivo functional analysis of ezrin during mouse blastocyst formation. *Dev. Biol.* **233**, 161–173 (2001).

26. Hirate, Y. *et al.* Polarity-dependent distribution of angiomotin localizes hippo signaling in preimplantation embryos. *Curr. Biol.* **23**, 1181–1194 (2013).

27. Chazaud, C. & Yamanaka, Y. Lineage specification in the mouse preimplantation embryo. *Dev.* **143**, 1063–1074 (2016).

28. Dard, N., Louvet-Vallée, S., Santa-Maria, A. & Maro, B. Phosphorylation of ezrin on threonine T567 plays a crucial role during compaction in the mouse early embryo. *Dev. Biol.* **271**, 87–97 (2004).

29. Liu, H. *et al.* Atypical PKC, Regulated by Rho GTPases and Mek/Erk, Phosphorylates Ezrin during eight-cell embryocompaction. *Dev. Biol.* **375**, 13–22 (2013).

30. Vinot, S. *et al.* Asymmetric distribution of PAR proteins in the mouse embryo begins at the 8-cell stage during compaction. *Dev. Biol.* **282**, 307–319 (2005).

31. Ralston, A. & Rossant, J. Cdx2 acts downstream of cell polarization to cell-autonomously promote trophectoderm fate in the early mouse embryo. *Dev. Biol.* **313**, 614–629 (2008).

32. Anani, S., Bhat, S., Honma-Yamanaka, N., Krawchuk, D. & Yamanaka, Y. Initiation of Hippo signaling is linked to polarity rather than to cell position in the pre-implantation mouse embryo. *Dev.* **141**, 2813–2824 (2014).

33. Alarcon, V. B. Cell Polarity Regulator PARD6B Is Essential for Trophectoderm Formation in the Preimplantation Mouse Embryo1. *Biol. Reprod.* **83**, 347–358 (2010).

34. Dard, N., Le, T., Maro, B. & Louvet-Valléee, S. Inactivation of aPKCλ reveals a context dependent allocation of cell lineages in preimplantation mouse embryos. *PLoS One* **4**, (2009).

35. Samarage, C. R. *et al.* Cortical Tension Allocates the First Inner Cells of the Mammalian Embryo. *Dev. Cell* **34**, 435–447 (2015).

36. Frum, T., Murphy, T. M. & Ralston, A. HIPPO signaling resolves embryonic cell fate conflicts during establishment of pluripotency in vivo. *Elife* **7**, 1–21 (2018).

37. Nishioka, N. *et al.* Tead4 is required for specification of trophectoderm in pre-implantation mouse embryos. *Mech. Dev.* **125**, 270–283 (2008).

38. Nishioka, N. *et al.* The Hippo Signaling Pathway Components Lats and Yap Pattern Tead4 Activity to Distinguish Mouse Trophectoderm from Inner Cell Mass. *Dev. Cell* **16**, 398–410 (2009).

39. Sasaki, H. Roles and regulations of Hippo signaling during preimplantation mouse development. *Dev. Growth Differ.* **59**, 12–20 (2017).

40. Yagi, R. *et al.* Transcription factor TEAD4 specifies the trophectoderm lineage at the beginning of mammalian development. *Development* **134**, 3827–3836 (2007).

41. Frum, T., Watts, J. L. & Ralston, A. TEAD4, YAP1 and WWTR1 prevent the premature onset of pluripotency prior to the 16-cell stage. *Development* **146**, dev179861 (2019).

42. Yamanaka, Y., Ralston, A., Stephenson, R. O. & Rossant, J. Cell and molecular regulation of the mouse blastocyst. *Dev. Dyn.* **235**, 2301–2314 (2006).

43. Leung, C. Y. & Zernicka-Goetz, M. Angiomotin prevents pluripotent lineage differentiation in mouse embryos via Hippo pathway-dependent and-independent mechanisms. *Nat. Commun.* **4**, 1–11 (2013).

44. Ralston, A. *et al.* Gata3 regulates trophoblast development downstream of Tead4 and in parallel to Cdx2. *Development* **137**, 395–403 (2010).

45. Rayon, T. *et al.* Notch and Hippo Converge on Cdx2 to Specify the Trophectoderm Lineage in the Mouse Blastocyst. *Dev. Cell* **30**, 410–422 (2014).

46. Watanabe, Y. *et al.* Notch and Hippo signaling converge on Strawberry Notch 1 (Sbno1) to synergistically activate Cdx2 during specification of the trophectoderm. *Sci. Rep.* **7**, 1–5 (2017).

47. Rayon, T. *et al.* Distinct mechanisms regulate Cdx2 expression in the blastocyst and in trophoblast stem cells. *Sci. Rep.* **6**, 1–10 (2016).

48. Menchero, S. *et al.* Transitions in cell potency during early mouse development are driven by Notch. *Elife* **8**, 1–29 (2019).

49. Niwa, H. *et al.* Interaction between Oct3/4 and Cdx2 determines trophectoderm differentiation. *Cell* **123**, 917–929 (2005).

50. Strumpf, D. *et al.* Cdx2 is required for correct cell fate specification and differentiation of trophectoderm in the mouse blastocyst. *Development* **132**, 2093–2102 (2005).

51. Blij, S., Frum, T., Akyol, A., Fearon, E. & Ralston, A. Maternal Cdx2 is dispensable for mouse development. *Dev.* **139**, 3969–3972 (2012).

52. Jedrusik, A., Cox, A., Wicher, K., Glover, D. M. & Zernicka-Goetz, M. Maternal-zygotic knockout reveals a critical role of Cdx2 in the morula to blastocyst transition. *Dev. Biol.* **398**, 147–152 (2015).

53. Wu, G. *et al.* Initiation of trophectoderm lineage specification in mouse embryos is independent of Cdx2. *Development* **137**, 4159–4169 (2010).

54. Dietrich, J. E. & Hiiragi, T. Stochastic patterning in the mouse pre-implantation embryo. *Development* **134**, 4219–4231 (2007).

55. Frum, T. *et al.* Oct4 Cell-autonomously promotes primitive endoderm development in the mouse blastocyst. *Dev. Cell* **25**, 610–622 (2013).

56. Lee, M. T. *et al.* Nanog, Pou5f1 and SoxB1 activate zygotic gene expression during the maternal-to-zygotic transition. *Nature* **503**, 360–364 (2013).

57. Guo, G. *et al.* Resolution of Cell Fate Decisions Revealed by Single-Cell Gene Expression Analysis from Zygote to Blastocyst. *Dev. Cell* **18**, 675–685 (2010).

58. Wicklow, E. *et al.* HIPPO Pathway Members Restrict SOX2 to the Inner Cell Mass Where It Promotes ICM Fates in the Mouse Blastocyst. *PLoS Genet.* **10**, (2014).

59. Manejwala, F. M., Cragoe, E. J. & Schultz, R. M. Blastocoel expansion in the preimplantation mouse embryo: Role of extracellular sodium and chloride and possible apical routes of their entry. *Dev. Biol.* **133**, 210–220 (1989).

60. Madan, P., Rose, K. & Watson, A. J. Na/K-ATPase β1 subunit expression is required for blastocyst formation and normal assembly of trophectoderm tight junction-associated proteins. *J. Biol. Chem.* **282**, 12127–12134 (2007).

61. Moriwaki, K., Tsukita, S. & Furuse, M. Tight junctions containing claudin 4 and 6 are essential for blastocyst formation in preimplantation mouse embryos. *Dev. Biol.* **312**, 509–522 (2007).

62. Chan, C. J. *et al.* Hydraulic control of mammalian embryo size and cell fate. *Nature* **571**, 112–116 (2019).

63. Niimura, S. Time-lapse videomicrographic analyses of contractions in mouse blastocysts. *J. Reprod. Dev.* **49**, 413–423 (2003).

64. Kurimoto, K. *et al.* An improved single-cell cDNA amplification method for efficient high-density oligonucleotide microarray analysis. *Nucleic Acids Res.* **34**, (2006).

65. Chazaud, C., Yamanaka, Y., Pawson, T. & Rossant, J. Early Lineage Segregation between Epiblast and Primitive Endoderm in Mouse Blastocysts through the Grb2-MAPK Pathway. *Dev. Cell* **10**, 615–624 (2006).

66. Xenopoulos, P., Kang, M., Puliafito, A., DiTalia, S. & Hadjantonakis, A. K. Heterogeneities in nanog expression drive stable commitment to pluripotency in the mouse blastocyst. *Cell Rep.* **10**, 1508–1520 (2015).

67. Schrode, N., Saiz, N., Di Talia, S. & Hadjantonakis, A. K. GATA6 levels modulate primitive endoderm cell fate choice and timing in the mouse blastocyst. *Dev. Cell* **29**, 454–467 (2014).

68. Bessonnard, S. *et al.* Gata6, Nanog and Erk signaling control cell fate in the inner cell mass through a tristable regulatory network. *Dev.* **141**, 3637–3648 (2014).

69. Frankenberg, S. *et al.* Primitive Endoderm Differentiates via a Three-Step Mechanism Involving Nanog and RTK Signaling. *Dev. Cell* **21**, 1005–1013 (2011).

70. Granier, C. *et al.* Nodal cis-regulatory elements reveal epiblast and primitive endoderm heterogeneity in the peri-implantation mouse embryo. *Dev. Biol.* **349**, 350–362 (2011).

71. Heurtier, V. *et al.* The molecular logic of Nanog-induced self-renewal in mouse embryonic stem cells. *Nat. Commun.* **10**, (2019).

72. Silva, J. *et al.* Nanog Is the Gateway to the Pluripotent Ground State. *Cell* **138**, 722–737 (2009).

73. Messerschmidt, D. M. & Kemler, R. Nanog is required for primitive endoderm formation through a non-cell autonomous mechanism. *Dev. Biol.* **344**, 129–137 (2010).

74. Kang, M., Piliszek, A., Artus, J. & Hadjantonakis, A. K. FGF4 is required for lineage restriction and salt-and-pepper distribution of primitive endoderm factors but not their initial expression in the mouse. *Dev.* **140**, 267–279 (2013).

75. Krawchuk, D., Honma-Yamanaka, N., Anani, S. & Yamanaka, Y. FGF4 is a limiting factor controlling the proportions of primitive endoderm and epiblast in the ICM of the mouse blastocyst. *Dev. Biol.* **384**, 65–71 (2013).

76. Bessonnard, S. *et al.* ICM conversion to epiblast by FGF/ERK inhibition is limited in time and requires transcription and protein degradation. *Sci. Rep.* **7**, 1–12 (2017).

77. Yamanaka, Y., Lanner, F. & Rossant, J. FGF signal-dependent segregation of primitive endoderm and epiblast in the mouse blastocyst. *Development* **137**, 715–724 (2010).

78. Freyer, L. *et al.* A loss-of-function and H2B-Venus transcriptional reporter allele for Gata6 in mice. *BMC Dev. Biol.* **15**, 38 (2015).

79. Mullen, A. C. *et al.* Master transcription factors determine cell-type-specific responses to TGF-β signaling. *Cell* **147**, 565–576 (2011).

80. Buecker, C. *et al.* Reorganization of enhancer patterns in transition from naive to primed pluripotency. *Cell Stem Cell* **14**, 838–53 (2014).

81. Kalkan, T. & Smith, A. Mapping the route from naive pluripotency to lineage specification. *Philos. Trans. R. Soc. B Biol. Sci.* **369**, (2014).

82. Meng, Y. *et al.* GATA6 phosphorylation by Erk1/2 propels exit from pluripotency and commitment to

primitive endoderm. *Dev. Biol.* **436**, 55–65 (2018).

83. Brewer, J. R., Molotkov, A., Mazot, P., Hoch, R. V. & Soriano, P. Fgfr1 regulates development through the combinatorial use of signaling proteins. *Genes Dev.* **29**, 1863–1874 (2015).

84. Molotkov, A., Mazot, P., Brewer, J. R., Cinalli, R. M. & Soriano, P. Distinct Requirements for FGFR1 and FGFR2 in Primitive Endoderm Development and Exit from Pluripotency. *Dev. Cell* **41**, 511-526.e4 (2017).

85. Kang, M., Garg, V. & Hadjantonakis, A. K. Lineage Establishment and Progression within the Inner Cell Mass of the Mouse Blastocyst Requires FGFR1 and FGFR2. *Dev. Cell* **41**, 496-510.e5 (2017).

86. Ohnishi, Y. *et al.* Cell-to-cell expression variability followed by signal reinforcement progressively segregates early mouse lineages. *Nat. Cell Biol.* **16**, 27–37 (2014).

87. Wigger, M. *et al.* Plasticity of the inner cell mass in mouse blastocyst is restricted by the activity of FGF/MAPK pathway. *Sci. Rep.* **7**, 1–13 (2017).

88. Azami, T. *et al.* Regulation of the ERK signalling pathway in the developing mouse blastocyst. *Development* **146**, dev177139 (2019).

89. Bassalert, C., Valverde-Estrella, L. & Chazaud, C. Primitive Endoderm Differentiation: From Specification to Epithelialization. *Curr. Top. Dev. Biol.* **128**, 81–104 (2018).

90. Neben, C. L., Lo, M., Jura, N. & Klein, O. D. Feedback regulation of RTK signaling in development. *Dev. Biol.* **447**, 71–89 (2019).

91. Patel, A. L. & Shvartsman, S. Y. Outstanding questions in developmental ERK signaling. *Dev.* **145**, (2018).

92. Le Bin, G. C. *et al.* Oct4 is required for lineage priming in the developing inner cell mass of the mouse blastocyst. *Dev.* **141**, 1001–1010 (2014).

93. Navarro, P. *et al.* OCT4/SOX2-independent Nanog autorepression modulates heterogeneous Nanog gene expression in mouse ES cells. *EMBO J.* **31**, 4547–4562 (2012).

94. Ema, M. *et al.* Krüppel-like factor 5 Is Essential for Blastocyst Development and the Normal Self-Renewal of Mouse ESCs. *Cell Stem Cell* **3**, 555–567 (2008).

95. Lin, S. C. J., Wani, M. A., Whitsett, J. A. & Wells, J. M. Klf5 regulates lineage formation in the pre-implantation mouse embryo. *Development* **137**, 3953–3963 (2010).

96. Azami, T. *et al.* Klf5 maintains the balance of primitive endoderm versus epiblast specification during mouse embryonic development by suppression of Fgf4. *Dev.* **144**, 3706–3718 (2017).

97. Artus, J., Piliszek, A. & Hadjantonakis, A. K. The primitive endoderm lineage of the mouse blastocyst: Sequential transcription factor activation and regulation of differentiation by Sox17. *Dev. Biol.* **350**, 393–404 (2011).

98. Artus, J., Kang, M., Cohen-Tannoudji, M. & Hadjantonakis, A. K. PDGF signaling is required for primitive endoderm cell survival in the inner cell mass of the mouse blastocyst. *Stem Cells* **31**, 1932–1941 (2013).

99. Saiz, N., Grabarek, J. B., Sabherwal, N., Papalopulu, N. & Plusa, B. Atypical protein kinase C couples cell sorting with primitive endoderm maturation in the mouse blastocyst. *Dev.* **140**, 4311–4322 (2013).

100. Plusa, B., Piliszek, A., Frankenberg, S., Artus, J. & Hadjantonakis, A. K. Distinct sequential cell behaviours direct primitive endoderm formation in the mouse blastocyst. *Development* **135**, 3081–3091 (2008).

101. Artus, J., Panthier, J.-J. & Hadjantonakis, A.-K. A role for PDGF signaling in expansion of the extra-embryonic endoderm lineage of the mouse blastocyst. *Development* **137**, 3361–3372 (2010).

102. Bessonnard, S., Vandormael-Pournin, S., Coqueran, S., Cohen-Tannoudji, M. & Artus, J. PDGF Signaling in Primitive Endoderm Cell Survival Is Mediated by PI3K-mTOR Through p53-Independent Mechanism. *Stem Cells* **37**, 888–898 (2019).

103. Meilhac, S. M. *et al.* Active cell movements coupled to positional induction are involved in lineage

segregation in the mouse blastocyst. *Dev. Biol.* **331**, 210–221 (2009).

104. Rong, L. *et al.* GATA-6 promotes cell survival by up-regulating BMP-2 expression during embryonic stem cell differentiation. *Mol. Biol. Cell* **23**, 3754–3763 (2012).

105. Graham, S. J. L. *et al.* BMP signalling regulates the pre-implantation development of extra-embryonic cell lineages in the mouse embryo. *Nat. Commun.* **5**, 1–11 (2014).

106. Yang, D. H., Cai, K. Q., Roland, I. H., Smith, E. R. & Xu, X. X. Disabled-2 is an epithelial surface positioning gene. *J. Biol. Chem.* **282**, 13114–13122 (2007).

107. Gerbe, F., Cox, B., Rossant, J. & Chazaud, C. Dynamic expression of Lrp2 pathway members reveals progressive epithelial differentiation of primitive endoderm in mouse blastocyst. *Dev. Biol.* **313**, 594–602 (2008).

108. Niakan K K, Ji H, M. R. *et al.* Sox17 promotes differentiation in mouse embryonic stem cells by directly regulating extraembryonic gene expression and indirectly antagonizing self-renewal. *Genes Dev.* **24**, 312–326 (2010).

109. Yang, D. H. *et al.* Disabled-2 is essential for endodermal cell positioning and structure formation during mouse embryogenesis. *Dev. Biol.* **251**, 27–44 (2002).

110. Moore, R., Cai, K. Q., Tao, W., Smith, E. R. & Xu, X. X. Differential requirement for Dab2 in the development of embryonic and extra-embryonic tissues. *BMC Dev. Biol.* **13**, 1 (2013).

111. Huang, C. L. *et al.* Disabled-2 is required for mesoderm differentiation of murine embryonic stem cells. *J. Cell. Physiol.* **225**, 92–105 (2010).

112. Prunier, C. & Howe, P. H. Disabled-2 (Dab2) is required for transforming growth factor β-induced epithelial to mesenchymal transition (EMT). *J. Biol. Chem.* **280**, 17540–17548 (2005).

113. Wang, C. & Song, B. Cell-type-specific expression of the platelet-derived growth factor alpha receptor: a role for GATA-binding protein. *Mol. Cell. Biol.* **16**, 712–723 (1996).

114. Moore, R., Cai, K. Q., Escudero, D. O. & Xu, X. X. Cell adhesive affinity does not dictate primitive endoderm segregation and positioning during murine embryoid body formation. *Genesis* **47**, 579–589 (2009).

115. Krupinski, P., Chickarmane, V. & Peterson, C. Simulating the Mammalian Blastocyst - Molecular and Mechanical Interactions Pattern the Embryo. *PLoS Comput. Biol.* **7**, (2011).

116. Krieg, M. *et al.* Tensile forces govern germ-layer organization in zebrafish. *Nat. Cell Biol.* **10**, 429–436 (2008).

117. Aksoy, I. *et al.* Sox transcription factors require selective interactions with oct4 and specific transactivation functions to mediate reprogramming. *Stem Cells* **31**, 2632–2646 (2013).

118. Aksoy, I. *et al.* Oct4 switches partnering from Sox2 to Sox17 to reinterpret the enhancer code and specify endoderm. *EMBO J.* **32**, 938–953 (2013).

119. Boroviak, T. *et al.* Lineage-Specific Profiling Delineates the Emergence and Progression of Naive Pluripotency in Mammalian Embryogenesis. *Dev. Cell* **35**, 366–382 (2015).

120. Simon, C. S. *et al.* A Gata4 nuclear GFP transcriptional reporter to study endoderm and cardiac development in the mouse. *Biol. Open* **7**, 1–11 (2018).

121. Molkentin, J. D., Lin, Q., Duncan, S. A. & Olson, E. N. Requirement of the transcription factor GATA4 for heart tube formation and ventral morphogenesis. *Genes Dev.* **11**, 1061–1072 (1997).

122. Niimi, T., Hayashi, Y., Futaki, S. & Sekiguchi, K. SOX7 and SOX17 regulate the parietal endoderm-specific enhancer activity of mouse laminin α1 gene. *J. Biol. Chem.* **279**, 38055–38061 (2004).

123. Lilly, A. J. *et al.* Interplay between SOX7 and RUNX1 regulates hemogenic endothelial fate in the yolk sac. *Dev.* **143**, 4341–4351 (2016).

124. Kinoshita, M., Shimosato, D., Yamane, M. & Niwa, H. Sox7 is dispensable for primitive endoderm differentiation from mouse ES cells Early development. *BMC Dev. Biol.* **15**, 1–11 (2015).

125. Molotkov, A. & Soriano, P. Distinct mechanisms for PDGF and FGF signaling in primitive endoderm development. *Dev. Biol.* **442**, 155–161 (2018).

126. Yeo, J. C. *et al.* Klf2 is an essential factor that sustains ground state pluripotency. *Cell Stem Cell* **14**, 864–872 (2014).

127. Guo, G. *et al.* Klf4 reverts developmentally programmed restriction of ground state pluripotency. *Development* **136**, 1063–1069 (2009).

128. Segre, J. A., Bauer, C. & Fuchs, E. Klf4 is a transcription factor required for establishing the barrier function of the skin. *Nat. Genet.* **22**, 356–360 (1999).

129. Jiang, J. *et al.* A core Klf circuitry regulates self-renewal of embryonic stem cells. *Nat. Cell Biol.* **10**, 353–360 (2008).

130. Avilion, A. A. *et al.* Multipotent cell lineages in early mouse development depend on SOX2 function. *Genes Dev.* **17**, 126–140 (2003).

131. Wu, F. R. *et al.* H3K27me3 may be associated with Oct4 and Sox2 in mouse preimplantation embryos. *Genet. Mol. Res.* **13**, 10121–10129 (2014).

132. Acampora, D. *et al.* Loss of the Otx2-Binding Site in the Nanog Promoter Affects the Integrity of Embryonic Stem Cell Subtypes and Specification of Inner Cell Mass-Derived Epiblast. *Cell Rep.* **15**, 2651–2664 (2016).

133. Zhu, Q. *et al.* The transcription factor Pou3f1 promotes neural fate commitment via activation of neural lineage genes and inhibition of external signaling pathways. *Elife* **2014**, 1–21 (2014).

134. Perea-Gomez, A. *et al.* Otx2 is required for visceral endoderm movement and for the restriction of posterior signals in the epiblast of the mouse embryo. *Development* **128**, 753–765 (2001).

135. Acampora, D., Di Giovannantonio, L. G. & Simeone, A. Otx2 is an intrinsic determinant of the embryonic stem cell state and is required for transition to a stable epiblast stem cell condition. *Dev.* **140**, 43–55 (2013).

136. Fiorenzano, A. *et al.* Cripto is essential to capture mouse epiblast stem cell and human embryonic stem cell pluripotency. *Nat. Commun.* **7**, (2016).

137. Cerchiari, A. E. *et al.* A strategy for tissue self-organization that is robust to cellular heterogeneity and plasticity. *Proc. Natl. Acad. Sci. U. S. A.* **112**, 2287–2292 (2015).

138. Rivera-Pérez, J. A. & Hadjantonakis, A. K. The dynamics of morphogenesis in the early mouse embryo. *Cold Spring Harb. Perspect. Biol.* **7**, 1–18 (2015).

139. Stower, M. J. & Srinivas, S. Heading forwards: Anterior visceral endoderm migration in patterning the mouse embryo. *Philos. Trans. R. Soc. B Biol. Sci.* **369**, (2014).

140. Takaoka, K., Yamamoto, M. & Hamada, H. Origin and role of distal visceral endoderm, a group of cells that determines anterior-posterior polarity of the mouse embryo. *Nat. Cell Biol.* **13**, 743–752 (2011).

141. Takaoka, K. & Hamada, H. Cell fate decisions and axis determination in the early mouse embryo. *Development* **139**, 3–14 (2012).

142. Takaoka, K., Nishimura, H. & Hamada, H. Both Nodal signalling and stochasticity select for prospective distal visceral endoderm in mouse embryos. *Nat. Commun.* **8**, 1–3 (2017).

143. Shen, M. M. Nodal signaling: developmental roles and regulation. *Development* **134**, 1023–1034 (2007).

144. Yamamoto, M. *et al.* Antagonism between Smad1 and Smad2 signaling determines the site of distal visceral endoderm formation in the mouse embryo. *J. Cell Biol.* **184**, 323–334 (2009).

145. Brennan, J. *et al.* Nodal signalling in the epiblast patterns the early mouse embryo. *Nature* **411**, 965–969 (2001).

146. Ding, J. *et al.* Cripto is required for correct orientation of the anterior-posterior axis in the mouse embryo. *Nature* **395**, 702–707 (1998).

147. Meno, C. *et al.* Lefty-1 Is Required for Left-Right Determination As a Regulator of Lefty-2 and Nodal. *Cell* **94**, 287–297 (1998).

148. Perea-Gomez, A. *et al.* Nodal antaginists in the anterior visceral endoderm prevent the formation of multiple primitive streaks. *Dev. Cell* **3**, 745–756 (2002).

149. Yamamoto, M. *et al.* Nodal antagonists regulate formation of the anteroposterior axis of the mouse embryo. *Nature* **428**, 387–392 (2004).

150. Takaoka, K. *et al.* The mouse embryo autonomously acquires anterior-posterior polarity at implantation. *Dev. Cell* **10**, 451–459 (2006).

151. Torres-Padilla, M. E. *et al.* The anterior visceral endoderm of the mouse embryo is established from both preimplantation precursor cells and by de novo gene expression after implantation. *Dev. Biol.* **309**, 97–112 (2007).

152. Martinez-Barbera, J. P., Rodriguez, T. A. & Beddington, R. S. P. The homeobox gene Hesx1 is required in the anterior neural ectoderm for normal forebrain formation. *Dev. Biol.* **223**, 422–430 (2000).

153. Srinivas, S., Rodriguez, T., Clements, M., Smith, J. C. & Beddington, R. S. P. Active cell migration drives the unilateral movements of the anterior visceral endoderm. *Development* **131**, 1157–1164 (2004).

154. Rodriguez, T. A., Srinivas, S., Clements, M. P., Smith, J. C. & Beddington, R. S. P. Induction and migration of the anterior visceral endoderm is regulated by the extra-embryonic ectoderm. *Development* **132**, 2513–2520 (2005).

155. Stuckey, D. W., Di Gregorio, A., Clements, M. & Rodriguez, T. A. Correct patterning of the primitive streak requires the anterior visceral endoderm. *PLoS One* **6**, 1–9 (2011).

156. Di-Gregorio, A. *et al.* BMP signalling inhibits premature neural differentiation in the mouse embryo. *Development* **134**, 3359–3369 (2007).

157. Rankin, S. A., Kormish, J., Kofron, M., Jegga, A. & Zorn, A. M. A gene regulatory network controlling hhex transcription in the anterior endoderm of the organizer. *Dev. Biol.* **351**, 297–310 (2011).

158. Soares, M. L. *et al.* Functional studies of signaling pathways in peri-implantation development of the mouse embryo by RNAi. *BMC Dev. Biol.* **5**, 1–11 (2005).

159. Kozmikova, I., Candiani, S., Fabian, P., Gurska, D. & Kozmik, Z. Essential role of Bmp signaling and its positive feedback loop in the early cell fate evolution of chordates. *Dev. Biol.* **382**, 538–554 (2013).

160. Lawson, K. A. *et al.* Bmp4 is required for the generation of primordial germ cells in the mouse embryo. *Genes Dev.* **13**, 424–436 (1999).

161. Galvin, K. E., Travis, E. D., Yee, D., Magnuson, T. & Vivian, J. L. Nodal signaling regulates the bone morphogenic protein pluripotency pathway in mouse embryonic stem cells. *J. Biol. Chem.* **285**, 19747–19756 (2010).

162. Ben-Haim, N. *et al.* The Nodal Precursor Acting via Activin Receptors Induces Mesoderm by Maintaining a Source of Its Convertases and BMP4. *Dev. Cell* **11**, 313–323 (2006).

163. Papanayotou, C. *et al.* A Novel Nodal Enhancer Dependent on Pluripotency Factors and Smad2/3 Signaling Conditions a Regulatory Switch During Epiblast Maturation. *PLoS Biol.* **12**, (2014).

164. Aragón, E. *et al.* Structural basis for distinct roles of SMAD2 and SMAD3 in FOXH1 pioneer-directed TGF-β signaling. *Genes Dev.* **1**, 1–19 (2019).

165. Ma, W. ge, Song, H., Das, S. K., Paria, B. C. & Dey, S. K. Estrogen is a critical determinant that specifies

the duration of the window of uterine receptivity for implantation. *Proc. Natl. Acad. Sci. U. S. A.* **100**, 2963–2968 (2003).

166. Matsumoto, H. *et al.* Extended uterine receptivity for blastocyst implantation and full-term fetal development in mice with vitrified-warmed ovarian tissue autotransplantation. *Reprod. Med. Biol.* **11**, 123–128 (2012).

167. Nichols, J., Chambers, I., Taga, T. & Smith, A. Physiological rationale for responsiveness of mouse embryonic stem cells to gp130 cytokines. *Development* **128**, 2333–2339 (2001).

168. Morris, S. A. *et al.* Dynamics of anterior-posterior axis formation in the developing mouse embryo. *Nat. Commun.* **3**, 610–673 (2012).

169. Saito, K. *et al.* Degradation of estrogen receptor α in activated blastocysts is associated with implantation in the delayed implantation mouse model. *Mol. Hum. Reprod.* **20**, 384–391 (2014).

170. Bedzhov, I., Graham, S. J. L., Leung, C. Y. & Zernicka-Goetz, M. Developmental plasticity, cell fate specification and morphogenesis in the early mouse embryo. *Philos. Trans. R. Soc. B Biol. Sci.* **369**, (2014).

171. Basak, S., Dhar, R. & Das, C. Steroids Modulate the Expression of α4 Integrin in Mouse Blastocysts and Uterus During Implantation1. *Biol. Reprod.* **66**, 1784–1789 (2002).

172. Matsumoto, H. Molecular and cellular events during blastocyst implantation in the receptive uterus: Clues from mouse models. *J. Reprod. Dev.* **63**, 445–454 (2017).

173. Joswig, A., Gabriel, H. D., Kibschull, M. & Winterhager, E. Apoptosis in uterine epithelium and decidua in response to implantation: Evidence for two different pathways. *Reprod. Biol. Endocrinol.* **1**, 1–9 (2003).

174. Ansell, J. D., Barlow, P. W. & McLaren, A. Binucleate and polyploid cells in the decidua of the mouse. *J. Embryol. Exp. Morphol.* **31**, 223–227 (1974).

175. NANCY, P. *et al.* Access To the Maternal-Fetal Interface. *Science (80-.).* **336**, 1317–1321 (2012).

176. Peng, S. *et al.* Dickkopf-1 secreted by decidual cells promotes trophoblast cell invasion during murine placentation. *Reproduction* **135**, 367–375 (2008).

177. Bany, B. M. & Cross, J. C. Post-implantation mouse conceptuses produce paracrine signals that regulate the uterine endometrium undergoing decidualization. *Dev. Biol.* **294**, 445–456 (2006).

178. Simmons, D. G., Fortier, A. L. & Cross, J. C. Diverse subtypes and developmental origins of trophoblast giant cells in the mouse placenta. *Dev. Biol.* **304**, 567–578 (2007).

179. Donnison, M., Broadhurst, R. & Pfeffer, P. L. Elf5 and Ets2 maintain the mouse extraembryonic ectoderm in a dosage dependent synergistic manner. *Dev. Biol.* **397**, 77–88 (2015).

180. Ng, R. K. *et al.* UKPMC Funders Group methylation of Elf5. *Cell* **10**, 1280–1290 (2009).

181. Georgiades, P. & Rossant, J. Ets2 is necessary in trophoblast for normal embryonic anteroposterior axis development. *Development* **133**, 1059–1068 (2006).

182. Polydorou, C. & Georgiades, P. Ets2-dependent trophoblast signalling is required for gastrulation progression after primitive streak initiation. *Nat. Commun.* **4**, 1–13 (2013).

183. Donnison, M. *et al.* Loss of the extraembryonic ectoderm in Elf5 mutants leads to defects in embryonic patterning. *Development* **132**, 2299–2308 (2005).

184. Mesnard, D. & Constam, D. B. Imaging proprotein convertase activities and their regulation in the implanting mouse blastocyst. *J. Cell Biol.* **191**, 129–139 (2010).

185. Takao, T., Asanoma, K., Tsunematsu, R., Kato, K. & Wake, N. The maternally expressed gene Tssc3 regulates the expression of MASH2 transcription factor in mouse trophoblast stem cells through the AKT-Sp1 signaling pathway. *J. Biol. Chem.* **287**, 42685–42694 (2012).

186. Wang, J., Mager, J., Schnedier, E. & Magnuson, T. The mouse PcG gene eed is required for Hox gene repression and extraembryonic development. *Mamm. Genome* **13**, 493–503 (2002).

187. Tanaka, M., Gertsenstein, M., Rossant, J. & Nagy, A. Mash2 acts cell autonomously in mouse spongiotrophoblast development. *Dev. Biol.* **190**, 55–65 (1997).

188. Hughes, M. *et al.* The Hand1, Stra13 and Gcm1 transcription factors override FGF signaling to promote terminal differentiation of trophoblast stem cells. *Dev. Biol.* **271**, 26–37 (2004).

189. Brown, K. *et al.* A comparative analysis of extra-embryonic endoderm cell lines. *PLoS One* **5**, (2010).

190. Pijuan-Sala, B. *et al.* A single-cell molecular map of mouse gastrulation and early organogenesis. *Nature* **566**, 490–495 (2019).

191. Bielinska, M., Narita, N. & Wilson, D. B. Distinct roles for visceral endoderm during embryonic mouse development. *Int. J. Dev. Biol.* **43**, 183–205 (1999).

192. Trichas, G. *et al.* Multi-cellular rosettes in the mouse visceral endoderm facilitate the ordered migration of anterior visceral endoderm cells. *PLoS Biol.* **10**, (2012).

193. Yoon, Y. *et al.* Extra-embryonic Wnt3 regulates the establishment of the primitive streak in mice. *Dev. Biol.* **403**, 80–88 (2015).

194. Kwon, G. S., Viotti, M. & Hadjantonakis, A. K. The Endoderm of the Mouse Embryo Arises by Dynamic Widespread Intercalation of Embryonic and Extraembryonic Lineages. *Dev. Cell* **15**, 509–520 (2008).

195. Costello, I. *et al.* Lhx1 functions together with Otx2, Foxa2, and Ldb1 to govern anterior mesendoderm, node, and midline development. *Genes Dev.* **29**, 2108–2122 (2015).

196. Igarashi, H. *et al.* Sox17 is essential for proper formation of the marginal zone of extraembryonic endoderm adjacent to a developing mouse placental disk †. *Biol. Reprod.* **99**, 578–589 (2018).

197. Shimoda, M. *et al.* Sox17 plays a substantial role in late-stage differentiation of the extraembryonic endoderm in vitro. *J. Cell Sci.* **120**, 3859–3869 (2007).

198. Trichas, G. *et al.* Nodal dependent differential localisation of dishevelled-2 demarcates regions of differing cell behaviour in the visceral endoderm. *PLoS Biol.* **9**, (2011).

199. Liu, J. *et al.* Integrins are required for the differentiation of visceral endoderm. *J. Cell Sci.* **122**, 233–242 (2009).

200. Artus, J. *et al.* BMP4 signaling directs primitive endoderm-derived XEN cells to an extraembryonic visceral endoderm identity. *Dev. Biol.* **361**, 245–262 (2012).

201. Paca, A. *et al.* BMP signaling induces visceral endoderm differentiation of XEN cells and parietal endoderm. *Dev. Biol.* **361**, 90–102 (2012).

202. Anderson, K. G. V. *et al.* Insulin fine-tunes self-renewal pathways governing naive pluripotency and extra-embryonic endoderm. *Nat. Cell Biol.* **19**, 1164–1177 (2017).

203. Yamamoto, M. *et al.* Antagonism between Smad1 and Smad2 signaling determines the site of distal visceral endoderm formation in the mouse embryo. *J. Cell Biol.* **184**, 323–334 (2009).

204. Loew, E., Grimley, J. S. & Ramanathan, S. robust signaling gradients through receptor. *Nat. Commun.* doi:10.1038/s41467-019-12533-7

205. Stary, M. *et al.* Parietal endoderm secreted SPARC promotes early cardiomyogenesis in vitro. *Exp. Cell Res.* **310**, 331–343 (2005).

206. Schlupf, J. & Steinbeisser, H. IGF antagonizes the Wnt/β-Catenin pathway and promotes differentiation of extra-embryonic endoderm. *Differentiation* **87**, 209–219 (2014).

207. Hrabchak, C., Ringuette, M. & Woodhouse, K. Recombinant mouse SPARC promotes parietal endoderm differentiation and cardiomyogenesis in embryoid bodies. *Biochem. Cell Biol.* **86**, 487–499 (2008).

208. LaMonica, K., Bass, M. & Grabel, L. The planar cell polarity pathway directs parietal endoderm migration. *Dev. Biol.* **330**, 44–53 (2009).

209. Mills, E. *et al.* Roles for Rho/ROCK and vinculin in parietal endoderm migration. *Cell Commun. Adhes.* **12**, 9–22 (2005).

210. Ninomiya, Y., Davies, T. J. & Gardner, R. L. Experimental analysis of the transdifferentiation of visceral to parietal endoderm in the mouse. *Dev. Dyn.* **233**, 837–846 (2005).

211. Cai, K. Q., Capo-Chichi, C. D., Rula, M. E., Yang, D. H. & Xu, X. X. M. Dynamic GATA6 expression in primitive endoderm formation and maturation in early mouse embryogenesis. *Dev. Dyn.* **237**, 2820–2829 (2008).

212. Bedzhov, I. & Zernicka-Goetz, M. Self-organizing properties of mouse pluripotent cells initiate morphogenesis upon implantation. *Cell* **156**, 1032–1044 (2014).

213. Martín-Belmonte, F. *et al.* Cell-Polarity Dynamics Controls the Mechanism of Lumen Formation in Epithelial Morphogenesis. *Curr. Biol.* **18**, 507–513 (2008).

214. Bedzhov, I. *et al.* Adhesion, but not a specific cadherin code, is indispensable for ES cell and induced pluripotency. *Stem Cell Res.* **11**, 1250–1263 (2013).

215. Li, S., Edgar, D., Fässler, R., Wadsworth, W. & Yurchenco, P. D. The role of laminin in embryonic cell polarization and tissue organization. *Dev. Cell* **4**, 613–624 (2003).

216. Meder, D., Shevchenko, A., Simons, K. & Füllekrug, J. Gp135/podocalyxin and NHERF-2 participate in the formation of a preapical domain during polarization of MDCK cells. *J. Cell Biol.* **168**, 303–313 (2005).

217. Shahbazi, M. N. *et al.* Pluripotent state transitions coordinate morphogenesis in mouse and human embryos. *Nature* **552**, 239–243 (2017).

218. Smith, A. Formative pluripotency: The executive phase in a developmental continuum. *Dev.* **144**, 365–373 (2017).

219. Morgani, S. M., Metzger, J. J., Nichols, J., Siggia, E. D. & Hadjantonakis, A. K. Micropattern differentiation of mouse pluripotent stem cells recapitulates embryo regionalized cell fate patterning. *Elife* **7**, 1–35 (2018).

220. Van Den Brink, S. C. *et al.* Symmetry breaking, germ layer specification and axial organisation in aggregates of mouse embryonic stem cells. *Dev.* **141**, 4231–4242 (2014).

221. Yoney, A. *et al.* WNT signaling memory is required for ACTIVIN to function as a morphogen in human gastruloids. *Elife* **7**, 1–28 (2018).

222. Harrison, S. E., Sozen, B., Christodoulou, N., Kyprianou, C. & Zernicka-Goetz, M. Assembly of embryonic and extraembryonic stem cells to mimic embryogenesis in vitro. *Science (80-.).* **356**, (2017).

223. Sozen, B. *et al.* Self-assembly of embryonic and two extra-embryonic stem cell types into gastrulating embryo-like structures. *Nat. Cell Biol.* **20**, 979–989 (2018).

224. Zhang, S. *et al.* Implantation initiation of self-assembled embryo-like structures generated using three types of mouse blastocyst-derived stem cells. *Nat. Commun.* **10**, (2019).

225. Souilhol, C. *et al.* NOTCH activation interferes with cell fate specification in the gastrulating mouse embryo. *Dev.* **142**, 3649–3660 (2015).

226. Becker, S. *et al.* A role for Indian hedgehog in extraembryonic endoderm differentiation in F9 cells and the early mouse embryo. *Dev. Biol.* **187**, 298–310 (1997).

227. Harman, R. M., Cowan, R. G., Ren, Y. & Quirk, S. M. Reduced signaling through the hedgehog pathway in the uterine stroma causes deferred implantation and embryonic loss. *Reproduction* **141**, 665–674 (2011).

228. Pan, Y. B. *et al.* Sonic hedgehog through Gli2 and Gli3 is required for the proper development of

placental labyrinth. *Cell Death Dis.* **6**, 1–11 (2015).

229. Wang, D. C. *et al.* Sonic Hedgehog promotes in vitro oocyte maturation and term development of embryos in Taiwan native goats. *Theriogenology* **103**, 52–58 (2017).

230. Lee, S. *et al.* Sonic hedgehog signaling mediates resveratrol to improve maturation of pig oocytes in vitro and subsequent preimplantation embryo development. *J. Cell. Physiol.* **233**, 5023–5033 (2018).

231. Ludwig, T. *et al.* Mouse mutants lacking the type 2 IGF receptor (IGF2R) are rescued from perinatal lethality in Igf2 and Igf1r null backgrounds. *Dev. Biol.* **177**, 517–535 (1996).

232. Inzunza, J. *et al.* Selective insulin-like growth factor-I antagonist inhibits mouse embryo development in a dose-dependent manner. *Fertil. Steril.* **93**, 2621–2626 (2010).

233. Green, C. J. & Day, M. L. Insulin-like growth factor 1 acts as an autocrine factor to improve early embryogenesis in vitro. *Int. J. Dev. Biol.* **57**, 837–844 (2013).

234. Chen, J. *et al.* Inhibition of phosphorylated Ser473-Akt from translocating into the nucleus contributes to 2-cell arrest and defective zygotic genome activation in mouse preimplantation embryogenesis. *Dev. Growth Differ.* **58**, 280–292 (2016).

235. Riley, J. K. *et al.* The PI3K/Akt pathway is present and functional in the preimplantation mouse embryo. *Dev. Biol.* **284**, 377–386 (2005).

236. Bulut-Karslioglu, A. *et al.* Inhibition of mTOR induces a paused pluripotent state. *Nature* **540**, 119–123 (2016).

237. Arnold, S. J., Maretto, S., Islam, A., Bikoff, E. K. & Robertson, E. J. Dose-dependent Smad1, Smad5 and Smad8 signaling in the early mouse embryo. *Dev. Biol.* **296**, 104–118 (2006).

238. Senft, A. D., Bikoff, E. K., Robertson, E. J. & Costello, I. Genetic dissection of Nodal and Bmp signalling requirements during primordial germ cell development in mouse. *Nat. Commun.* **10**, 1–11 (2019).

239. Tang, F. *et al.* Tracing the derivation of embryonic stem cells from the inner cell mass by single-cell RNA-seq analysis. *Cell Stem Cell* **6**, 468–478 (2010).

240. Reyes de Mochel, N. S. *et al.* BMP signaling is required for cell cleavage in preimplantation-mouse embryos. *Dev. Biol.* **397**, 45–55 (2015).

241. Coucouvanis, E. & Martin, G. R. BMP signaling plays a role in visceral endoderm differentiation and cavitation in the early mouse embryo. *Development* **126**, 535–546 (1999).

242. Robertson, E. J. Dose-dependent nodal/smad signals pattern the early mouse embryo. *Semin. Cell Dev. Biol.* **32**, 73–79 (2014).

243. Conlon, F. L., Barth, K. S. & Robertson, E. J. A novel retrovirally induced embryonic lethal mutation in the mouse: Assessment of the developmental fate of embryonic stem cells homozygous for the 413.d proviral intergration. *Development* **111**, 969–981 (1991).

244. Conlon, F. L. *et al.* A primary requirement for nodal in the formation and maintenance of the primitive streak in the mouse. *Development* **120**, 1919–1928 (1994).

245. Zhou, X., Sasaki, H., Lowe, L., Hogan, B. L. & Kuehn, M. R. Nodal is a novel TGF-beta-like gene expressed in the mouse node during gastrulation. *Nature* **361**, 543–547 (1993).

246. Tadjuidje, E. *et al.* Nodal signalling in Xenopus: The role of Xnr5 in left/right asymmetry and heart development. *Open Biol.* **6**, (2016).

247. Lapraz, F., Haillot, E. & Lepage, T. A deuterostome origin of the Spemann organiser suggested by Nodal and ADMPs functions in Echinoderms. *Nat. Commun.* **6**, (2015).

248. Montague, T. G. & Schier, A. F. Vg1-nodal heterodimers are the endogenous inducers of mesendoderm. *Elife* **6**, 1–24 (2017).

249. Schier, a F. & Shen, M. M. Nodal signalling in vertebrate development. *Nature* **403**, 385–389 (2000).

250. Collignon, J., Varlet, I. & Robertson, E. J. Relationship between asymmetric nodal expression and the direction of embryonic turning. *Nature* **381**, 155–158 (1996).

251. Grande, C. & Patel, N. H. Nodal signalling is involved in left-right asymmetry in snails. *Nature* **457**, 1007–1011 (2009).

252. Watanabe, H. *et al.* Nodal signalling determines biradial asymmetry in Hydra. *Nature* **515**, 112–115 (2014).

253. Beck, S. *et al.* Extraembryonic proteases regulate Nodal signalling during gastrulation. *Nat. Cell Biol.* **4**, 981–985 (2002).

254. Constam, D. B. Riding shotgun: A dual role for the epidermal growth factor-Cripto/FRL-1/ Cryptic protein cripto in nodal trafficking. *Traffic* **10**, 783–791 (2009).

255. Ellis, P. S. *et al.* Pronodal acts via FGFR3 to govern duration of Shh expression in the prechordal mesoderm. *Dev.* **142**, 3821–3832 (2015).

256. Shen, M. M. Nodal signaling: developmental roles and regulation. *Development* **134**, 1023–34 (2007).

257. Arnold, S. J. & Robertson, E. J. Making a commitment: cell lineage allocation and axis patterning in the early mouse embryo. *Nat. Rev. Mol. Cell Biol.* **10**, 91–103 (2009).

258. Gray, P. C., Harrison, C. A. & Vale, W. CriptoはActRIIと複合体を形成しActivinシグナルを阻害する (PNAS, 2003).pdf. **100**, 5193–5198 (2003).

259. Levine, A. J. & Brivanlou, A. H. GDF3 at the Crossroads of TGF-B signaling. *Cell Cycle* 1069–1073 (2006).

260. Pelliccia, J. L., Jindal, G. A. & Burdine, R. D. Gdf3 is required for robust nodal signaling during germ layer formation and left-right patterning. *Elife* **6**, 1–23 (2017).

261. Chen, C. *et al.* The Vg1-related protein Gdf3 acts in a Nodal signaling pathway in the pre-gastrulation mouse embryo. *Development* **133**, 319–329 (2006).

262. Andersson, O., Bertolino, P. & Ibáñez, C. F. Distinct and cooperative roles of mammalian Vg1 homologs GDF1 and GDF3 during early embryonic development. *Dev. Biol.* **311**, 500–511 (2007).

263. Tanaka, C., Sakuma, R., Nakamura, T., Hamada, H. & Saijoh, Y. Long-range action of Nodal requires interaction with GDF1. *Genes Dev.* **21**, 3272–3282 (2007).

264. Fuerer, C., Nostro, M. C. & Constam, D. B. Nodal·Gdf1 heterodimers with bound prodomains enable serum-independent nodal signaling and endoderm differentiation. *J. Biol. Chem.* **289**, 17854–17871 (2014).

265. Aykul, S. *et al.* Biochemical and cellular analysis reveals ligand binding specificities, a molecular basis for ligand recognition, and membrane association-dependent activities of cripto-1 and cryptic. *J. Biol. Chem.* **292**, 4138–4151 (2017).

266. Aykul, S., Ni, W., Mutatu, W. & Martinez-Hackert, E. Human cerberus prevents nodal-receptor binding, inhibits nodal signaling, and suppresses nodal-mediated phenotypes. *PLoS One* **10**, 1–23 (2015).

267. Siebold, C., Yamashita, T., Monnier, P. P., Mueller, B. K. & Pasterkamp, R. J. RGMs: Structural Insights, Molecular Regulation, and Downstream Signaling RGMs: A Small Gene Family with Widespread Effects. *Trends Cell Biol.* **27**, 365–378 (2017).

268. Saito, T. *et al.* Structural Basis of the Human Endoglin-BMP9 Interaction: Insights into BMP Signaling and HHT1. *Cell Rep.* **19**, 1917–1928 (2017).

269. Massagué, J., Seoane, J. & Wotton, D. Smad transcription factors. *Genes Dev.* **19**, 2783–2810 (2005).

270. Goto, K., Kamiya, Y., Imamura, T., Miyazono, K. & Miyazawa, K. Selective inhibitory effects of Smad6 on bone morphogenetic protein type I receptors. *J. Biol. Chem.* **282**, 20603–20611 (2007).

271. Yan, X. *et al.* Smad7 protein interacts with receptor-regulated Smads (R-Smads) to inhibit transforming growth factor-β (TGF-β)/Smad signaling. *J. Biol. Chem.* **291**, 382–392 (2016).

272. Inoue, Y. & Imamura, T. Regulation of TGF-β family signaling by E3 ubiquitin ligases. *Cancer Sci.* **99**, 2107–2112 (2008).

273. Hill, C. S. Transcriptional control by the SMADs. *Cold Spring Harb. Perspect. Biol.* **8**, (2016).

274. Charney, R. M. *et al.* Foxh1 Occupies cis-Regulatory Modules Prior to Dynamic Transcription Factor Interactions Controlling the Mesendoderm Gene Program. *Dev. Cell* **40**, 595-607.e4 (2017).

275. Deheuninck, J. & Luo, K. Ski and SnoN, potent negative regulators of TGF-β signaling. *Cell Res.* **19**, 47–57 (2009).

276. Levy, L. *et al.* Arkadia Activates Smad3/Smad4-Dependent Transcription by Triggering Signal-Induced SnoN Degradation. *Mol. Cell. Biol.* **27**, 6068–6083 (2007).

277. Le Scolan, E. *et al.* Transforming growth factor-β suppresses the ability of ski to inhibit tumor metastasis by inducing its degradation. *Cancer Res.* **68**, 3277–3285 (2008).

278. Tsuneyoshi, N. *et al.* The SMAD2/3 corepressor SNON maintains pluripotency through selective repression of mesendodermal genes in human ES cells. *Genes Dev.* **26**, 2471–2476 (2012).

279. Bertero, A. *et al.* Activin/Nodal signaling and NANOG orchestrate human embryonic stem cell fate decisions by controlling the H3K4me3 chromatin mark. *Genes Dev.* **29**, 702–717 (2015).

280. Wang, Q. *et al.* The p53 Family Coordinates Wnt and Nodal Inputs in Mesendodermal Differentiation of Embryonic Stem Cells. *Cell Stem Cell* **20**, 70–86 (2017).

281. Nowotschin, S. *et al.* The T-box transcription factor eomesodermin is essential for AVE induction in the mouse embryo. *Genes Dev.* **27**, 997–1002 (2013).

282. Bertero, A. *et al.* Activin/Nodal signaling and NANOG orchestrate human embryonic stem cell fate decisions by controlling the H3K4me3 chromatin mark. *Genes Dev.* **29**, 702–717 (2015).

283. Kang, J. S., Alliston, T., Delston, R. & Derynck, R. Repression of Runx2 function by TGF-β through recruitment of class II histone deacetylases by Smad3. *EMBO J.* **24**, 2543–2555 (2005).

284. Ross, S. *et al.* Smads orchestrate specific histone modifications and chromatin remodeling to activate transcription. *EMBO J.* **25**, 4490–4502 (2006).

285. Dahle, Ø., Kumar, A. & Kuehn, M. R. Nodal signaling recruits the histone demethylase Jmjd3 to counteract Polycomb-mediated repression at target genes. *Sci. Signal.* **3**, (2010).

286. Xi, Q. *et al.* A poised chromatin platform for TGF-β access to master regulators. *Cell* **147**, 1511–1524 (2011).

287. Beyer, T. A. *et al.* Switch enhancers interpret TGF-β and hippo signaling to control cell fate in human embryonic stem cells. *Cell Rep.* **5**, 1611–1624 (2013).

288. De Dieuleveult, M. *et al.* Genome-wide nucleosome specificity and function of chromatin remodellers in ES cells. *Nature* **530**, 113–116 (2016).

289. Kishigami, S. & Mishina, Y. BMP signaling and early embryonic patterning. *Cytokine Growth Factor Rev.* **16**, 265–278 (2005).

290. Krishnakumar, R. *et al.* FOXD3 Regulates Pluripotent Stem Cell Potential by Simultaneously Initiating and Repressing Enhancer Activity. *Cell Stem Cell* **18**, 104–117 (2016).

291. Carey, T. S. *et al.* BRG1 Governs Nanog Transcription in Early Mouse Embryos and Embryonic Stem Cells via Antagonism of Histone H3 Lysine 9/14 Acetylation . *Mol. Cell. Biol.* **35**, 4158–4169 (2015).

292. Xi, Q., He, W., Zhang, X. H. F., Le, H. Van & Massague, J. Genome-wide impact of the BRG1 SWI/SNF chromatin remodeler on the transforming growth factor β transcriptional program. *J. Biol. Chem.* **283**,

1146–1155 (2008).

293. Kato, Y., Habas, R., Katsuyama, Y., Näär, A. M. & He, X. A component of the ARC/mediator complex required for TGFβ/nodal signalling. *Nature* **418**, 641–646 (2002).

294. Müller, J. & Verrijzer, P. Biochemical mechanisms of gene regulation by polycomb group protein complexes. *Curr. Opin. Genet. Dev.* **19**, 150–158 (2009).

295. Bertero, A. *et al.* The SMAD2/3 interactome reveals that TGFβ controls m 6 A mRNA methylation in pluripotency. *Nature* **555**, 256–259 (2018).

296. Burdine, R. D. & Schier, A. F. Conserved and divergent mechanisms in left − right axis formation Conserved and divergent mechanisms in left – right axis formation. *Genes Dev* **14**, 763–776 (2000).

297. van Boxtel, A. L., Economou, A. D., Heliot, C. & Hill, C. S. Long-Range Signaling Activation and Local Inhibition Separate the Mesoderm and Endoderm Lineages. *Dev. Cell* **44**, 179-191.e5 (2018).

298. Guzman-Ayala, M. *et al.* Graded Smad2/3 activation is converted directly into levels of target gene expression in embryonic stem cells. *PLoS One* **4**, (2009).

299. Hagos, E. G. & Dougan, S. T. Time-dependent patterning of the mesoderm and endoderm by Nodal signals in zebrafish. *BMC Dev. Biol.* **7**, 1–18 (2007).

300. van Boxtel, A. L. *et al.* A Temporal Window for Signal Activation Dictates the Dimensions of a Nodal Signaling Domain. *Dev. Cell* **35**, 175–185 (2015).

301. Dubrulle, J. *et al.* Response to Nodal morphogen gradient is determined by the kinetics of target gene induction. *Elife* **4**, 1–27 (2015).

302. Mavrakis, K. J. *et al.* Arkadia enhances Nodal/TGF-β signaling by coupling phospho-Smad2/3 activity and turnover. *PLoS Biol.* **5**, 0586–0603 (2007).

303. Warmflash, A. *et al.* Dynamics of TGF-β signaling reveal adaptive and pulsatile behaviors reflected in the nuclear localization of transcription factor Smad4. *Proc. Natl. Acad. Sci. U. S. A.* **109**, (2012).

304. Sorre, B., Warmflash, A., Brivanlou, A. H. & Siggia, E. D. Encoding of temporal signals by the TGF-β Pathway and implications for embryonic patterning. *Dev. Cell* **30**, 334–342 (2014).

305. Niederländer, C., Walsh, J. J., Episkopou, V. & Jones, C. M. Arkadia enhances nodal-related signalling to induce mesendoderm. *Nature* **410**, 830–834 (2001).

306. Dunn, N. R., Vincent, S. D., Oxburgh, L., Robertson, E. J. & Bikoff, E. K. Combinatorial activities of Smad2 and Smad3 regulate mesoderm formation and patterning in the mouse embryo. *Development* **131**, 1717–1728 (2004).

307. Vincent, S. D., Dunn, N. R., Hayashi, S., Norris, D. P. & Robertson, E. J. Cell fate decisions within the mouse organizer are governed by graded Nodal signals. *Genes Dev.* **17**, 1646–1662 (2003).

308. Cheng, S. K., Olale, F., Brivanlou, A. H. & Schier, A. F. Lefty blocks a subset of TGF?? signals by antagonizing EGF-CFC coreceptors. *PLoS Biol.* **2**, (2004).

309. Fullerton, P. T., Monsivais, D., Kommagani, R. & Matzuk, M. M. Follistatin is critical for mouse uterine receptivity and decidualization. *Proc. Natl. Acad. Sci. U. S. A.* **114**, E4772–E4781 (2017).

310. Shiratori, H. & Hamada, H. TGFβ signaling in establishing left-right asymmetry. *Semin. Cell Dev. Biol.* **32**, 80–84 (2014).

311. Haillot, E., Molina, M. D., Lapraz, F. & Lepage, T. The Maternal Maverick/GDF15-like TGF-β Ligand Panda Directs Dorsal-Ventral Axis Formation by Restricting Nodal Expression in the Sea Urchin Embryo. *PLoS Biol.* **13**, 1–38 (2015).

312. Luo, K. Signaling Cross Talk between TGF-b / Smad. *Cold Spring Harb. Persepctives Biol.* **9**, a022137 (2017).

313. Nakatake, Y. *et al.* Klf4 Cooperates with Oct3/4 and Sox2 To Activate the Lefty1 Core Promoter in Embryonic Stem Cells. *Mol. Cell. Biol.* **26**, 7772–7782 (2006).

314. Gao, Z., Zhu, X. & Dou, Y. The MIR-302/367 cluster: A comprehensive update on its evolution and functions. *Open Biol.* **5**, (2015).

315. Dai, H. Q. *et al.* TET-mediated DNA demethylation controls gastrulation by regulating Lefty-Nodal signalling. *Nature* **538**, 528–532 (2016).

316. Morkel, M. *et al.* β-Catenin regulates Cripto- and Wnt3-dependent gene expression programs in mouse axis and mesoderm formation. *Development* **130**, 6283–6294 (2003).

317. Vincent, S. D., Norris, D. P., Ann Le Good, J., Constam, D. B. & Robertson, E. J. Asymmetric Nodal expression in the mouse is governed by the combinatorial activities of two distinct regulatory elements. *Mech. Dev.* **121**, 1403–1415 (2004).

318. Adachi, H. *et al.* Determination of left/right asymmetric expression of nodal by a left side-specific enhancer with sequence similarity to a lefty-2 enhancer. *Genes Dev.* **13**, 1589–1600 (1999).

319. Norris, D. P. & Robertson, E. J. Asymmetric and node-specific nodal expression patterns are controlled by two distinct cis-acting regulatory elements. *Genes Dev.* **13**, 1575–1588 (1999).

320. Krebs, L. T. *et al.* Notch signaling regulates left-right asymmetry determination by inducing Nodal expression. *Genes Dev.* **17**, 1207–1212 (2003).

321. Kitajima, K., Oki, S., Ohkawa, Y., Sumi, T. & Meno, C. Wnt signaling regulates left-right axis formation in the node of mouse embryos. *Dev. Biol.* **380**, 222–232 (2013).

322. Li, Z. *et al.* BMP4 signaling acts via dual-specificity phosphatase 9 to control ERK activity in mouse embryonic stem cells. *Cell Stem Cell* **10**, 171–182 (2012).

323. Liu, X. *et al.* Araf kinase antagonizes Nodal-Smad2 activity in mesendoderm development by directly phosphorylating the Smad2 linker region. *Nat. Commun.* **4**, 1711–1728 (2013).

324. Singh, A. M. *et al.* Signaling network crosstalk in human pluripotent cells: A Smad2/3-regulated switch that controls the balance between self-renewal and differentiation. *Cell Stem Cell* **10**, 312–326 (2012).

325. Molina, M. D. *et al. MAPK and GSK3/ß-TRCP-mediated degradation of the maternal Ets domain transcriptional repressor Yan/Tel controls the spatial expression of nodal in the sea urchin embryo*. *PLoS Genetics* **14**, (2018).

326. Clements, M., Pernaute, B., Vella, F. & Rodriguez, T. A. Crosstalk between Nodal/activin and MAPK p38 signaling is essential for anterior-posterior axis specification. *Curr. Biol.* **21**, 1289–1295 (2011).

327. Wu, Q., Fukuda, K., Weinstein, M., Graff, J. M. & Saga, Y. Smad2 and p38 signaling pathways act in concert to determine xy primordial germ cell fate in mice. *Dev.* **142**, 575–586 (2015).

328. Cavalieri, V. & Spinelli, G. Early asymmetric cues triggering the dorsal/ventral gene regulatory network of the sea urchin embryo. *Elife* **3**, e04664 (2014).

329. Maekawa, M. *et al.* Requirement of the MAP kinase signaling pathways for mouse preimplantation development. *Development* **132**, 1773–1783 (2005).

330. Natale, D. R., Paliga, A. J. M., Beier, F., D'Souza, S. J. A. & Watson, A. J. p38 MAPK signaling during murine preimplantation development. *Dev. Biol.* **268**, 76–88 (2004).

331. Bell, C. E. & Watson, A. J. p38 MAPK Regulates Cavitation and Tight Junction Function in the Mouse Blastocyst. *PLoS One* **8**, (2013).

332. Estarás, C., Benner, C. & Jones, K. A. SMADs and YAP Compete to Control Elongation of β-Catenin: LEF-1-Recruited RNAPII during hESC Differentiation. *Mol. Cell* **58**, 780–793 (2014).

333. Chu, J. & Shen, M. M. Functional redundancy of EGF-CFC genes in epiblast and extraembryonic patterning during early mouse embryogenesis. *Dev. Biol.* **342**, 63–73 (2010).

334. Matzuk, M. M. *et al.* Functional analysis of activins during mammalian development. *Nature* **374**, 354–357 (1995).

335. Song, J. *et al.* The type II activin receptors are essential for egg cylinder growth, gastrulation, and rostral head development in mice. *Dev. Biol.* **213**, 157–169 (1999).

336. Matzuk, M. M., Kumar, T. R. & Bradley, A. Different phenotypes for mice deficient in either activins or activin receptor type II. *Nature* **374**, 356–360 (1995).

337. Gu, Z. *et al.* The type I activin receptor ActRIB is required for egg cylinder organization and gastrulation in the mouse. *Genes Dev.* **12**, 844–857 (1998).

338. Jornvall, H., Reissmann, E., Andersson, O., Mehrkash, M. & Ibanez, C. F. ALK7, a Receptor for Nodal, Is Dispensable for Embryogenesis and Left-Right Patterning in the Mouse. *Mol. Cell. Biol.* **24**, 9383–9389 (2004).

339. Matzuk, M. M. *et al.* Multiple defects and perinatal death in mice deficient in follistatin. *Nature* **374**, 360–363 (1995).

340. Zhu, Y. P., Liu, Z., Fu, Z. X. & Li, D. C. Smad3 mutant mice develop colon cancer with overexpression of COX-2. *Oncol. Lett.* **13**, 1535–1538 (2017).

341. Yuan, Z., Richardson, J. A., Parada, L. F. & Graft, J. M. Smad3 mutant mice develop metastatic colorectal cancer. *Cell* **94**, 703–714 (1998).

342. Datto, M. B. *et al.* Targeted Disruption of Smad3 Reveals an Essential Role in Transforming Growth Factor β-Mediated Signal Transduction. *Mol. Cell. Biol.* **19**, 2495–2504 (1999).

343. Mesnard, D., Guzman-Ayala, M. & Constam, D. B. Nodal specifies embryonic visceral endoderm and sustains pluripotent cells in the epiblast before overt axial patterning. *Development* **133**, 2497–2505 (2006).

344. Sirard, C. *et al.* The tumor suppressor gene Smad4/Dpc4 is required for gastrulation and later for anterior development of the mouse embryo. *Genes Dev.* **12**, 107–119 (1998).

345. Hoodless, P. A. *et al.* FoxH1 (Fast) functions to specify the anterior primitive streak in the mouse. *Genes Dev.* **15**, 1257–1271 (2001).

346. Belo, J. A. *et al.* Cerberus-like is a secreted BMP and nodal antagonist not essential for mouse development. *Genesis* **26**, 265–270 (2000).

347. Simon, C. S. *et al.* Functional characterisation of cis-regulatory elements governing dynamic Eomes expression in the early mouse embryo. *Dev.* **144**, 1249–1260 (2017).

348. Kimura-Yoshida, C. *et al.* Crucial roles of Foxa2 in mouse anterior-posterior axis polarization via regulation of anterior visceral endoderm-specific genes. *Proc. Natl. Acad. Sci. U. S. A.* **104**, 5919–5924 (2007).

349. Lu, C. C. & Robertson, E. J. Multiple roles for Nodal in the epiblast of the mouse embryo in the establishment of anterior-posterior patterning. *Dev. Biol.* **273**, 149–159 (2004).

350. Guzman-Ayala, M., Ben-Haim, N., Beck, S. & Constam, D. B. Nodal protein processing and fibroblast growth factor 4 synergize to maintain a trophoblast stem cell microenvironment. *Proc. Natl. Acad. Sci. U. S. A.* **101**, 15656–15660 (2004).

351. Camus, A., Perea-Gomez, A., Moreau, A. & Collignon, J. Absence of Nodal signaling promotes precocious neural differentiation in the mouse embryo. *Dev. Biol.* **295**, 743–755 (2006).

352. Papanayotou, C. Activin / Nodal signalling before implantation : setting the stage for embryo patterning. **3**, (2014).

353. James, D., Levine, A. J., Besser, D. & Hemmati-Brivanlou, A. TGFbeta/activin/nodal signaling is necessary for the maintenance of pluripotency in human embryonic stem cells. *Development* **132**, 1273–1282

(2005).

354. Albano, R. M., Groome, N. & Smith, J. C. Activins are expressed in preimplantation mouse embryos and in ES and EC cells and are regulated on their differentiation. *Development* **117**, 711–723 (1993).

355. Lu, R. Z., Matsuyama, S., Nishihara, M. & Takahashi, M. Developmental Expression of Activin/Inhibin βA, βB, and α Subunits, and Activin Receptor-IIB Genes in Preimplantation Mouse Embryos1. *Biol. Reprod.* **49**, 1163–1169 (1993).

356. Albano, R. M. & Smith, J. C. Follistatin expression in ES and F9 cells and in preimplantation mouse embryos. *Int. J. Dev. Biol.* **38**, 543–547 (1994).

357. Rankin, C. T., Bunton, T., Lawler, a M. & Lee, S. J. Regulation of left-right patterning in mice by growth/differentiation factor-1. *Nat. Genet.* **24**, 262–265 (2000).

358. Park, C. B. & Dufort, D. Nodal Expression in the Uterus of the Mouse Is Regulated by the Embryo and Correlates with Implantation1. *Biol. Reprod.* **84**, 1103–1110 (2011).

359. Peng, J. *et al.* Uterine activin-like kinase 4 regulates trophoblast development during mouse placentation. *Mol. Endocrinol.* **29**, 1684–1693 (2015).

360. Beppu, H. *et al.* BMP type II receptor is required for gastrulation and early development of mouse embryos. *Dev. Biol.* **221**, 249–258 (2000).

361. Reyes de Mochel, N. S. *et al.* BMP signaling is required for cell cleavage in preimplantation-mouse embryos. *Dev. Biol.* **397**, 45–55 (2015).

362. La Rosa, I. *Bone Morphogenetic Proteins in Preimplantation Embryos*. *Vitamins and Hormones* **99**, (Elsevier Inc., 2015).

363. Komekado, H., Yamamoto, H., Chiba, T. & Kikuchi, A. Glycosylation and palmitoylation of Wnt-3a are coupled to produce an active form of Wnt-3a. *Genes to Cells* **12**, 521–534 (2007).

364. Takada, R. *et al.* Monounsaturated Fatty Acid Modification of Wnt Protein: Its Role in Wnt Secretion. *Dev. Cell* **11**, 791–801 (2006).

365. Fu, J., Jiang, M., Mirando, A. J., Yu, H. M. I. & Hsu, W. Reciprocal regulation of Wnt and Gpr177/mouse Wntless is required for embryonic axis formation. *Proc. Natl. Acad. Sci. U. S. A.* **106**, 18598–18603 (2009).

366. Fu, J., Ivy Yu, H. M., Maruyama, T., Mirando, A. J. & Hsu, W. Gpr177/mouse Wntless is essential for Wnt-mediated craniofacial and brain development. *Dev. Dyn.* **240**, 365–371 (2011).

367. Maruyama, E. O., Yu, H. M. I., Jiang, M., Fu, J. & Hsu, W. Gpr177 Deficiency Impairs Mammary Development and Prohibits Wnt-Induced Tumorigenesis. *PLoS One* **8**, (2013).

368. Miranda, M. *et al.* Identification of the WNT1 residues required for palmitoylation by Porcupine. *FEBS Lett.* **588**, 4815–4824 (2014).

369. Farah, O., Biechele, S., Rossant, J. & Dufort, D. Porcupine-Dependent Wnt activity within the uterine epithelium is essential for fertility. *Biol. Reprod.* **97**, 688–697 (2017).

370. Biechele, S., Cockburn, K., Lanner, F., Cox, B. J. & Rossant, J. Porcn-dependent Wnt signaling is not required prior to mouse gastrulation. *Dev.* **140**, 2961–2971 (2013).

371. Biechele, S., Cox, B. J. & Rossant, J. Porcupine homolog is required for canonical Wnt signaling and gastrulation in mouse embryos. *Dev. Biol.* **355**, 275–285 (2011).

372. Morrell, N. T. *et al.* Liposomal packaging generates Wnt protein with in vivo biological activity. *PLoS One* **3**, (2008).

373. Bovolenta, P., Esteve, P., Ruiz, J. M., Cisneros, E. & Lopez-Rios, J. Beyond Wnt inhibition: New functions of secreted Frizzled-related proteins in development and disease. *J. Cell Sci.* **121**, 737–746 (2008).

374. Mii, Y. & Taira, M. Secreted Frizzled-related proteins enhance the diffusion of Wnt ligands and expand their signalling range. *Development* **136**, 4083–4088 (2009).

375. Yamamoto, H., Yoo, S. K., Nishita, M., Kikuchi, A. & Minami, Y. Wnt5a modulates glycogen synthase kinase 3 to induce phosphorylation of receptor tyrosine kinase Ror2. *Genes to Cells* **12**, 1215–1223 (2007).

376. Minami, Y., Oishi, I., Endo, M. & Nishita, M. Ror-family receptor tyrosine kinases in noncanonical Wnt signaling: Their implications in developmental morphogenesis and human diseases. *Dev. Dyn.* **239**, 1–15 (2010).

377. He, X., Semenov, M., Tamai, K. & Zeng, X. LDL receptor-related proteins 5 and 6 in Wnt/β-catenin signaling: Arrows point the way. *Development* **131**, 1663–1677 (2004).

378. Tamai, K. *et al.* A Mechanism for Wnt Coreceptor Activation. *Mol. Cell* **13**, 149–156 (2004).

379. MacDonald, B. T., Tamai, K. & He, X. Wnt/β-Catenin Signaling: Components, Mechanisms, and Diseases. *Dev. Cell* **17**, 9–26 (2009).

380. Semënov, M. V. *et al.* Head inducer dickkopf-1 is a ligand for Wnt coreceptor LRP6. *Curr. Biol.* **11**, 951–961 (2001).

381. Semënov, M., Tamai, K. & He, X. SOST is a ligand for LRP5/LRP6 and a Wnt signaling inhibitor. *J. Biol. Chem.* **280**, 26770–26775 (2005).

382. Shimomura, Y. *et al.* APCDD1 is a novel Wnt inhibitor mutated in hereditary hypotrichosis simplex. *Nature* **464**, 1043–1047 (2010).

383. Yamamoto, A., Nagano, T., Takehara, S., Hibi, M. & Aizawa, S. Shisa promotes head formation through the inhibition of receptor protein maturation for the caudalizing factors, Wnt and FGF. *Cell* **120**, 223–235 (2005).

384. Lee, E., Salic, A., Krüger, R., Heinrich, R. & Kirschner, M. W. The roles of APC and axin derived from experimental and theoretical analysis of the Wnt pathway. *PLoS Biol.* **1**, 116–132 (2003).

385. Choi, J., Sun, Y. P., Costantini, F., Jho, E. H. & Joo, C. K. Adenomatous polyposis coli is down-regulated by the ubiquitin-proteasome pathway in a process facilitated by Axin. *J. Biol. Chem.* **279**, 49188–49198 (2004).

386. Su, Y. Y. *et al.* APC Is Essential for Targeting Phosphorylated β-Catenin to the SCFβ-TrCP Ubiquitin Ligase. *Mol. Cell* **32**, 652–661 (2008).

387. Luo, W. *et al.* Protein phosphatase 1 regulates assembly and function of the β-catenin degradation complex. *EMBO J.* **26**, 1511–1521 (2007).

388. Zeng, X. *et al.* W289(W2285_ref13).pdf. *Nature* **438**, 873–877 (2005).

389. Zeng, X. *et al.* Initiation of Wnt signaling: Control of Wnt coreceptor Lrp6 phosphorylation/activation via frizzled, dishevelled and axin functions. *Development* **135**, 367–375 (2008).

390. MacDonald, B. T., Yokota, C., Tamai, K., Zeng, X. & He, X. Wnt signal amplification via activity, cooperativity, and regulation of multiple intracellular PPPSP motifs in the Wnt co-receptor LRP6. *J. Biol. Chem.* **283**, 16115–16123 (2008).

391. Taelman, V. F. *et al.* Wnt signaling requires sequestration of Glycogen Synthase Kinase 3 inside multivesicular endosomes. *Cell* **143**, 1136–1148 (2010).

392. Kim, H., Vick, P., Hedtke, J., Ploper, D. & De Robertis, E. M. Wnt Signaling Translocates Lys48-Linked Polyubiquitinated Proteins to the Lysosomal Pathway. *Cell Rep.* **11**, 1151–1159 (2015).

393. Tejeda-Muñoz, N., Albrecht, L. V., Bui, M. H. & De Robertis, E. M. Wnt canonical pathway activates macropinocytosis and lysosomal degradation of extracellular proteins. *Proc. Natl. Acad. Sci. U. S. A.* **116**, 10402–10411 (2019).

394. Benchabane, H., Hughes, E. G., Takacs, C. M., Baird, J. R. & Ahmed, Y. Adenomatous polyposis coli is present near the minimal level required for accurate graded responses to the Wingless morphogen. *Development* **135**, 963–971 (2008).

395. Savvidou, I. *et al.* β-catenin inhibitor BC2059 is efficacious as monotherapy or in combination with proteasome inhibitor bortezomib in multiple myeloma. *Mol. Cancer Ther.* **16**, 1765–1778 (2017).

396. Fagotto, F., Glück, U. & Gumbiner, B. M. Nuclear localization signal-independent and importin/karyopherin-independent nuclear import of β-catenin. *Curr. Biol.* **8**, 181–190 (1998).

397. Städeli, R., Hoffmans, R. & Basler, K. Transcription under the Control of Nuclear Arm/β-Catenin. *Curr. Biol.* **16**, 378–385 (2006).

398. Kim, G. *et al.* Nuclear β-catenin localization and mutation of the CTNNB1 gene: a context-dependent association. *Mod. Pathol.* **31**, 1553–1559 (2018).

399. Wu, X. *et al.* Rac1 Activation Controls Nuclear Localization of β-catenin during Canonical Wnt Signaling. *Cell* **133**, 340–353 (2008).

400. Ehyai, S. *et al.* A p38 mitogen-activated protein kinase-regulated myocyte enhancer factor 2-β-catenin interaction enhances canonical Wnt signaling. *Mol. Cell. Biol.* **36**, 330–346 (2016).

401. Chen, J. R. *et al.* Dietary-induced serum phenolic acids promote bone growth via p38 MAPK/β-catenin canonical Wnt signaling. *J. Bone Miner. Res.* **25**, 2399–2411 (2010).

402. Atcha, F. A. *et al.* A Unique DNA Binding Domain Converts T-Cell Factors into Strong Wnt Effectors. *Mol. Cell. Biol.* **27**, 8352–8363 (2007).

403. Hoppler, S. P. & Kavanagh, C. L. Wnt signalling: Variety at the core. *J. Cell Sci.* **120**, 385–393 (2007).

404. Tago, K. I. *et al.* Inhibition of Wnt signaling by ICAT, a novel β-catenin-interacting protein. *Genes Dev.* **14**, 1741–1749 (2000).

405. Zhang, W. *et al.* Novel Cross Talk of Kruppel-Like Factor 4 and -Catenin Regulates Normal Intestinal Homeostasis and Tumor Repression. *Mol. Cell. Biol.* **26**, 2055–2064 (2006).

406. Singh, A. M. *et al.* Chibby, an antagonist of the Wnt/β-catenin pathway, facilitates cardiomyocyte differentiation of murine embryonic stem cells. *Circulation* **115**, 617–626 (2007).

407. Li, F.-Q. *et al.* Chibby Promotes Adipocyte Differentiation through Inhibition of -Catenin Signaling. *Mol. Cell. Biol.* **27**, 4347–4354 (2007).

408. Tanaka, S. S., Kojima, Y., Yamaguchi, Y. L., Nishinakamura, R. & Tam, P. P. L. Impact of WNT signaling on tissue lineage differentiation in the early mouse embryo. *Dev. Growth Differ.* **53**, 843–856 (2011).

409. Funa, N. S. *et al.* β-Catenin Regulates Primitive Streak Induction through Collaborative Interactions with SMAD2/SMAD3 and OCT4. *Cell Stem Cell* **16**, 639–652 (2015).

410. Wang, S. & Jones, K. A. CK2 Controls the Recruitment of Wnt Regulators to Target Genes In Vivo. *Curr. Biol.* **16**, 2239–2244 (2006).

411. Sierra, J., Yoshida, T., Joazeiro, C. A. & Jones, K. A. The APC tumor suppressor counteracts β-catenin activation and H3K4 methylation at Wnt target genes. *Genes Dev.* **20**, 586–600 (2006).

412. Krieghoff, E., Behrens, J. & Mayr, B. Nucleo-cytoplasmic distribution of β-catenin is regulated by retention. *J. Cell Sci.* **119**, 1453–1463 (2006).

413. Gayrard, C., Bernaudin, C., Déjardin, T., Seiler, C. & Borghi, N. Src- and confinement-dependent FAK activation causes E-cadherin relaxation and β-catenin activity. *J. Cell Biol.* **217**, 1063–1077 (2018).

414. Gortazar, A. R., Martin-Millan, M., Bravo, B., Plotkin, L. I. & Bellido, T. Crosstalk between caveolin-1/extracellular signal-regulated kinase (ERK) and β-catenin survival pathways in osteocyte mechanotransduction. *J. Biol. Chem.* **288**, 8168–8175 (2013).

415. Cha, B. *et al.* Mechanotransduction activates canonical Wnt/β-catenin signaling to promote lymphatic vascular patterning and the development of lymphatic and lymphovenous valves. *Genes Dev.* **30**, 1454–1469 (2016).

416. Liu, Z. *et al.* CFTR-β-catenin interaction regulates mouse embryonic stem cell differentiation and embryonic development. *Cell Death Differ.* **24**, 98–110 (2017).

417. Mo, S. *et al.* Caveolin-1 regulates dorsoventral patterning through direct interaction with β-catenin in zebrafish. *Dev. Biol.* **344**, 210–223 (2010).

418. Chairoungdua, A., Smith, D. L., Pochard, P., Hull, M. & Caplan, M. J. Exosome release of β-catenin: A novel mechanism that antagonizes Wnt signaling. *J. Cell Biol.* **190**, 1079–1091 (2010).

419. Azzolin, L. *et al.* Role of TAZ as mediator of wnt signaling. *Cell* **151**, 1443–1456 (2012).

420. Llado, V. *et al.* Repression of intestinal stem cell function and tumorigenesis through direct phosphorylation of β-catenin and yap by PKCζ. *Cell Rep.* **10**, 740–754 (2015).

421. Yu, F. X. *et al.* Regulation of the Hippo-YAP pathway by G-protein-coupled receptor signaling. *Cell* **150**, 780–791 (2012).

422. Azzolin, L. *et al.* YAP/TAZ incorporation in the β-catenin destruction complex orchestrates the Wnt response. *Cell* **158**, 157–170 (2014).

423. Codelia, V. A., Sun, G. & Irvine, K. D. Regulation of YAP by mechanical strain through Jnk and Hippo signaling. *Curr. Biol.* **24**, 2012–2017 (2014).

424. Varelas, X. *et al.* The Hippo Pathway Regulates Wnt/β-Catenin Signaling. *Dev. Cell* **18**, 579–591 (2010).

425. Barry, E. R. *et al.* Restriction of intestinal stem cell expansion and the regenerative response by YAP. *Nature* **493**, 106–110 (2013).

426. Johnson, R. L. & Martin, J. F. Proliferation and Heart Size. 458–461 (2011).

427. Park, H. W. *et al.* Alternative Wnt Signaling Activates YAP/TAZ. *Cell* **162**, 780–794 (2015).

428. Nichols, J. & Smith, A. Pluripotency in the embryo and in culture. *Cold Spring Harb. Perspect. Biol.* **4**, 1–14 (2012).

429. Umehara, H. *et al.* Efficient Derivation of Embryonic Stem Cells by Inhibition of Glycogen Synthase Kinase-3. *Stem Cells* **25**, 2705–2711 (2007).

430. Descalzo, S. M., Rué, P., Garcia-Ojalvo, J. & Arias, A. M. Correlations between the levels of Oct4 and Nanog as a signature for naïve pluripotency in mouse embryonic stem cells. *Stem Cells* **30**, 2683–2691 (2012).

431. Wagner, R. T., Xu, X., Yi, F., Merrill, B. J. & Cooney, A. J. Canonical Wnt/β-catenin regulation of liver receptor homolog-1 mediates pluripotency gene expression. *Stem Cells* **28**, 1794–1804 (2010).

432. Zhang, X., Peterson, K. A., Liu, X. S., Mcmahon, A. P. & Ohba, S. Gene regulatory networks mediating canonical wnt signal-directed control of pluripotency and differentiation in embryo stem cells. *Stem Cells* **31**, 2667–2679 (2013).

433. del Valle, I. *et al.* E-cadherin is required for the proper activation of the Lifr/Gp130 signaling pathway in mouse embryonic stem cells. *Dev.* **140**, 1684–1692 (2013).

434. Faunes, F. *et al.* A membrane-associated β-catenin/Oct4 complex correlates with ground-state pluripotency in mouse embryonic stem cells. *Development* **140**, 1171–1183 (2013).

435. Muñoz Descalzo, S. *et al.* A competitive protein interaction network buffers Oct4-mediated differentiation to promote pluripotency in embryonic stem cells. *Mol. Syst. Biol.* **9**, 1–10 (2013).

436. Kelly, K. F. *et al.* ??-catenin enhances Oct-4 activity and reinforces pluripotency through a TCF-independent mechanism. *Cell Stem Cell* **8**, 214–227 (2011).

437. Abu-Remaileh, M. *et al.* Oct-3/4 regulates stem cell identity and cell fate decisions by modulating Wnt/β-catenin signalling. *EMBO J.* **29**, 3236–3248 (2010).

438. Sumi, T., Oki, S., Kitajima, K. & Meno, C. Epiblast Ground State Is Controlled by Canonical Wnt/β-Catenin Signaling in the Postimplantation Mouse Embryo and Epiblast Stem Cells. *PLoS One* **8**, (2013).

439. Davidson, K. C. *et al.* Wnt/β-catenin signaling promotes differentiation, not self-renewal, of human embryonic stem cells and is repressed by Oct4. *Proc. Natl. Acad. Sci. U. S. A.* **109**, 4485–4490 (2012).

440. Haegel, H. *et al.* Lack of β-catenin affects mouse development at gastrulation. *Development* **121**, 3529–3537 (1995).

441. Huelsken, J. *et al.* Requirement for β-catenin in anterior-posterior axis formation in mice. *J. Cell Biol.* **148**, 567–578 (2000).

442. Brault, V. *et al.* Inactivation of the β-catenin gene by Wnt1-Cre-mediated deletion results in dramatic brain malformation and failure of craniofacial development. *Development* **128**, 1253–1264 (2001).

443. Valenta, T. *et al.* Probing transcription-specific outputs of β-catenin in vivo. *Genes Dev.* **25**, 2631–2643 (2011).

444. Kimura-Yoshida, C. *et al.* Canonical Wnt signaling and its antagonist regulate anterior-posterior axis polarization by guiding cell migration in mouse visceral endoderm. *Dev. Cell* **9**, 639–650 (2005).

445. Matsuda, K. & Kondoh, H. Dkk1-dependent inhibition of Wnt signaling activates Hesx1 expression through its 5' enhancer and directs forebrain precursor development. *Genes to Cells* **19**, 374–385 (2014).

446. Stuckey, D. W. *et al.* Coordination of cell proliferation and anterior-posterior axis establishment in the mouse embryo. *Development* **138**, 1521–1530 (2011).

447. Miura, S., Singh, A. P. & Mishina Yuji, Y. Bmpr1a is required for proper migration of the AVE through regulation of Dkk1 expression in the pre-streak mouse embryo. *Dev. Biol.* **341**, 246–254 (2010).

448. Dang, L. T. H. & Tropepe, V. FGF dependent regulation of Zfhx1b gene expression promotes the formation of definitive neural stem cells in the mouse anterior neurectoderm. *Neural Dev.* **5**, 1–16 (2010).

449. Lighthouse, J. K., Zhang, L., Hsieh, J. C., Rosenquist, T. & Holdener, B. C. MESD is essential for apical localization of megalin/LRP2 in the visceral endoderm. *Dev. Dyn.* **240**, 577–588 (2011).

450. Ferrer-vaquer, A. *et al.* art%3A10.1186%2F1471-213X-10-121. (2010).

451. Marikawa, Y. Wnt/β-catenin signaling and body plan formation in mouse embryos. *Semin. Cell Dev. Biol.* **17**, 175–184 (2006).

452. Barrow, J. R. *et al.* Wnt3 signaling in the epiblast is required for proper orientation of the anteroposterior axis. *Dev. Biol.* **312**, 312–320 (2007).

453. Tortelote, G. G. *et al.* Wnt3 function in the epiblast is required for the maintenance but not the initiation of gastrulation in mice. *Dev. Biol.* **374**, 164–173 (2013).

454. Muñoz-Descalzo, S., Hadjantonakis, A. K. & Arias, A. M. Wnt/ß-catenin signalling and the dynamics of fate decisions in early mouse embryos and embryonic stem (ES) cells. *Semin. Cell Dev. Biol.* **47–48**, 101–109 (2015).

455. Arkell, R. M., Fossat, N. & Tam, P. P. L. Wnt signalling in mouse gastrulation and anterior development: New players in the pathway and signal output. *Curr. Opin. Genet. Dev.* **23**, 454–460 (2013).

456. Wray, J. *et al.* Inhibition of glycogen synthase kinase-3 alleviates Tcf3 repression of the pluripotency network and increases embryonic stem cell resistance to differentiation. *Nat. Cell Biol.* **13**, 838–45 (2011).

457. Moser, A. R. *et al.* Homozygosity for the Minallele of Apc results in disruption of mouse development

prior to gastrulation. *Dev. Dyn.* **203**, 422–433 (1995).

458. Zeng, L. *et al.* The mouse Fused locus encodes axin, an inhibitor of the Wnt signaling pathway that regulates embryonic axis formation. *Cell* **90**, 181–192 (1997).

459. Yu, H. M. I. *et al.* The role of Axin2 in calvarial morphogenesis and craniosynostosis. *Development* **132**, 1995–2005 (2005).

460. Merrill, B. J. *et al.* Tcf3: A transcriptional regulator of axis induction in the early embryo. *Development* **131**, 263–274 (2004).

461. Chazaud, C. & Rossant, J. Disruption of early proximodistal patterning and AVE formation in Apc mutants. *Development* **133**, 3379–3387 (2006).

462. Harada, N. *et al.* Harada N, 1999.pdf. **18**, 5931–5942 (1999).

463. Kemler, R. *et al.* Stabilization of β-catenin in the mouse zygote leads to premature epithelial-mesenchymal transition in the epiblast. *Development* **131**, 5817–5824 (2004).

464. Fossat, N., Jones, V., Garcia-Garcia, M. J. & Tam, P. P. L. Modulation of WNT signaling activity is key to the formation of the embryonic head. *Cell Cycle* **11**, 26–32 (2012).

465. Morkel, M. *et al.* β-Catenin regulates Cripto- and Wnt3-dependent gene expression programs in mouse axis and mesoderm formation. *Development* **130**, 6283–6294 (2003).

466. Kemp, C., Willems, E., Abdo, S., Lambiv, L. & Leyns, L. Expression of all Wnt genes and their secreted antagonists during mouse blastocyst and postimplantation development. *Dev. Dyn.* **233**, 1064–1075 (2005).

467. Kemp, C. R. *et al.* Expression of Frizzled5, Frizzled7, and Frizzled10 during early mouse development and interactions with canonical Wnt signaling. *Dev. Dyn.* **236**, 2011–2019 (2007).

468. Xie, H. *et al.* Inactivation of nuclear Wnt-β-catenin signaling limits blastocyst competency for implantation. *Development* **135**, 717–727 (2008).

469. Goad, J., Ko, Y. A., Kumar, M., Syed, S. M. & Tanwar, P. S. Differential Wnt signaling activity limits epithelial gland development to the anti-mesometrial side of the mouse uterus. *Dev. Biol.* **423**, 138–151 (2017).

470. Tepekoy, F., Akkoyunlu, G. & Demir, R. The role of Wnt signaling members in the uterus and embryo during pre-implantation and implantation. *J. Assist. Reprod. Genet.* 337–346 (2014). doi:10.1007/s10815-014-0409-7

471. Messerschmidt, D. *et al.* B-Catenin-Mediated Adhesion Is Required for Successful Preimplantation Mouse Embryo Development. *Dev.* **143**, 1993–1999 (2016).

472. Krivega, M., Essahib, W. & Van de Velde, H. WNT3 and membrane-associated β-catenin regulate trophectoderm lineage differentiation in human blastocysts. *Mol. Hum. Reprod.* **21**, 711–722 (2015).

473. He, S., Pant, D., Schiffmacher, A., Meece, A. & Keefer, C. L. Lymphoid Enhancer Factor 1-Mediated Wnt Signaling Promotes the Initiation of Trophoblast Lineage Differentiation in Mouse Embryonic Stem Cells. *Stem Cells* **26**, 842–849 (2008).

474. de Vries, W. N. *et al.* Maternal β-catenin and E-cadherin in mouse development. *Development* **131**, 4435–4445 (2004).

475. Hyenne, V. *et al.* Conditional knock-out reveals that zygotic vezatin-null mouse embryos die at implantation. *Mech. Dev.* **124**, 449–462 (2007).

476. Nichols, J., Silva, J., Roode, M. & Smith, A. Suppression of Erk signalling promotes ground state pluripotency in the mouse embryo. *Development* **136**, 3215–3222 (2009).

477. Nichols, J. & Smith, A. Pluripotency in the embryo and in culture. *Cold Spring Harb. Perspect. Biol.* **4**, (2012).

478. Nichols, J. & Smith, A. Naive and Primed Pluripotent States. *Cell Stem Cell* **4**, 487–492 (2009).

479. Evans, M. J. & Kaufman, M. H. Establishment in culture of pluripotential cells from mouse embryos. *Nature* **292**, 154–156 (1981).

480. Silva, J. & Smith, A. Capturing Pluripotency. *Cell* **132**, 532–536 (2008).

481. Brons, I. G. M. *et al.* Derivation of pluripotent epiblast stem cells from mammalian embryos. *Nature* **448**, 191–195 (2007).

482. Tesar, P. J. *et al.* New cell lines from mouse epiblast share defining features with human embryonic stem cells. *Nature* **448**, 196–199 (2007).

483. Shahbazi, M. N., Siggia, E. D. & Zernicka-Goetz, M. Self-organization of stem cells into embryos: A window on early mammalian development. *Science (80-.).* **364**, 948–951 (2019).

484. Hayashi, K., Ohta, H., Kurimoto, K., Aramaki, S. & Saitou, M. Reconstitution of the mouse germ cell specification pathway in culture by pluripotent stem cells. *Cell* **146**, 519–532 (2011).

485. Kuijk, E. W., Chuva de Sousa Lopes, S. M., Geijsen, N., Macklon, N. & Roelen, B. A. J. The different shades of mammalian pluripotent stem cells. *Hum. Reprod. Update* **17**, 254–271 (2011).

486. Kunath, T. *et al.* Imprinted X-inactivation in extra-embryonic endoderm cell lines from mouse blastocysts. *Development* **132**, 1649–1661 (2005).

487. Artus, J., Panthier, J. J. & Hadjantonakis, A. K. A role for PDGF signaling in expansion of the extra-embryonic endoderm lineage of the mouse blastocyst. *Development* **137**, 3361–3372 (2010).

488. Julio, M. K. *et al.* Regulation of extra-embryonic endoderm stem cell differentiation by Nodal and Cripto signaling. *Development* **138**, 3885–3895 (2011).

489. Cho, L. T. Y. *et al.* Conversion from mouse embryonic to extra-embryonic endoderm stem cells reveals distinct differentiation capacities of pluripotent stem cell states. *Dev.* **139**, 2866–2877 (2012).

490. Tanaka, S., Kunath, T., Hadjantonakis, A. K., Nagy, A. & Rossant, J. Promotion to trophoblast stem cell proliferation by FGF4. *Science (80-.).* **282**, 2072–2075 (1998).

491. Shahbazi, M. N. *et al.* Self-organization of the human embryo in the absence of maternal tissues. *Nat. Cell Biol.* **18**, 700–708 (2016).

492. Chhabra, S., Liu, L., Goh, R. & Warmflash, A. *Dissecting the dynamics of signaling events in the BMP, WNT, and NODAL cascade during self-organized fate patterning in human gastruloids*. *bioRxiv* (2018). doi:10.1101/440164

493. Simunovic, M. & Brivanlou, A. H. Embryoids, organoids and gastruloids: New approaches to understanding embryogenesis. *Dev.* **144**, 976–985 (2017).

494. Martinez Arias, A. & Steventon, B. On the nature and function of organizers. *Dev.* **145**, (2018).

495. Huch, M., Knoblich, J. A., Lutolf, M. P. & Martinez-Arias, A. The hope and the hype of organoid research. *Dev.* **144**, 938–941 (2017).

496. Turner, D. A., Baillie-Johnson, P. & Martinez Arias, A. Organoids and the genetically encoded self-assembly of embryonic stem cells. *BioEssays* **38**, 181–191 (2016).

497. Sasai, Y., Eiraku, M. & Suga, H. In vitro organogenesis in three dimensions: Self-organising stem cells. *Dev.* **139**, 4111–4121 (2012).

498. Hiramatsu, R. *et al.* External mechanical cues trigger the establishment of the anterior-posterior axis in early mouse embryos. *Dev. Cell* **27**, 131–144 (2013).

499. Turner, D. A. *et al.* Wnt/β-catenin and FGF signalling direct the specification and maintenance of a neuromesodermal axial progenitor in ensembles of mouse embryonic stem cells. *Dev.* **141**, 4243–4253 (2014).

500. Turner, D. A. *et al.* Anteroposterior polarity and elongation in the absence of extraembryonic tissues and of spatially localised signalling in gastruloids: Mammalian embryonic organoids. *Dev.* **144**, 3894–3906 (2017).

501. Beccari, L. *et al.* Multi-axial self-organization properties of mouse embryonic stem cells into gastruloids. *Nature* **562**, 272–276 (2018).

502. Turner, D. A., Rué, P., Mackenzie, J. P., Davies, E. & Martinez Arias, A. Brachyury cooperates with Wnt/β-catenin signalling to elicit primitive-streak-like behaviour in differentiating mouse embryonic stem cells. *BMC Biol.* **12**, 8–11 (2014).

503. Warmflash, A., Sorre, B., Etoc, F., Siggia, E. D. & Brivanlou, A. H. A method to recapitulate early embryonic spatial patterning in human embryonic stem cells. *Nat. Methods* **11**, 847–854 (2014).

504. Deglincerti, A. *et al.* Self-organization of the in vitro attached human embryo. *Nature* **533**, 251–254 (2016).

505. Etoc, F. *et al.* A Balance between Secreted Inhibitors and Edge Sensing Controls Gastruloid Self-Organization. *Dev. Cell* **39**, 302–315 (2016).

506. Ma, Z. *et al.* Self-organizing human cardiac microchambers mediated by geometric confinement. *Nat. Commun.* **6**, (2015).

507. Rivron, N. C. *et al.* Blastocyst-like structures generated solely from stem cells. *Nature* **557**, 106–111 (2018).

508. Srinivas, S., Rodriguez, T., Clements, M., Smith, J. C. & Beddington, R. S. P. Active cell migration drives the unilateral movements of the anterior visceral endoderm. *Development* **131**, 1157–1164 (2004).

509. Hamilton, T. G., Klinghoffer, R. A., Corrin, P. D. & Soriano, P. Evolutionary divergence of platelet-derived growth factor alpha receptor signaling mechanisms. *Mol. Cell. Biol.* **23**, 4013–25 (2003).

510. Hadjantonakis, A. K. & Papaioannou, V. E. Dynamic in vivo imaging and cell tracking using a histone fluorescent protein fusion in mice. *BMC Biotechnol.* **4**, 1–14 (2004).

511. Lou, X., Kang, M., Xenopoulos, P., Mu??oz-Descalzo, S. & Hadjantonakis, A. K. A rapid and efficient 2D/3D nuclear segmentation method for analysis of early mouse embryo and stem cell image data. *Stem Cell Reports* **2**, 382–397 (2014).

512. Senft, A. D. *et al.* Combinatorial Smad2/3 Activities Downstream of Nodal Signaling Maintain Embryonic/Extra-Embryonic Cell Identities during Lineage Priming. *Cell Rep.* **24**, 1977-1985.e7 (2018).

513. El Nagar, S. *et al.* Otx2 promotes granule cell precursor proliferation and Shh-dependent medulloblastoma maintenance in vivo. *Oncogenesis* **7**, (2018).

514. Dykes, I. M. *et al.* A Requirement for Zic2 in the regulation of nodal expression underlies the establishment of left-sided identity. *Sci. Rep.* **8**, 1–16 (2018).

515. Norris, D. P., Brennan, J., Bikoff, E. K. & Robertson, E. J. The Foxh1-dependent autoregulatory enhancer controls the level of Nodal signals in the mouse embryo. *Development* **129**, 3455–3468 (2002).

516. Blakeley, P. *et al.* Erratum to Defining the three cell lineages of the human blastocyst by single-cell RNA-seq (Development, (2015) 142, 3151-3165). *Dev.* **142**, 3613 (2015).

517. Moley, K. H., Gynecology, M. M. C. & Biology, C. Concentrations Trigger Apoptosis in the Mouse Blastocyst via Down-Regulation of the IGF-1 Receptor *. *Society* **141**, 4784–4792 (2009).

518. Bedzhov, I., Liszewska, E., Kanzler, B. & Stemmler, M. P. Igf1r signaling is indispensable for preimplantation development and is activated via a novel function of E-cadherin. *PLoS Genet.* **8**, (2012).

ABSTRACT

During the early mouse embryogenesis, cell-fate specification events result in the formation of the pre-implantation blastocyst. Those events are mainly regulated by the action of signaling cascades activated upon fixation of the signaling molecules at the cell membrane. The activity of these signaling pathways allow the transcriptional regulation of a specific pool of genes responsible for cell-fate decisions and the formation of tissues. Here, I am interested in the roles of both ACTIVIN/NODAL and βCATENIN signaling pathways in the specification of cell identities during the maturation of the mouse blastocyst.

Key words: mouse, embryo, pre-implantation, blastocyst, cell-fate, specification, ACTIVIN/NODAL, βCATENIN, signaling, pathways.

RESUMÉ

Lors du développement précoce de l'embryon de souris, divers évènements de spécification des destins cellulaires induisent la formation du blastocyste pré-implantatoire. Ces évènements sont majoritairement contrôlés par l'action de voies de signalisation activées via la fixation de molécules signal à la membrane de la cellule. L'activité de ces voies de signalisation permet la régulation de la transcription de gènes cible responsable de l'acquisition d'une identité cellulaire et de son arrangement sous forme de tissu. Ici je m'intéresse aux rôles des voies ACTIVINE/NODAL et βCATENIN dans la spécification de ces identités cellulaires lors de la formation du blastocyste de souris.

Mots clefs : souris, embryon, pré-implantatoire, blastocyste, destins, spécification, ACTIVIN/NODAL, βCATENIN, signalisation, voies.